UNCLASSIFIED

AD NUMBER
ADB012311
LIMITATION CHANGES
TO: **Approved for public release; distribution is unlimited.**
FROM: **Distribution authorized to U.S. Gov't. agencies only; Test and Evaluation; 17 JUN 1976. Other requests shall be referred to Space and Missile Systems Organization, PO box 92960, Los Angeles, CA.**
AUTHORITY
SAMSO ltr 13 May 1981

THIS PAGE IS UNCLASSIFIED

THIS REPORT HAS BEEN DELIMITED
AND CLEARED FOR PUBLIC RELEASE
UNDER DOD DIRECTIVE 5200.20 AND
NO RESTRICTIONS ARE IMPOSED UPON
ITS USE AND DISCLOSURE.

DISTRIBUTION STATEMENT A

APPROVED FOR PUBLIC RELEASE;
DISTRIBUTION UNLIMITED.

(12) (2)

B.S.

ADTC-TR-76-58

FINAL REPORT

LDG 540 GYRO TEST

PREPARED BY

CENTRAL INERTIAL GUIDANCE TEST FACILITY
6585TH TEST GROUP
HOLLOMAN AIR FORCE BASE, NEW MEXICO

JUNE 1976

DISTRIBUTION LIMITED TO US GOVERNMENT AGENCIES ONLY: (TEST AND EVALUATION): (17 JUNE 1976). OTHER REQUESTS FOR THIS DOCUMENT MUST BE REFERRED TO SAMSO/YAD, P.O. BOX 92960, WORLDWAY POSTAL CENTER, LOS ANGELES CA 90009.

ARMAMENT DEVELOPMENT AND TEST CENTER

AIR FORCE SYSTEMS COMMAND - UNITED STATES AIR FORCE

EGLIN AIR FORCE BASE, FLORIDA

THIS TECHNICAL REPORT HAS BEEN REVIEWED AND IS APPROVED.

Richard E Clark

RICHARD E. CLARK, Colonel, USAF
Director, Guidance Test Division

UNCLASSIFIED

SECURITY CLASSIFICATION OF THIS PAGE (When Data Entered)

REPORT DOCUMENTATION PAGE

READ INSTRUCTIONS BEFORE COMPLETING FORM

1. REPORT NUMBER: 14 ADTC-TR-76-58

2. GOVT ACCESSION NO.

3. RECIPIENT'S CATALOG NUMBER

4. TITLE (and Subtitle): 6 LDG 540 Gyro Test .

5. TYPE OF REPORT & PERIOD COVERED: 9 Final Report, 30 Sep[redacted]r 1975 [redacted] 22 Jan[redacted]1976,

6. PERFORMING ORG. REPORT NUMBER

7. AUTHOR(s): 10
Steven Cox, Mr
Craig Price, 1st Lt, USAF
Frank Connor, Capt, USAF

8. CONTRACT OR GRANT NUMBER(s): ~~SAMSNP02~~

9. PERFORMING ORGANIZATION NAME AND ADDRESS
6585th Test Group (GDP)
Holloman AFB, NM 88330

10. PROGRAM ELEMENT, PROJECT, TASK AREA & WORK UNIT NUMBERS: 12 217p.

11. CONTROLLING OFFICE NAME AND ADDRESS
SAMSO/YAD
P.O. Box 92960
Worldway Postal Center, Los Angeles, CA 90009

12. REPORT DATE: 11 Jun[redacted]76

13. NUMBER OF PAGES

14. MONITORING AGENCY NAME & ADDRESS (if different from Controlling Office)

15. SECURITY CLASS. (of this report): Unclassified

15a. DECLASSIFICATION/DOWNGRADING SCHEDULE

16. DISTRIBUTION STATEMENT (of this Report)
Distribution limited to U. S. Government Agencies only: (Test and Evaluation): (17 Jun 1976). Other requests for this document must be referred to SAMSO/YAD P.O. Box 92960, Worldway Postal Center, Los Angeles, CA 90009.

17. DISTRIBUTION STATEMENT (of the abstract entered in Block 20, if different from Report)

18. SUPPLEMENTARY NOTES

19. KEY WORDS (Continue on reverse side if necessary and identify by block number)

Gyro	Power Spectral Density
Gyroscope	Inertial Instrument
Bendix	

20. ABSTRACT (Continue on reverse side if necessary and identify by block number)

Two Bendix LDG 540 gyroscopes were tested at the Central Inertial Guidance Test Facility, 6585th Test Group, Holloman Air Force Base, New Mexico during the period from 30 September 1975 to 22 January 1976. The purpose of the tests was to characterize the gyro output noise signature in the frequency range from 10^{-5} to 10 Hz with the gyro in a quiescent environment. A description of the test item is presented as well as descriptions of the support electronics, test equipment, fixtures, data acquisition system, and test procedures. A complete

DD FORM 1 JAN 73 1473 EDITION OF 1 NOV 65 IS OBSOLETE

UNCLASSIFIED 404 038

SECURITY CLASSIFICATION OF THIS PAGE (When Data Entered)

00001

cont

set of the individual test results are included in the appendices along with the monitored environmental influences of temperature, pad motion, and the gyro wheel supply electronics. The results are presented both in time domain plots, and the frequency domain power spectral density (PSD) plots.

Both gyros were sensitive to temperature and wheel current variations. The best low frequency performance was obtained from the second twenty-four hour test on gyro S/N 1. At the six hour point (4.6 x 10^{-5} Hz) the PSD of gyro S/N 1 had a value of .0006 $(deg/hr)^2/Hz$. From the six hour point, the gyro noise output rolls off at about 10 to 12 db/decade as frequency increases except for several power peaks between .0004 and .002 Hz. The larger peaks seen in the PSD of gyro S/N 1 were not present in gyro S/N 2. However, the PSD of gyro S/N 2 output was ten times larger than that of gyro S/N 1 at the six hour point.

FOREWORD

This report covers the results of tests performed by the Central Inertial Guidance Test Facility (CIGTF) on the Bendix LDG 540 gyroscope from 30 September 1975 to 22 January 1976. The Space and Missile Systems Organization (SAMSO) was the responsible development organization and provided reimbursable expenses under JON: SAMSNP02. The report was prepared by the Test Engineer, 1st Lt Craig Price; the Test Analyst, Mr. Stephen Cox; and the Test Director, Captain Richard Rumph.

ABSTRACT

Two Bendix LDG 540 gyroscopes were tested at the Central Inertial Guidance Test Facility, 6585th Test Group, Holloman Air Force Base, New Mexico during the period from 30 September 1975 to 22 January 1976. The purpose of the tests was to characterize the gyro output noise signature in the frequency range from 10^{-5} to 10 Hz with the gyro in a quiescent environment. A description of the test item is presented as well as descriptions of the support electronics, test equipment, fixtures, data acquisition system, and test procedures. A complete set of the individual test results are included in the appendices along with the monitored environmental influences of temperature, pad motion, and the gyro wheel supply electronics. The results are presented both in time domain plots, and the frequency domain power spectral density (PSD) plots.

Both gyros were sensitive to temperature and wheel current variations. The best low frequency performance was obtained from the second twenty-four hour test on gyro S/N 1. At the six hour point (4.6×10^{-5} Hz) the PSD of gyro S/N 1 had a value of .0006 $(deg/hr)^2/Hz$. From the six hour point, the gyro noise output rolls off at about 10 to 12 db/decade as frequency increases except for several power peaks between .0004 and .002 Hz. The larger peaks seen in the PSD of gyro S/N 1 were not present in gyro S/N 2. However, the PSD of gyro S/N 2 output was ten times larger than that of gyro S/N 1 at the six hour point.

TABLE OF CONTENTS

Table of Contents (Continued)

LIST OF TABLES

LIST OF FIGURES

LIST OF FIGURES (Continued)

LIST OF FIGURES (Continued)

LIST OF FIGURES (Continued)

LIST OF FIGURES (Continued)

LIST OF FIGURES (Continued)

LIST OF FIGURES (Continued)

LIST OF FIGURES (Continued)

1. INTRODUCTION

1.1 Authority

Laboratory testing of a sequence of 6 different gyroscopes was requested by the Space and Missile Systems Organization, Los Angeles Air Force Station, California in a Program Introduction dated 12 February 1975, titled "Space Gyro Testing".

In accordance with AFSC Supplement 1 to AFR 80-14, the Guidance Test Division of the 6585th Test Group documented this test program in a Statement of Capability dated 12 March 1975.

This report documents the results of testing performed on one gyro in the sequence, the Bendix LDG 540.

The gyro and its support equipment are unclassified to both visual and physical access. All test procedures, schedules and data are unclassified.

1.2 Test Objective

The objective of this test program is to measure and characterize the noise output for each gyro in the sequence. Each gyro is subjected to the same test environment with the intent to provide a valid basis for comparing the gyros. Power spectral density measurements of the output noise are presented for the frequency range from 10^{-5} - 10 Hz.

1.3 Test History

Testing on the LDG 540 began in September 1975 and continued through January 1976. A detailed history of the test effort is given in Appendix A.

2. TEST ITEM DESCRIPTION

2.1 General

The LDG 540 is a single degree-of-freedom gas bearing gyroscope with an AC torquer and a liquid hydrostatic float suspension. The unit weighs approximately 1.5 pounds and is generally cylindrical with diameter 2.4 inches and length 3.7 inches.

2.2 Instruments Tested

Two instruments were provided to CIGTF for testing; S/N 1 and S/N 2. The units were built by Bendix however they were owned by the Marshal Space Flight Center, Huntsville, Alabama. Gyro S/N 1 was intended for use as the primary test instrument with S/N 2 serving as a back-up.

2.3 Support Electronics

Figure 1 shows the basic interconnections of the gyro support electronics. The two frequency synthesizers were synchronized and their outputs were applied to three identical precision power supplies. The wheel supply voltages were passed to the gyro with the supply sense leads connected at the breakout box. The hydrostatic suspension pump supply voltages were also passed to the gyro but the sense leads were tied at the terminal board. The 100 v maximum output of the control panel power supply was stepped-up to 115 v by a variac and applied to the control panel. The sense leads were jumpered at the supply.

GYRO SUPPORT ELECTRONICS

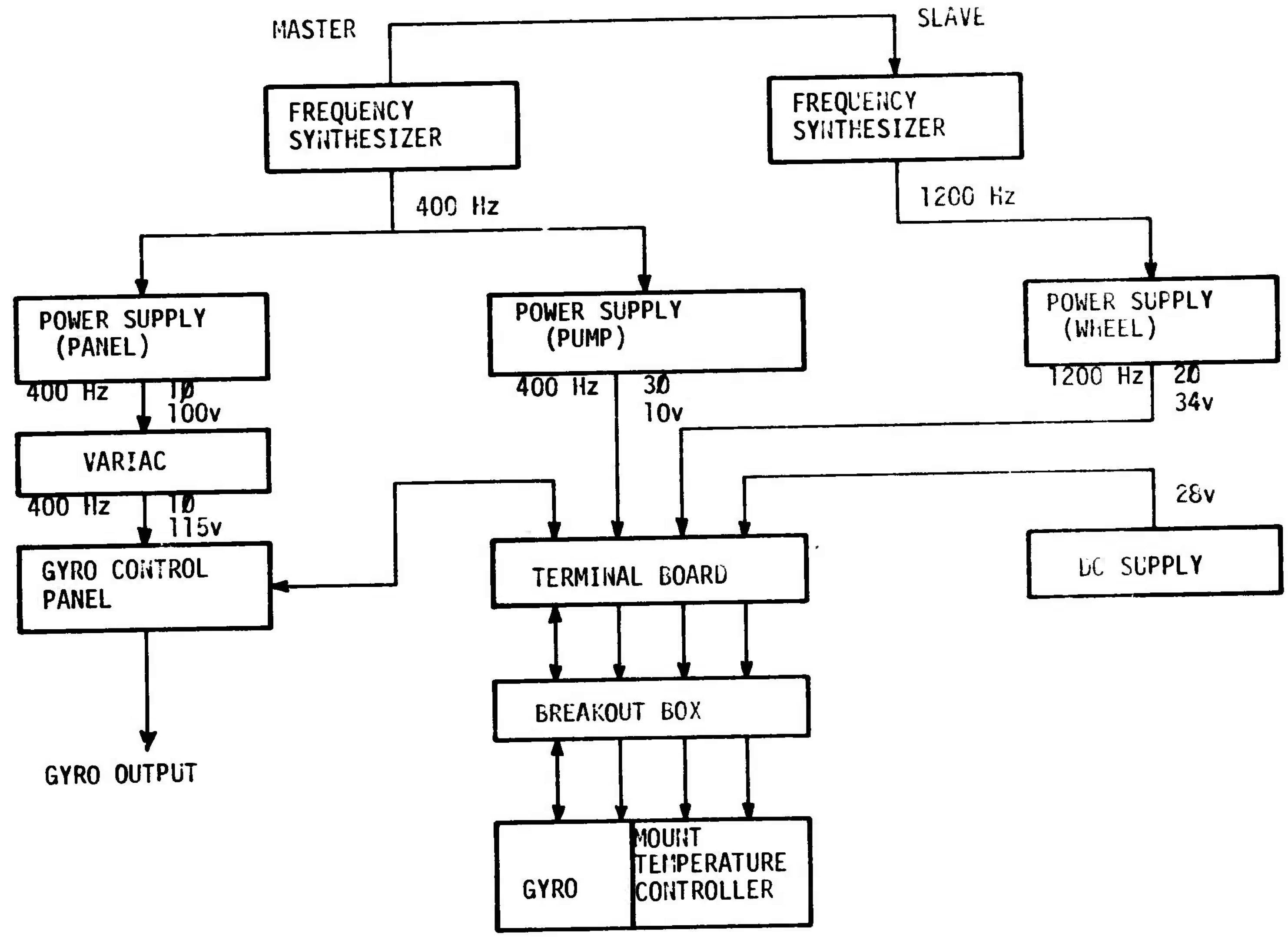

FIGURE 1

The control panel generated its own reference frequencies and performed all of the functions of the AC gyro servo loop. A sensitivity switch on the panel allowed for a 3:1 change in the maximum torquing rate. The panel along with the terminal board and breakout box was supplied by Bendix but had also been built at the Marshall Space Flight Center.

Finally, the DC supply provided 28 volts to the mount temperature controller. Since the gyro does not depend on bouyance for float suspension, there is no temperature control on the gyro itself so the gyro mount is temperature controlled to provide a stable environment.

An itemized list of the support electronics used is given in Table I.

3. TEST EQUIPMENT AND FIXTURES

3.1 Precision Positioning Table

For the eight point tests, the gyro was mounted on the Hughes M-1 table in the components test laboratory. The M-1 has an air bearing table top with better than 1 arc second positioning accuracy and a trunion axis which allows the table axis to be vertical or horizontal as necessary for the tests.

3.2 Drift Fixture

The mounting arrangement for the gyro during drift tests is illustrated in Figure 2. The 2 1/2 x 2 1/2 foot aluminum plate was bolted to the floor-level concrete isolated test pier. The 1 1/2 foot diameter aluminum disk was held securely to the square plate by 3 "L" shaped clamps. Both plates had a hole drilled at their centers through which a dowel rod was slipped, providing a pivot for the disk. This allowed for coarse positioning of the gyro input axis before tightening of the "L" clamps. The gyro mount was then attached to the disk. A styrofoam box was placed over the gyro and mount to provide additional temperature stability for the gyro.

TABLE 1

GYRO SUPPORT ELECTRONICS

QTY	ITEM	MAKE	MODEL	DESCRIPTION
2	Frequency Synthesizer	Rockland	5100	.01 PPM, .001 Hz - 2 MHz
3	Power Supplies	NH Research	SF-1250W	25 PPM, 5-100v, 1-3Ø
1	Variac	General Radio	-	-
1	Power Supply	Kepco	SC-32-2.5	0-32v DC
1	Control Panel	-	-	-

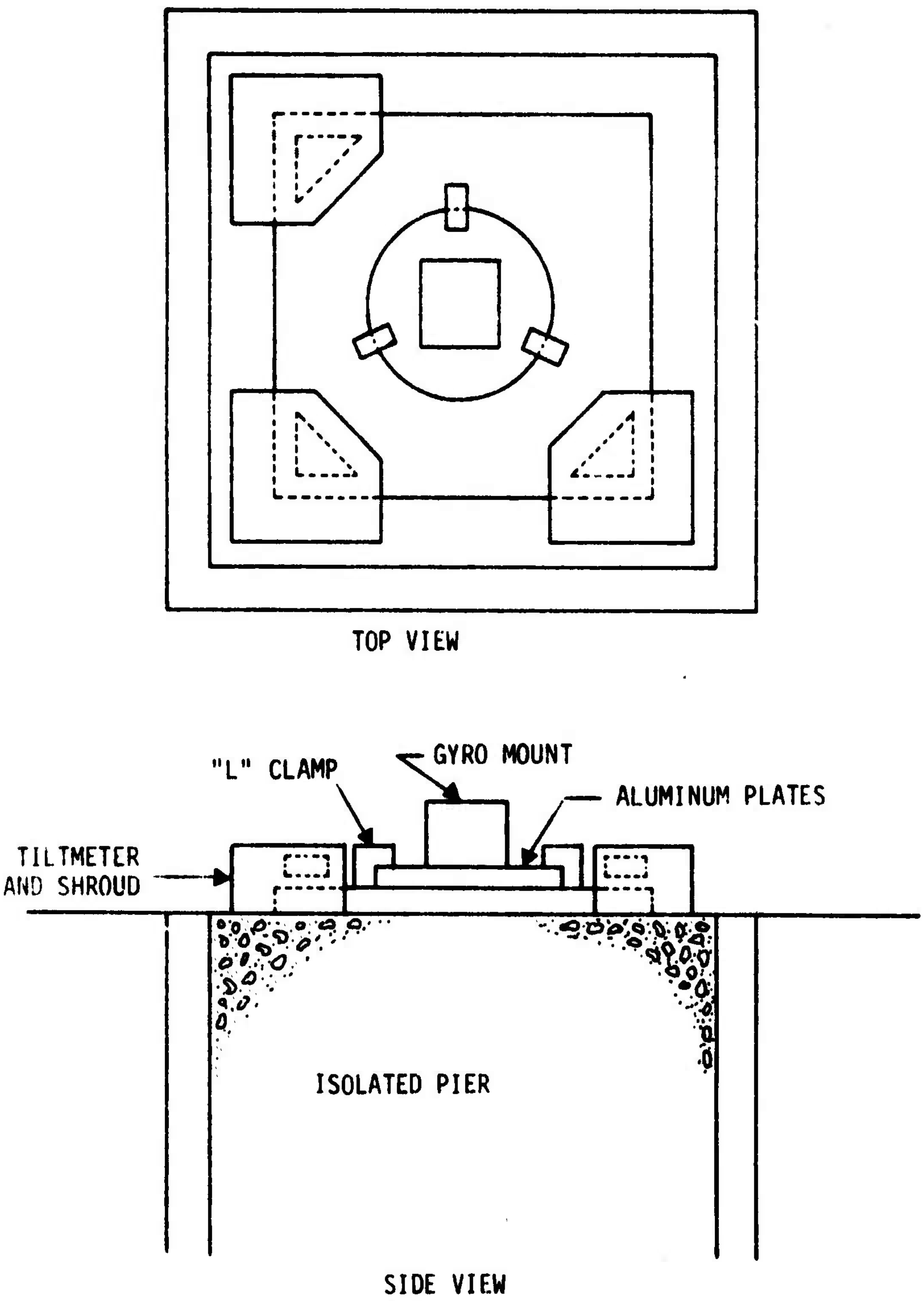

FIGURE 2. GYRO DRIFT MOUNTING CONFIGURATION

Three tiltmeters with styrofoam temperature shrouds were placed on 3 corners of the square plate.

3.3 Data Acquisition

A block diagram of the data acquisition system is given in Figure 3 with an itemized list of the equipment in Table II.

The three tiltmeters were placed on the pad such that they all sensed rotations about the gyro input axis. The DC output voltages proportional to angular displacements were fed to the input of the multichannel filter.

The wheel current and voltage monitors were connected at the wheel supply output and passed their outputs to the multichannel filter.

The ambient temperature sensor was a ribbon thermistor suspended approximately 10 inches to one side of the gyro mount. The gyro temperature sensor was an identical thermistor which was taped around the gyro case. Both thermistors were connected to temperature bridges whose DC outputs were input to the multichannel filter.

The multichannel filter used has 8 independent channels, each consisting of an 8 pole Butterworth filter with selectable cutoff frequencies from .01 -150 Hz. The output noise of each channel is approximately 1 mv RMS.

The output of the gyro taken from the "Filter Out" terminals of the control panel was passed through two cascaded single channel filters. Each filter consisted of 3 cascaded poles so that the net result was a 6 pole filter. The output noise of the 6 pole filter was less than .1 mv RMS which made it more suitable for the low level gyro signals.

DATA ACQUISITION SYSTEM

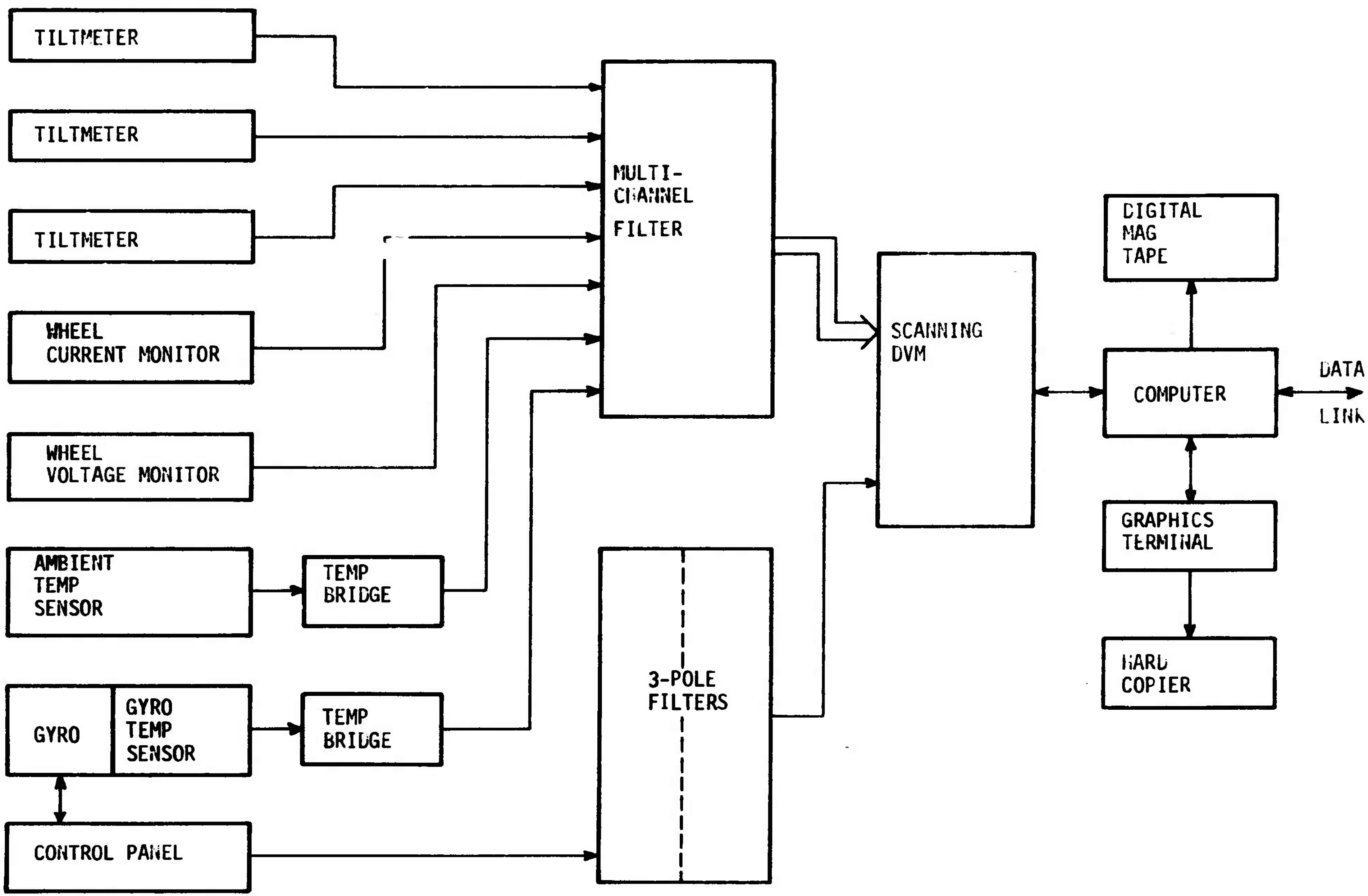

FIGURE 3

TABLE II

DATA ACQUISITION EQUIPMENT

QTY	ITEM	MAKE	MODEL	DESCRIPTION
3	Tiltmeter	Autonetics	SE541A	2-axis tiltmeter
1	Wheel Voltage Monitor	NH Research	4106	High resolution AC voltmeter
1	Wheel Current Monitor	Fluke or NH Research	803BR 4106	Differential voltmeter High resolution AC voltmeter
2	Temperature Sensor	Minco	7B	Thermal ribbon
2	Temperature Bridge	Harrel	CI207A	Resistive bridge
1	Multi-channel Filter	Rockland	816	16 channel 8 pole analog filter (.01-150 Hz)
2	3-Pole Filter	C.S. Draper Labs	---	3 Pole analog filter (.16-.0003 Hz)
1	DVM	Hewlett Packard	3480B/85A	4-1/2 digit scanning digital voltmeter
1	Computer	Hewlett Packard	2100A	32767 word minicomputer
1	Terminal	Tektronics	4015-1	Graphics terminal
1	Copier	Tektronics	4610	Thermal hard copier
1	Tape Drive	Hewlett Packard	7970B	9 track digital magnetic tape drive

The outputs of both filters were passed to the scanning digital voltmeter. On command from the computer, the DVM point sampled each of the 8 inputs with .1 mv resolution and 1 v range. The computer saved the data and waited on its internal time base for the next sample time. After 32 such sample, save and wait cycles, the computer wrote its stored data onto the digital magnetic tape unit and repeated the process until the preselected number of samples had been taken. Up to 32767 samples could be selected for one test.

Table III gives the scale factors used for each of the environmental monitor signals. The .1 mv resolution of the DVM can be multiplied by the sensor channel scale factor to get the signal resolution.

TABLE III

SENSOR SCALE FACTORS

SENSOR	GYRO S/N 1 TESTS	GYRO S/N 2 TESTS
Tiltmeters	5 $\widehat{\text{sec}}$/volt	5 $\widehat{\text{sec}}$/volt
Ambient temperature	56°F/volt	56°F/volt
Gyro case temperature	11.6°F/volt	-
Wheel current	.05 amps/volt	.0016 amps/volt
Wheel voltage	.4 volts/volt	.04 volts/volt

3.4 Fourier Analysis

At the conclusion of the test, the operator obtained a different computer operating system over the data link. Each channel of data was taken off of the magnetic tape up to 4096 points at a time, scaled into appropriate units, and run through a least squares straight line fit for computing slope, bias, and variance about the line. The data was then plotted on the graphics terminal along with the results of the least squares fit. The bias and slope were removed from the data and a Fast Fourier Transform was applied. The resulting frequency domain data was temporarily stored on disk and then self conjugate multiplied and plotted to obtain the PSD. The stored frequency domain data could be used for correlations, transfer functions and other analyses.

The power spectral density routine used is one which maintains the total power in a signal. Thus any input sine wave of amplitude A on a test T seconds in length has a PSD amplitude of $\frac{A^2T}{2}$ with frequency resolution of $\frac{1}{T}$. The total power in the PSD is then $(\frac{A^2T}{2}) \times (\frac{1}{T}) = \frac{A^2}{2}$ which is the proper result.

Often the PSD's are smoothed before plotting. The operation is essentially Hanning and consists of replacing the PSD value V at each point k with

$$V_k = \frac{1}{4} V_{k-1} + \frac{1}{2} V_k + \frac{1}{4} V_{k+1}.$$

Hanning may be applied repeatedly for higher degrees of smoothing.

Tilt rate information is obtained utilizing the differentiation property of the Fourier transform. The tilt data is Fourier transformed into the frequency domain and the multiplied by $j\omega$ ($j = \sqrt{-1}$) with ω evaluated at each frequency. This results in the Fourier transform of the derivative of the input data (tilt rate). This result is then either conjugate multiplied for obtaining the PSD or inverse transformed to obtain a synthesized time plot of tilt rate. The tilt rate time plot is dominated by high frequencies however some low frequency variations are present in the plot.

4. TEST PROCEDURES AND RESULTS

4.1 Eight Point and Scale Factor Test

4.1.1 Procedure

In order to confirm proper operation of the instrument preliminary 8 point tests were run on the Hughes M-1 table at CIGTF. The gyro was mounted on the table top with OA vertical up and parallel to the table top rotational axis. An east-west determination was run for coarse alignment. Data was then taken with the input axis pointing north, east, south and then west. Next, the table was repositioned with its rotational axis horizontal so that the gyro was oriented OA north. Data was then taken with the input axis pointing down, east, up, then west. The entire procedure was repeated three times.

The control panel sensitivity switch was placed in the high rate mode for the eight point tests because the loop would saturate for several of the positions if it were in the low rate mode. For the drift tests described later, however, the low rate mode was used for increased resolution. For this reason, a separate scale factor determination test was conducted with the loop in the low rate position.

Again starting with an east/west determination, the gyro input axis was then positioned +1° and -1° from the west orientation. The known difference in earth rate between the two positions divided by the change in the gyro output provides the low rate scale factor with sufficient accuracy for the drift tests.

4.1.2 Test Results

The coefficients obtained from the eight position tests for Gyro S/N 1 are presented in Table IV confirming proper operation of the gyro.

TABLE IV

EIGHT POINT TEST RESULTS GYRO S/N 1

	S (DEG/HR/VOLT)	DI (DEG/HR/G)	DS (DEG/HR/G)	DF+DSS	DF+DII	DF+DO	PHI (DEG)
TEST 1	2.89788	-.07782	.39492	.08230	.00580	-.00797	.00659
TEST 2	2.90624	-.02577	.40139	.07992	-.00291	.00363	-.03305
TEST 3	2.89654	-.05691	.39300	.06952	-.00724	-.01159	.00659
MEAN	2.90022	-.05350	.39644	.07725	-.00145	-.00531	-.00662

The explanation of the gyro model used in obtaining the coefficients is found in Appendix B. A full eight position test was not conducted on Gyro S/N 2. The results of the low rate scale factor test for both Gyro S/N 1 and Gyro S/N 2 are presented in Table V.

TABLE V

SCALE FACTOR TEST RESULTS

	GYRO S/N 1	GYRO S/N 2
SCALE FACTOR	.92753 °/hr/volt	.95993 °/hr/volt

4.2 Drift Tests

4.2.1 Procedure

The gyro was attached to the test pier as described in Section 3.2 and illustrated in Figure 2. The input axis of the gyro was positioned approximately west and then incremented slightly north or south using earth rate to bias the gyro output to near zero. This allows use of the most sensitive DVM scales, provides the least output sensitivity to changes in the gyro parameters and is most similar to the low rates which will be seen in a space application. The gyro was maintained in this position for all of the drift tests.

Table VI describes the sample times and filter cutoff frequencies used on the gyro and environmental signals. The 24 hour test parameters were chosen to give the maximum low frequency information under the constraints of a 4096 point data processing limitation and a .01 Hz low pass filter minimum cutoff frequency. With .01 Hz cutoff, the sampling frequency needs to be at least .02 Hz and to minimize aliasing should be about twice this rate. The 21 second sample period chosen meets this requirement as well as resulting in very nearly a 24 hour test with 4096 samples. The parameters for the other two tests were chosen in a similar manner with the objective of covering higher frequency regions with minimum overlap.

TABLE VI

DRIFT TEST SAMPLING PARAMETERS

SAMPLE PERIOD	NUMBER OF SAMPLES	TEST LENGTH	816 CUTOFF	3-POLE CUTOFF
21 sec	4096	24 hours	.01 Hz	.011 Hz
1 sec	4096	1 hour	.2 Hz	.159 Hz
.05 sec	4096	3 min	5 Hz	-

The 816 filter was used for the monitor signals for each test and the 3-pole filter was used for the gyro signal in all but the 3 minute test. Since the maximum cutoff frequency of the 3-pole filter was .159 Hz, the 816 filter had to be used.

Shorted filter tests were conducted to insure that the total data acquisition system noise was below the signals being measured. To perform these tests, the filter inputs were shorted, the filters were set to the appropriate cutoff frequencies and full length tests were run at each of the 3 sample rates.

4.2.2 Test Results

Appendix C gives a detailed description of the data plot formats used in this report. Plots and more detailed discussions of the gyro drift tests are presented in Appendix D in the following order:

(a) Time domain plots of the raw data:

(1) Gyro

(2) Average Tilt

(3) Average Tilt Rate

(4) Ambient Temperature

(5) Gyro Case Temperature

(6) Gyro Wheel Voltage

(7) Gyro Wheel Current

(b) Frequency domain PSD plots of the data:

(1) Gyro Data Unsmoothed (for 24 hour tests only)

(2) Gyro Data Smoothed

(3) Average Tilt Rate

(4) Ambient Temperature

(5) Gyro Case Temperature

(6) Gyro Wheel Voltage

(7) Gyro Wheel Current

(c) Other plots as explained in the text.

Gyro S/N 1 data is presented first, starting with the 24 hour tests, and followed respectively by the one hour test and the three minute test. The data from Gyro S/N 2 is then presented in the same order.

The mean and trend is removed from all time domain data prior to converting it into the frequency domain as described in paragraph 3.4. This was done to permit characterization of the random noise instead of trends. The time domain data plots are made prior to removal of mean and trend but do have appropriate scaling. However since the means are subsequently removed, the signals are not calibrated to read the correct absolute values.

Appendix E presents the results of the shorted filter 3 minute, one hour, and twenty four hour tests. The raw time domain data is presented first followed by PSD plots. The PSD plots were obtained by appropriate scaling of the time domain data. This was done to allow a direct comparison between the actual data and recording channel noise.

Testing started with Gyro S/N 1. When Gyro S/N 1 failed, as described in Appendix A, testing was completed on Gyro S/N 2. The probable cause of the Gyro S/N 1 failure was later traced to low fluid charge. The impending malfunction of Gyro S/N 1 did not appear to have an adverse affect on the noise level in the low frequency spectrum. Therefore, a complete set of drift test data taken from Gyro S/N 1 before the failure, is presented. A sample set (except for the third 24 hour test) of drift tests results for Gyro S/N 2 is also given.

4.3 Wheel Off Tests

4.3.1 Procedure

In order to investigate the contribution of the gyro loop to the output noise, the wheel was turned off with the gyro mounted on the drift fixture and data was taken at each of the 3 sample rates used for the drift tests.

4.3.2 Wheel Off Test Results

Appendix F presents the plots of the wheel off test results along with a brief discussion of the data. Essentially, the wheel off tests were not significantly different than the shorted filter tests presented in Appendix E.

4.4 OA Noise Sensitivity Test

4.4.1 Procedure

The purpose of the OA noise sensitivity tests was to investigate the effect of output axis rates on the total noise output of the gyro. The instrument was placed onto the M-1 table with OA vertical and parallel to the table rotational axis and IA west. A square wave rate was then applied to the table top such that it rotated through .1° in 100 seconds at a constant rate and then reversed direction. The gyro output was sampled at 1 Hz for an hour.

Since the table top is known to be seismically noisier than the pad used for the drift tests, two baseline tests were run with the gyro mounted onto the table top but with no motion applied. In one test the table top was locked down by its mechanical brake and in the other the brake was released and the table top held in place by the table servo loop.

4.4.2 Output Axis Sensitivity Test Results

The results of the Output Axis Sensitivity Test are presented in Appendix G. Temperature and wheel supply parameters were not monitored during this test. Therefore, only the gyro data and table rate information are presented.

5. SUMMARY OF RESULTS

The test environment and test procedures were adequate for testing the gyros. The shorted filter tests revealed that the noise level of the data acquisition system was well below the output noise level of the gyros below .1 Hz. The wheel off test confirmed that there was essentially little difference between the gyro torquer loop noise and noise created by the data acquisition equipment. Induced rates from pad motion also proved to be much smaller than the measured noise level of the gyros below .01 Hz.

Both gyros were found to be sensitive to temperature variations in the low frequency region of the twenty-four hour tests. Therefore, the best gyro performance figures in the low frequency spectrum are obtained from the twenty-four hour test #2 of gyro S/N #1 which had the best temperature stability; and from the temperature compensated example shown in the first twenty-four hour test of the same gyro. Using the PSD plots of these two best twenty-four hour tests, the PSD of the one hour test, and the PSD of the three minute test, gyro performance can be summarized as follows: At the six hour point of interest (4.6×10^{-5} Hz) the PSD has a value of approximately .0006 $(deg/hr)^2/Hz$. From the six hour point, the gyro noise output rolls off at about 10 to 12 db/decade as frequency increases except for several power peaks between .0004 and .002 Hz caused in part by wheel current variations.

The mid frequency range in the twenty-four hour tests of both gyros was sensitive to wheel current variations. This sensitivity to wheel current variations was shown more dramatically in the PSD of Gyro S/N 1 where the basic frequency of the variations was approximately twice that seen in the Gyro S/N 2 data.

Some unexplained spikes were also displayed in the mid frequency range of the Gyro S/N 1 twenty-four hour PSD plot. These spikes may have been evidence of an impending gyro failure and caused by degradation in the gyro. Gyro S/N 1 did fail shortly after this series of drift tests, and the observed behavior was not seen in the Gyro S/N 2 data. However, additional tests on the repaired Gyro S/N 1 would be required to support this hypothesis.

A summary of the variances of the gyro output noise from each test is presented in Table VII. An entry in Table VII exists for each test. The value in the table is the variance of the data after the mean and slope were removed.

TABLE VII

VARIANCE $(DEG/HR)^2$ OF GYRO DATA

	TEST	VARIANCE
GYRO S/N 1	24 Hour #1	2.956×10^{-6}
	24 Hour #2	3.365×10^{-6}
	24 Hour #3	3.125×10^{-6}
	1 Hour	2.688×10^{-6}
	3 Min	$.1745 \times 10^{-6}$
GYRO S/N 2	24 Hour #1	$.8811 \times 10^{-6}$
	24 Hour #2	$.9759 \times 10^{-6}$
	1 Hour	$.9720 \times 10^{-6}$
	3 Min	1.433×10^{-6}

APPENDIX A

TEST HISTORY

30 September 1975	Gyros S/N 1 and S/N 2 delivered to CIGTF by Bendix representative.
9 October 1975	Eight point tests and scale factor test completed on S/N 1.
21 October 1975	Mounted gyro to drift fixture.
30 October 1975	Completed preparations for drift tests.
3 November 1975	Discovered 21 minute cycling of wheel current at .5 MA p-p which was causing variations in gyro data at .005 °/hr p-p. Resistive load tests eliminated the wheel supply as the source of the cycling and removal of the current and voltage monitor units eliminated the possibility of circuit loadings. Changing the wheel run voltage did not eliminate the variations nor did de-synchronizing the wheel speed.
1 December 1975	Concluded that wheel current cycling was characteristic of gyro and began drift testing.
12 December 1975	Completed drift testing on S/N 1 and began wheel off tests. Servo loop saturated during the test and it was suspected that the gyro float was not fully suspended. (Bendix later determined that the suspension fluid had leaked and refilling the gyro restored normal operation.)

16 December 1975	Wheel off tests resumed using S/N 2.
17 December 1975	Completion of wheel off tests.
8 January 1976	Began developing techniques for OA sensitivity testing of S/N 2.
16 January 1976	Began one hour drift tests on S/N 2 for baseline prior to OA sensitivity test. Made use of a weekend to run two 24 hour drift tests.
19 January 1976	Began OA sensitivity tests on S/N 2.
20 January 1976	Completed OA sensitivity tests.
22 January 1976	Ran scale factor test on S/N 2. Returned instruments and equipment to Bendix representatives.

WHEEL RUN LOG

LDG 540 S/N 1

TABLE A-I

WHEEL ON			WHEEL OFF			TIME	
DATE	TIME	RUN UP TIME SEC	DATE	TIME	RUN DN TIME SEC	RUN TIME	TOTAL RUN TIME
1-10-75	0800	--	1-10-75	1540	105	7 hrs 40 min	7 hrs 40 min
2-10-75	0930	--	2-10-75	1115	--	1 hr 45 min	9 hrs 25 min
7-10-75	0950	15	7-10-75	1009	105	19 min	9 hrs 44 min
7-10-75	1015	18	7-10-75	1430	115	4 hrs 15 min	13 hrs 59 min
8-10-75	0840	16	8-10-75	1355	105	5 hrs 15 min	19 hrs 14 min
9-10-75	0820	16	9-10-75	1530	110	7 hrs 10 min	26 hrs 24 min
10-10-75	0915	18	10-10-75	1400	108	4 hrs 45 min	31 hrs 09 min
23-10-75	1005	16	23-10-75	1010	115	5 min	31 hrs 14 min
23-10-75	1015	18	23-10-75	1600	115	5 hrs 45 min	36 hrs 59 min
24-10-75	0820	16	24-10-75	1010	120	1 hr 50 min	38 hrs 49 min
24-10-75	1230	18	28-10-75	1045	110	94 hrs 15 min	133 hrs 04 min
28-10-75	1055	17	30-10-75	1506	100	52 hrs 11 min	185 hrs 15 min
30-10-75	1603	18	3-11-75	1035	110	90 hrs 32 min	275 hrs 47 min
3-11-75	1300	18	7-11-75	0920	110	92 hrs 20 min	368 hrs 07 min
10-11-75	1000	--	18-11-75	1230	110	194 hrs 30 min	562 hrs 32 min
18-11-75	1235	18	19-11-75	0755	110	19 hrs 20 min	581 hrs 51 min
19-11-75	1102	18	26-11-75	1245	105	169 hrs 43 min	751 hrs 40 min
26-11-75	1334	18	12-12-75	1325	105	383 hrs 51 min	1135 hrs 31 min

WHEEL RUN LOG

LDG 540 S/N 2

TABLE A-II

WHEEL ON			WHEEL OFF			TIME	
DATE	TIME	RUN UP TIME (SEC)	DATE	TIME	RUN DOWN TIME (SEC)	RUN TIME	TOTAL RUN TIME
7-11-75	0955	18	7-11-75	1504	87	5 hrs 09 min	5 hrs 09 min
7-01-76	1410	18	7-01-76	1415	--	05 min	5 hrs 14 min
7-01-76	1428	18	10-01-76	1455	110	72 hrs 27 min	77 hrs 41 min
10-01-76	1535	18	15-01-76	0835	--	113 hrs	190 hrs 41 min
15-01-76	0945	18	15-01-76	1233	100	2 hrs 48 min	193 hrs 29 min
15-01-76	1250	18	16-01-76	1320	80	24 hrs 30 min	217 hrs 59 min
16-01-76	1335	18	19-01-76	1210	100	70 hrs 35 min	288 hrs 34 min
19-01-76	1310	18	22-01-76	1430	85	73 hrs 20 min	362 hrs 54 min

APPENDIX B

GYRO MODEL

Using the input axis performance model for a single degree of freedom (SDF) gyro described in Reference 2 as a guide, the following performance model is assumed:

$$SV = D_F + D_I a_I + D_O a_O + D_S a_S + D_{II} a_I^2 + D_{SS} a_S^2$$

$$+ D_{IO} a_I a_O + D_{IS} a_I a_S + D_{OS} a_O a_S + \omega_I$$

where

V	Gyro torquer output (volts)
S	Gyro axis torquer scale factor (°/hr/volt)
D	Gyro drift coefficient
a_I	Acceleration, with respect to inertial space, of the gyro case along the input axis (g)
a_O	Acceleration, with respect to inertial space, of the gyro case along the output axis (g)
a_S	Acceleration, with respect to inertial space, of the gyro case along the spin axis (g)
ω_I	Angular velocity, with respect to inertial space, of the gyro case about the input axis (°/hr)

The eight point tests were conducted to insure that the gyro being tested was representative of its type. Accurate determination of the drift coefficients was not considered to be one of the test objectives. Therefore the following assumptions were made.

1. Errors in test table positioning were negligible.
2. The input and spin axes of the gyro were orthogonal.
3. Small angle approximations (i.e, $\sin\phi = \phi$ and $\cos\phi = 1$) were made on the input axes misalignment with the cardinal headings.

Using the assumed performance model, and starting as shown in Figure B-1 with the test table axis local vertical, the input axis north, spin axis east, output axis up, and with a small misalignment angle ϕ, rotation through the four cardinal headings produces the following equations:

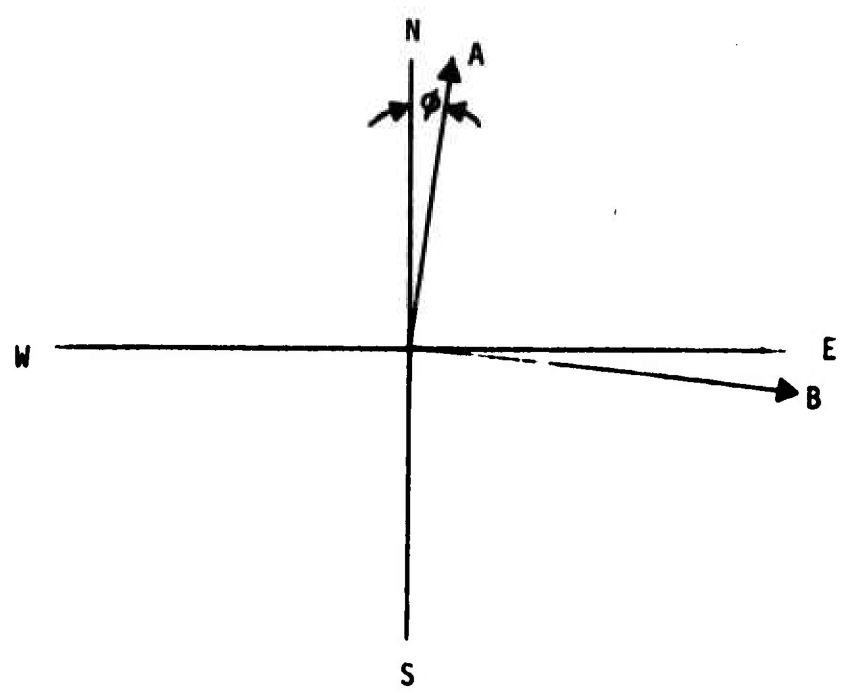

FIGURE B-1

1. $S \quad V_N = D_F + D_0 + E_H \cos\phi$

2. $S \quad V_E = D_F + D_0 - E_H \sin\phi$

3. $S \quad V_S = D_F + D_0 - E_H \cos\phi$

4. $S \quad V_W = D_F + D_0 + E_H \sin\phi$

Rotating 90° to table axis horizontal (OA to the north) then repeating the above process produces four more equations:

5. $S \quad V_U = D_F + D_I \cos\phi - D_S \sin\phi + D_{II} \sin^2\phi + D_{SS} \sin^2\phi$

$$- D_{IS} \sin\phi \cos\phi + E_V \cos\phi$$

6. $S \quad V_W = D_F - D_I \sin\phi - D_S \sin\phi + D_{II} \sin^2\phi + D_{SS} \cos^2\phi$

$$+ D_{IS} \sin\phi \cos\phi - E_V \sin\phi$$

7. $S \quad V_D = D_F - D_I \cos\phi + D_S \sin\phi + D_{II} \sin^2\phi + D_{SS} \sin^2\phi$

$$- D_{IS} \sin\phi \cos\phi - E_V \cos\phi$$

8. $S \quad V_E = D_F + D_I \sin\phi + D_S \cos\phi + D_{II} \sin^2\phi + D_{SS} \cos^2\phi$

$$+ D_{IS} \sin\phi \cos\phi + E_V \sin\phi$$

where:

E_H = The horizontal component of earth rate at the test site latitude = 12.595672°/hr

E_V = The vertical component of earth rate at the test site latitude = 8.14556175°/hr

from equations 1 - 4 we get:

$$S = 2 E_H/(V_N - V_S)$$

$$\phi = (V_W - V_E)/(V_N - V_S)$$

$$D_F + D_O = S (V_N + V_E + V_S + V_W)/4$$

and equations 5 - 8 yield the following:

* $D_I = S [V_U - V_D + \phi(V_E - V_W)]/2 - E_V$

* $D_S = S [V_E - V_W - \phi(V_U - V_D)]/2$

** $D_F + D_{SS} = S (V_W + V_E)/2$

** $D_F + D_{II} = S (V_U + V_D)/2$

* Note that $(\phi^2 + 1)$ is equivalent to $(\sin^2 + \cos^2) = 1$ since small angle assumptions were made.

** The equations also yield a ϕ^2 term and a $\phi\ D_{IS}$ term. Both ϕ and the cross axis term, D_{IS} are assumed small, so they are dropped.

APPENDIX C

PLOT FORMATS

In order to understand the information contained in the plots, Figures C-1 and C-2 have been highlighted with descriptions of the various axes, scale factors and other data.

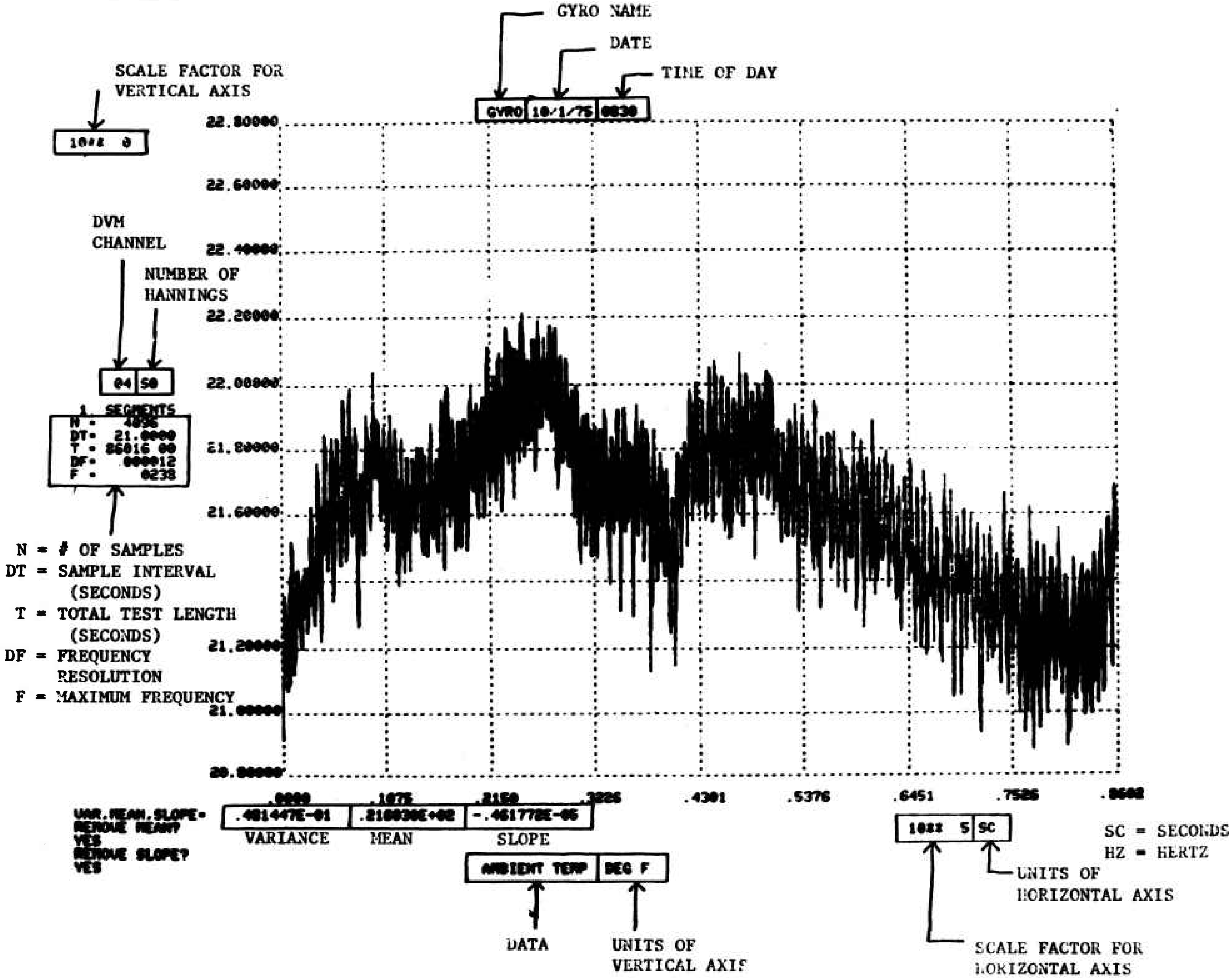
GYRO NAME
DATE
TIME OF DAY
SCALE FACTOR FOR VERTICAL AXIS
10** 0
GYRO
10/1/75
0830
22.80000
22.60000
22.40000
22.20000
22.00000
21.80000
21.60000
21.20000
21.00000
20.80000
DVM CHANNEL
NUMBER OF HANNINGS
04
50
1 SEGMENTS
N = 4096
DT = 21.0000
T = 86016 00
DF = 000012
F = 0238
N = # OF SAMPLES
DT = SAMPLE INTERVAL (SECONDS)
T = TOTAL TEST LENGTH (SECONDS)
DF = FREQUENCY RESOLUTION
F = MAXIMUM FREQUENCY
.0000
.1075
.2150
.3226
.4301
.5376
.6451
.7526
.8602
VAR.MEAN.SLOPE=
REMOVE MEAN?
YES
REMOVE SLOPE?
YES
.481447E-01
.218030E+02
-.461778E-05
VARIANCE
MEAN
SLOPE
AMBIENT TEMP
DEG F
DATA
UNITS OF VERTICAL AXIS
10** 5
SC
SC = SECONDS
HZ = HERTZ
UNITS OF HORIZONTAL AXIS
SCALE FACTOR FOR HORIZONTAL AXIS

FIGURE C-1

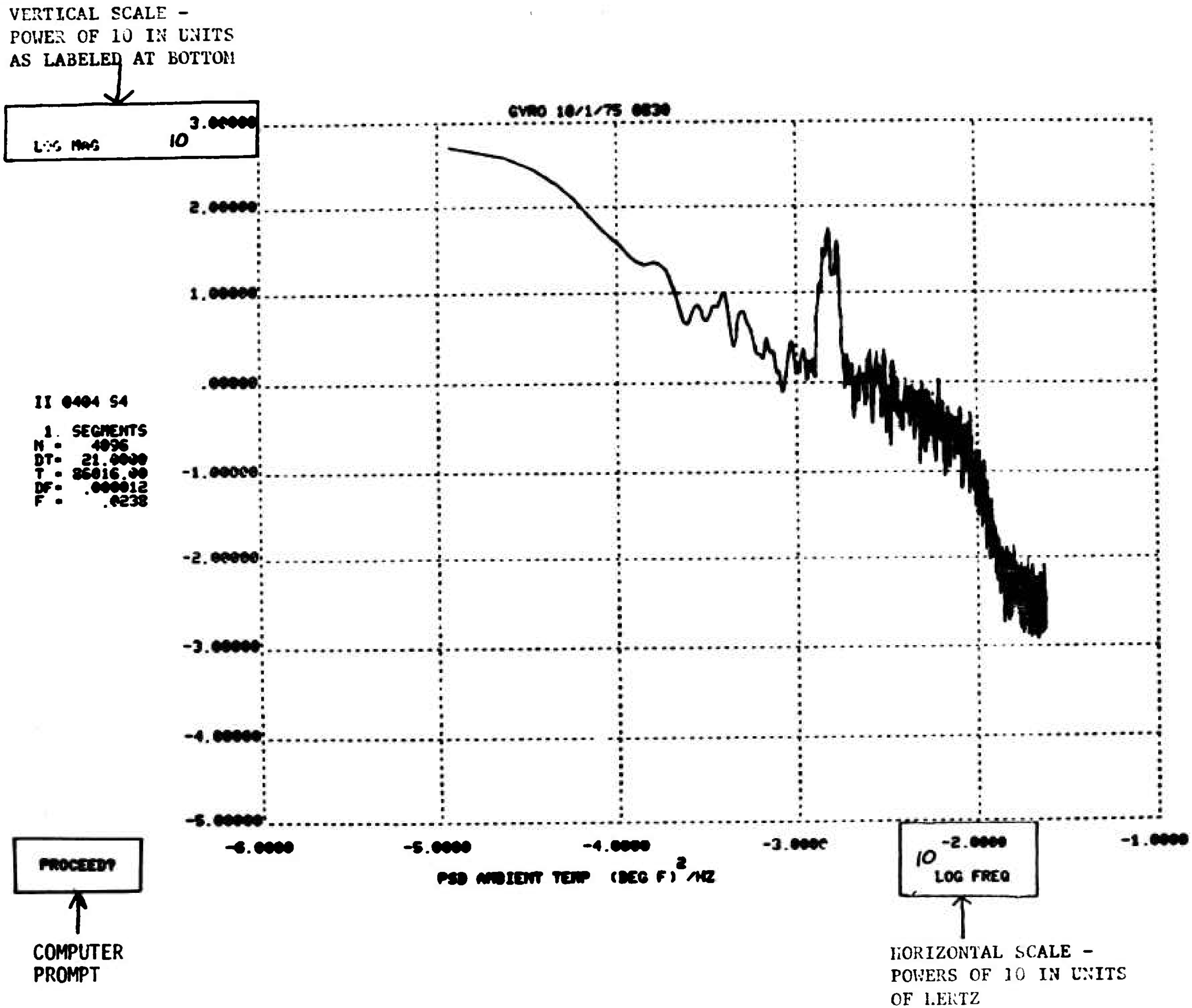
VERTICAL SCALE -
POWER OF 10 IN UNITS
AS LABELED AT BOTTOM
LOG MAG 10
GYRO 10/1/75 0830
3.00000
2.00000
1.00000
.00000
-1.00000
-2.00000
-3.00000
-4.00000
-5.00000
II 0404 S4
1. SEGMENTS
N = 4096
DT= 21.0000
T = 86016.00
DF= .000012
F = .0238
-6.0000
-5.0000
-4.0000
-3.000C
-2.0000
-1.0000
10 LOG FREQ
PSD AMBIENT TEMP (DEG F)2/HZ
PROCEED?
COMPUTER
PROMPT
HORIZONTAL SCALE -
POWERS OF 10 IN UNITS
OF HERTZ

FIGURE C-2

APPENDIX D

GYRO DRIFT TESTS

24 HOUR TEST #1, GYRO S/N 1

The twenty-four hour test #1 results for Gyro S/N 1 are shown in Figure D-1 through Figure D-16. Figure D-1 is the raw time domain gyro data. Figure D-2 is the average tilt obtained by averaging the data obtained from the three tiltmeters monitoring pad motion. The average tilt is then differentiated, as discussed in paragraph 3.4, to obtain the tilt rate which is presented in Figure D-3.

A plot of ambient temperature is shown in Figure D-4. Both the gyro data, Figure D-1, and the tilt data, Figure D-2, appear to be strongly influenced by the ambient temperature. Note that the peak-to-peak amplitude of the change in temperature is about 1.5 degrees. The gyro case temperature, Figure D-5, also follows the changes in ambient temperature, Figure D-4. However, since the peak-to-peak change in case temperature is only approximately .1 degree, the temperature isolation provided by the styrofoam shroud is apparent. Figures D-6 and D-7 respectively show the monitored gyro wheel voltage, and the gyro wheel current.

The unsmoothed PSD of the gyro data is presented in Figure D-8 for reference. Figure D-9 shows the gyro PSD smoothed by four iterations of Hanning as discussed in paragraph 3.4. All other PSD plots presented have the same smoothing applied as the gyro data in Figure D-9. Note also that the gyro PSD has the gradual roll off of the cascaded filter while the environmental PSD's have the sharp knee of the 8-pole Butterworth filter. Figure D-10 is a PSD of the tilt rate. The power level shown in the tilt rate PSD is

well below that recorded in the gyro PSD. Therefore, the base motion of the test environment should have little effect on the gyro output. Figures D-11 and D-12 show the PSD of the ambient temperature and the PSD of the gyro case temperature. As would be expected from the earlier look at the time domain data, Figures D-4 and D-5, the PSD of the gyro case temperature is much lower than the PSD of the ambient temperature. Figures D-13 and D-14 respectively show the PSD of the gyro wheel voltage and current. The cause of the variations in wheel current is unknown. One theory suggests that wheel motor pole slippage could be responsible for the current variations.

The significance of recording channel noise on each recorded signal can be observed by comparing the PSD's produced by the test with the appropriately scaled shorted filter PSD in Appendix E. For the 24 hour test of gyro S/N #1 the gyro output, tilt rate, and ambient temperature are all well above the noise level shown in Appendix E. Gyro temperature rises significantly above the noise level at frequencies below .008 Hz. Wheel voltage and current both appear dominated by the noise level except for the large spikes in the mid frequency range of the wheel current PSD.

As mentioned above, the gyro data seems sensitive to temperature changes. Compensation of the gyro data for temperature was accomplished by appropriate scaling and shifting of the gyro case temperature data. The PSD generated by the temperature compensated gyro data showed an improvement in the low frequency noise level, but an increase in the noise level of the high frequency end. This indicated that the gyro was apparently not sensitive to the higher frequency components of temperature. Hence, the gyro case temperature data was transformed into the frequency domain, the high frequency components were removed, then a transformation

back to the time domain was made. These manipulations created temperature data with only its low frequency components, which were then subtracted from the gyro data. Figure D-15 shows the gyro data with the temperature removed in this manner. Figure D-16 shows the PSD of the gyro with temperature removed, and the improvement in the low frequency noise level can clearly be seen.

The gyro wheel current PSD, Figure D-13, shows a large peak at approximately .0008 Hz along with its first 4 or 5 harmonics. The gyro output PSD appears to be sensitive to the .0008 Hz wheel current variations and the first harmonic but insensitive to the higher harmonics.

Also of significance in the gyro PSD is a double power peak in the vicinity of .0004 to .0007 Hz, and another peak at approximately .0011 Hz. No apparent cause for these peaks could be determined. Reference 1 suggests that PSD data could possibly be used for early detection of degraded performance. The gyro did fail shortly after this series of tests were conducted, and the phenomenon was not seen in gyro S/N 2 data which will be shown later. However, a retest of gyro S/N 1 after repair would be required to positively support this hypothesis.

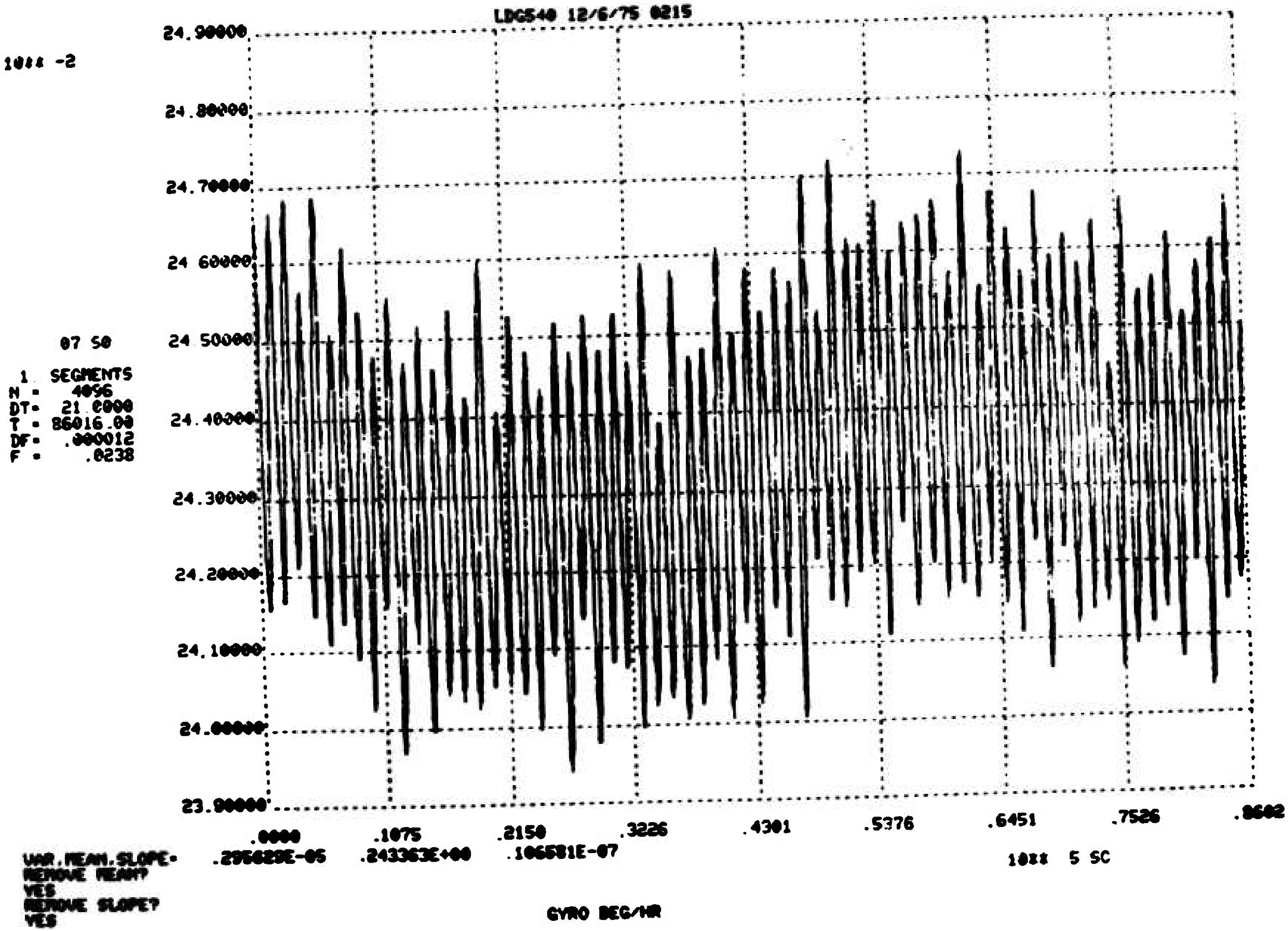

FIGURE D-1. S/N 1 GYRO DATA, DEGREE/HOUR (24 HOUR TEST #1)

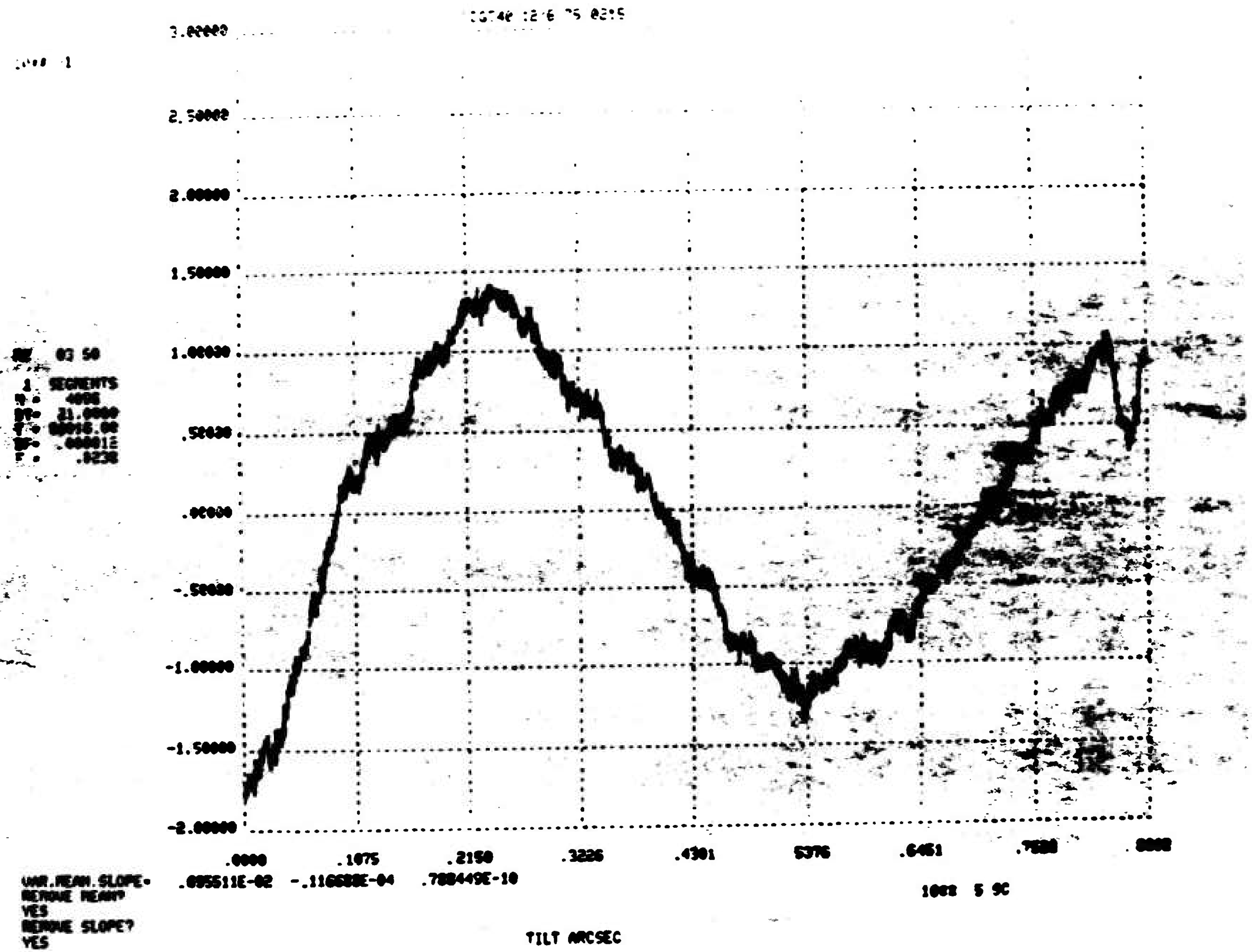

FIGURE D-2. AVERAGE TILT, ARC SECONDS (S/N 1 24 HOUR TEST #1)

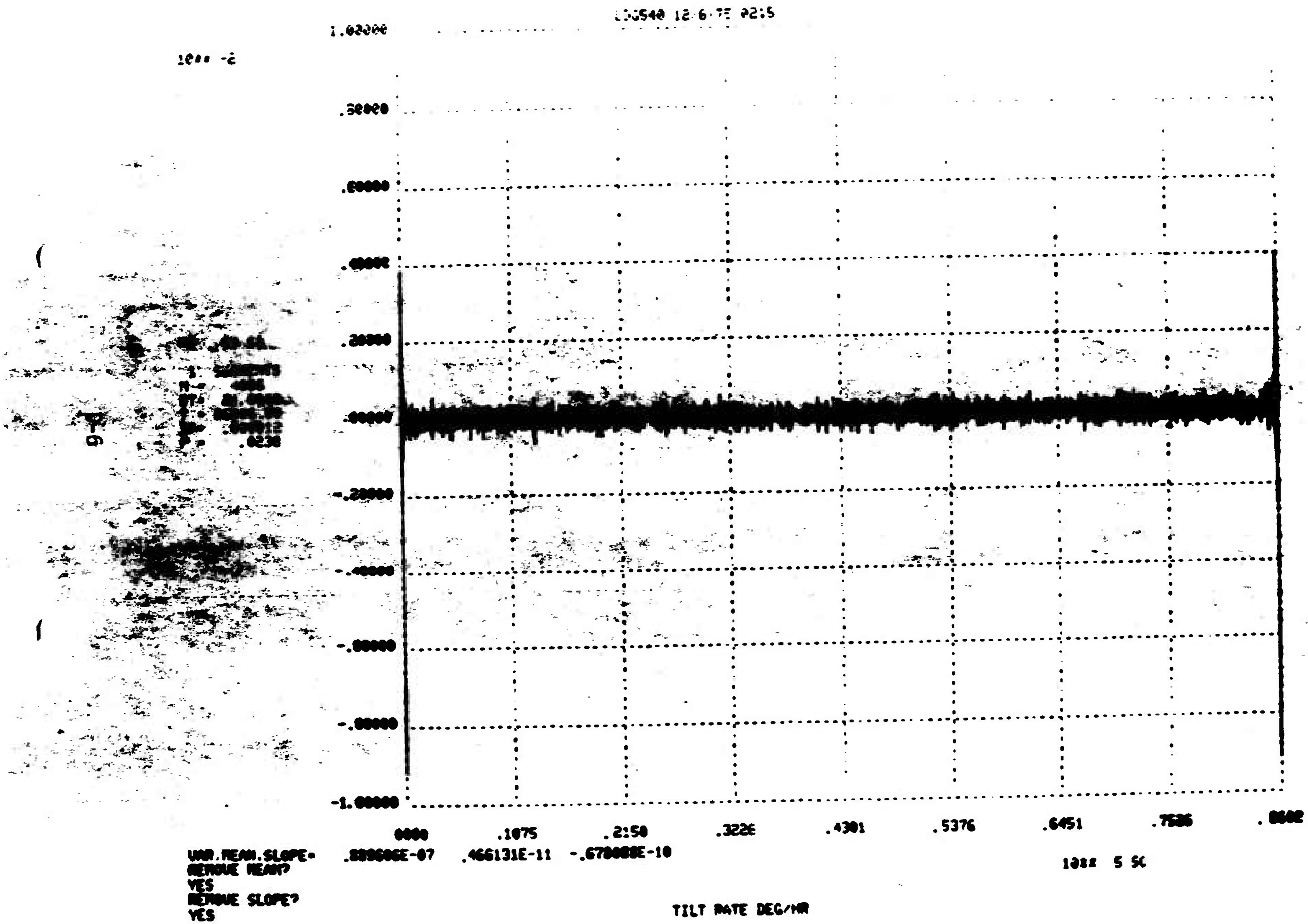

FIGURE D-3. TILT RATE, DEGREE/HOUR (S/N 1 24 HOUR TEST #1)

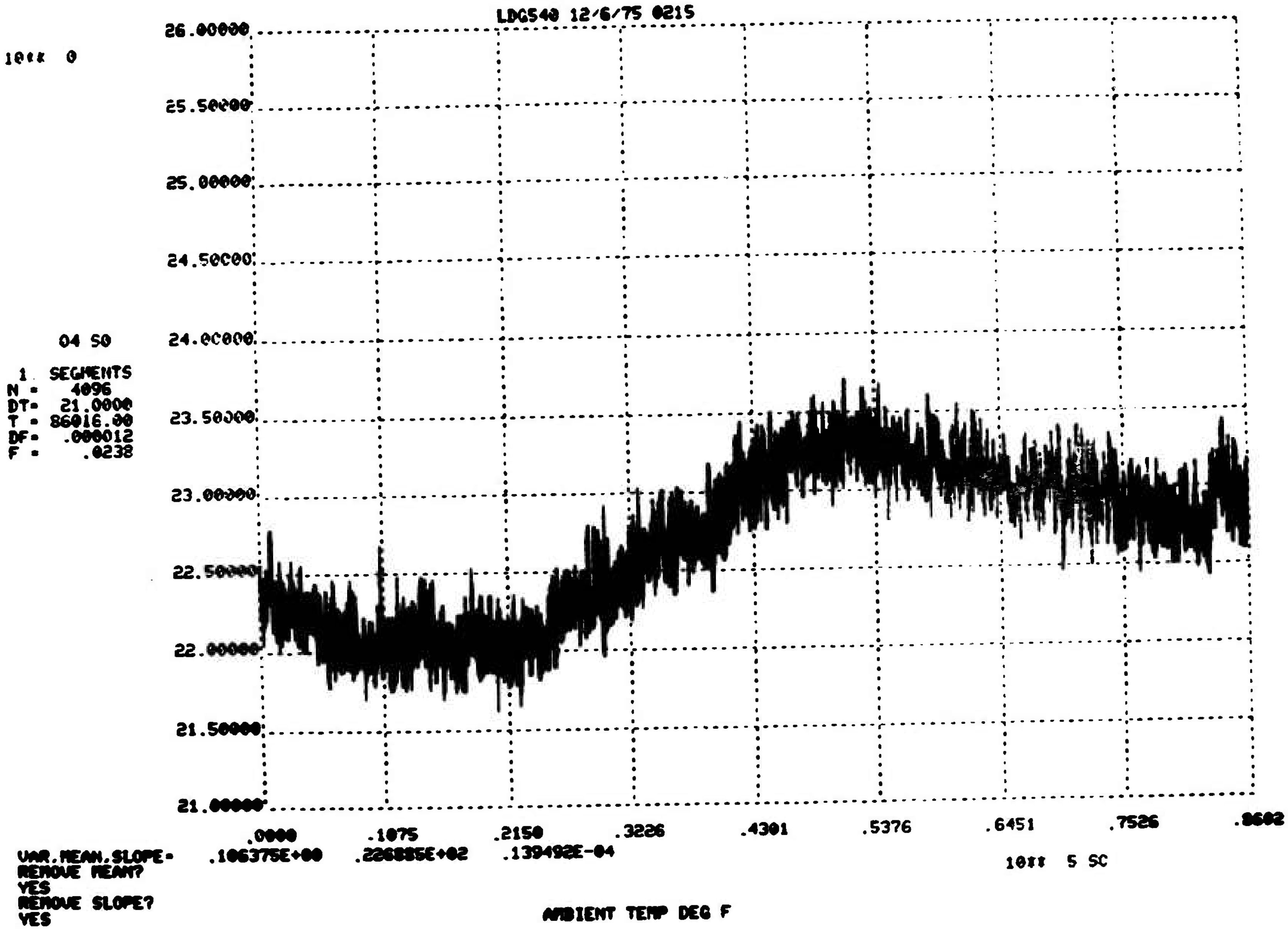

FIGURE D-4. AMBIENT TEMPERATURE, DEGREE F (S/N 1 24 HOUR TEST #1)

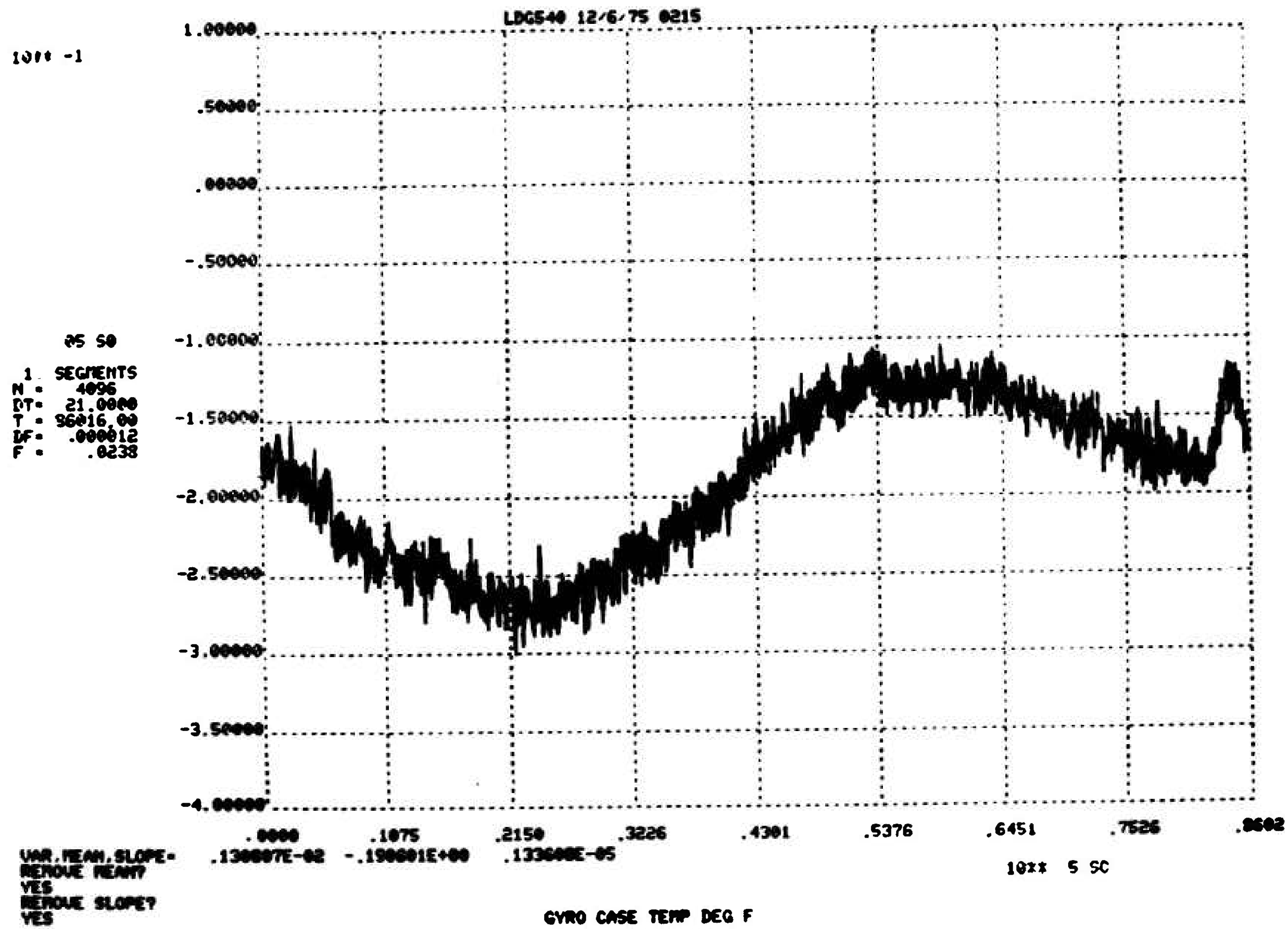

FIGURE D-5. S/N 1 GYRO CASE TEMPERATURE, DEGREE F (24 HOUR TEST #1)

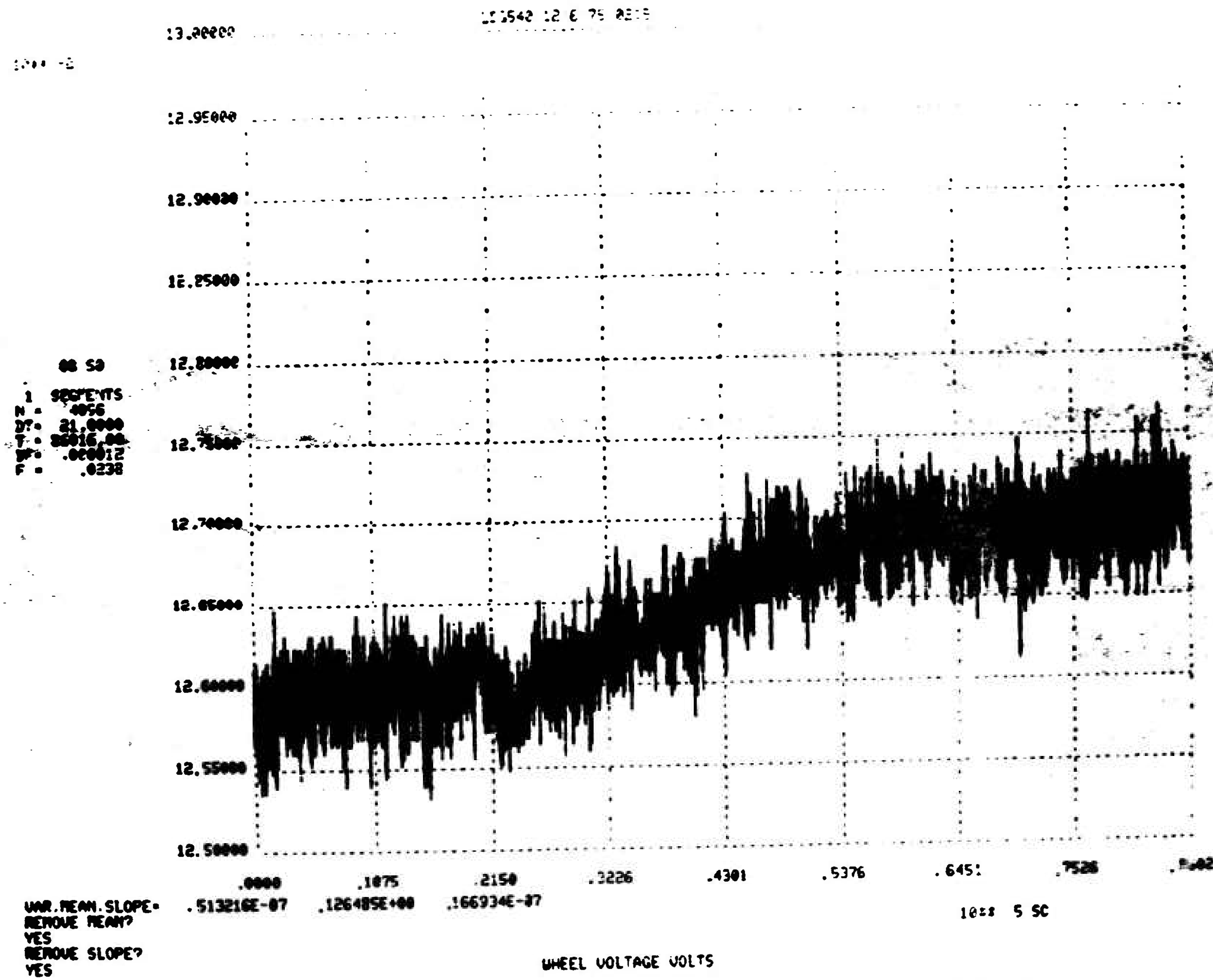

FIGURE D-6. S/N 1 GYRO WHEEL VOLTAGE, VOLTS (24 HOUR TEST #1)

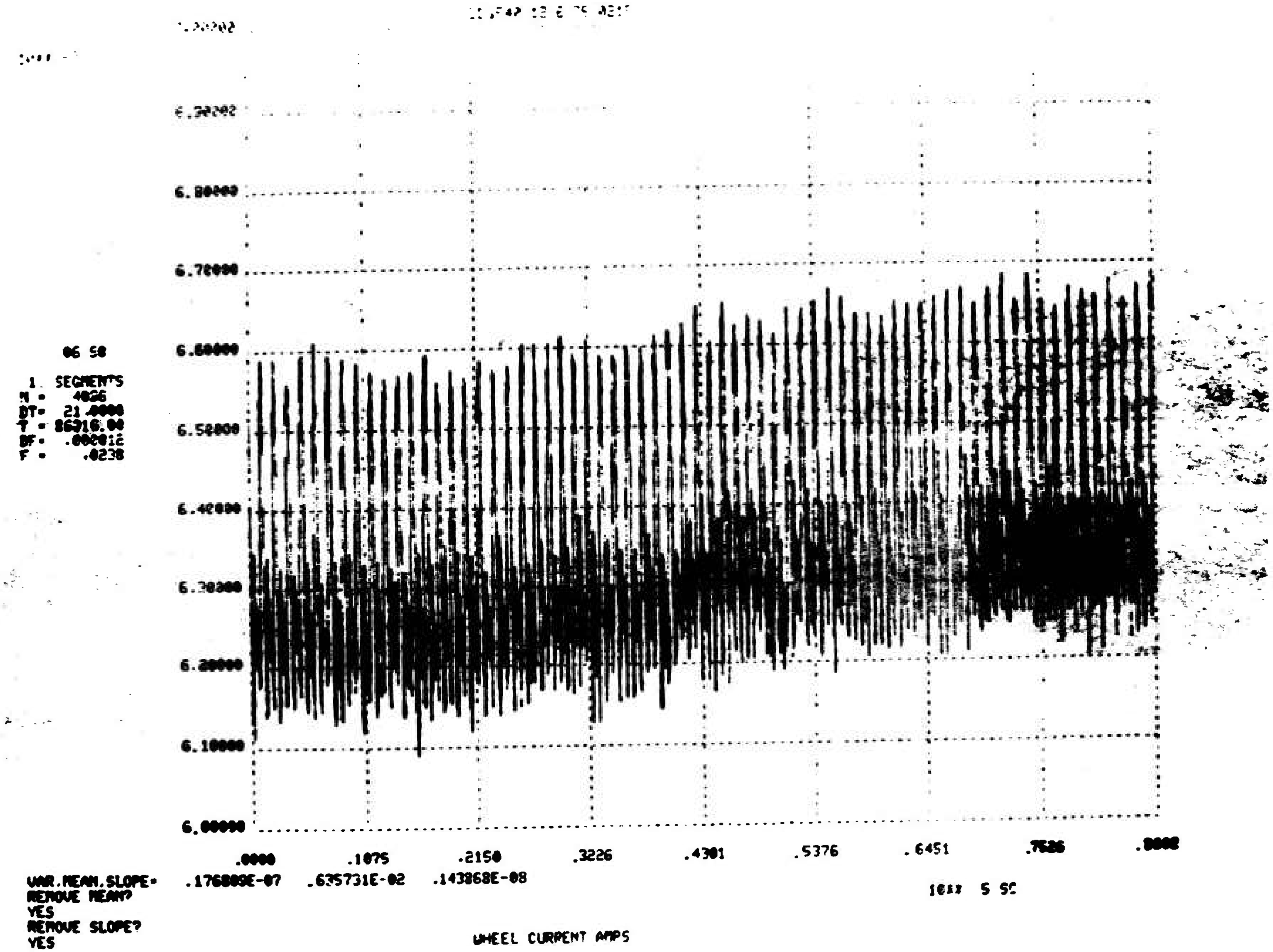

FIGURE D-7. S/N 1 GYRO WHEEL CURRENT, AMPS (24 HOUR TEST #1)

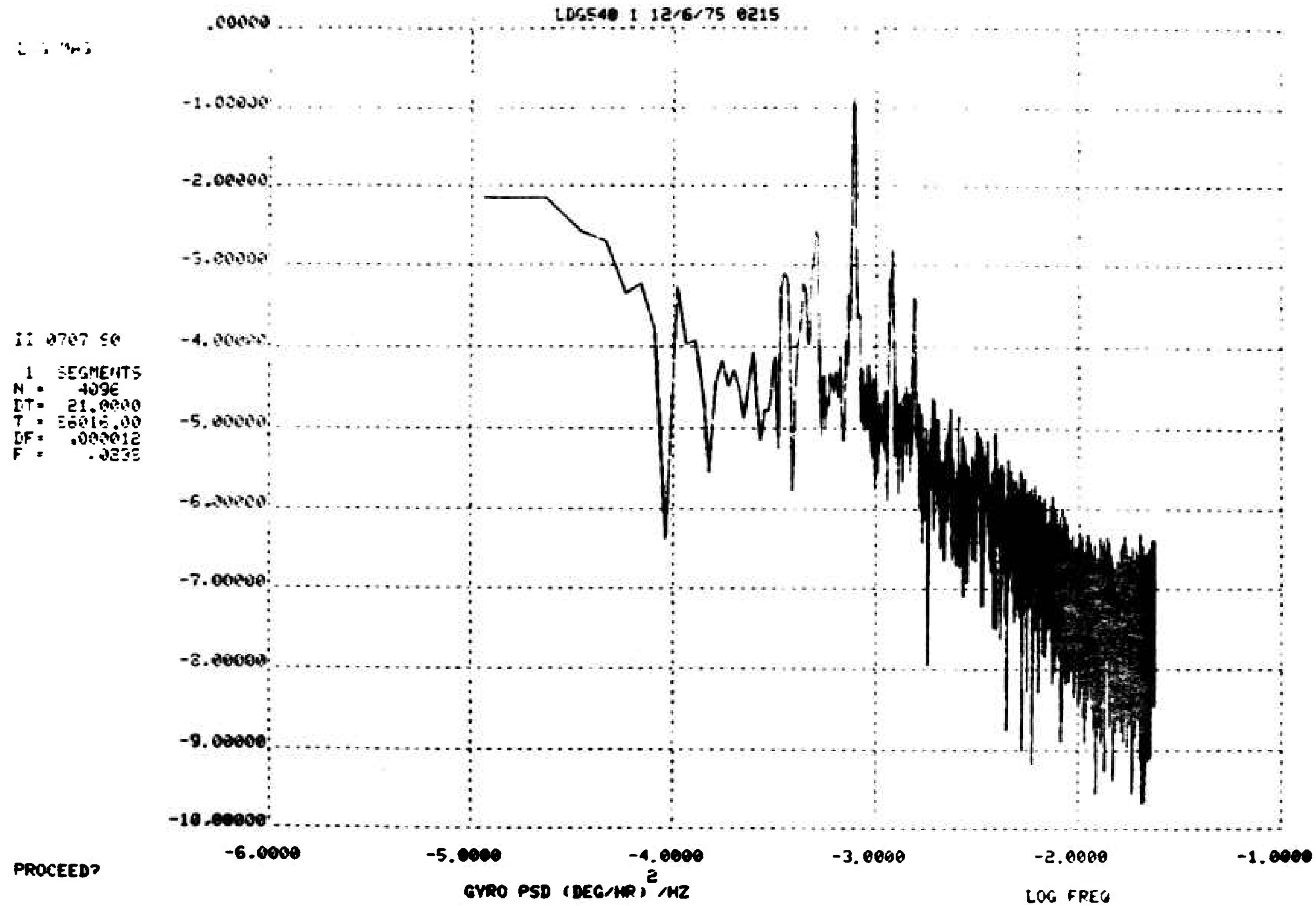

FIGURE D-8. UNSMOOTHED PSD S/N 1 GYRO DATA, (DEGREE/HOUR)^2/HZ (24 HOUR TEST #1)

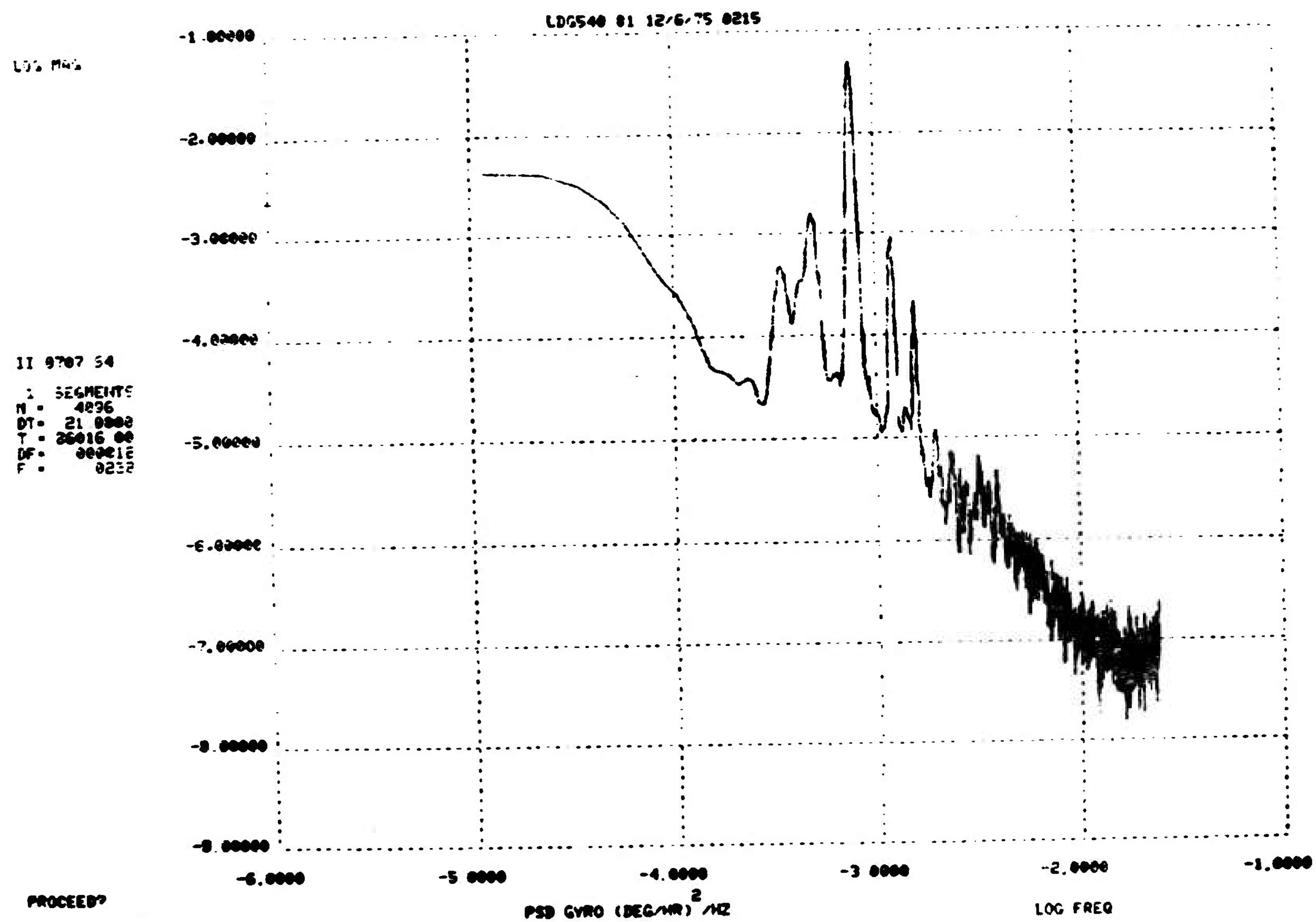

FIGURE D-9. SMOOTHED PSD S/N 1 GYRO DATA, (DEGREE/HOUR)^2/HZ (24 HOUR TEST #1)

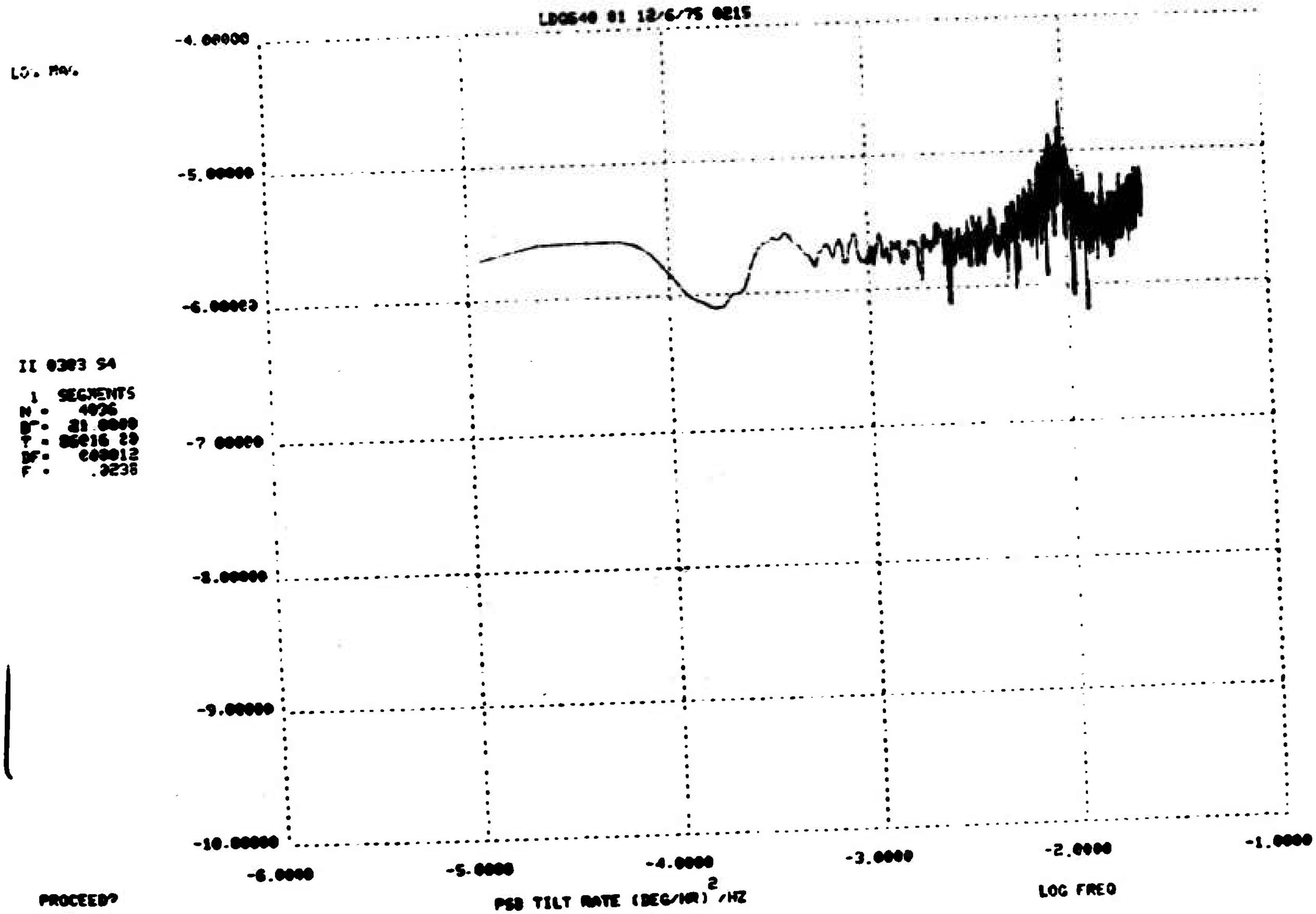

FIGURE D-10. PSD TILT RATE, (DEGREE/HOUR)^2/HZ (S/N 1 24 HOUR TEST #1)

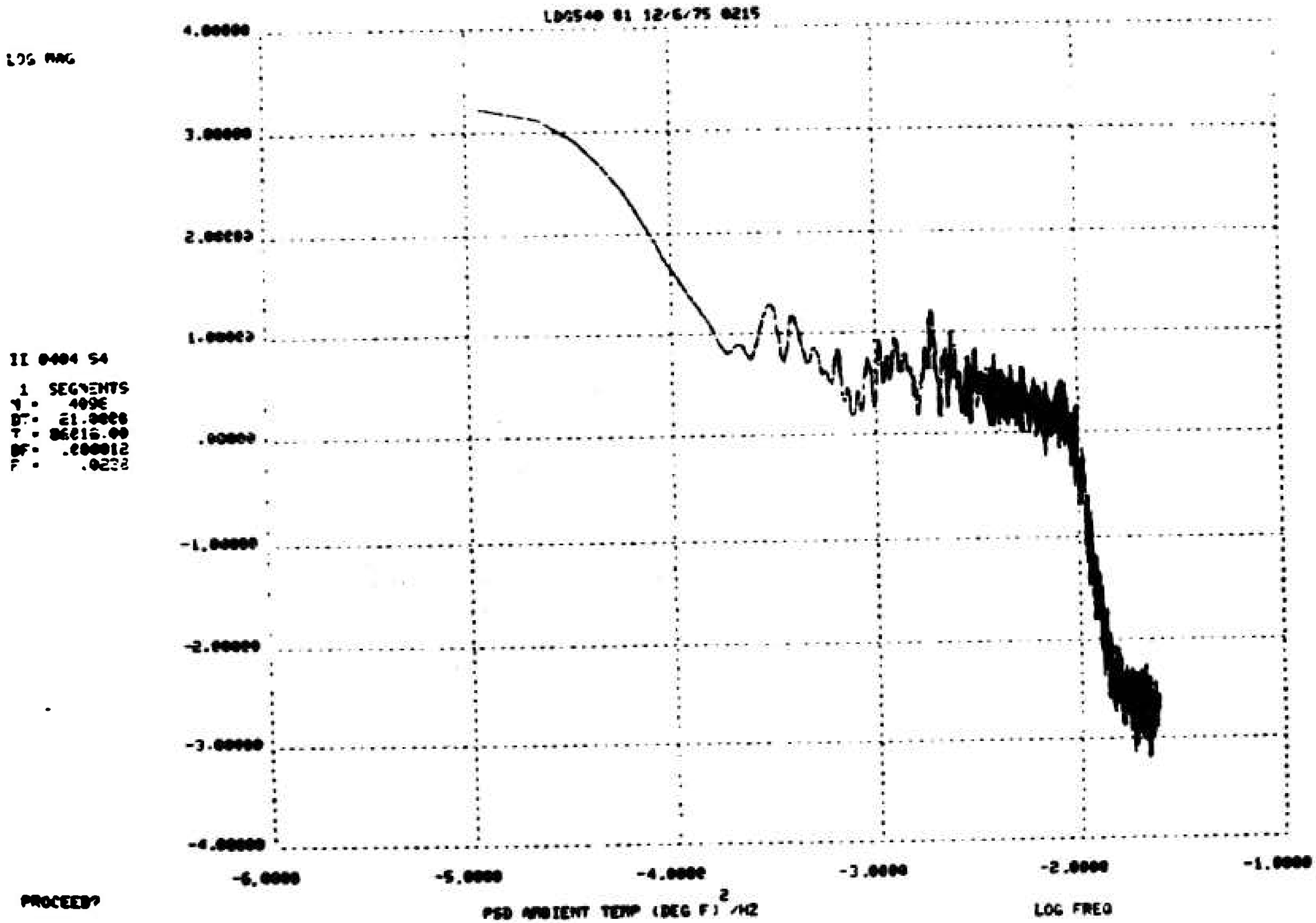

FIGURE D-11. PSD AMBIENT TEMPERATURE, (DEGREE F)^2/HZ (S/N 1 24 HOUR TEST #1)

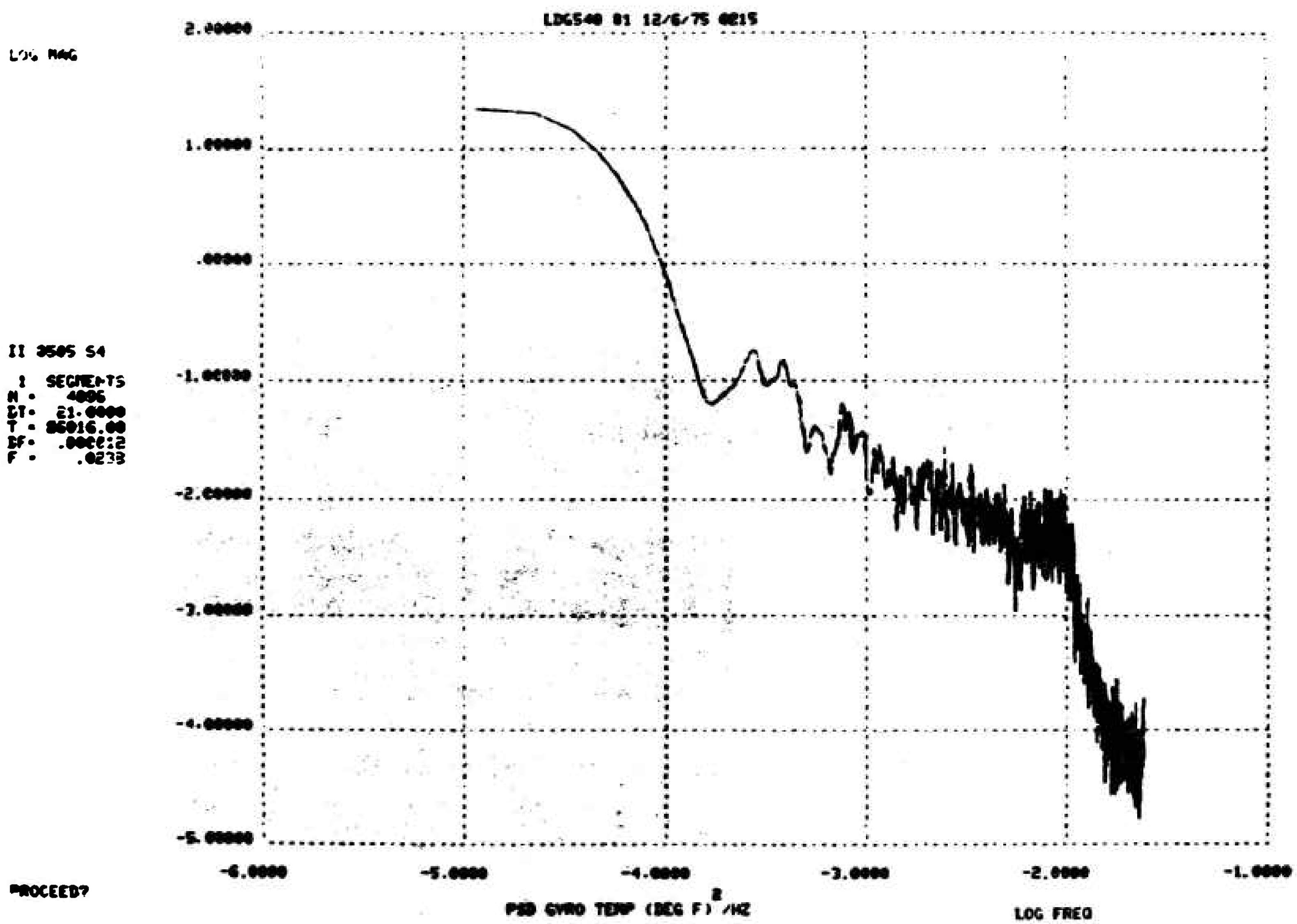

FIGURE D-12. PSD S/N 1 GYRO CASE TEMPERATURE, (DEGREE F)^2/HZ (24 HOUR TEST #1)

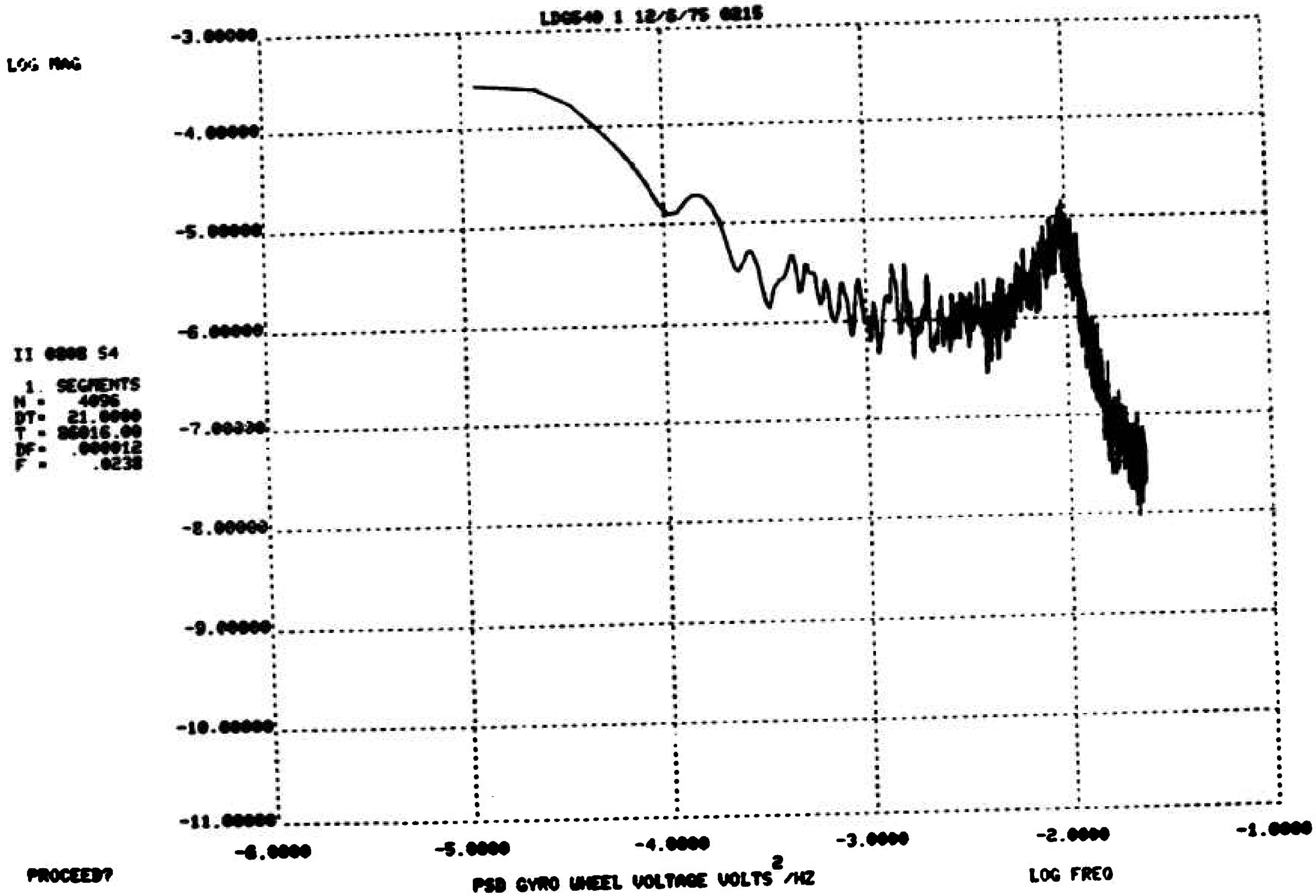

FIGURE D-13. PSD S/N 1 GYRO WHEEL VOLTAGE, $(VOLTS)^2/HZ$ (24 HOUR TEST #1)

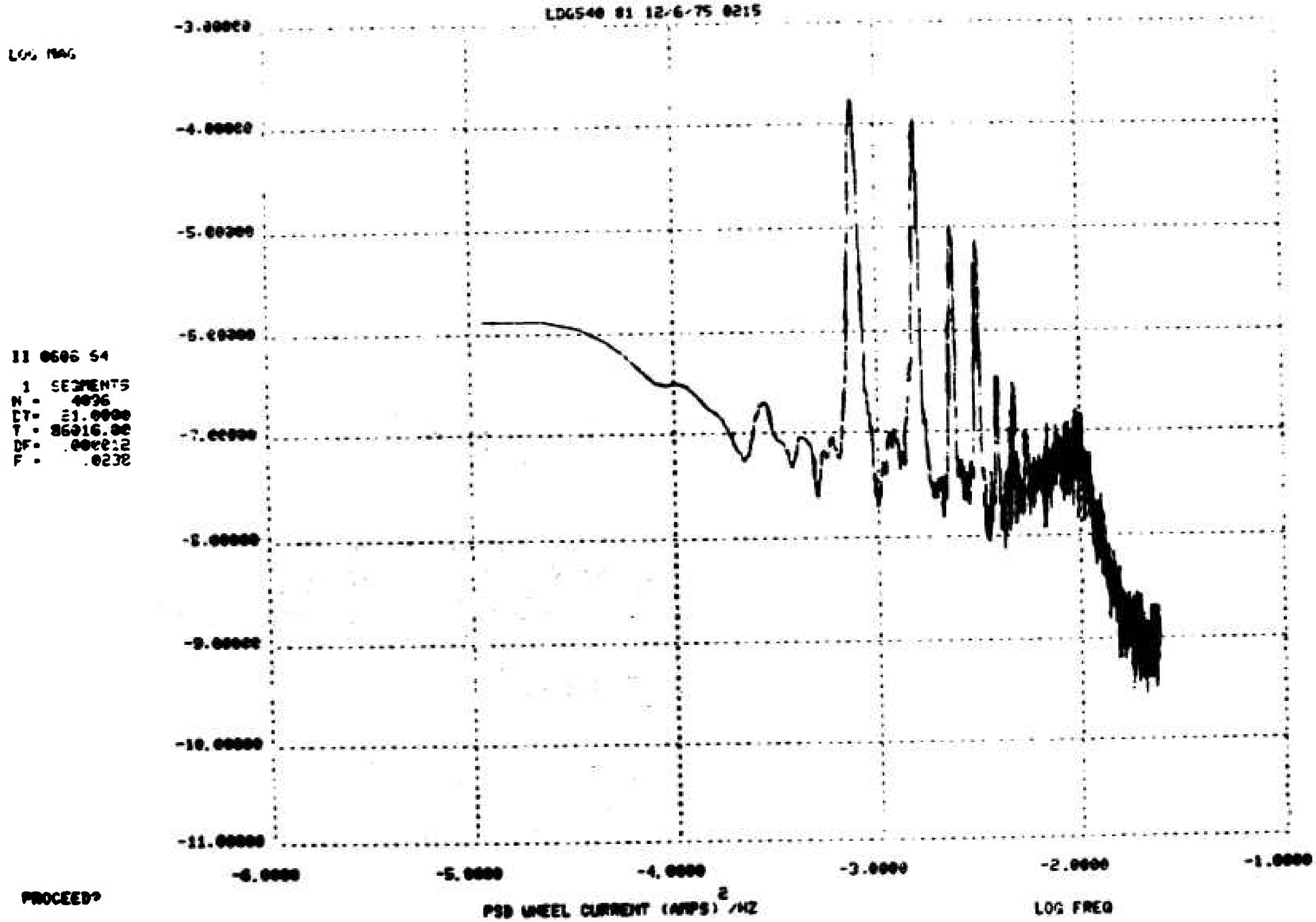

FIGURE D-14. S/N 1 PSD GYRO WHEEL CURRENT, (AMPS)^2/HZ (24 HOUR TEST #1)

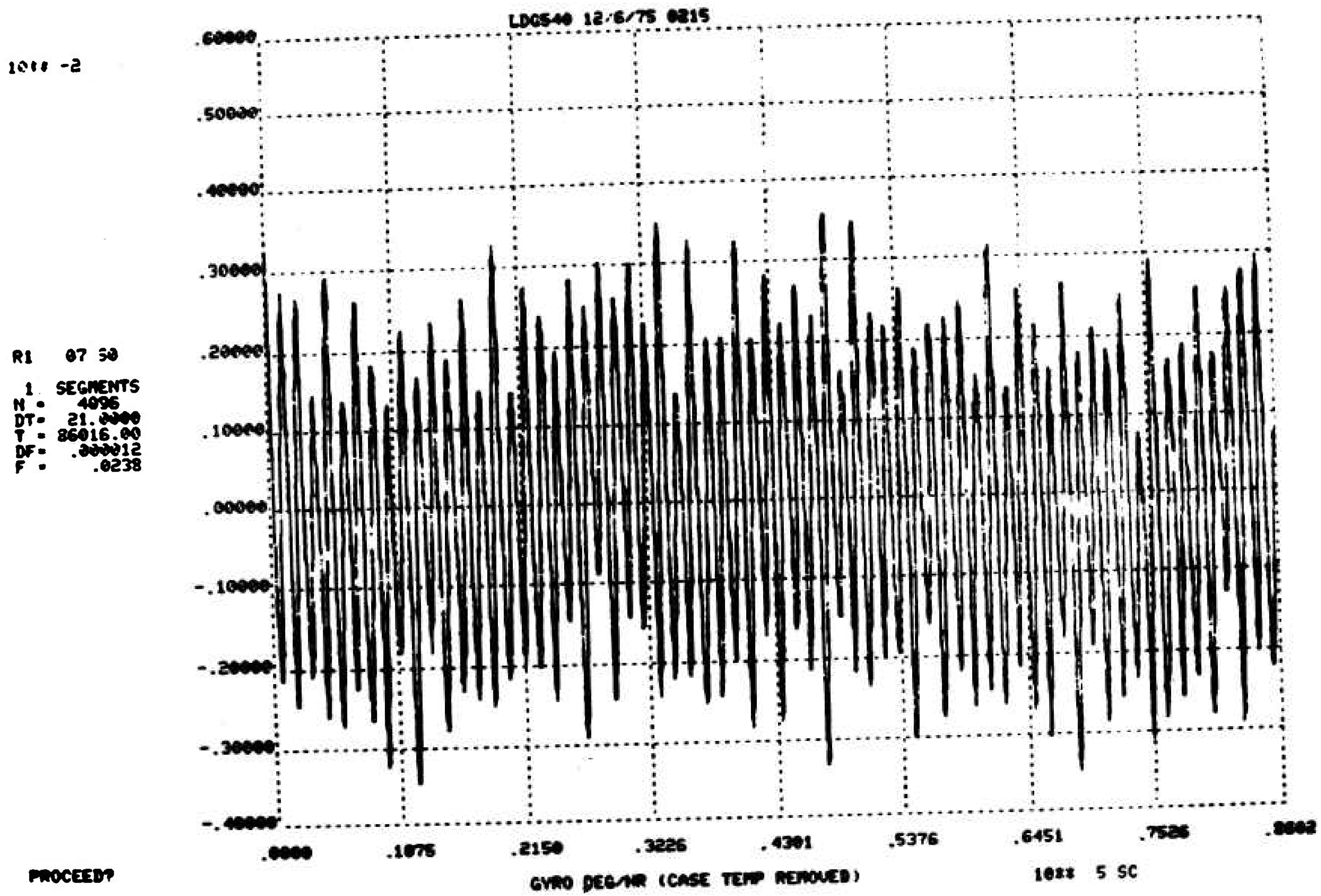

FIGURE D-15. S/N 1 GYRO DATA WITH TEMPERATURE REMOVED, DEGREE/HOUR (24 HOUR TEST #1)

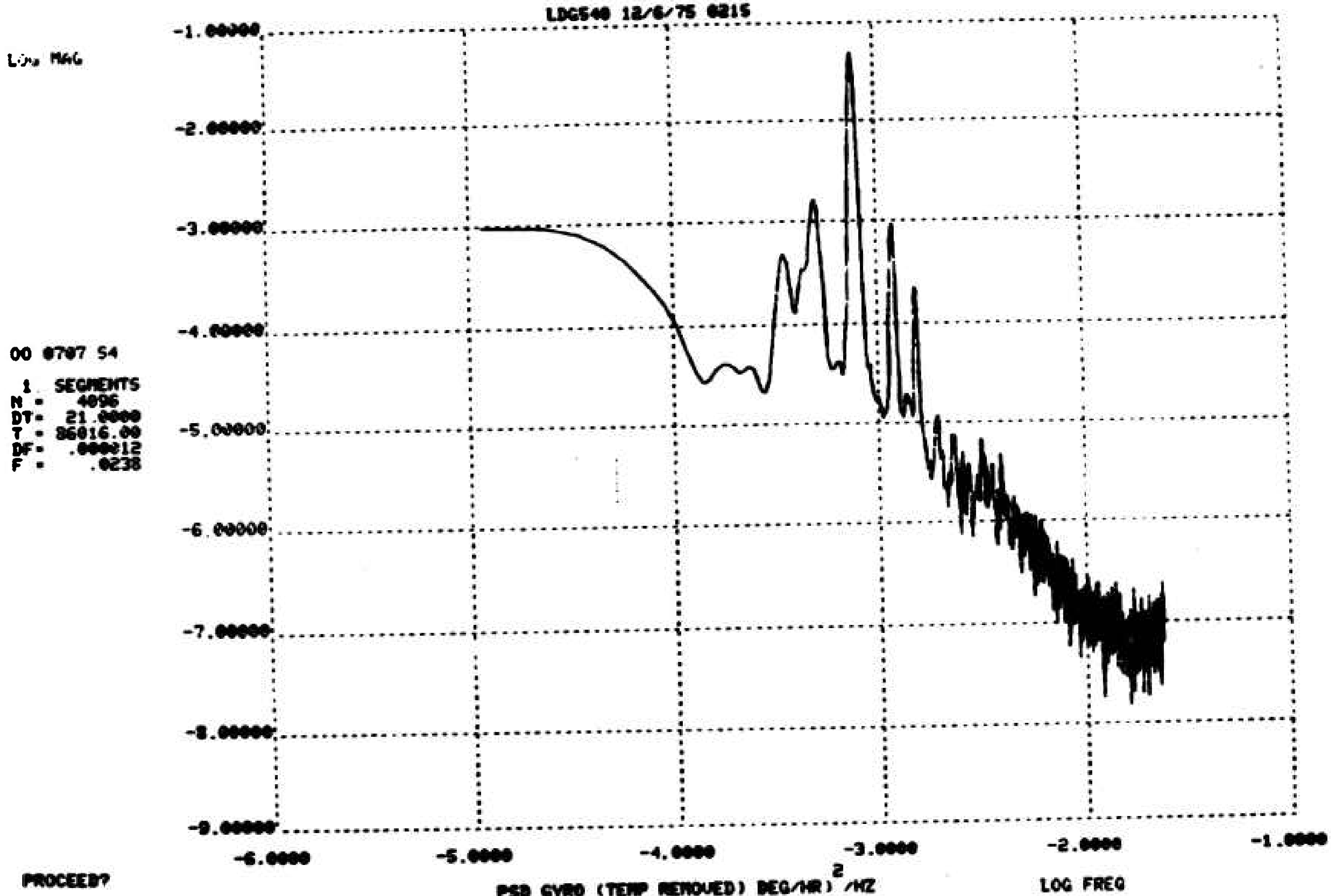

FIGURE D-16. PSD S/N 1 GYRO DATA WITH TEMPERATURE REMOVED, $(\text{DEGREE/HOUR})^2/\text{HZ}$ (24 HOUR TEST #1)

24 HOUR TEST #2 GYRO S/N 1

Gyro S/N #1, test results for twenty-four hour test #2 are shown in Figure D-17 through Figure D-28. The gyro wheel current plots are not present because wheel current was not monitored during this test. The PSD of the gyro, Figure D-23, has the quietest uncompensated low frequency response of all the tests conducted on the LDG 540 gyro series. Note that on this test the ambient temperature, Figure D-20, was very stable throughout the test with the obvious exceptions at the beginning and the end.

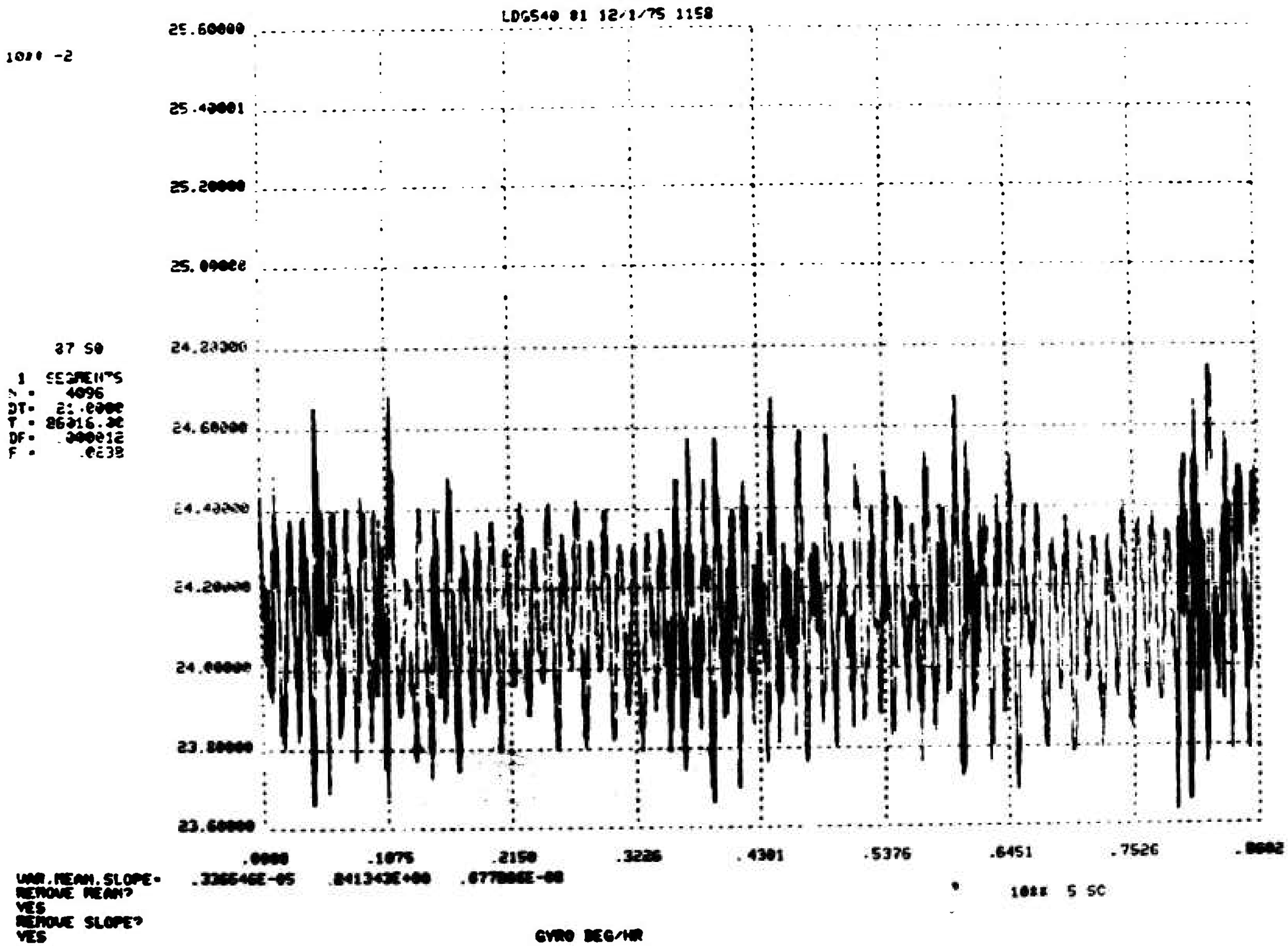

FIGURE D-17. S/N 1 GYRO DATA, DEGREE/HOUR (24 HOUR TEST #2)

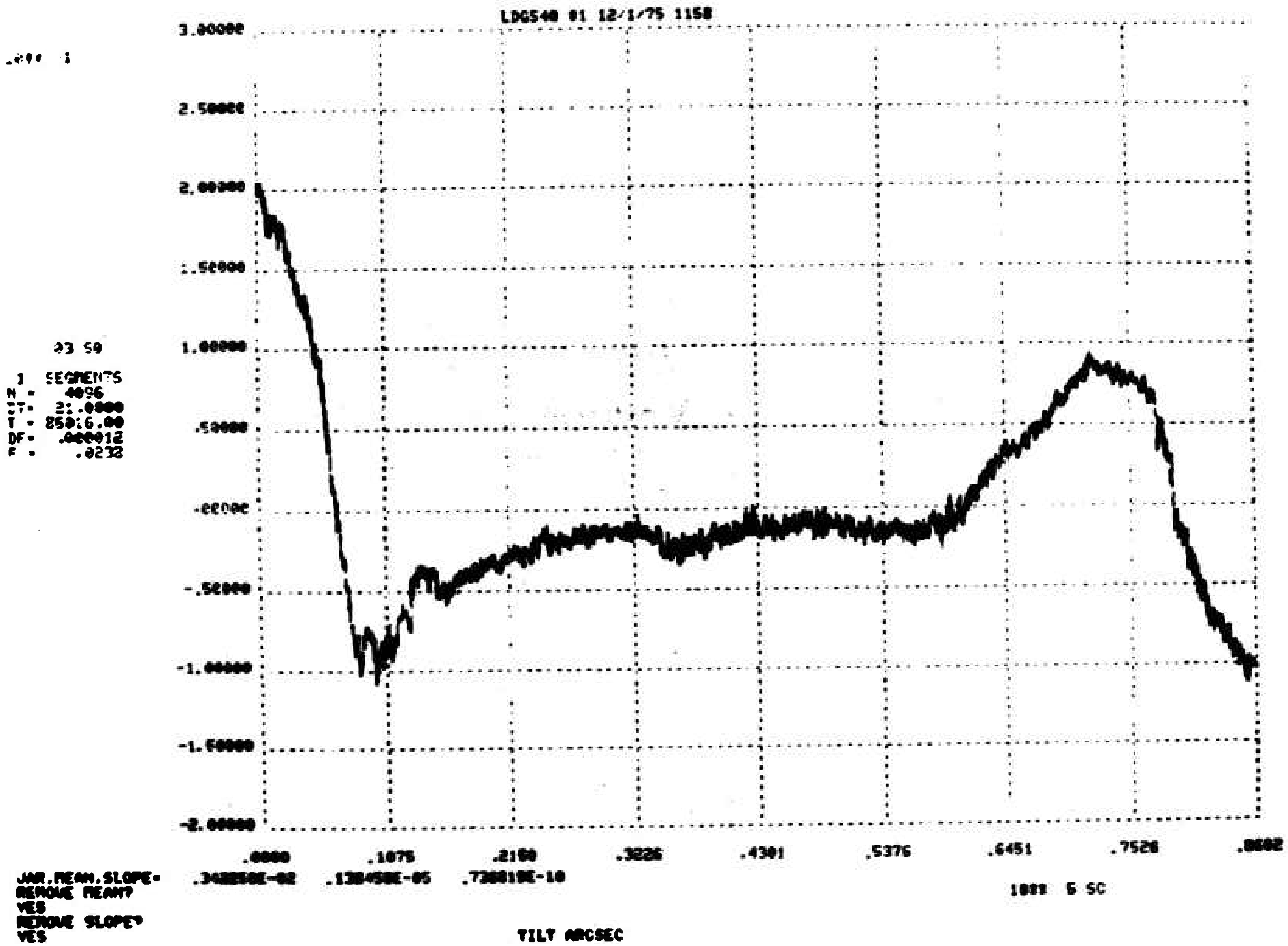

FIGURE D-18. AVERAGE TILT, ARC SECONDS (S/N 1 24 HOUR TEST #2)

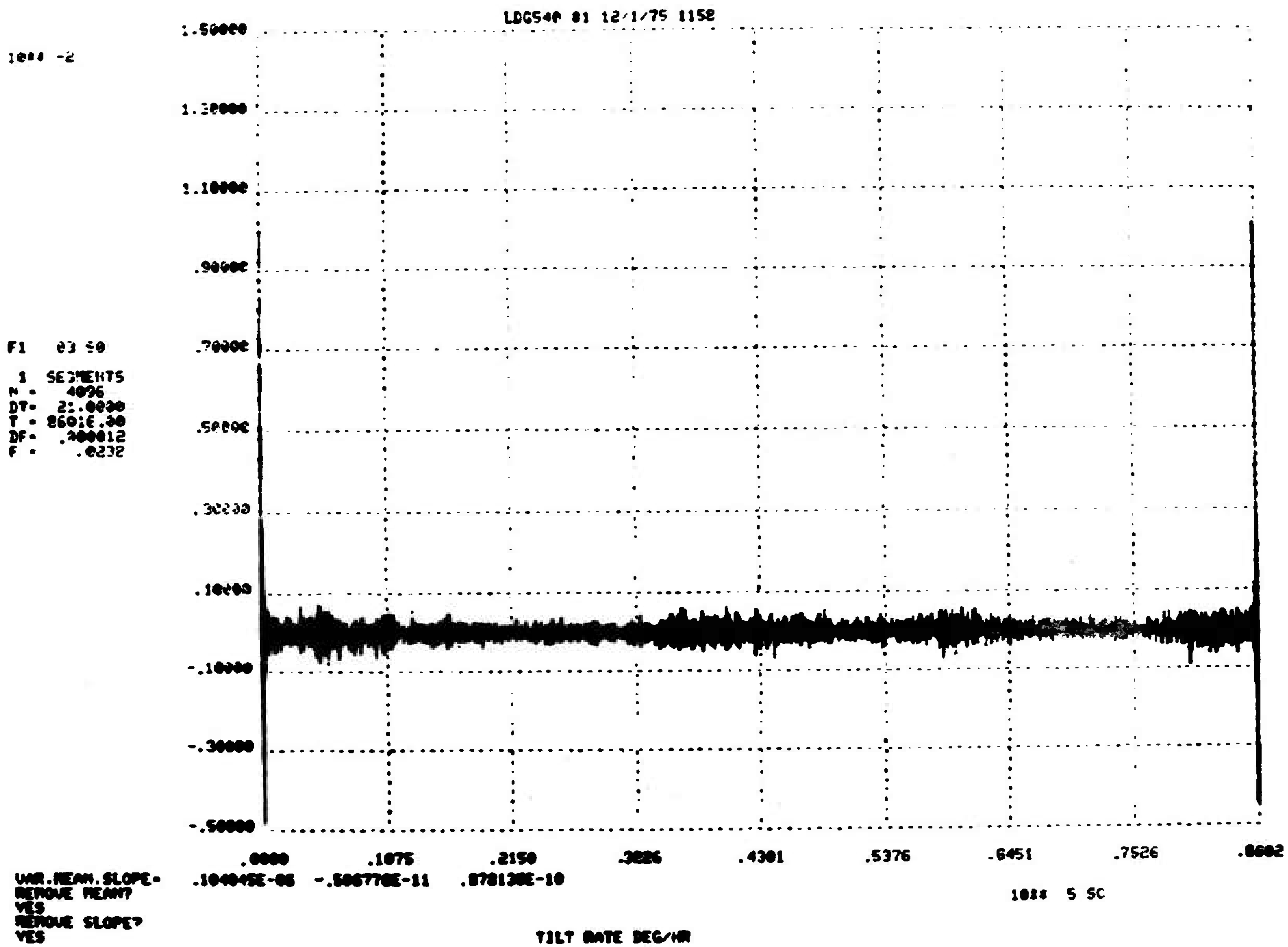

FIGURE D-19. TILT RATE, DEGREE/HOUR (S/N 1 24 HOUR TEST #2)

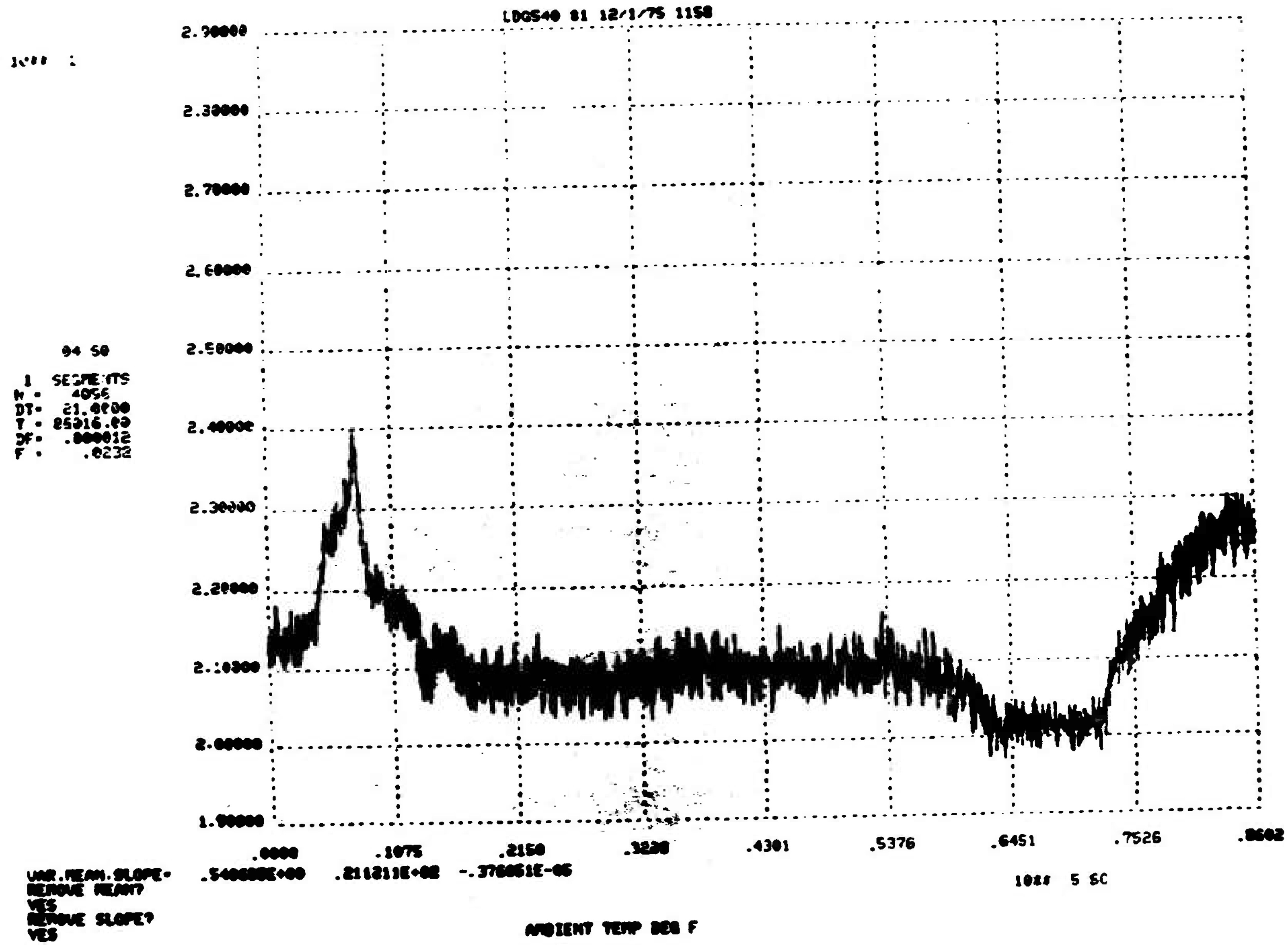

FIGURE D-20. AMBIENT TEMPERATURE, DEGREE F (S/N 1 24 HOUR TEST #2)

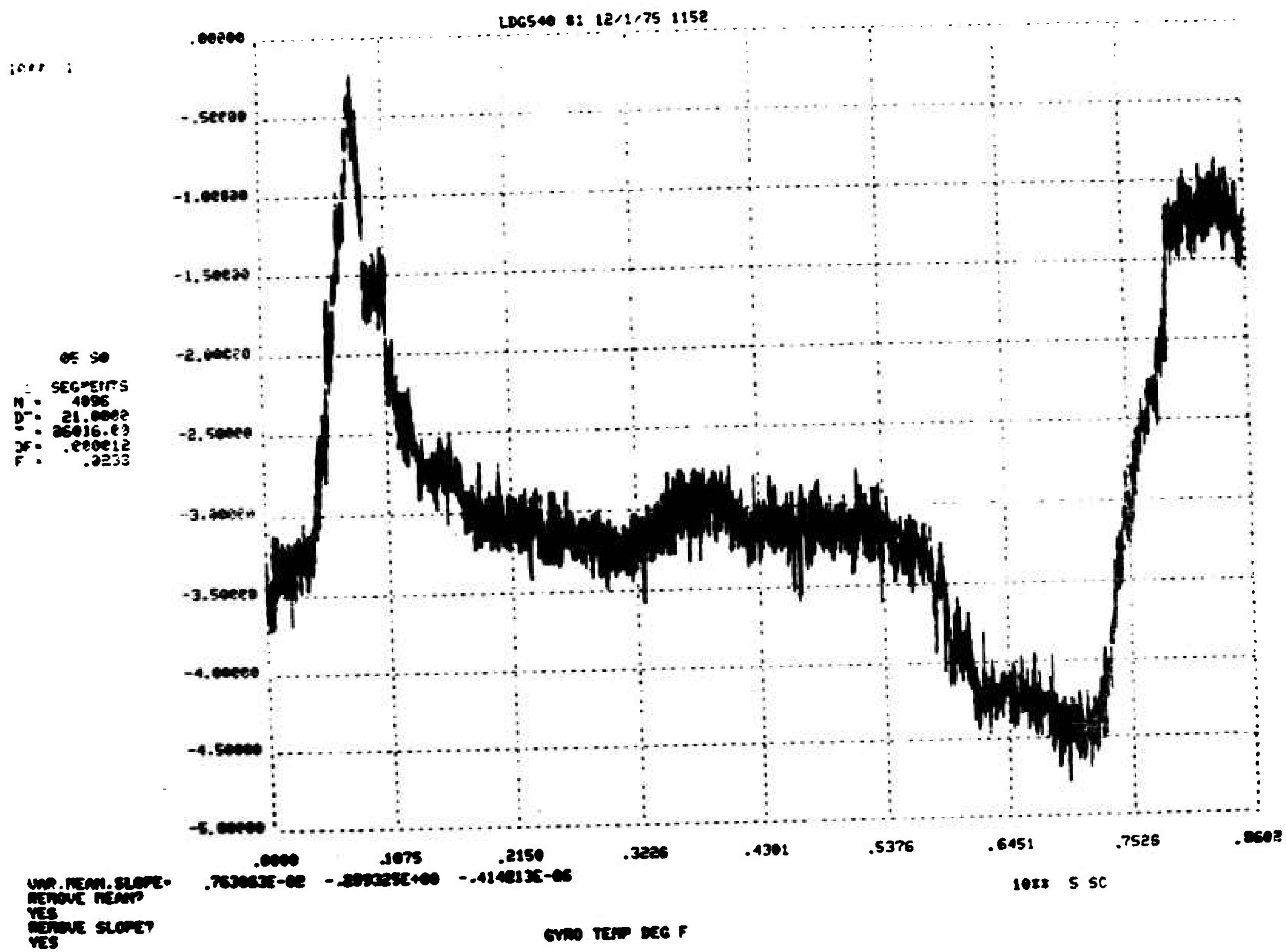

FIGURE D-21. S/N 1 GYRO CASE TEMPERATURE, DEGREE F (24 HOUR TEST #2)

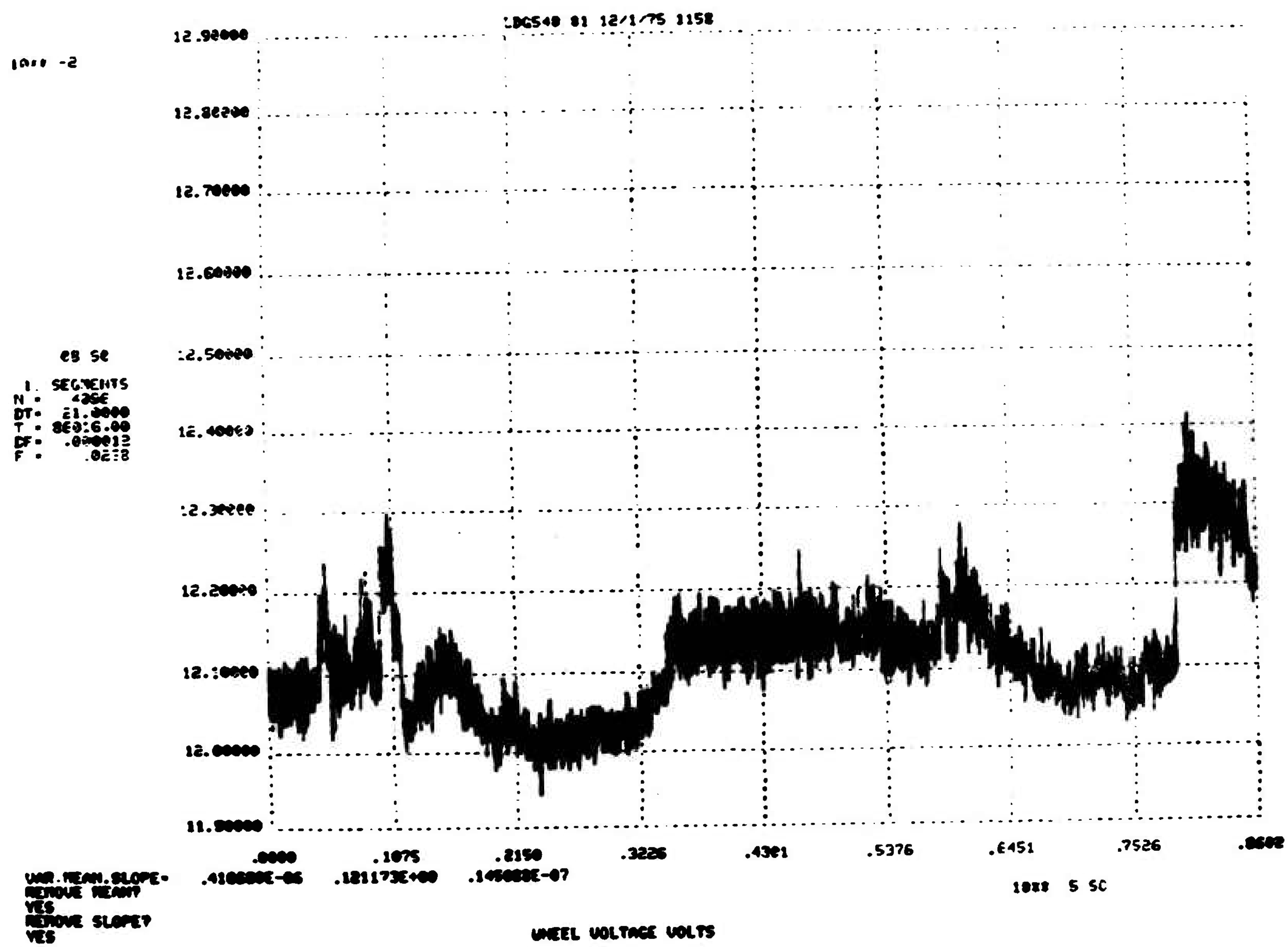

FIGURE D-22. S/N 1 GYRO WHEEL VOLTAGE, VOLTS (24 HOUR TEST #2)

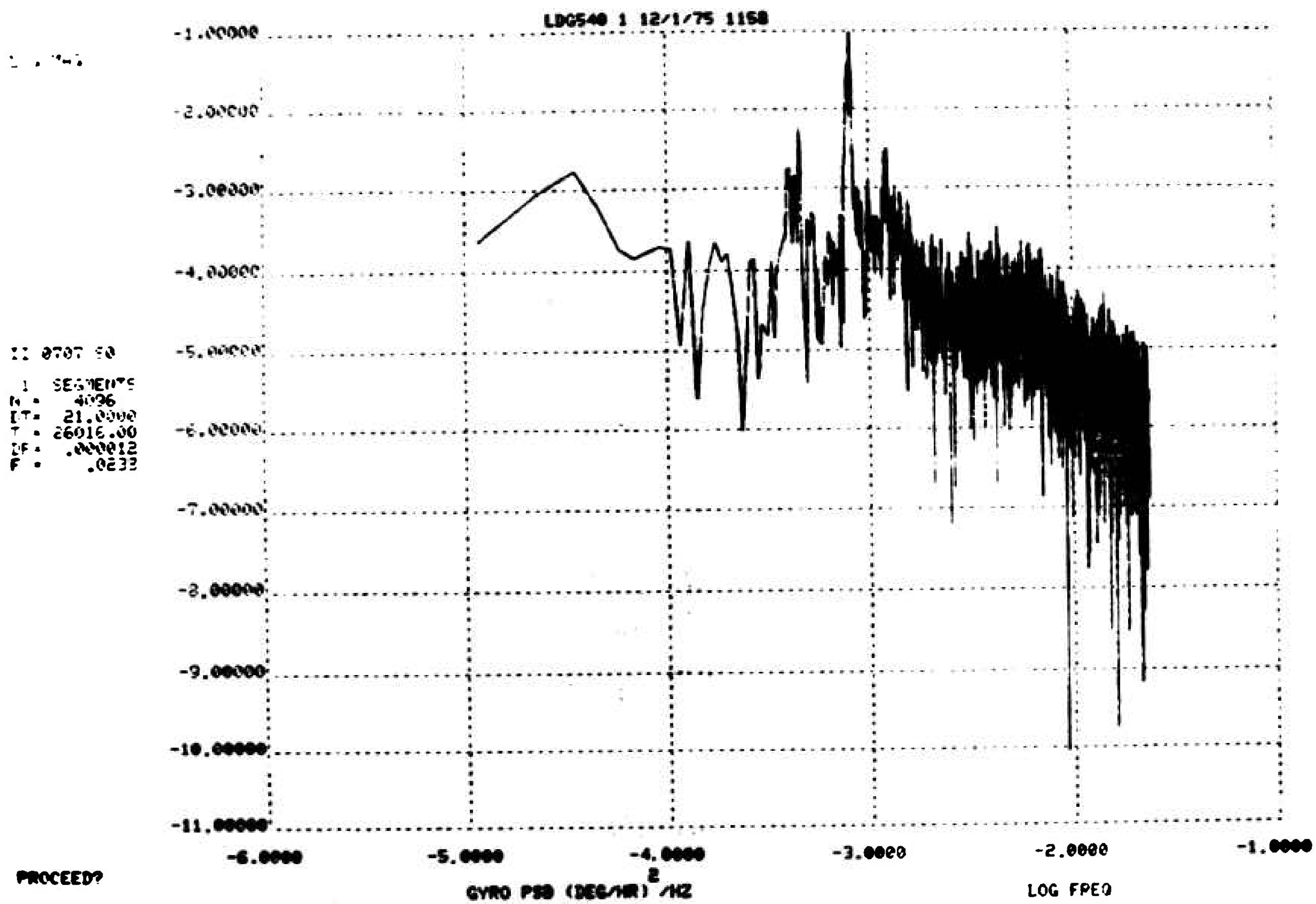

FIGURE D-23. UNSMOOTHED PSD S/N 1 GYRO DATA, (DEGREE/HOUR)^2/HZ (24 HOUR TEST #2)

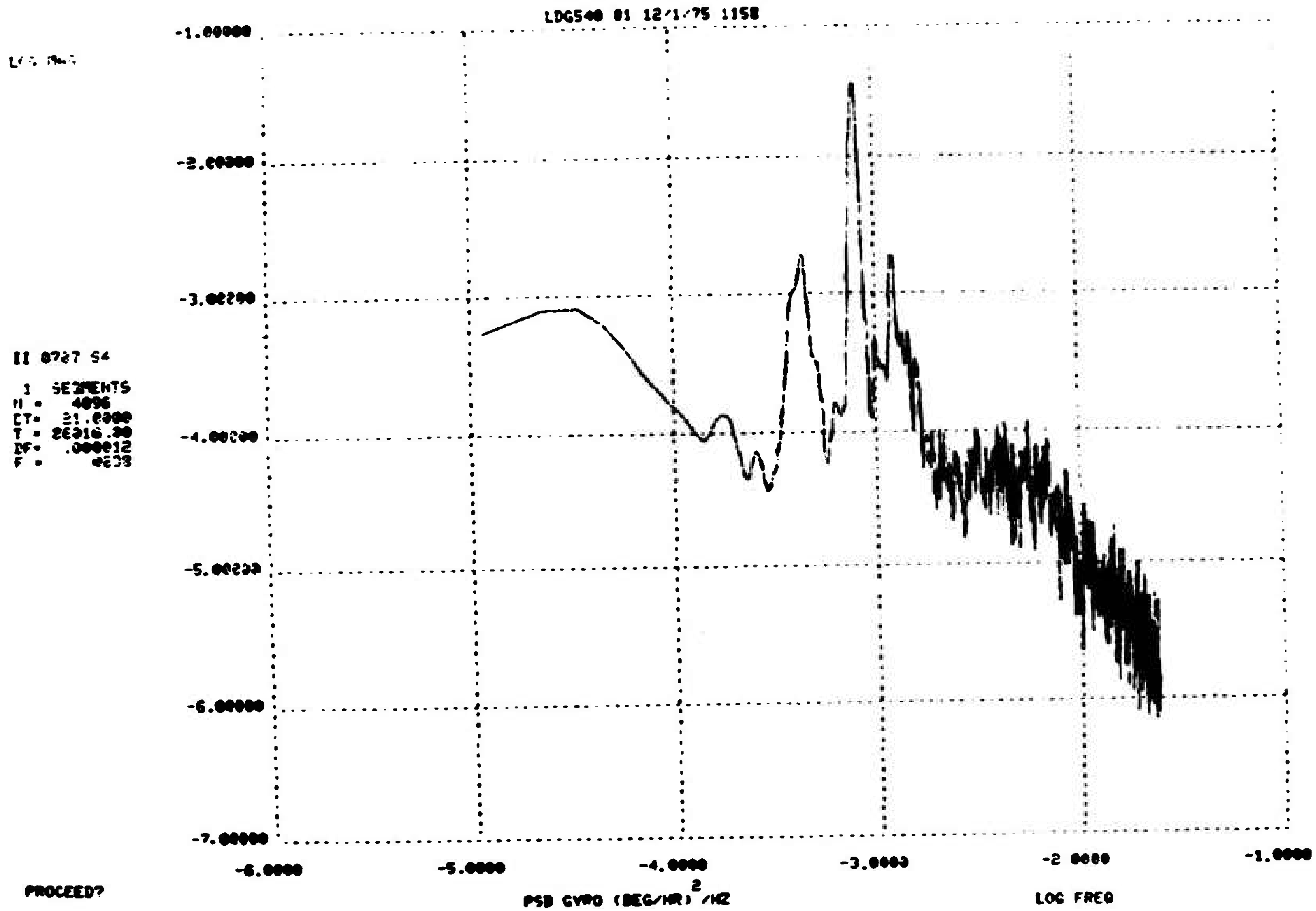

FIGURE D-24. SMOOTHED PSD S/N 1 GYRO DATA, (DEGREE/HOUR)^2/HZ (24 HOUR TEST #2)

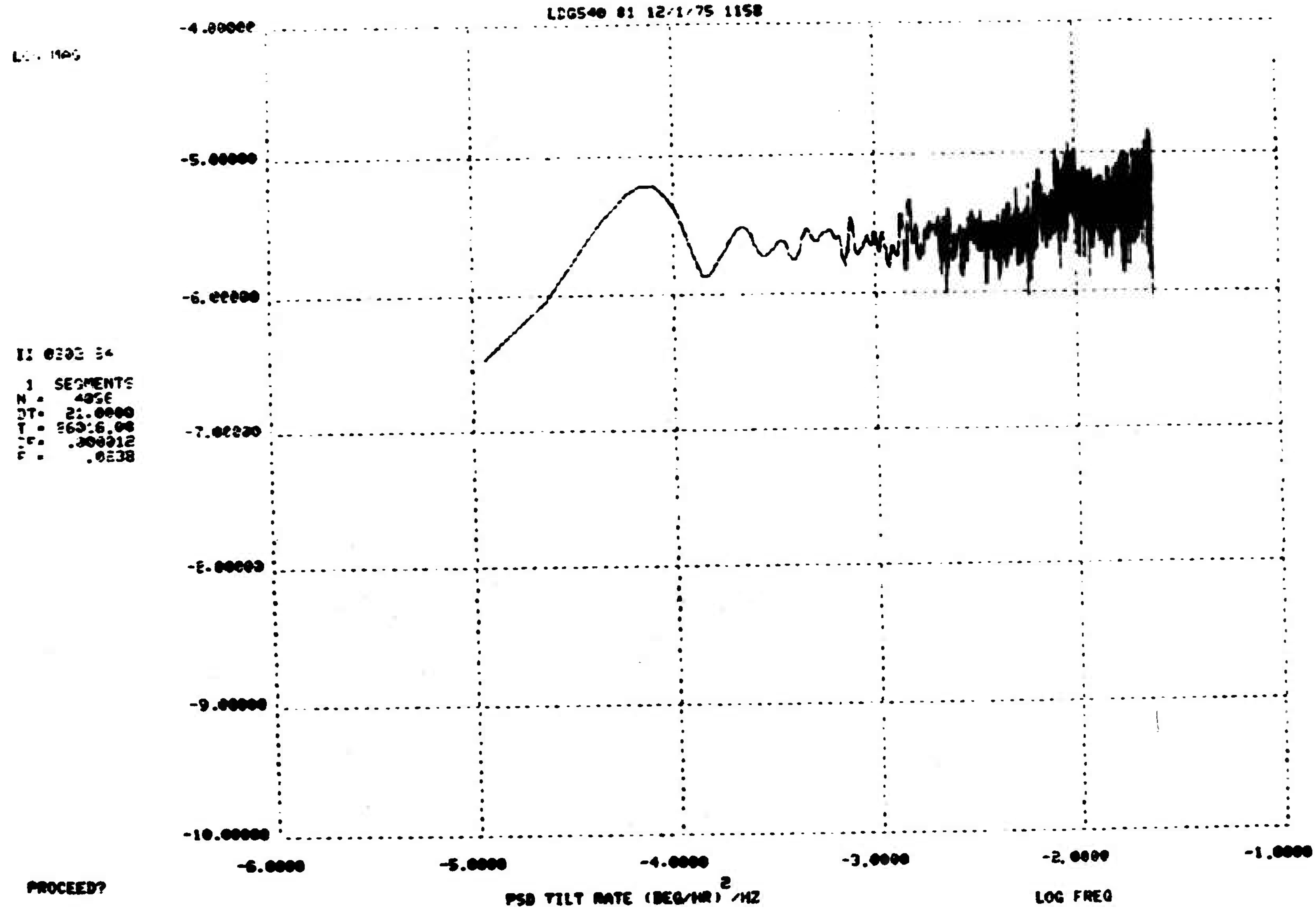

FIGURE D-25. PSD TILT RATE, (DEGREE/HOUR)^2/HZ (S/N 1 24 HOUR TEST #2)

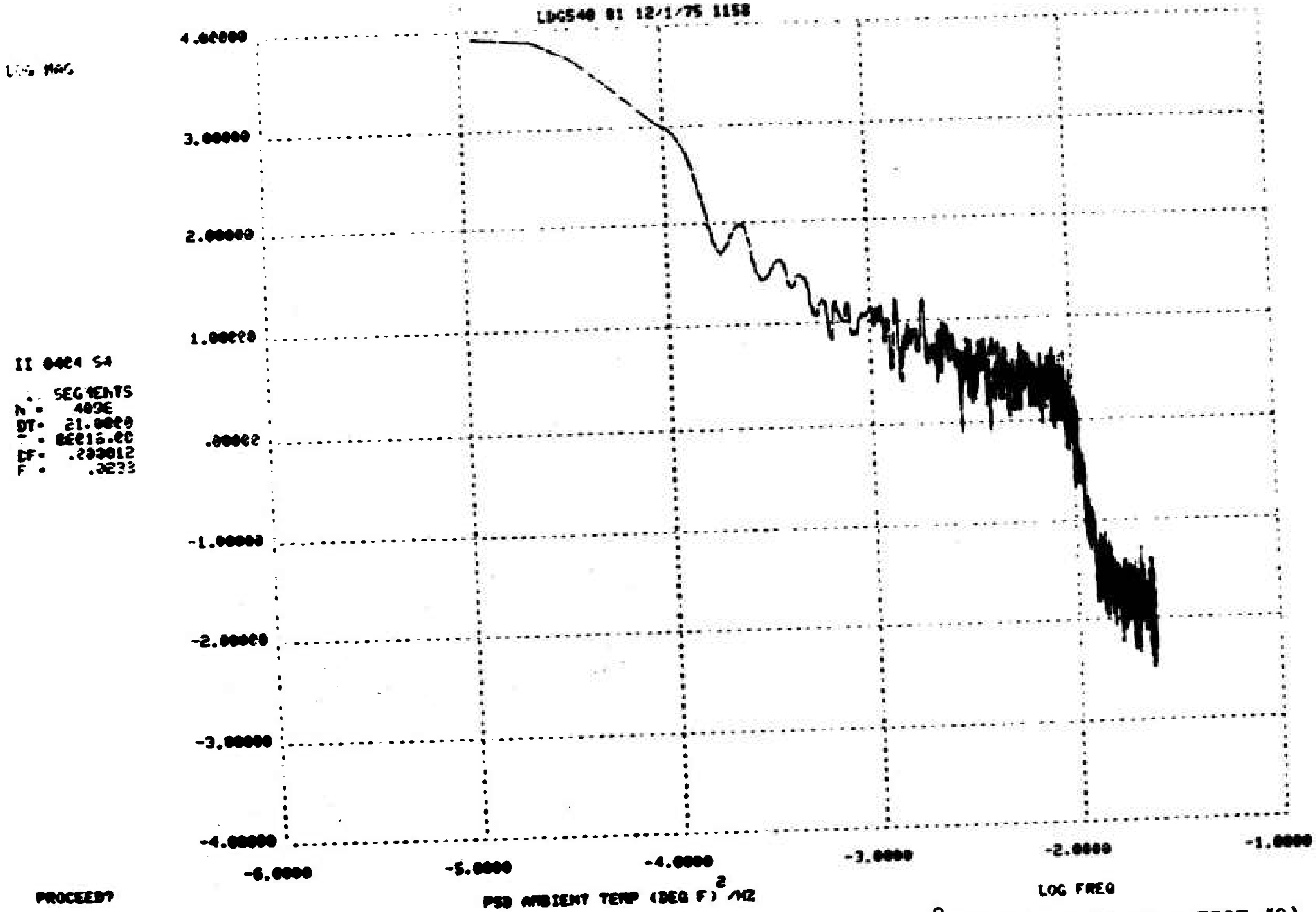

FIGURE D-26. PSD AMBIENT TEMPERATURE, (DEGREE F)^2/HZ (S/N 1 24 HOUR TEST #2)

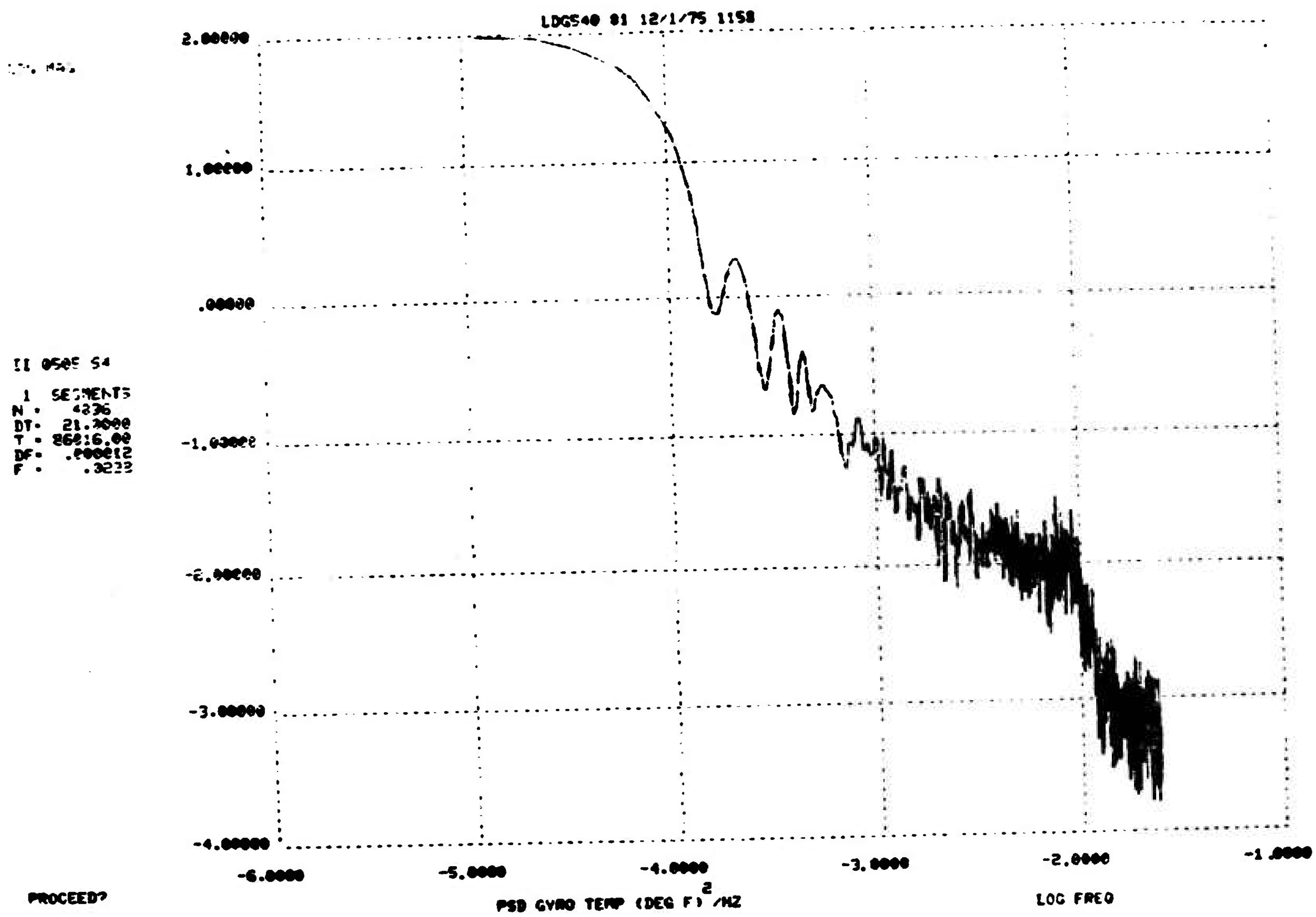

FIGURE D-27. PSD S/N 1 GYRO CASE TEMPERATURE, (DEGREE F)^2/HZ (24 HOUR TEST #2)

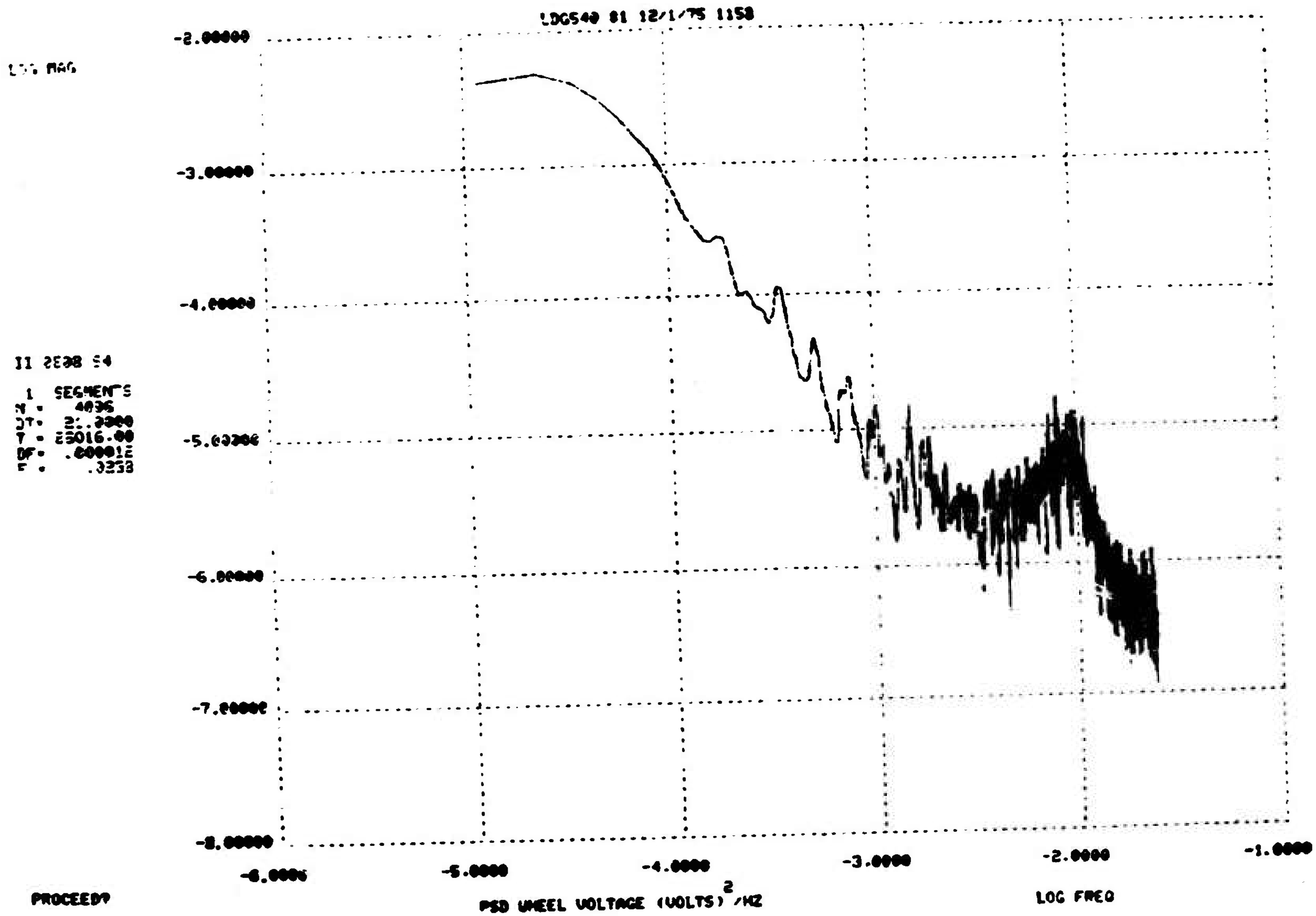

FIGURE D-28. PSD S/N 1 GYRO WHEEL VOLTAGE, $(VOLTS)^2/HZ$ (24 HOUR TEST #2)

24 HOUR TEST #3 GYRO S/N #1

Figure D-29 through Figure D-42 show the results of the third twenty-four test on Gyro S/N #1. This was the last test conducte on Gyro S/N #1 prior to its failure.

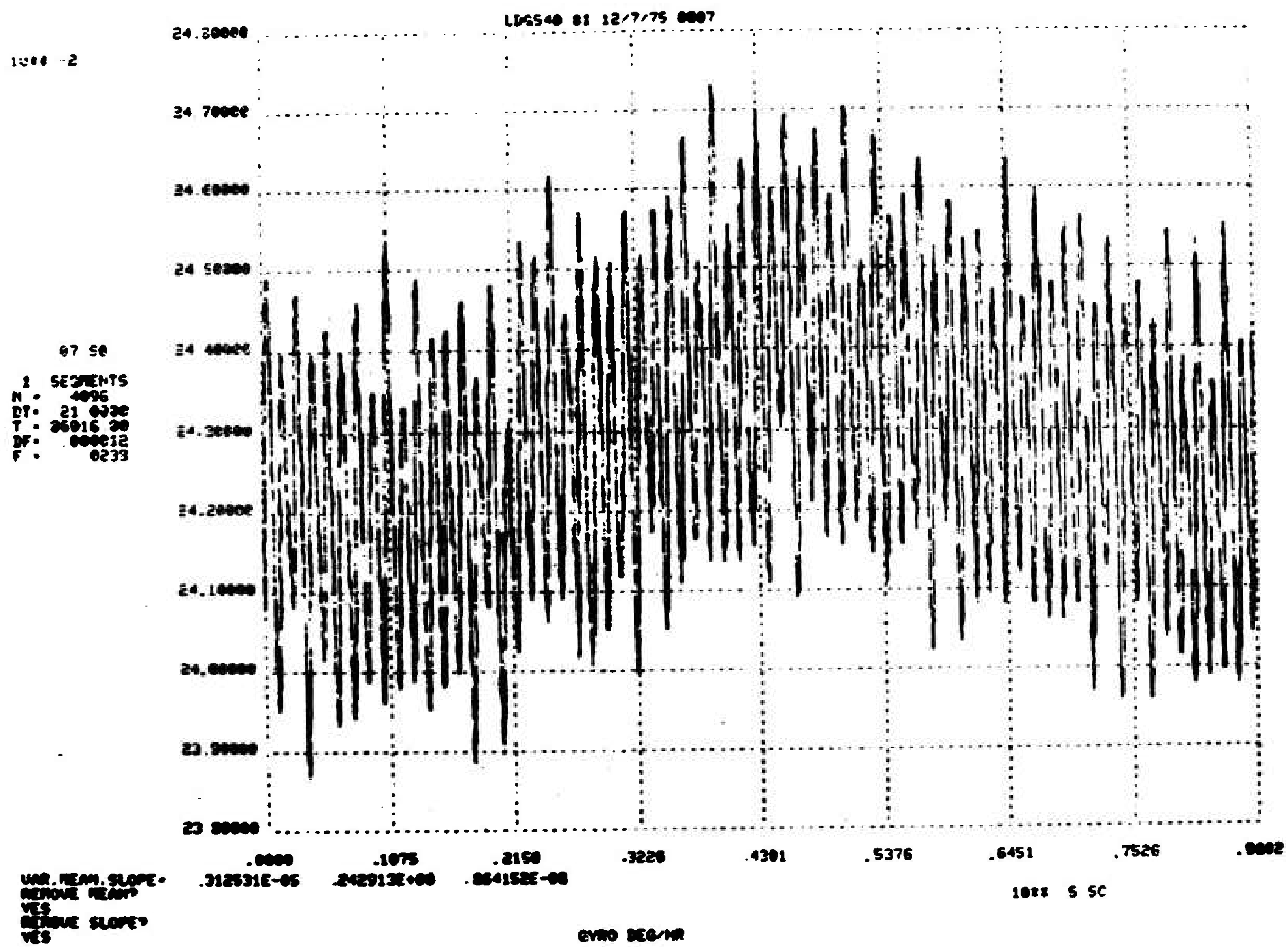

FIGURE D-29. S/N 1 GYRO DATA, DEGREE/HOUR (24 HOUR TEST #3)

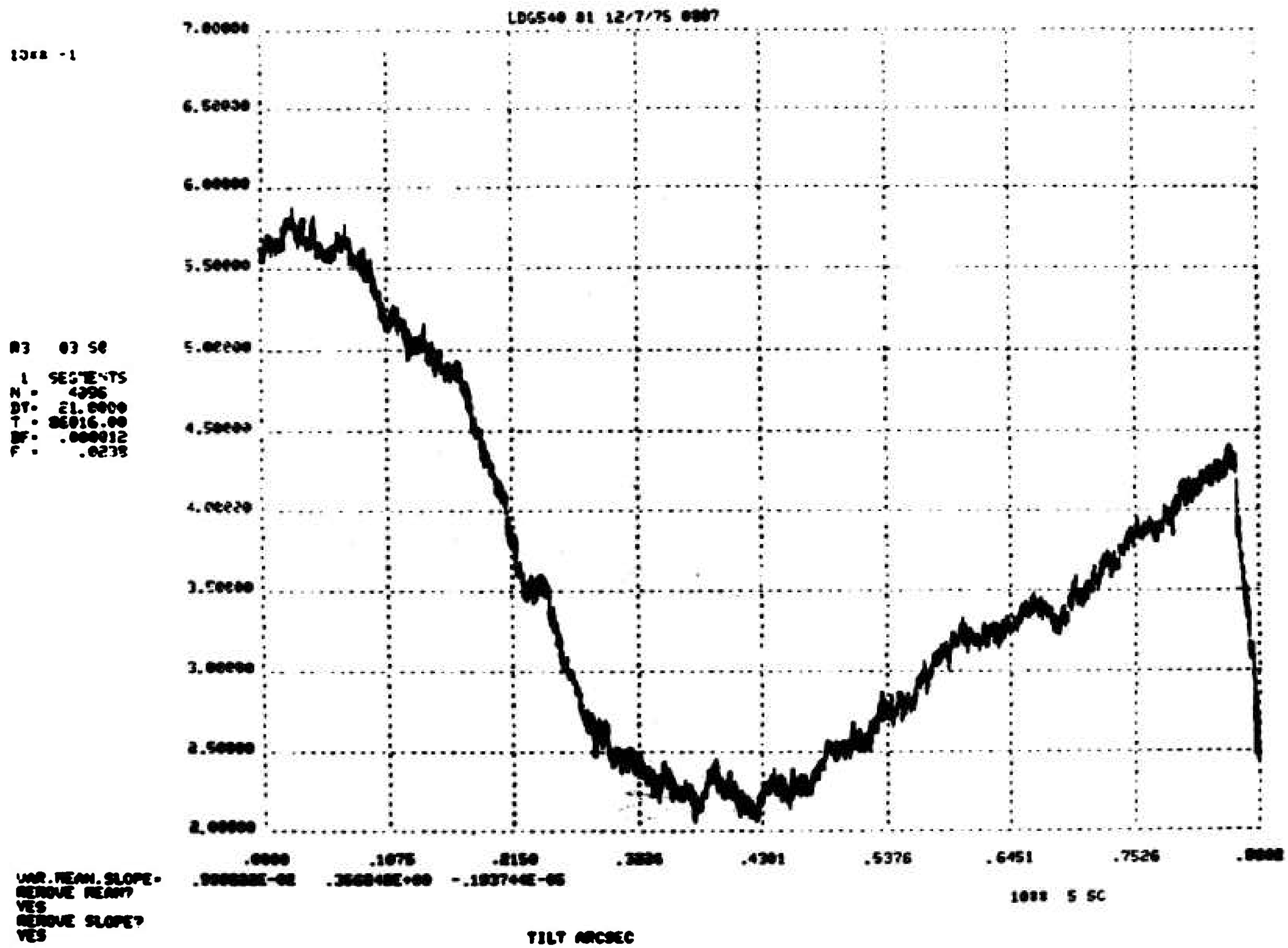

FIGURE D-30. AVERAGE TILT, ARC SECONDS (S/N 1 24 HOUR TEST #3)

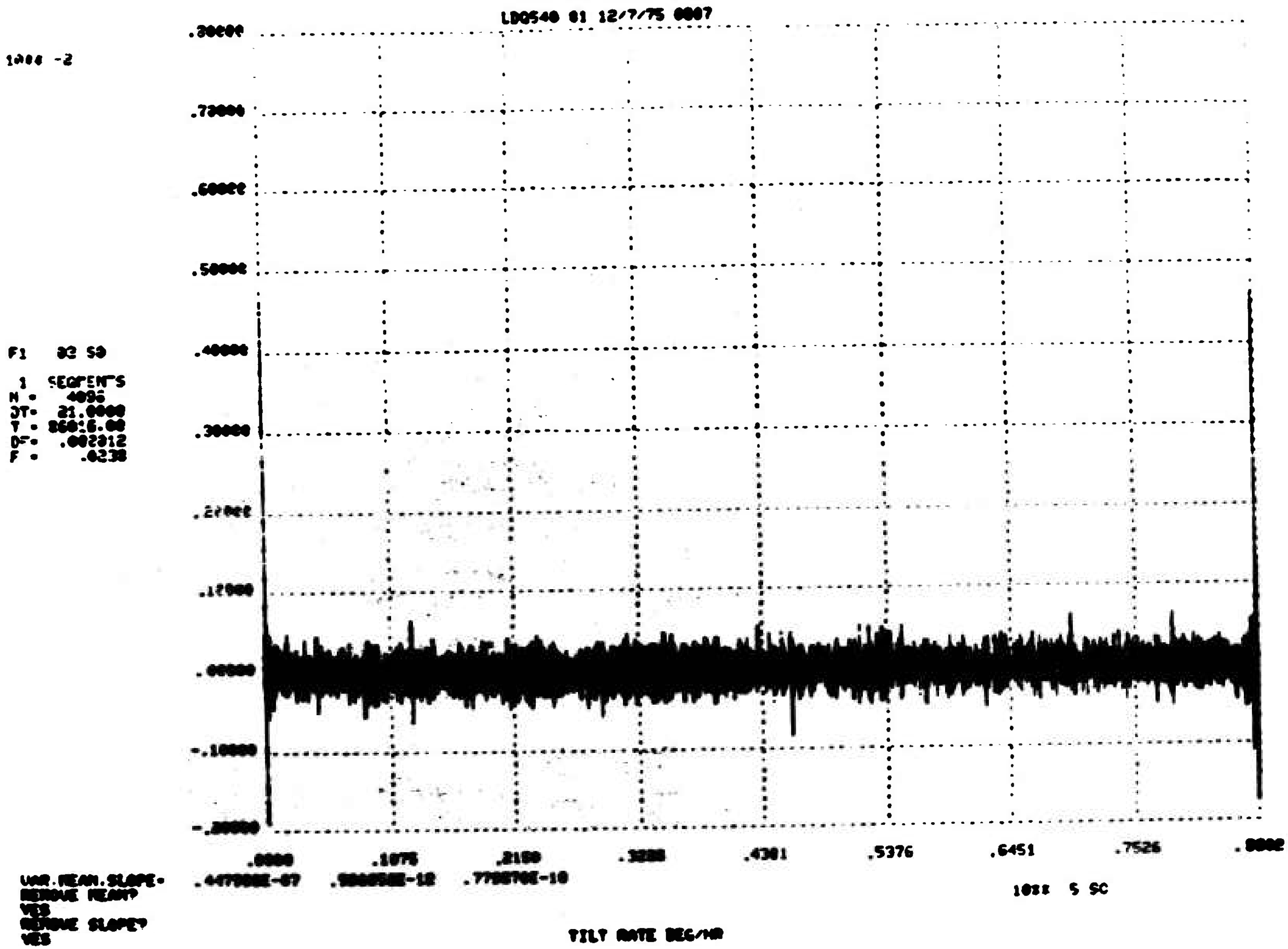

FIGURE D-31. TILT RATE, DEGREE/HOUR (S/N 1 24 HOUR TEST #3)

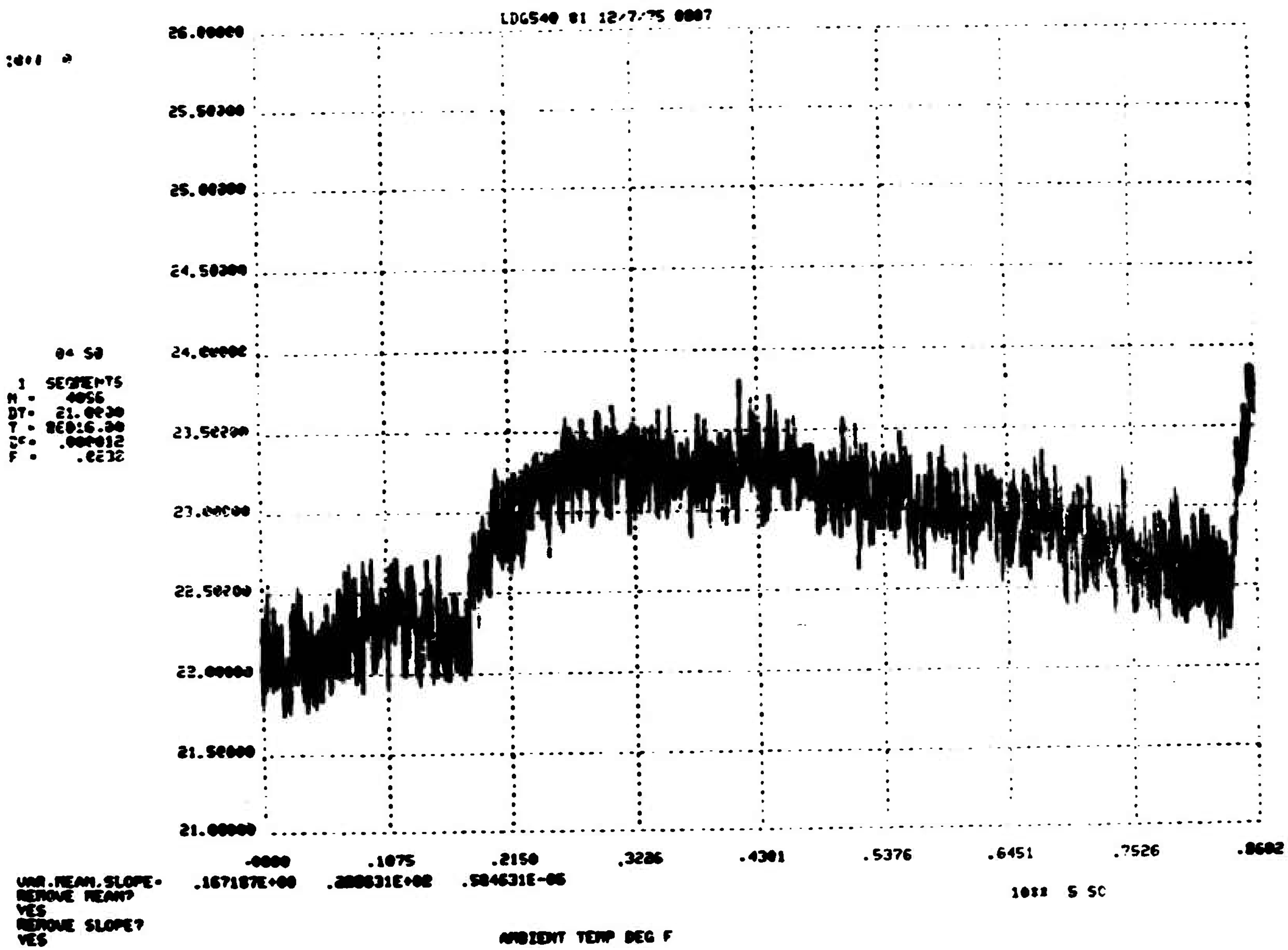

FIGURE D-32. AMBIENT TEMPERATURE, DEGREE F (S/N 1 24 HOUR TEST #3)

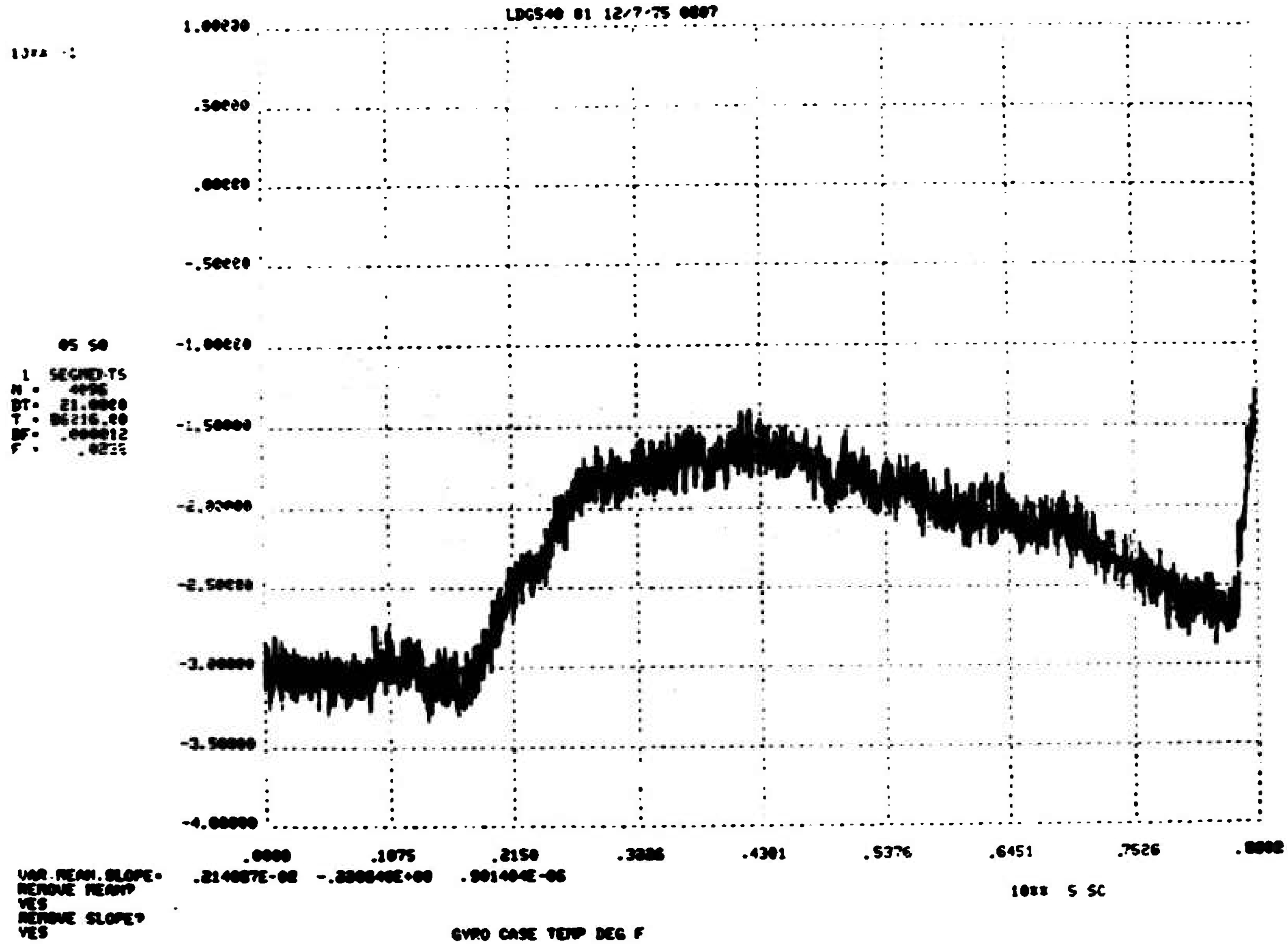

FIGURE D-33. S/N 1 GYRO CASE TEMPERATURE, DEGREE F (24 HOUR TEST #3)

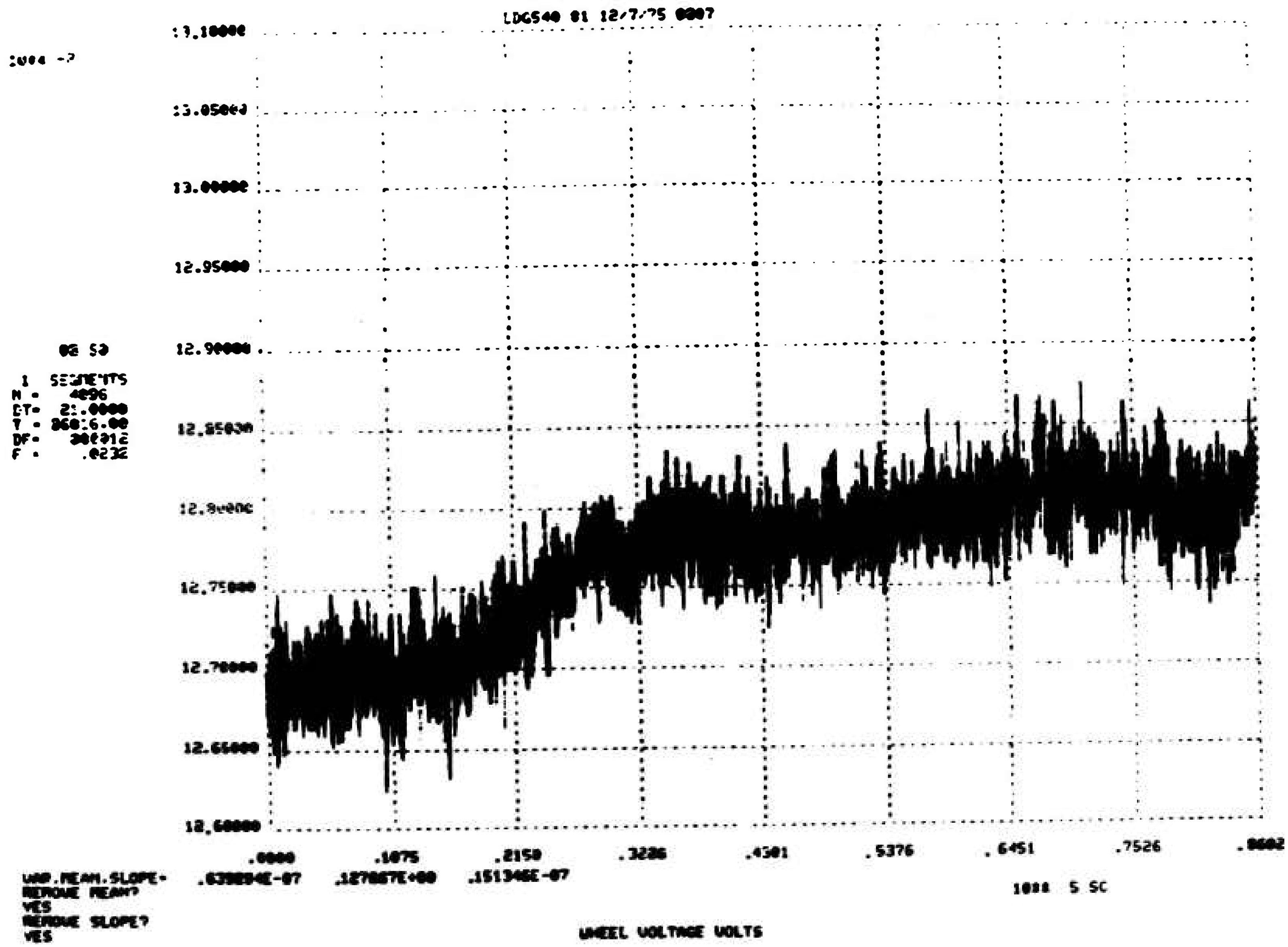

FIGURE D-34. S/N 1 GYRO WHEEL VOLTAGE, VOLTS (24 HOUR TEST #3)

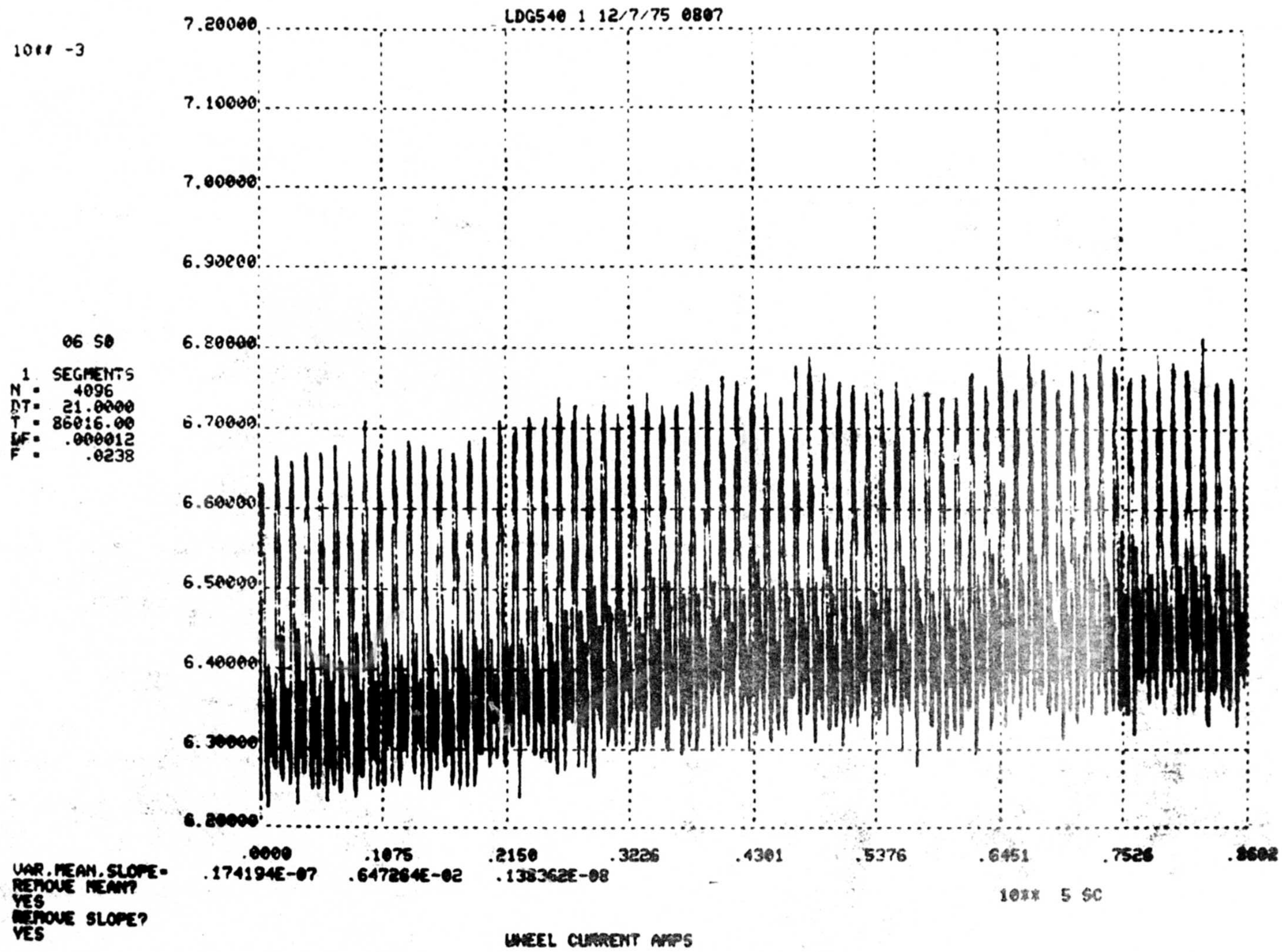

FIGURE D-35. S/N 1 GYRO WHEEL CURRENT, AMPS (24 HOUR TEST #3)

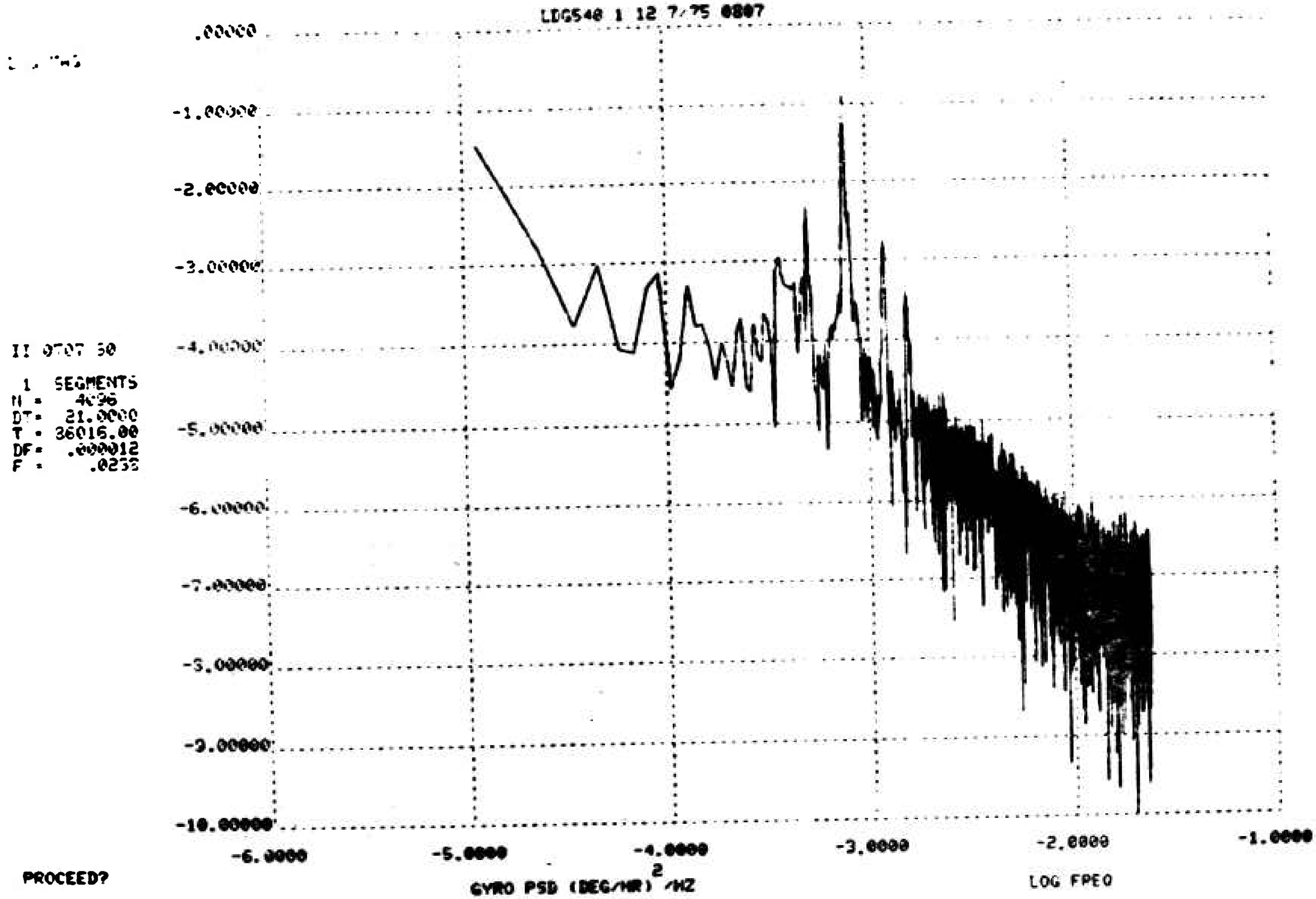

FIGURE D-36. UNSMOOTHED PSD S/N 1 GYRO DATA, $(DEGREE/HOUR)^2/HZ$ (24 HOUR TEST #3)

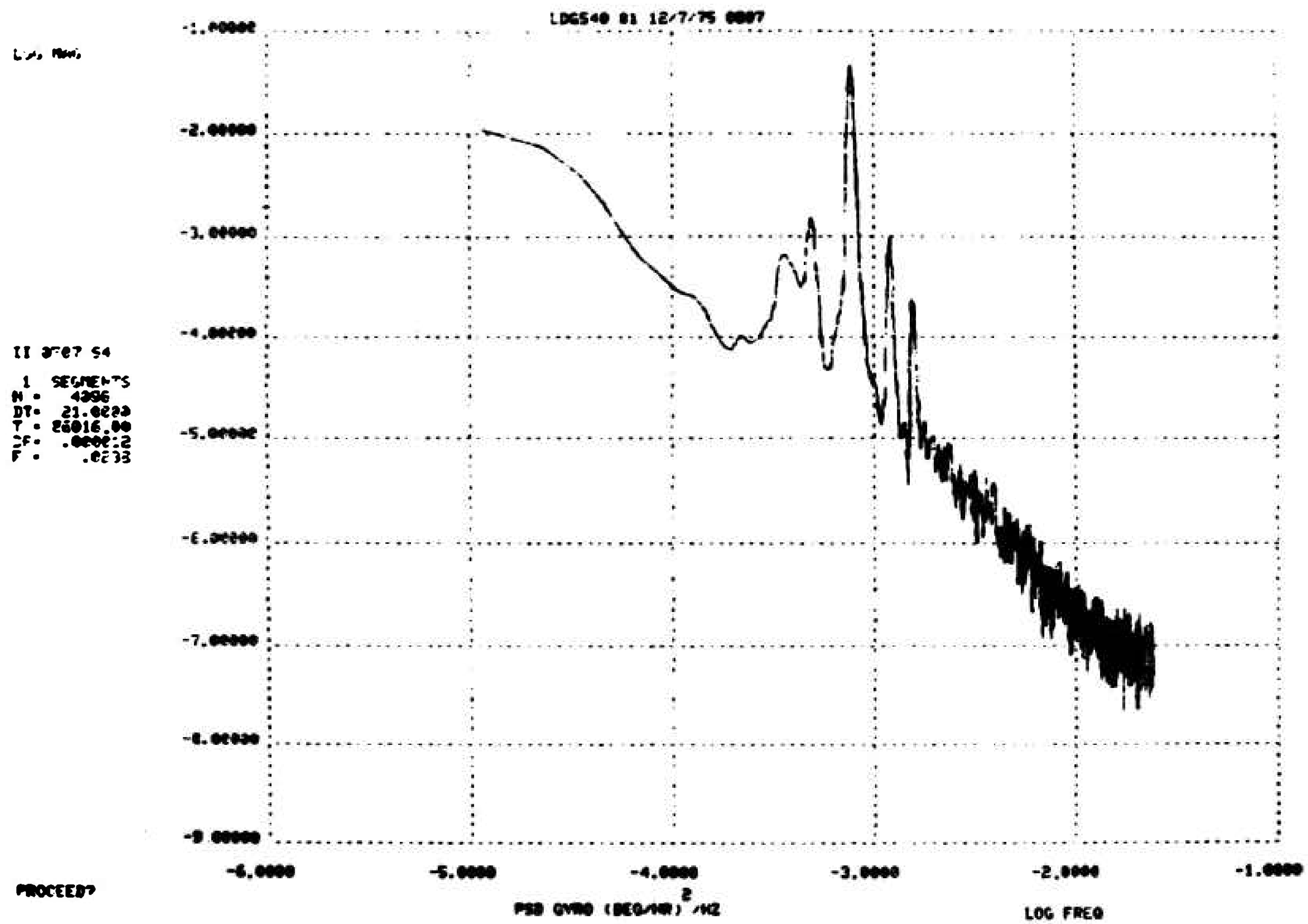

FIGURE D-37. SMOOTHED PSD S/N 1 GYRO DATA, $(\text{DEGREE/HOUR})^2/\text{HZ}$ (24 HOUR TEST #3)

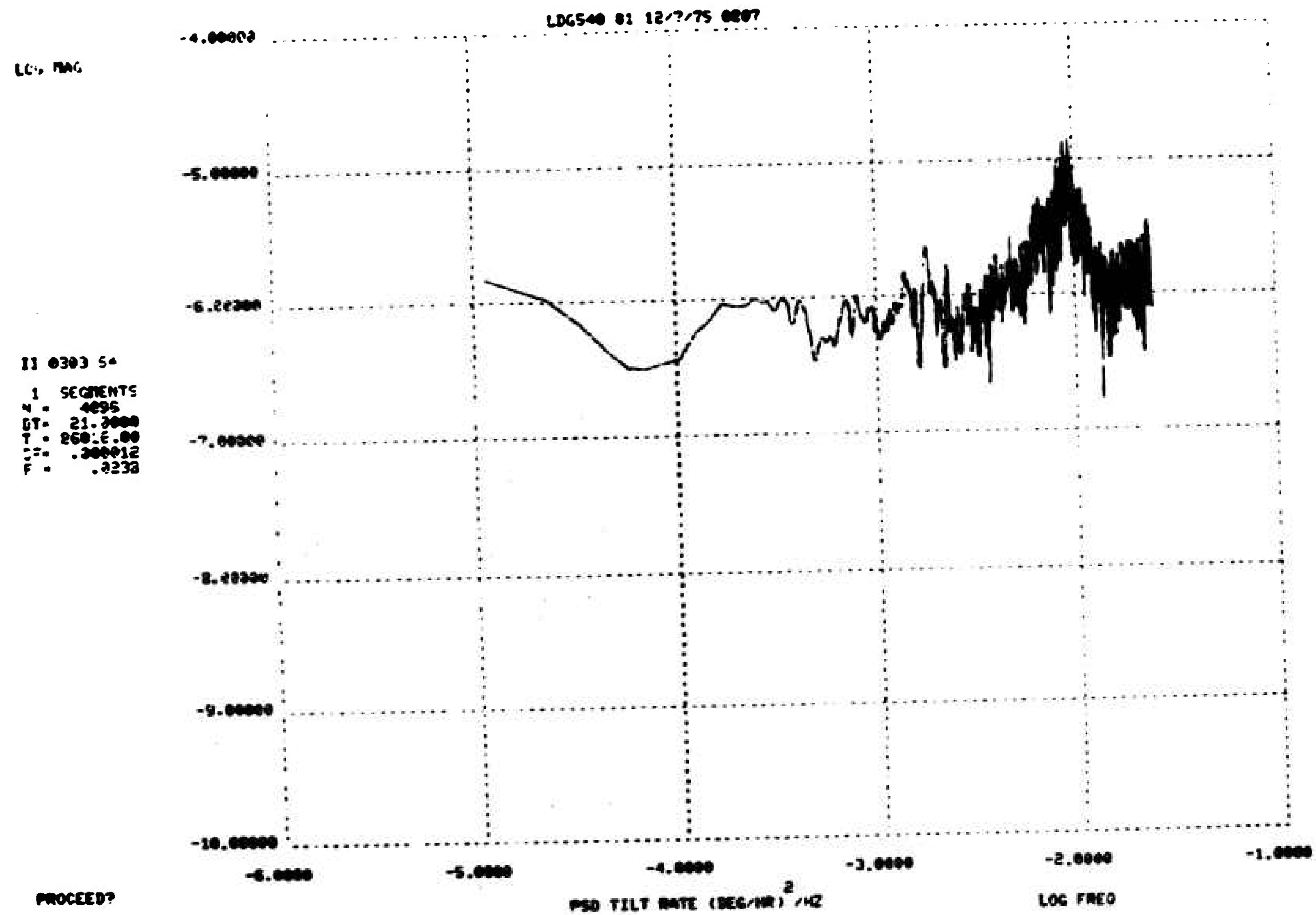

FIGURE D-38. PSD TILT RATE, $(DEGREE/HOUR)^2/HZ$ (S/N 1 24 HOUR TEST #3)

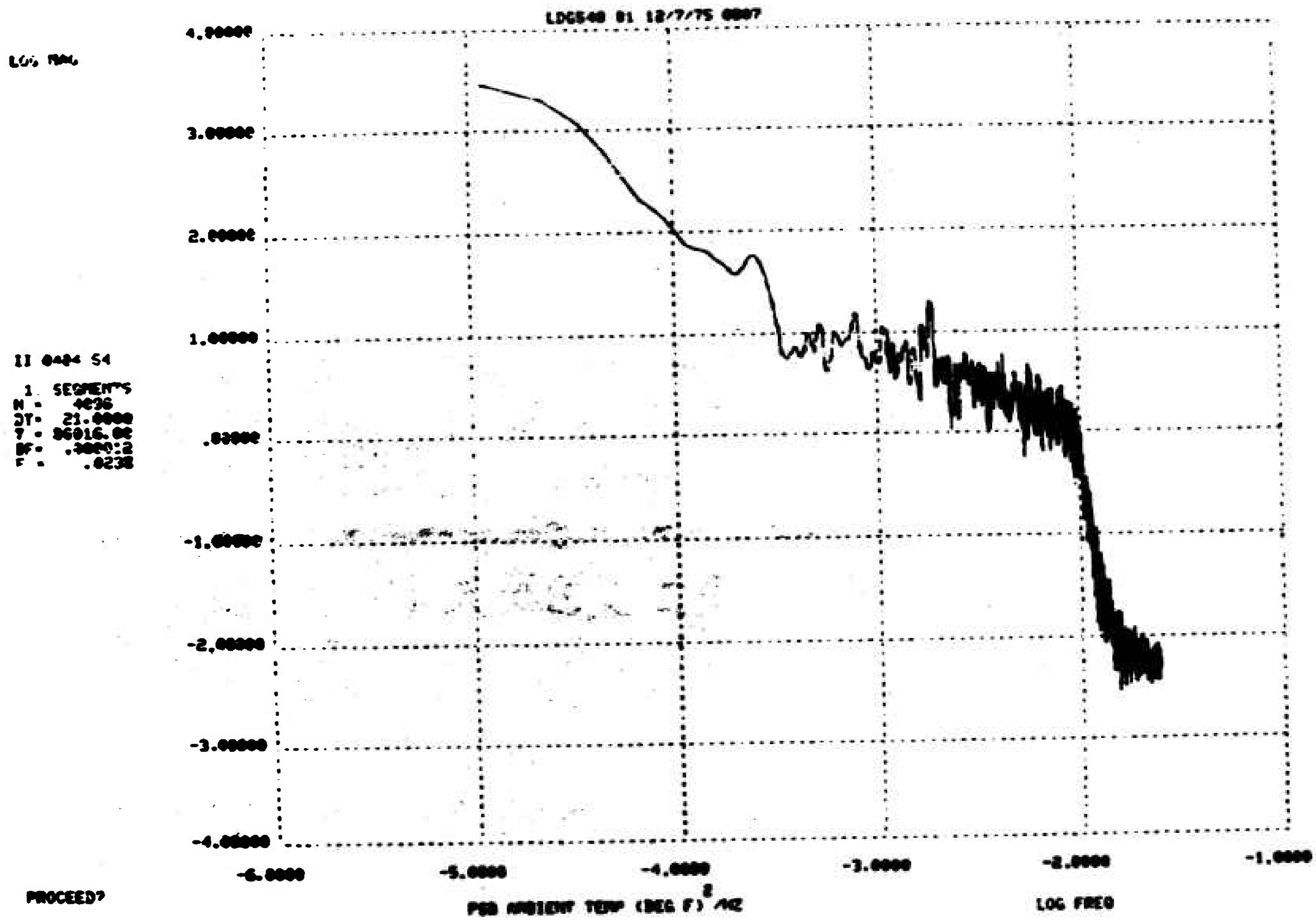

FIGURE D-39. PSD AMBIENT TEMPERATURE, (DEGREE F)^2/HZ (S/N 1 24 HOUR TEST #3)

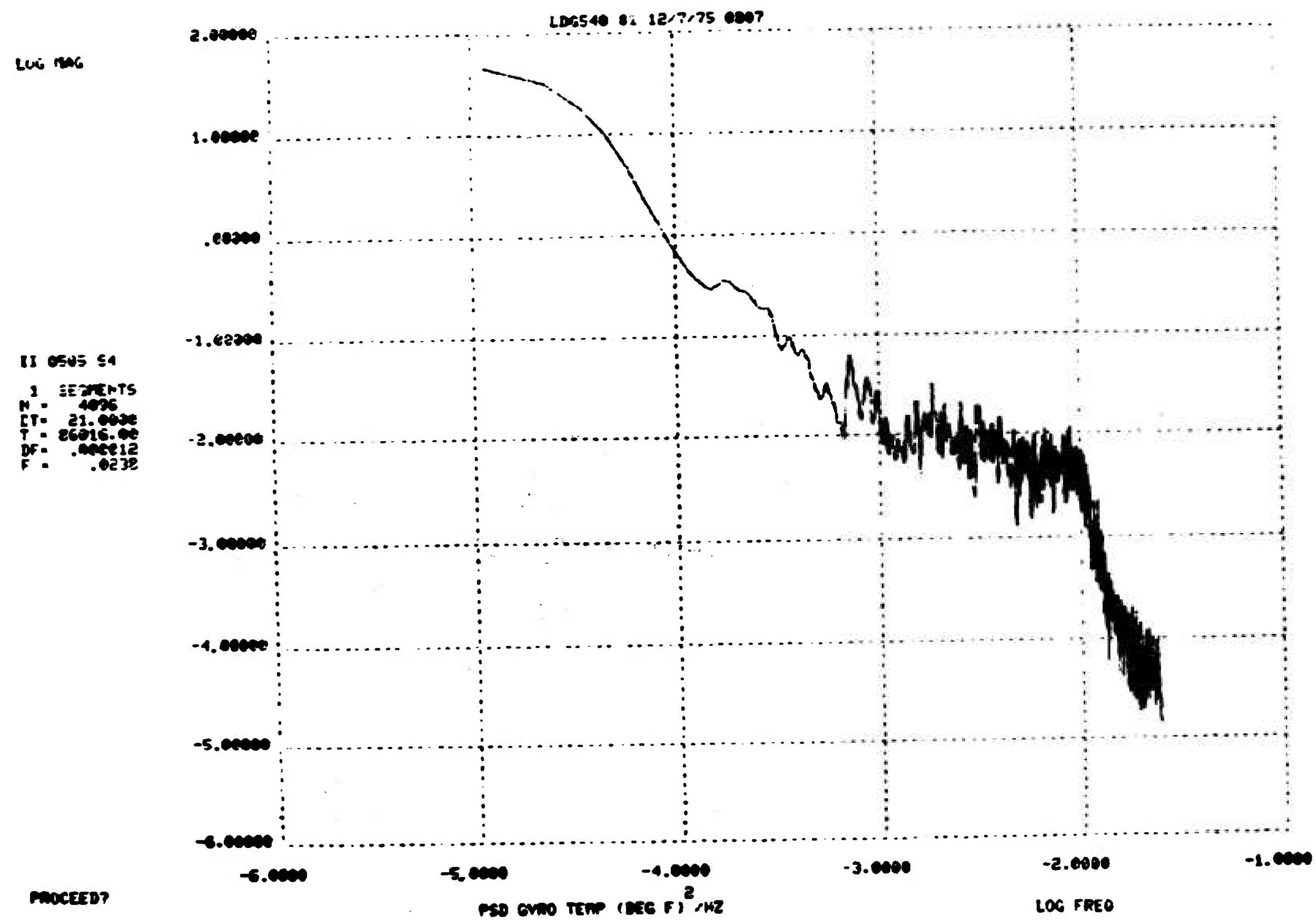

FIGURE D-40. PSD S/N 1 GYRO CASE TEMPERATURE, (DEGREE F)^2/HZ (24 HOUR TEST #3)

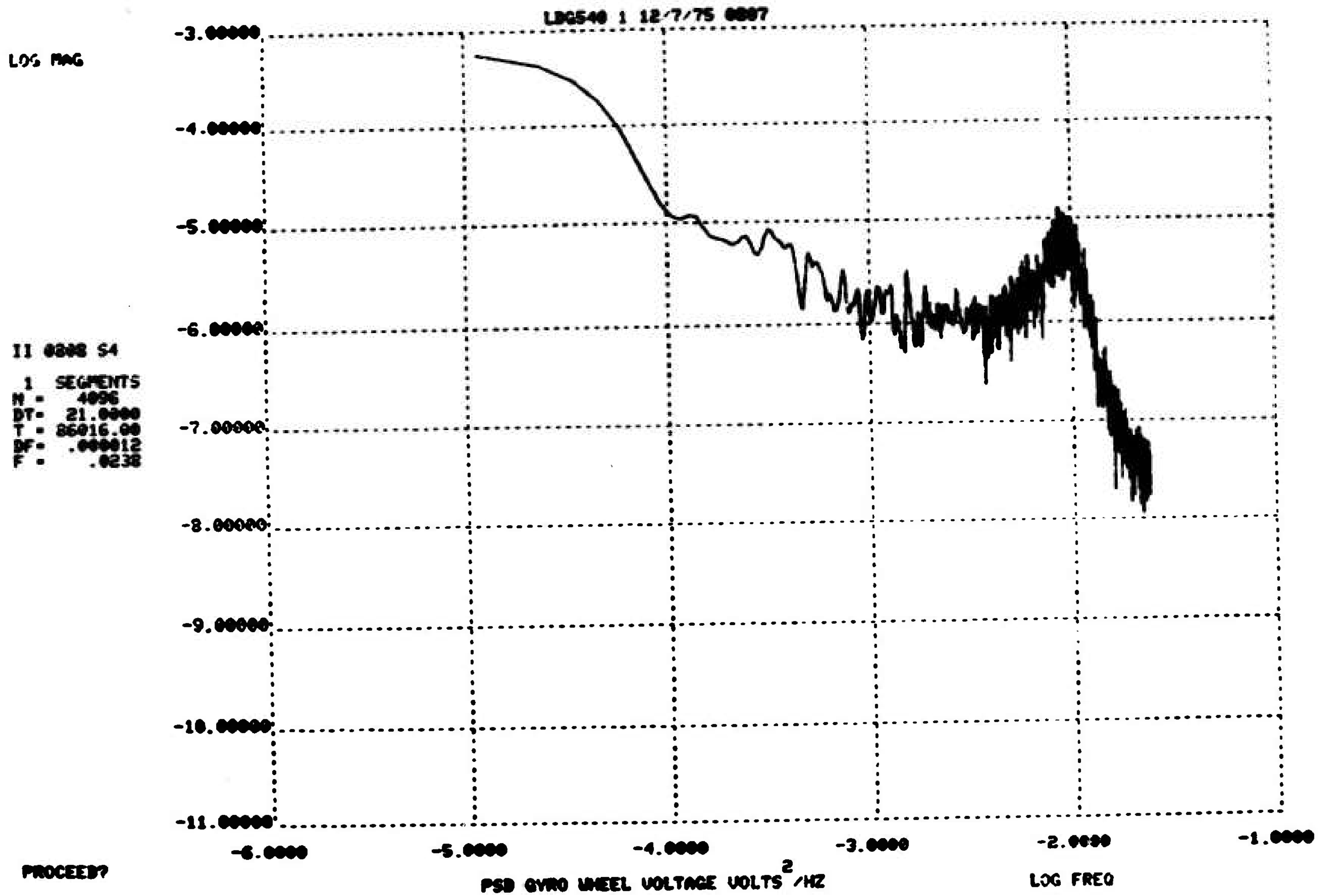

FIGURE D-41. PSD S/N 1 GYRO WHEEL VOLTAGE, $(VOLTS)^2/HZ$ (24 HOUR TEST #3)

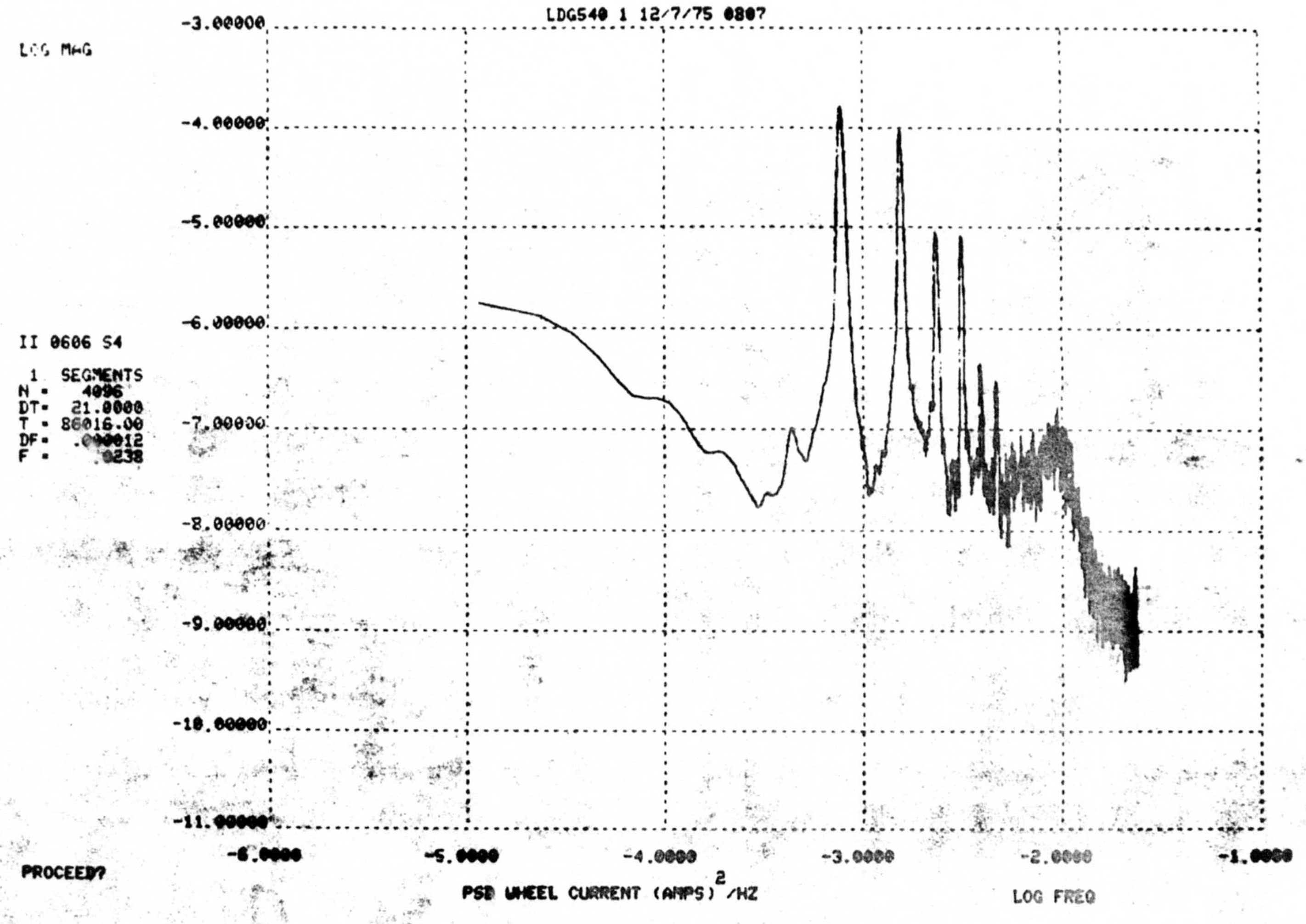

FIGURE D-42. PSD S/N 1 GYRO WHEEL CURRENT, $(\text{AMPS})^2$/HZ (24 HOUR TEST #3)

1 HOUR TEST S/N 1

The one hour test results are shown in Figure D-43 through Figure D-55. The gyro output PSD, Figure D-50 was well above the noise level shown in Appendix E for this test. Tilt PSD information Figure D-51 appears to start rising significantly above the noise level at approximately .05 Hz. This will be seen more clearly in the three minute test to be shown later. Ambient temperature and gyro temperature PSD, Figure D-52 and D-53, break away from the noise level at about .08 Hz. However, the gyro temperature appears to remain strongly influenced by noise until approximately .008 Hz as seen in the twenty-four hour tests. Wheel voltage and current PSD's Figure D-54 and D-55 are still dominated by noise except for the low frequency end of the wheel current PSD which corresponds to the spikes observed in the twenty-four hour tests.

The low frequency end of the gyro PSD, Figure D-50, is characterized by the gyro response to wheel current variations. The twenty-four hour test illustrated the response to wheel current more vividly. The spike in the gyro PSD at approximately .08 Hz is probably a response to the spike seen in the gyro case temperature PSD, Figure D-53. The gyro temperature controller cycling has been postulated as the cause of the spike.

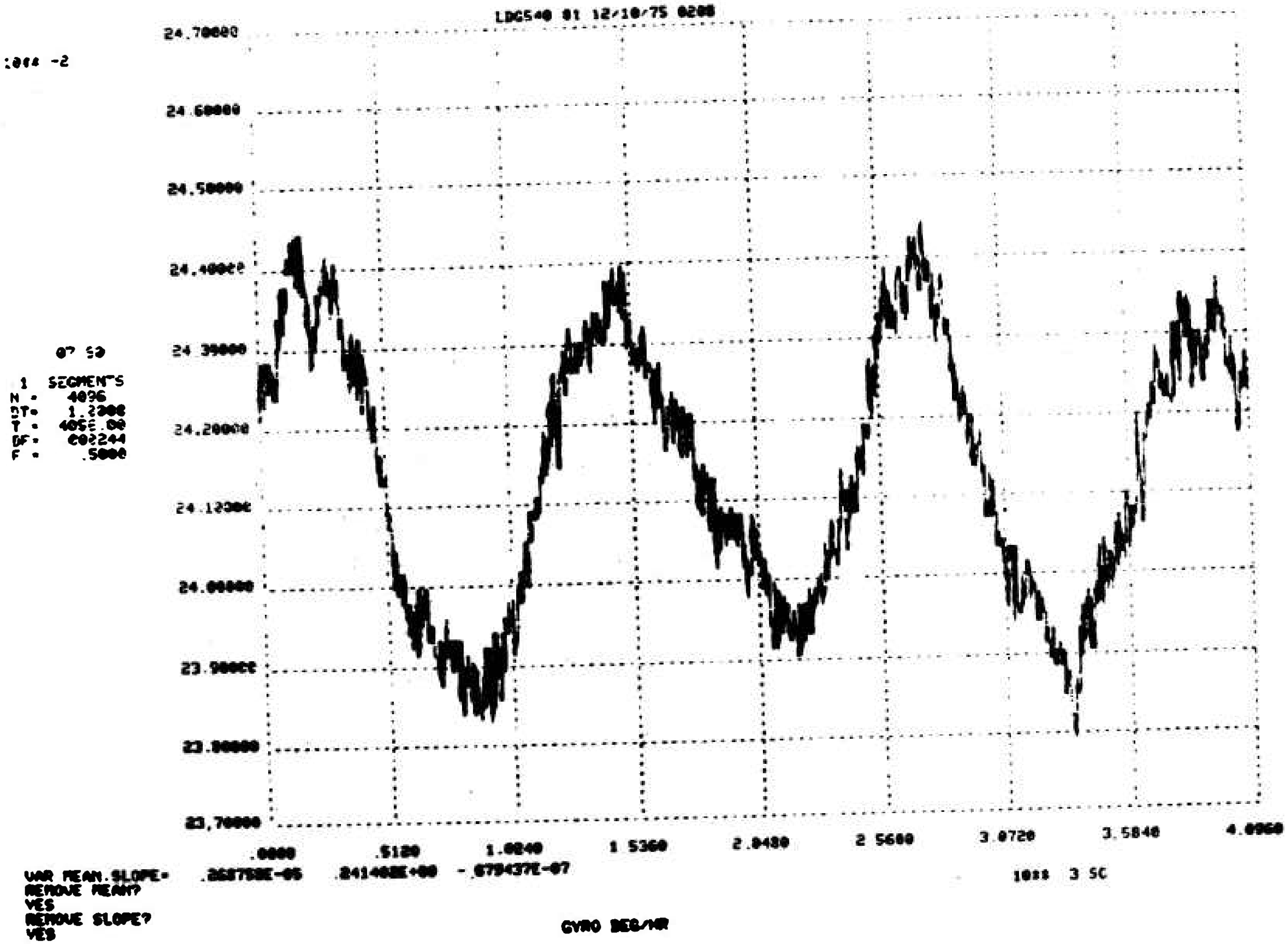

FIGURE D-43. S/N 1 GYRO DATA, DEGREE/HOUR (1 HOUR TEST)

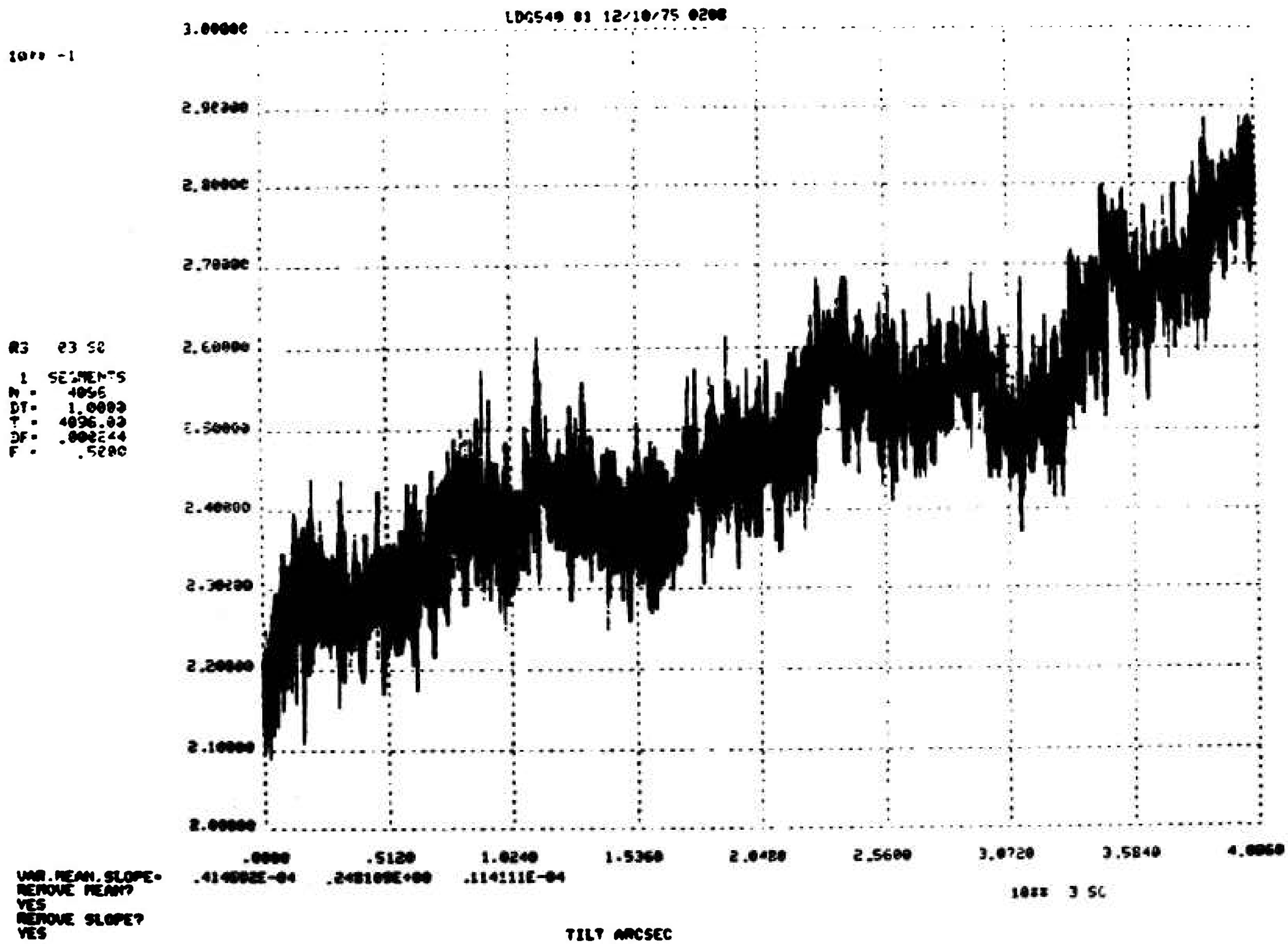

FIGURE D-44. AVERAGE TILT, ARC SECONDS (1 HOUR TEST S/N 1)

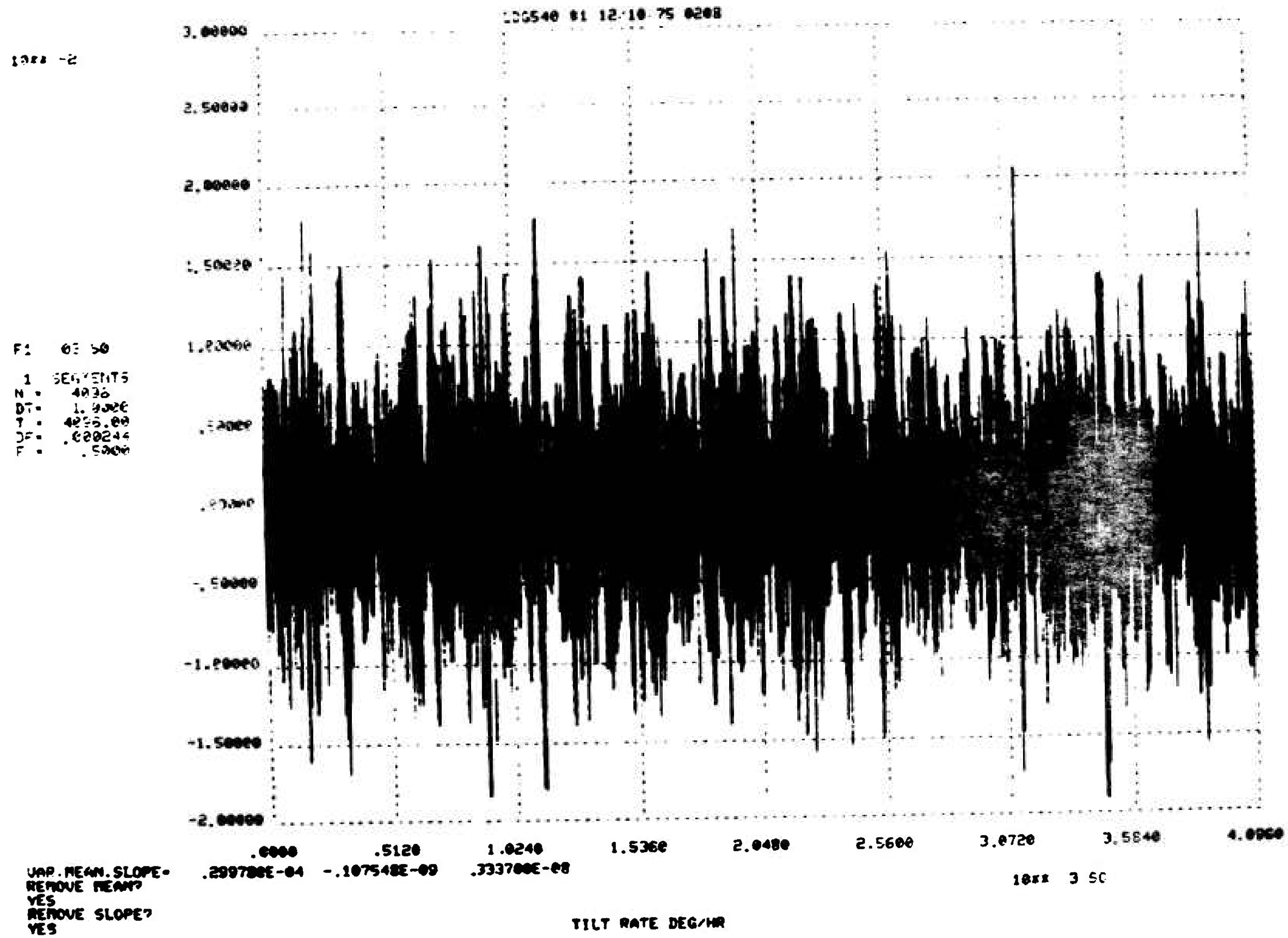

FIGURE D-45. TILT RATE, DEGREE/HOUR (1 HOUR TEST S/N 1)

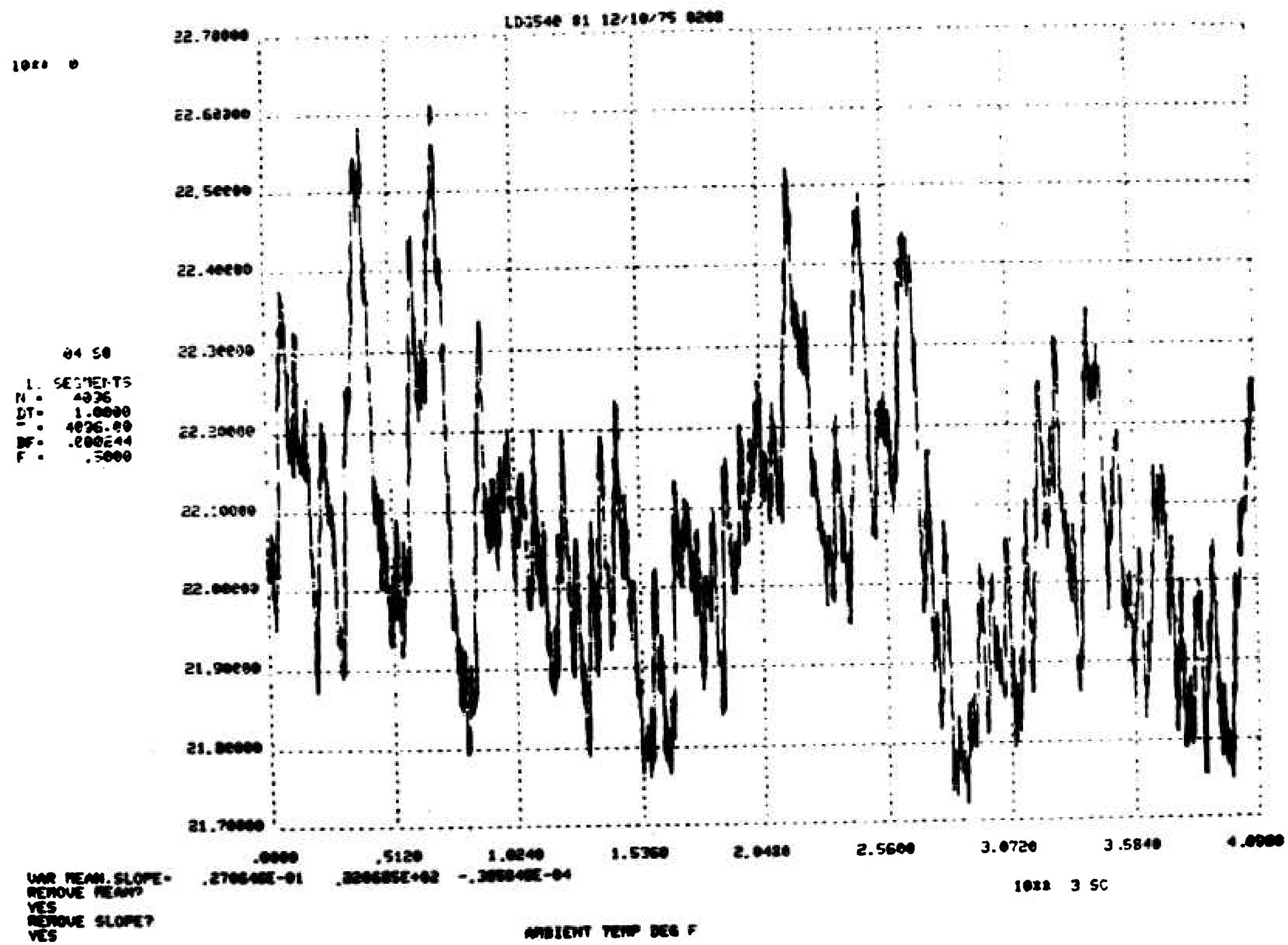

FIGURE D-46. AMBIENT TEMPERATURE, DEGREE F (1 HOUR TEST S/N 1)

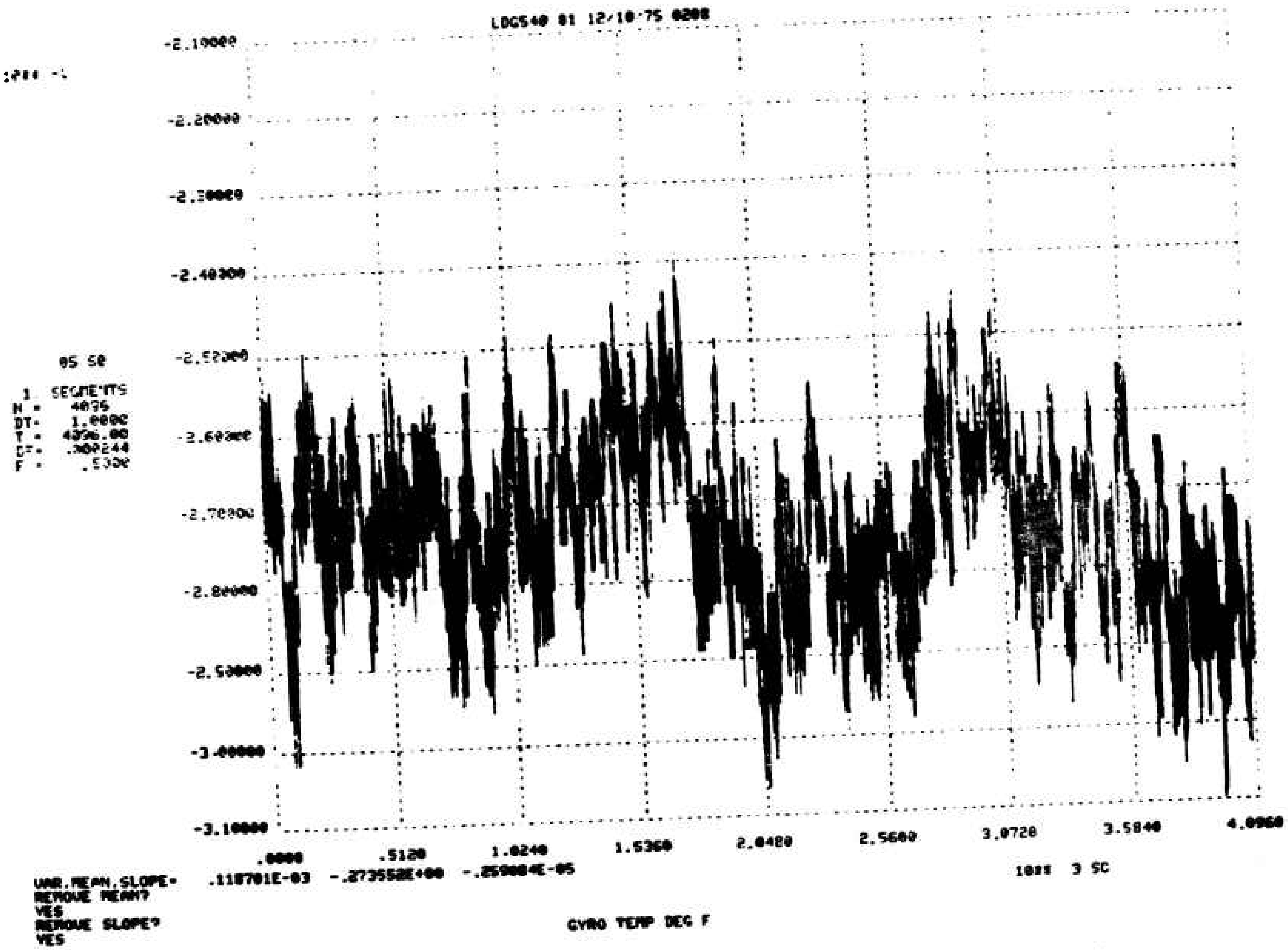

FIGURE D-47. S/N 1 GYRO CASE TEMPERATURE, DEGREE F (1 HOUR TEST)

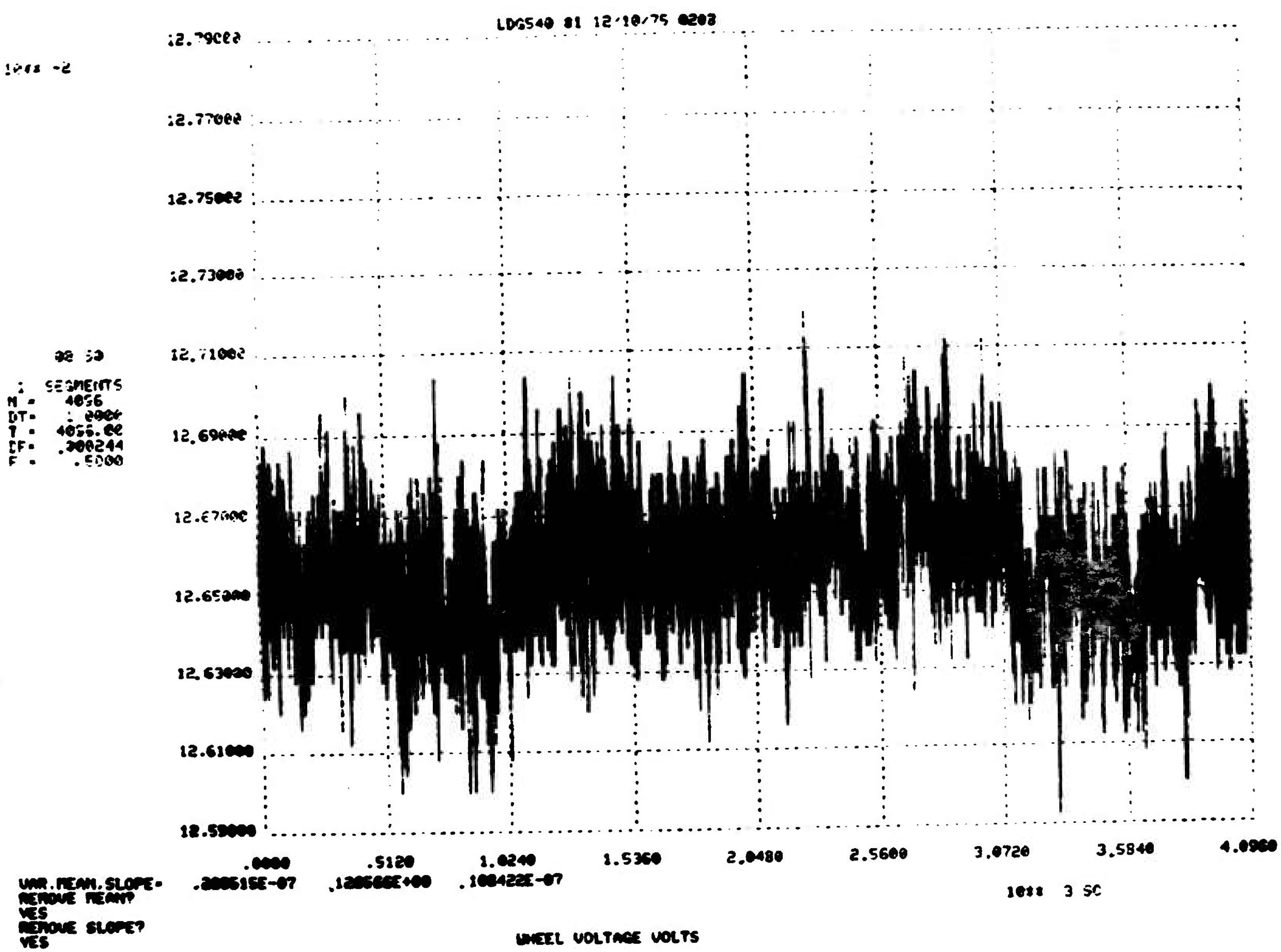

FIGURE D-48. S/N 1 GYRO WHEEL VOLTAGE, VOLTS (1 HOUR TEST)

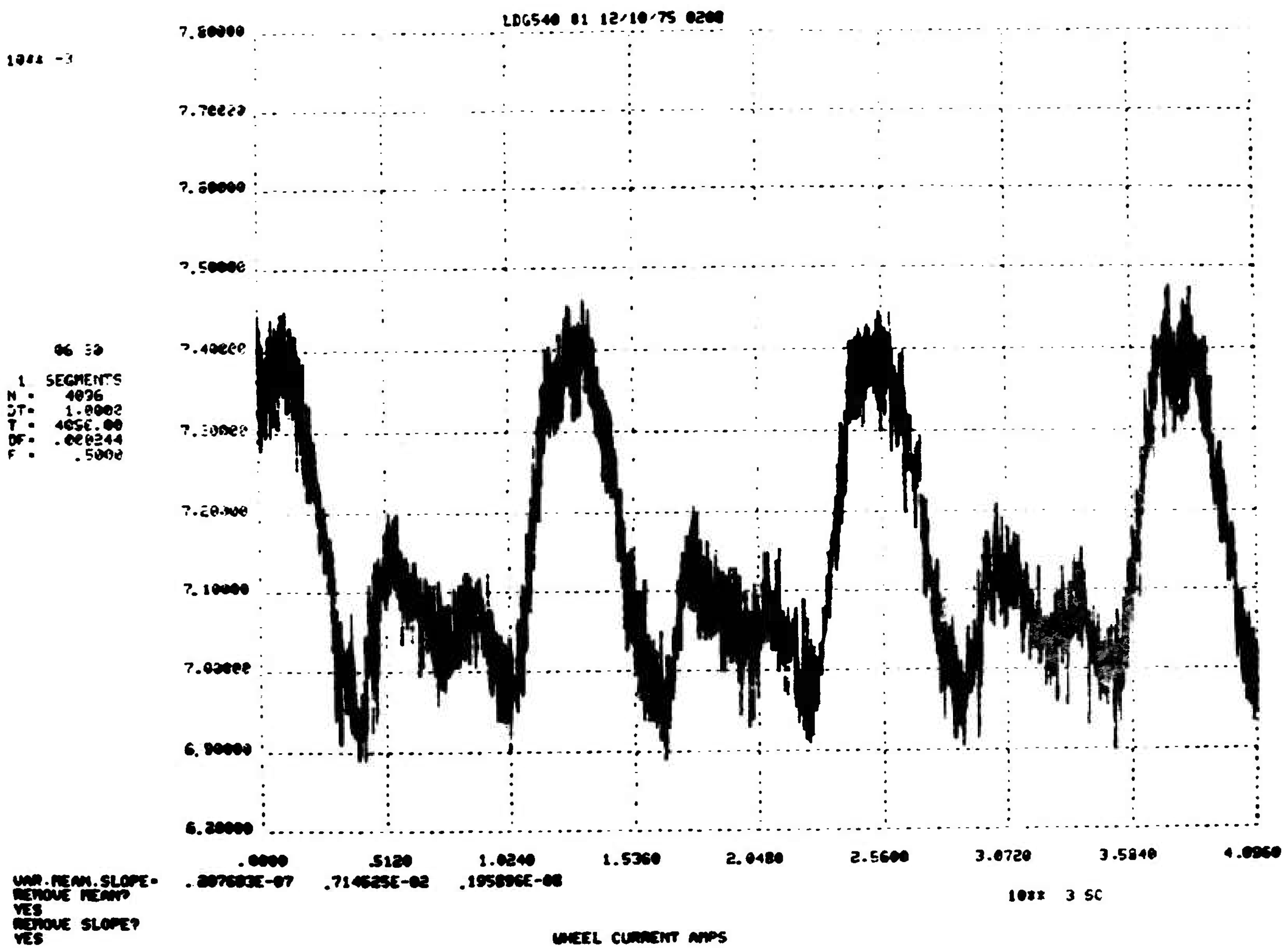

FIGURE D-49. S/N 1 GYRO WHEEL CURRENT, AMPS (1 HOUR TEST)

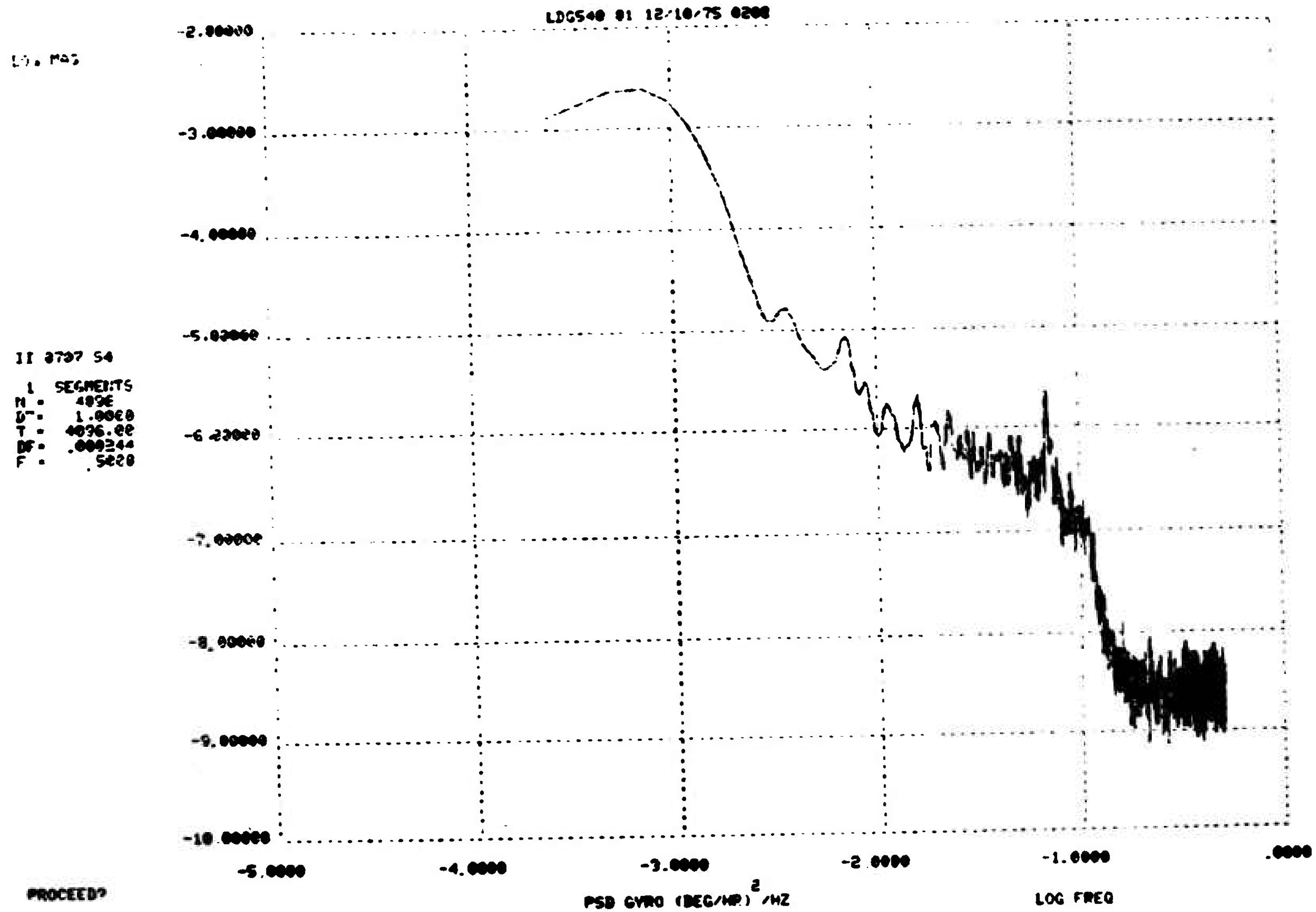

FIGURE D-50. PSD S/N 1 GYRO DATA, (DEGREE/HOUR)^2/HZ (1 HOUR TEST)

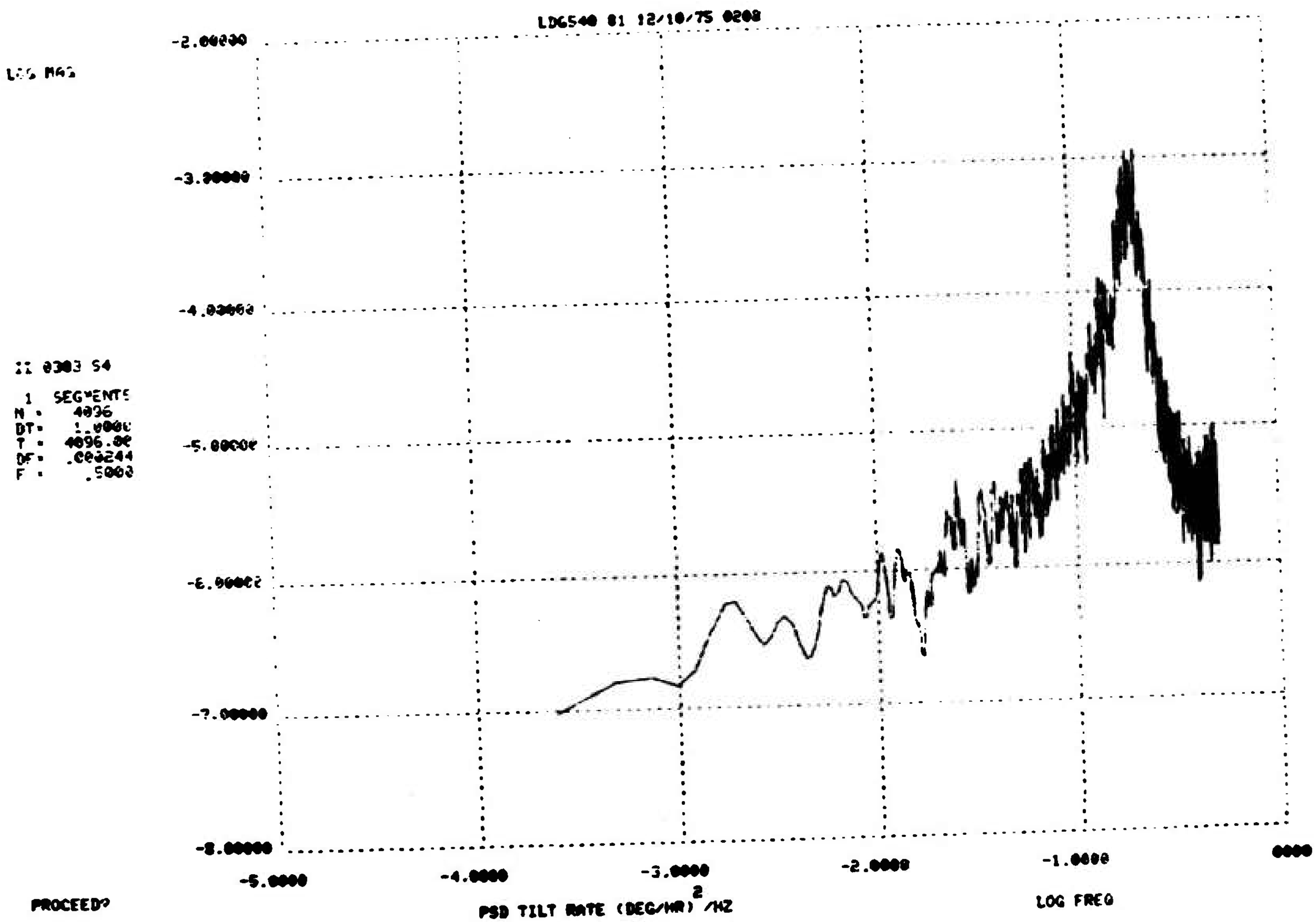

FIGURE D-51. PSD TILT RATE, (DEGREE/HOUR)^2/HZ (1 HOUR TEST S/N 1)

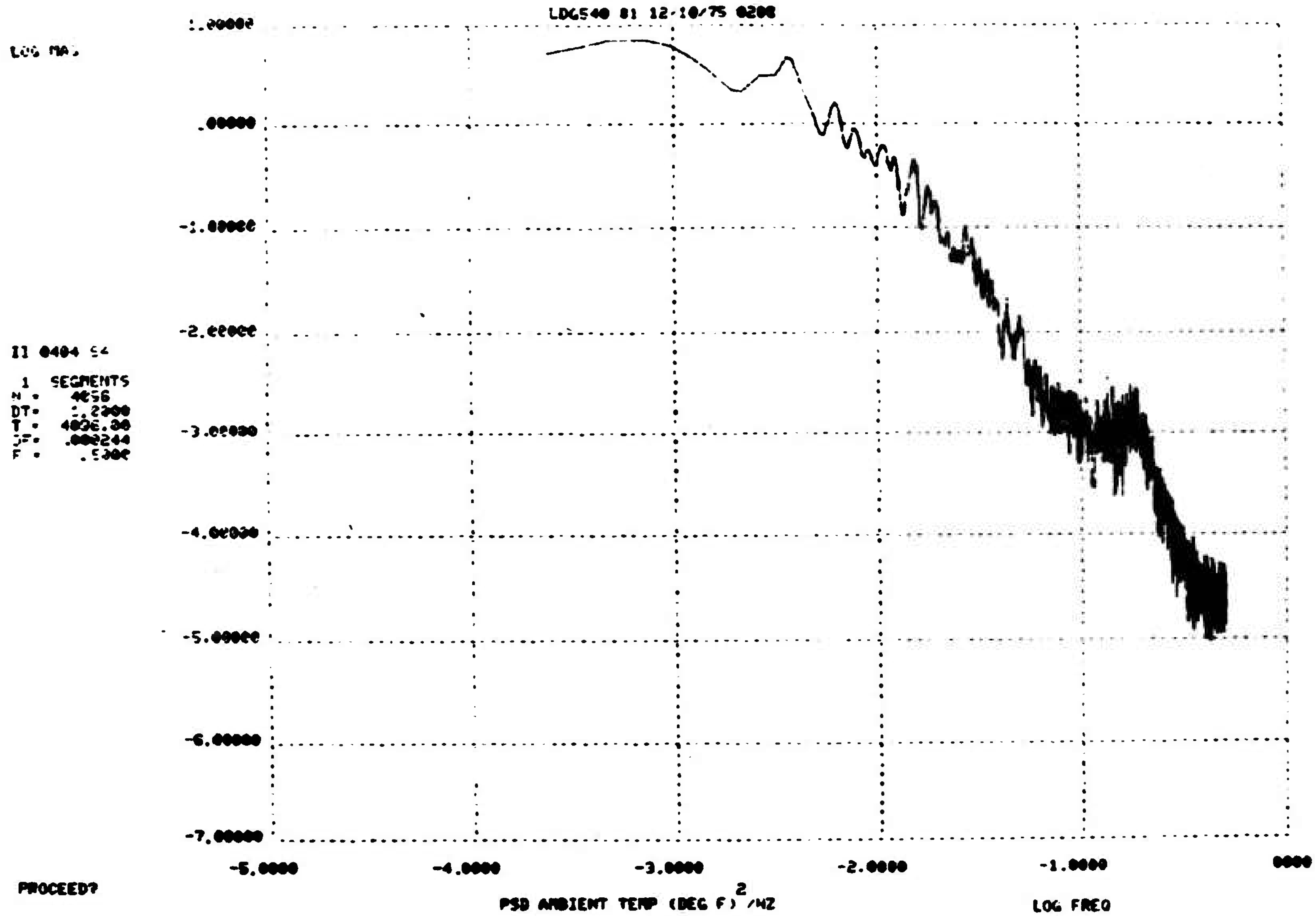

FIGURE D-52. PSD AMBIENT TEMPERATURE, (DEGREE F)^2/HZ (1 HOUR TEST S/N 1)

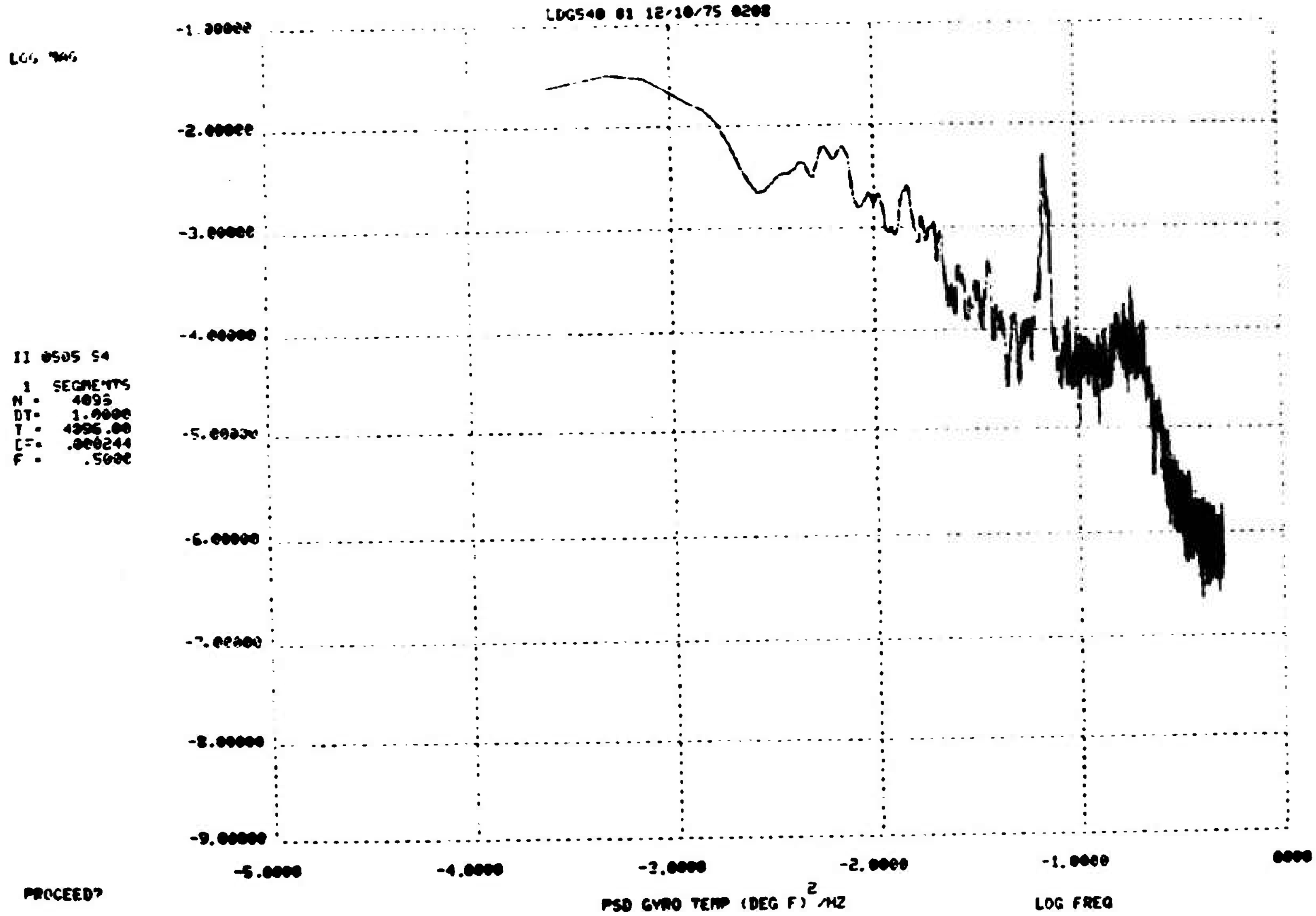

FIGURE D-53. PSD S/N 1 GYRO CASE TEMPERATURE, (DEGREE F)^2/HZ (1 HOUR TEST)

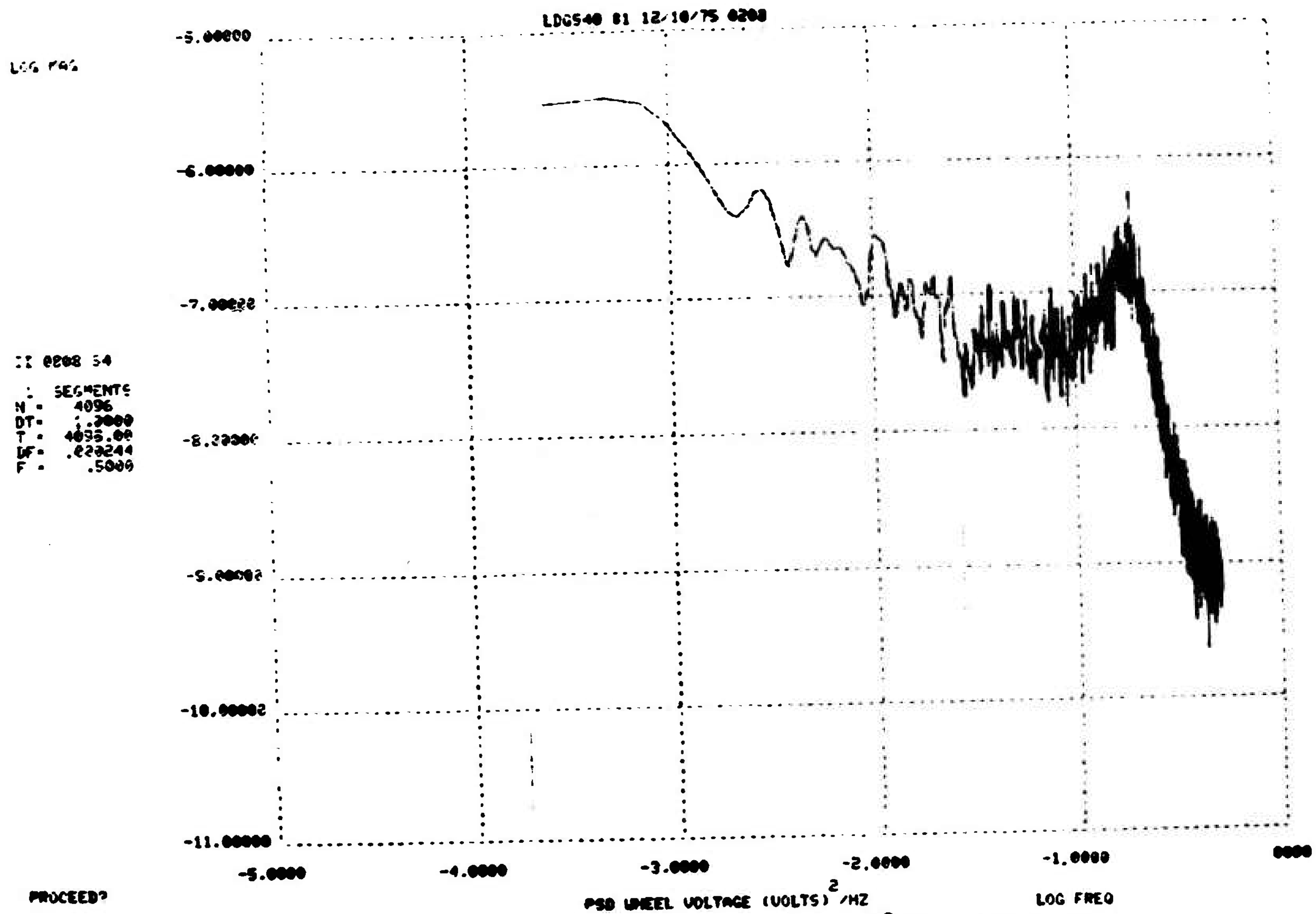

FIGURE D-54. PSD S/N 1 WHEEL VOLTAGE, $(VOLTS)^2/HZ$ (1 HOUR TEST)

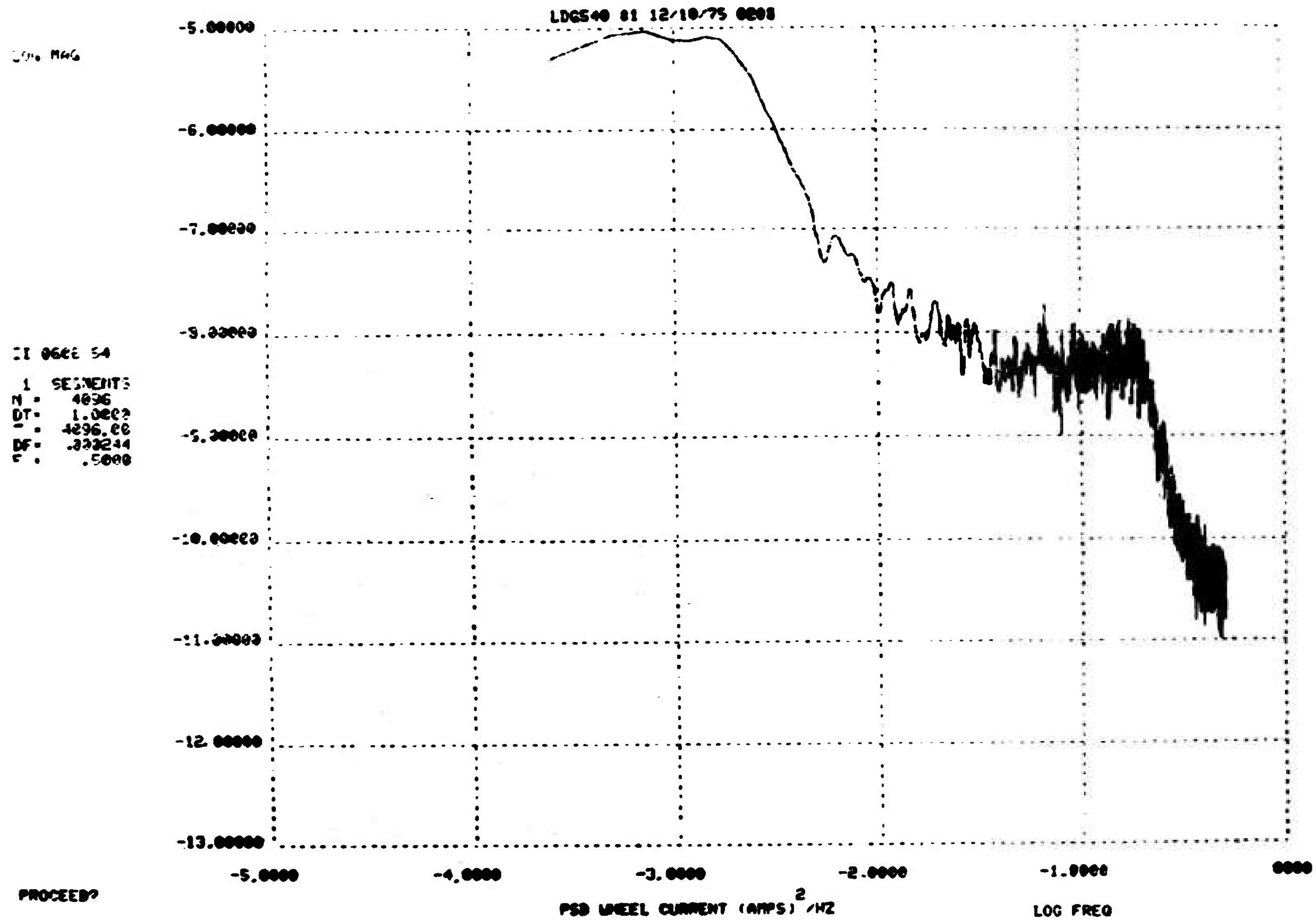

FIGURE D-55. PSD S/N 1 WHEEL CURRENT, (AMPS)^2/HZ (1 HOUR TEST)

3-MINUTE TEST S/N 1

The results of the three minute test for Gyro S/N 1 are shown in Figure D-56 through Figure D-64. PSD plots of temperature and gyro wheel supply voltage and current are not presented. The data acquisition noise PSD plots from Appendix E show considerable noise domination in both the gyro PSD, Figure D-63, and the tilt rate PSD, Figure D-64. The gyro data channel noise level is much higher for this test than it was for the longer tests presented earlier. This is because the 816 filter was used on the gyro data for this test. The gyro output starts rising above the noise level below .1 Hz. The tilt rate PSD shows significant information above the noise level below .05 Hz, and in the vicinity of .1 to .5 Hz where microseisms occur.

The gyro PSD shows little or no perceptible response above the noise level at the frequencies where microseism response is seen in the tilt rate PSD. Why the gyro did not respond could not be determined. Two possible explanations are offered: Reference 3 argues that tilt rate information above 10^{-3} Hz is dominated by lateral acceleration. In this case, the gyro would not be expected to record a significant response. On the other hand, this test could be approaching the high frequency response limit of the gyro or gyro servo loop. Throughout the longer tests shown earlier the gyro output noise level has continuously rolled off as frequency increased.

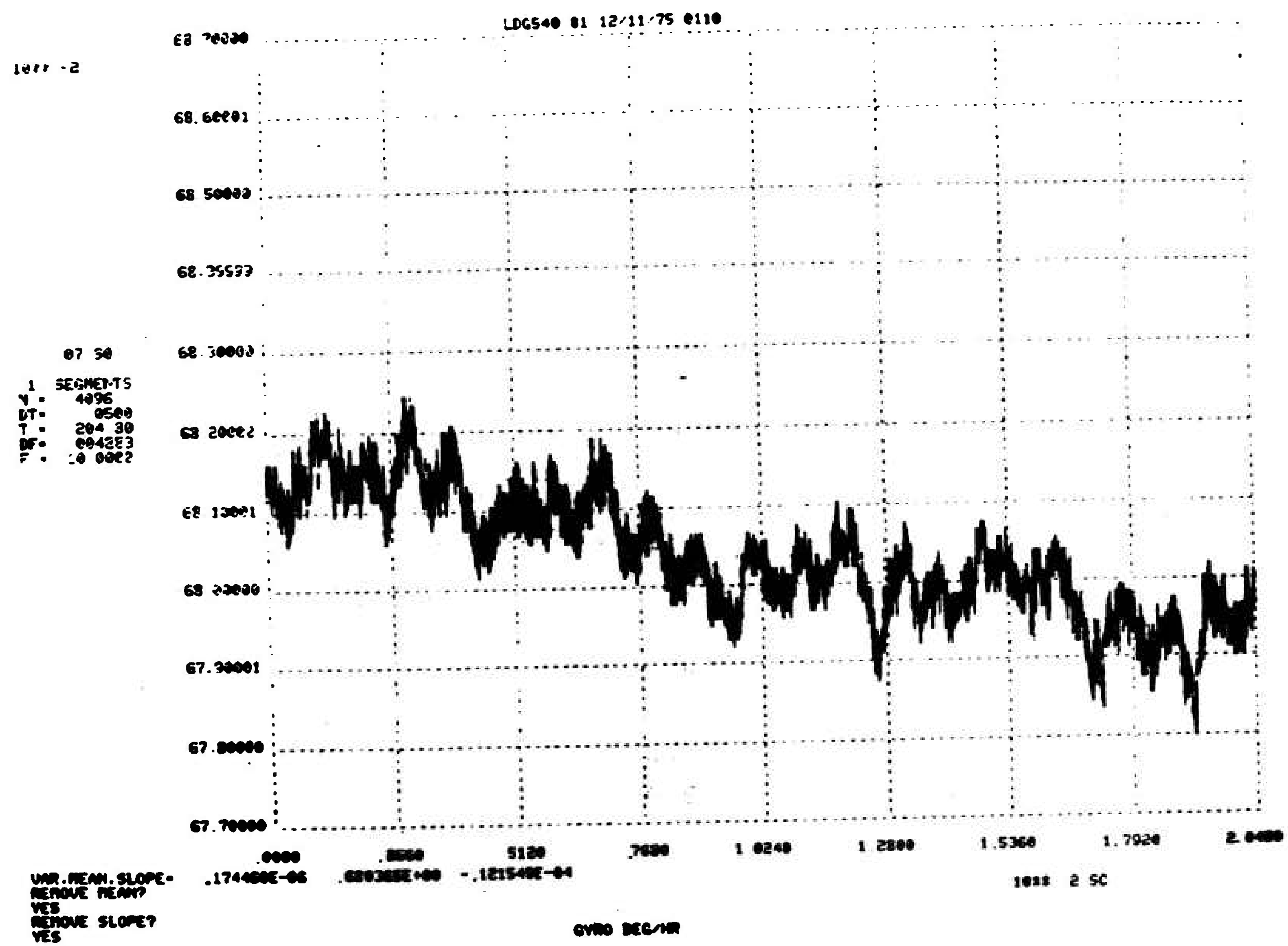

FIGURE D-56. S/N 1 GYRO DATA, DEGREE/HOUR (3 MINUTE TEST)

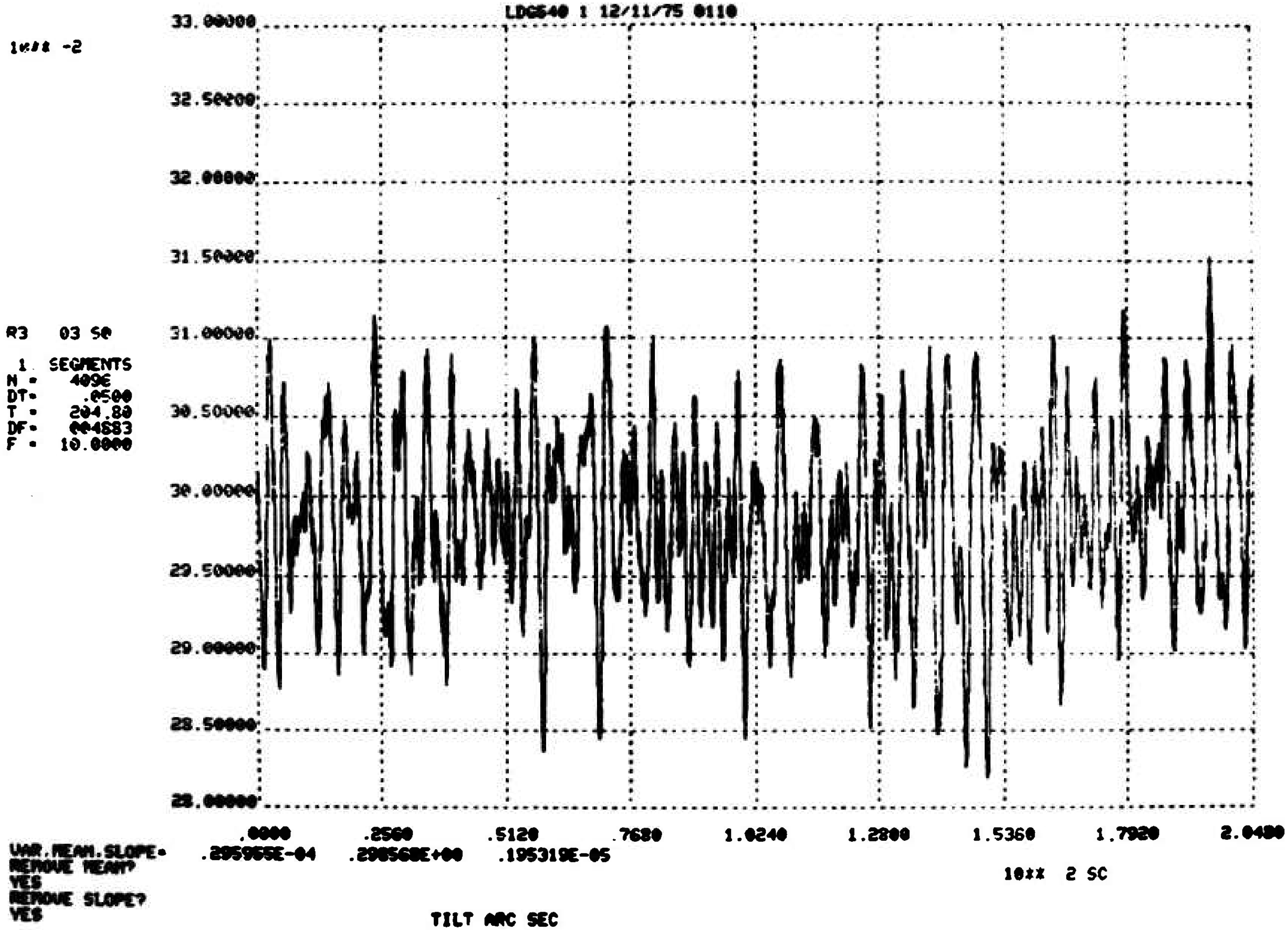

FIGURE D-57. AVERAGE TILT, ARC SECONDS (3 MINUTE TEST S/N 1)

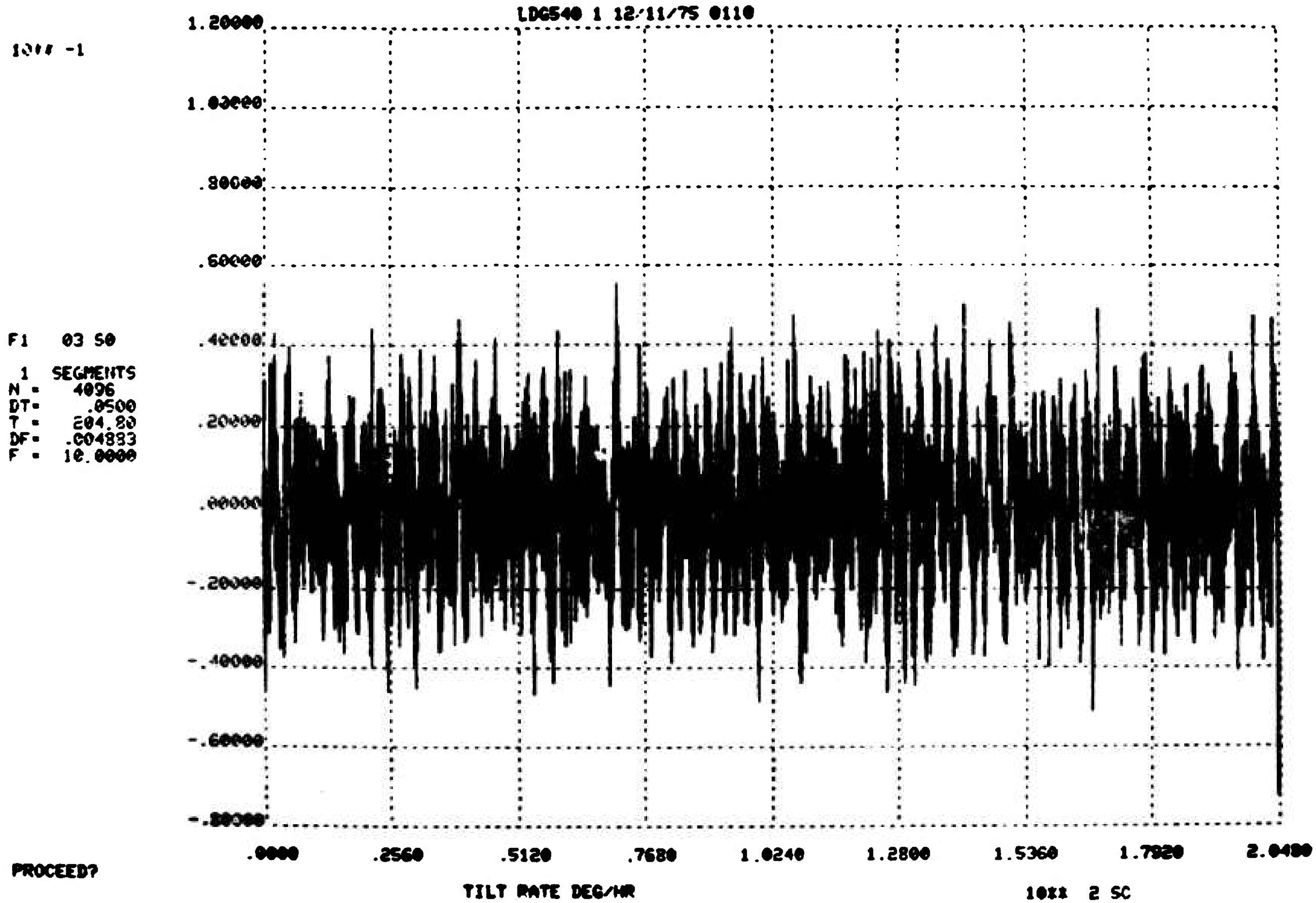

FIGURE D-58. TILT RATE, DEGREE/HOUR (3 MINUTE TEST S/N 1)

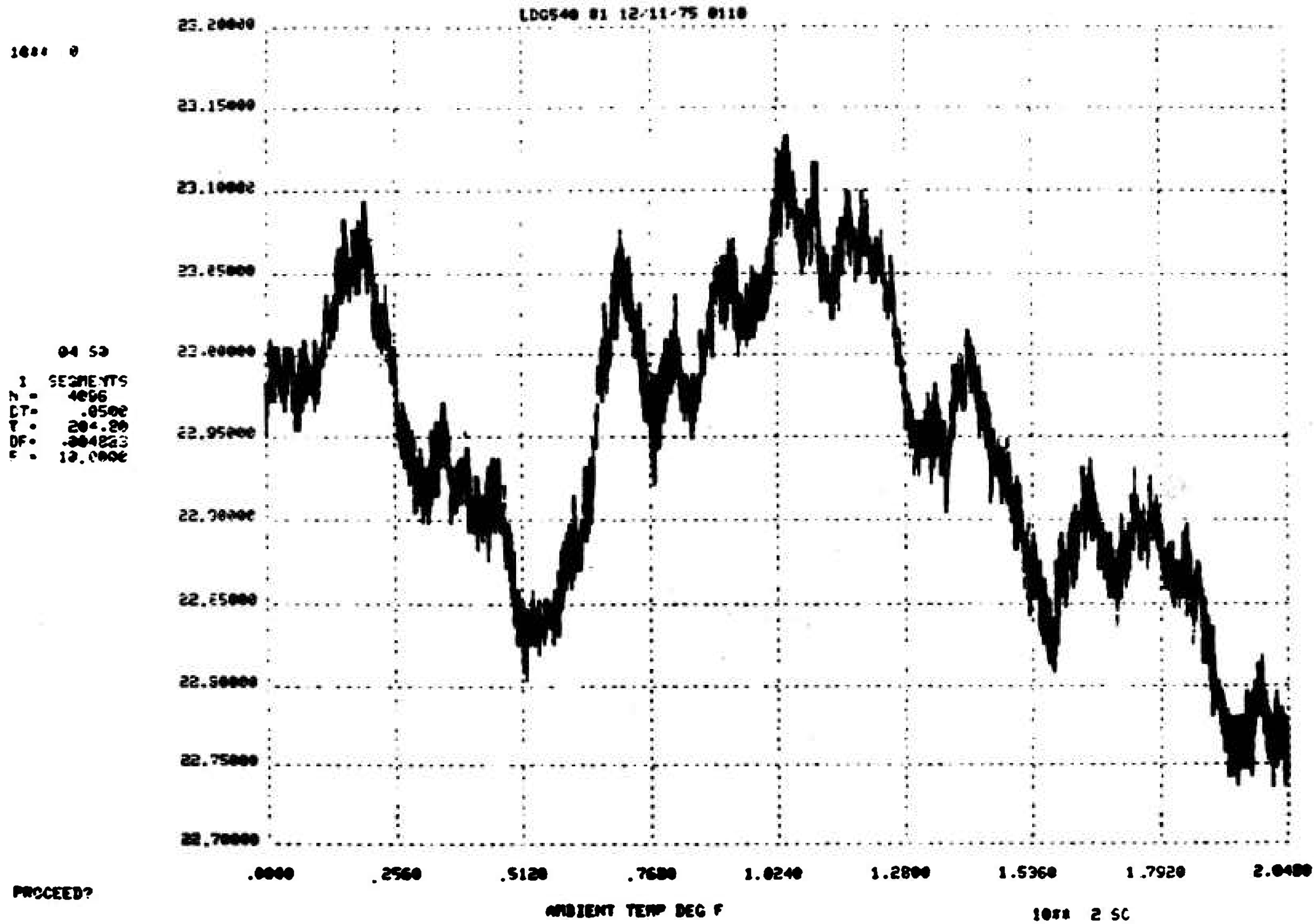

FIGURE D-59. AMBIENT TEMPERATURE, DEGREE F (3 MINUTE TEST S/N 1)

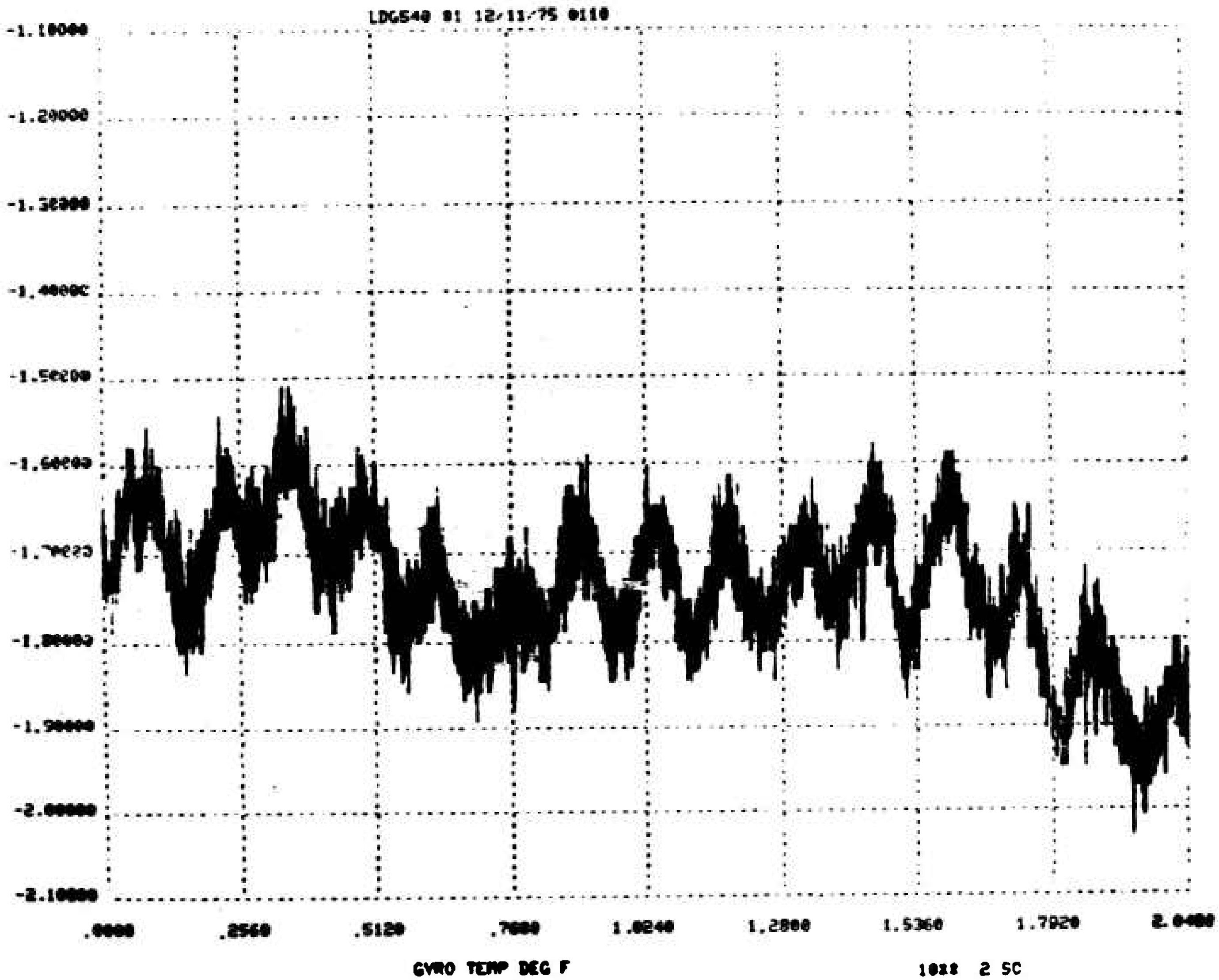

ES 50

: SEGMENTS
N = 4056
DT= .0500
T = 204.80
DF= .004883
F = 10.0200

PROCEED?

FIGURE D-60. S/N 1 GYRO CASE TEMPERATURE, DEGREE F (3 MINUTE TEST)

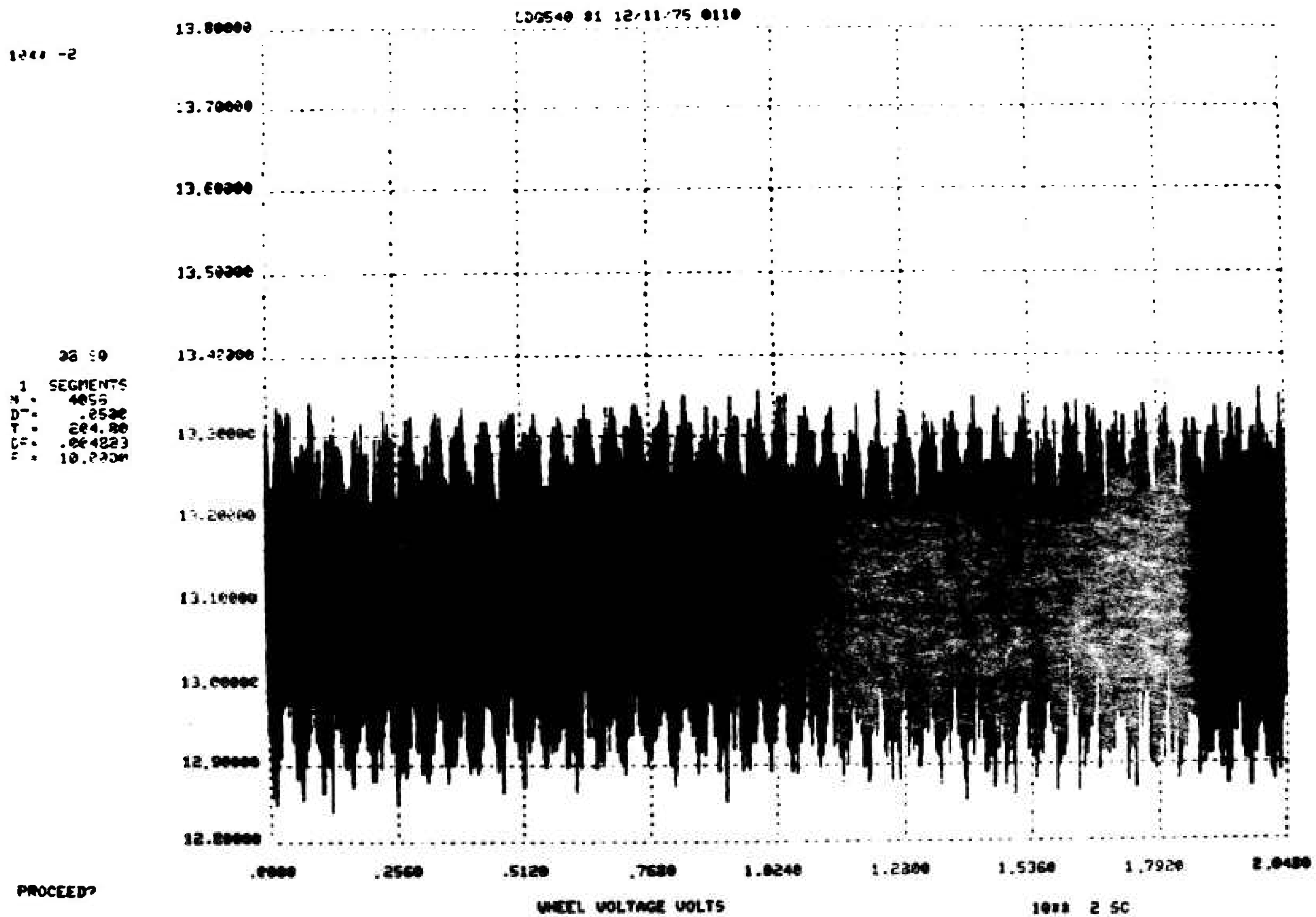

FIGURE D-61. S/N 1 GYRO WHEEL VOLTAGE, VOLTS (3 MINUTE TEST)

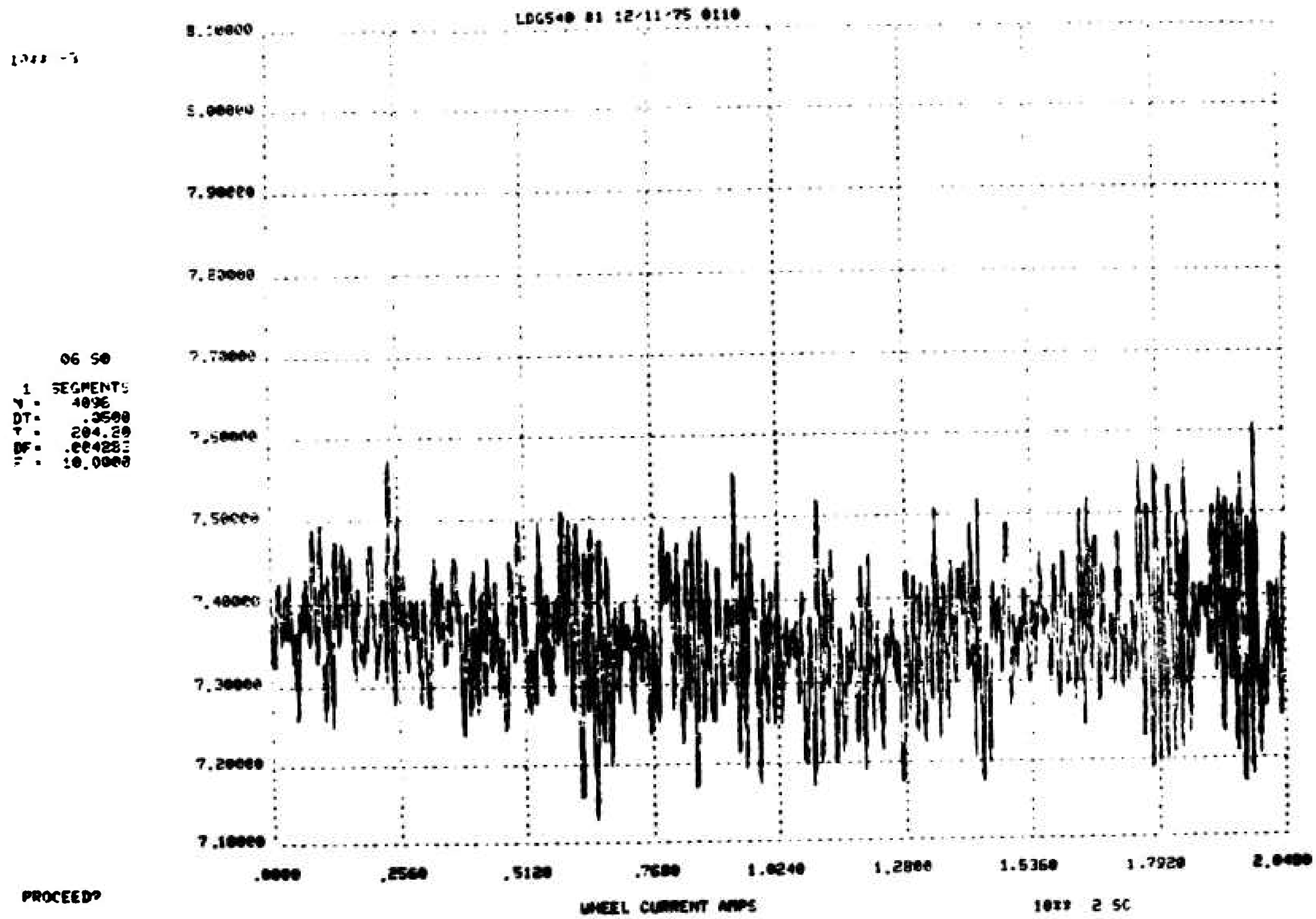

FIGURE D-62. S/N 1 GYRO WHEEL CURRENT, AMPS (3 MINUTE TEST)

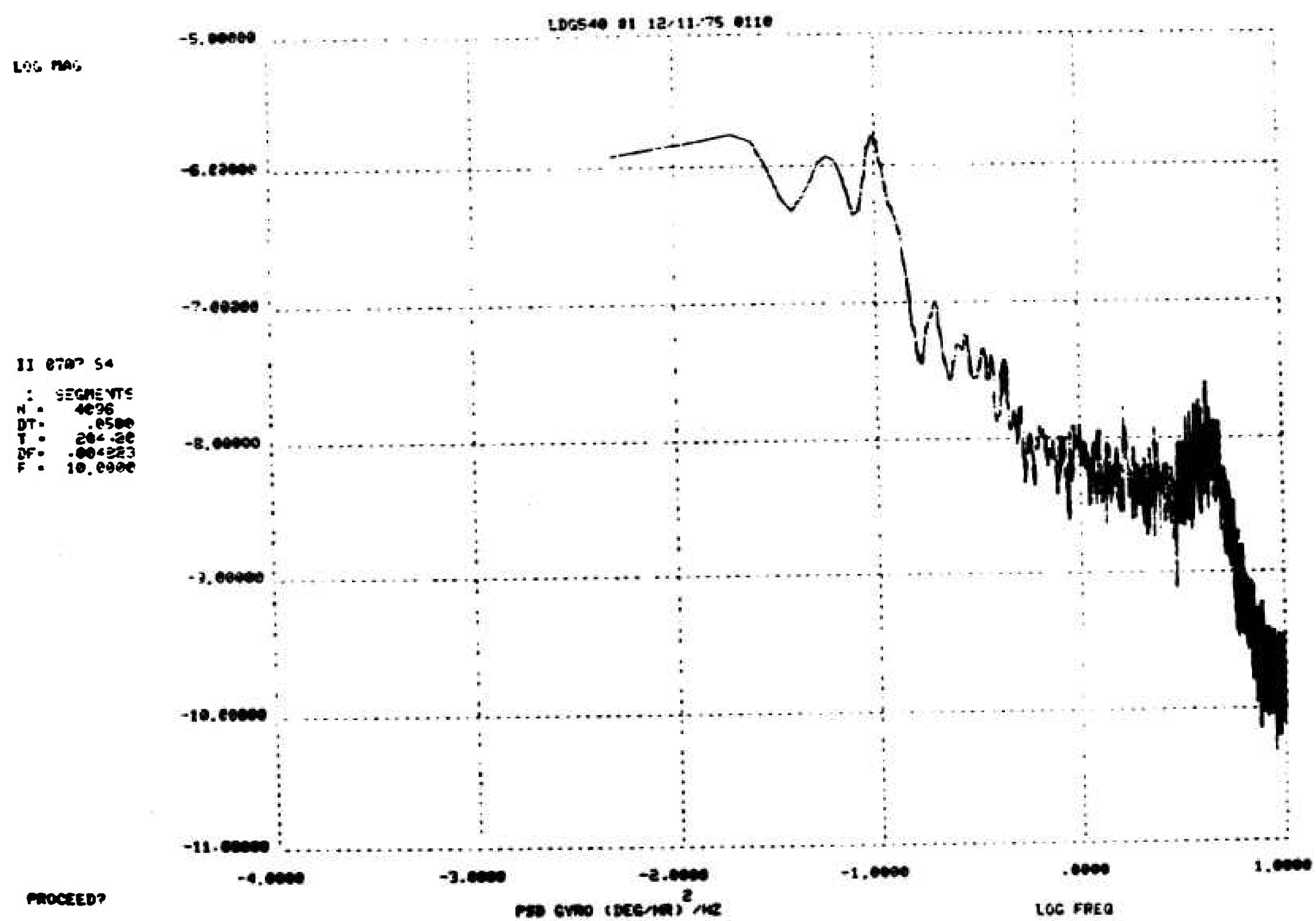

FIGURE D-63. PSD S/N 1 GYRO DATA, (DEGREE/HOUR)^2/HZ (3 MINUTE TEST)

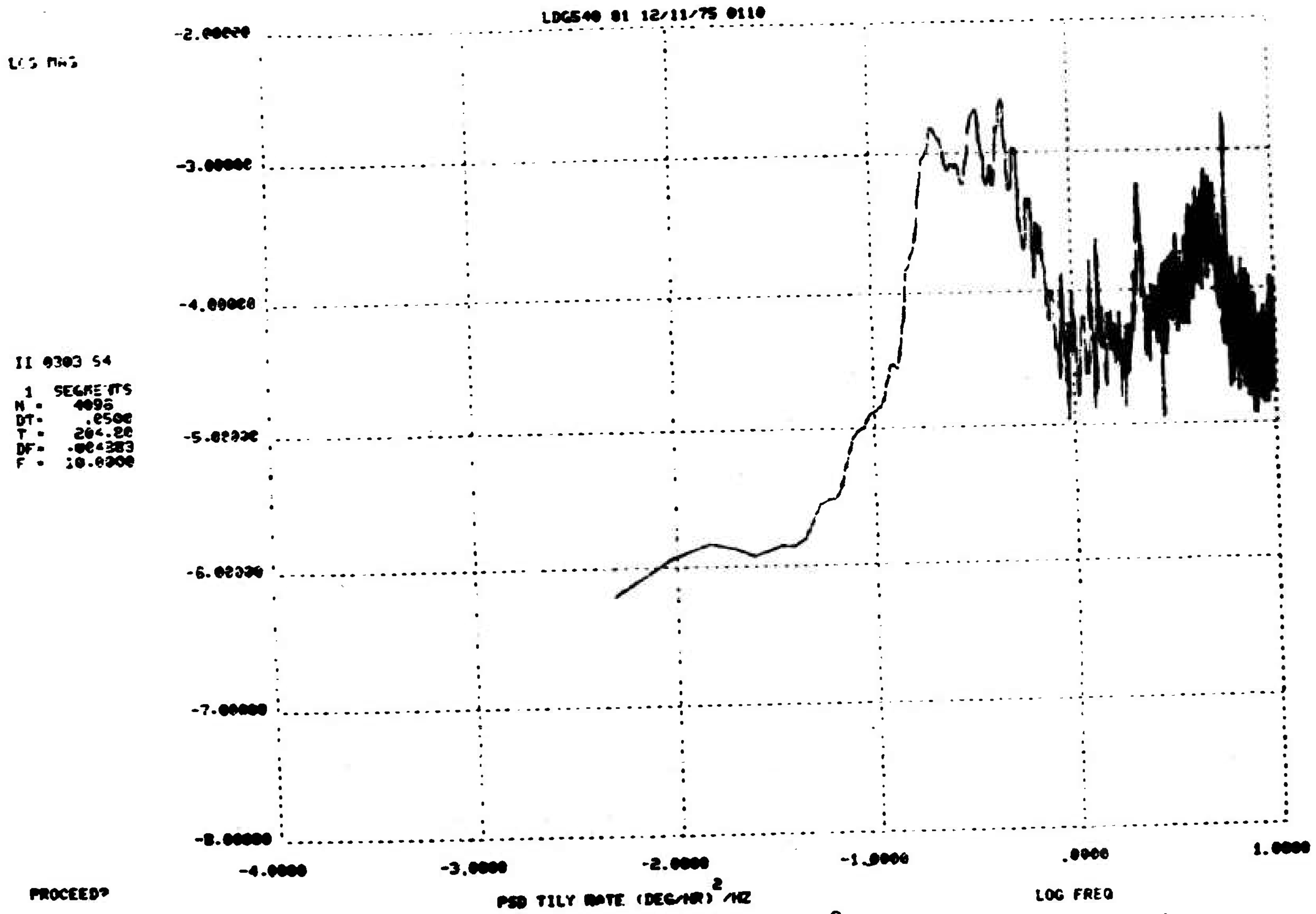

FIGURE D-64. PSD TILT RATE, (DEGREE/HOUR)^2/HZ (3 MINUTE TEST S/N 1)

24 HOUR TEST #1 S/N 2

Shown in Figure D-65 through Figure D-76 are the results of the first 24 hour test on Gyro S/N 2. The gyro output, and all monitored functions for the twenty-four tests of gyro S/N 2 were significantly above the noise level recorded in Appendix E. Note that the lowest frequency regions of the gyro PSD, Figure D-72, compare favorably with the results obtained from Gyro S/N 1. The mid frequency regions of the gyro PSD still appear dependent upon the gyro wheel current, Figure D-76. However, the frequency of the predominant wheel current variations in Gyro S/N 2, Figure D-70, was much lower than shown in Figure D-65 for Gyro S/N 1.

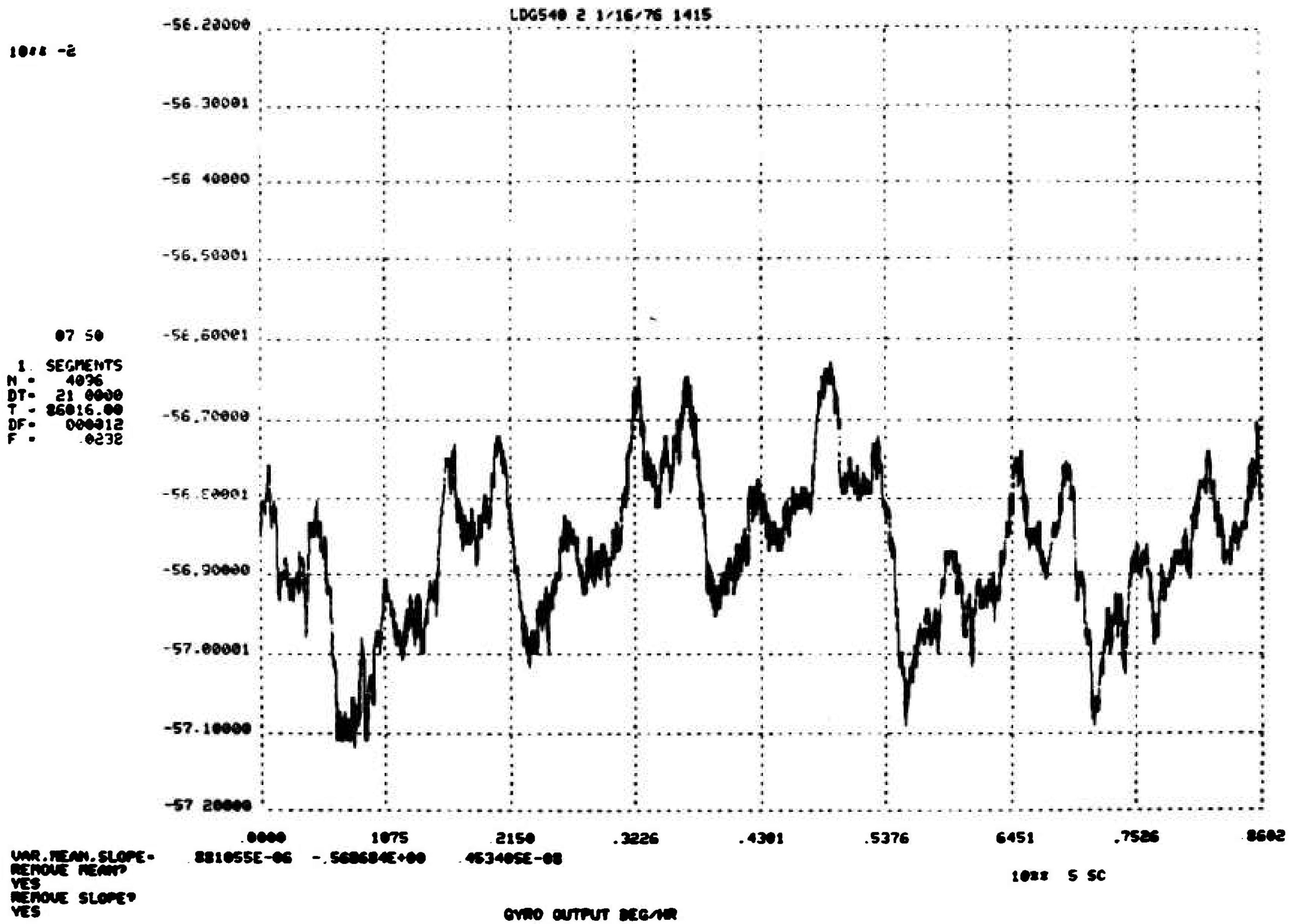

FIGURE D-65. S/N 2 GYRO DATA, DEGREE/HOUR (24 HOUR TEST #1)

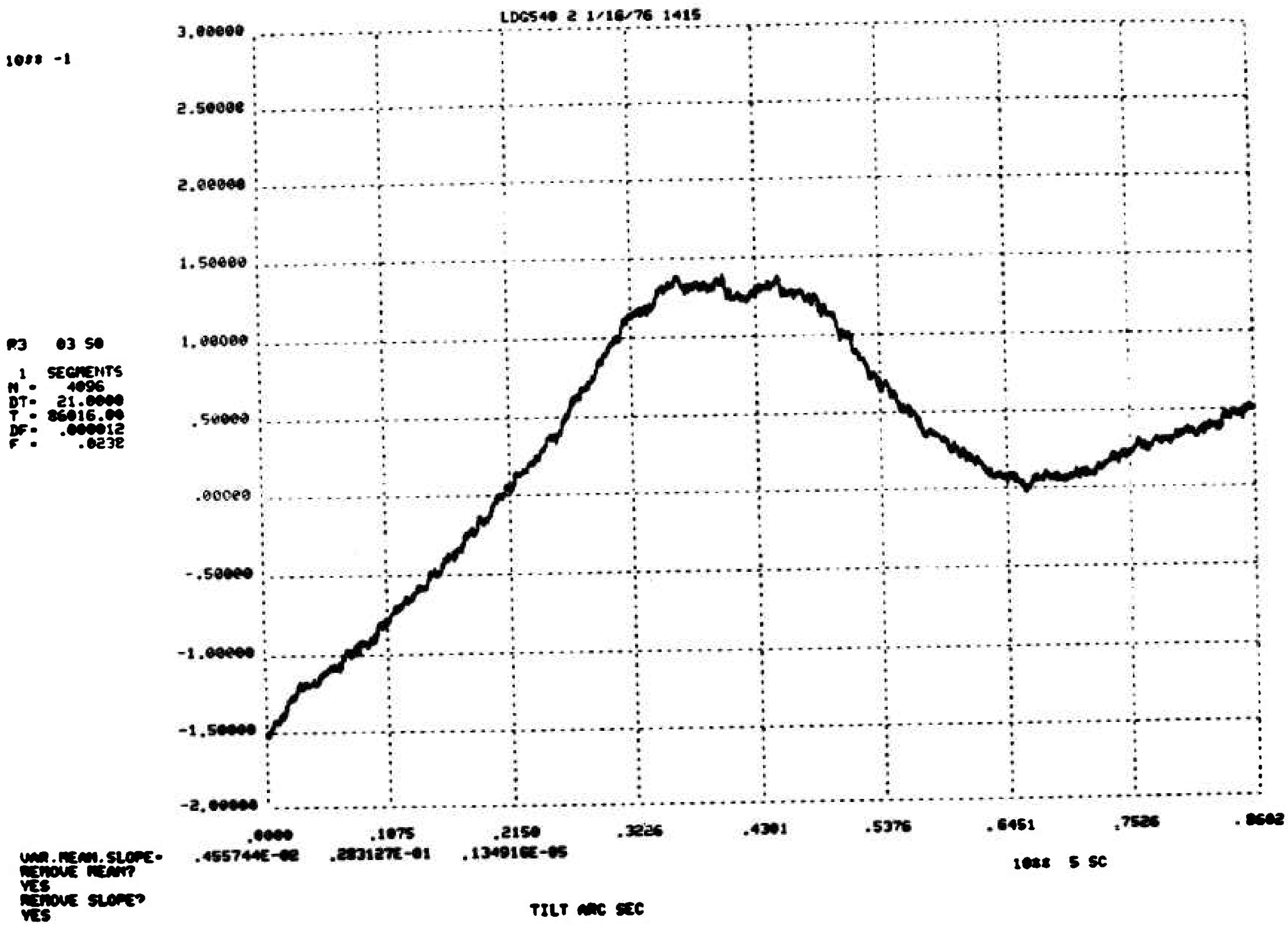

FIGURE D-66. AVERAGE TILT, ARC SECONDS (S/N 2 24 HOUR TEST #1)

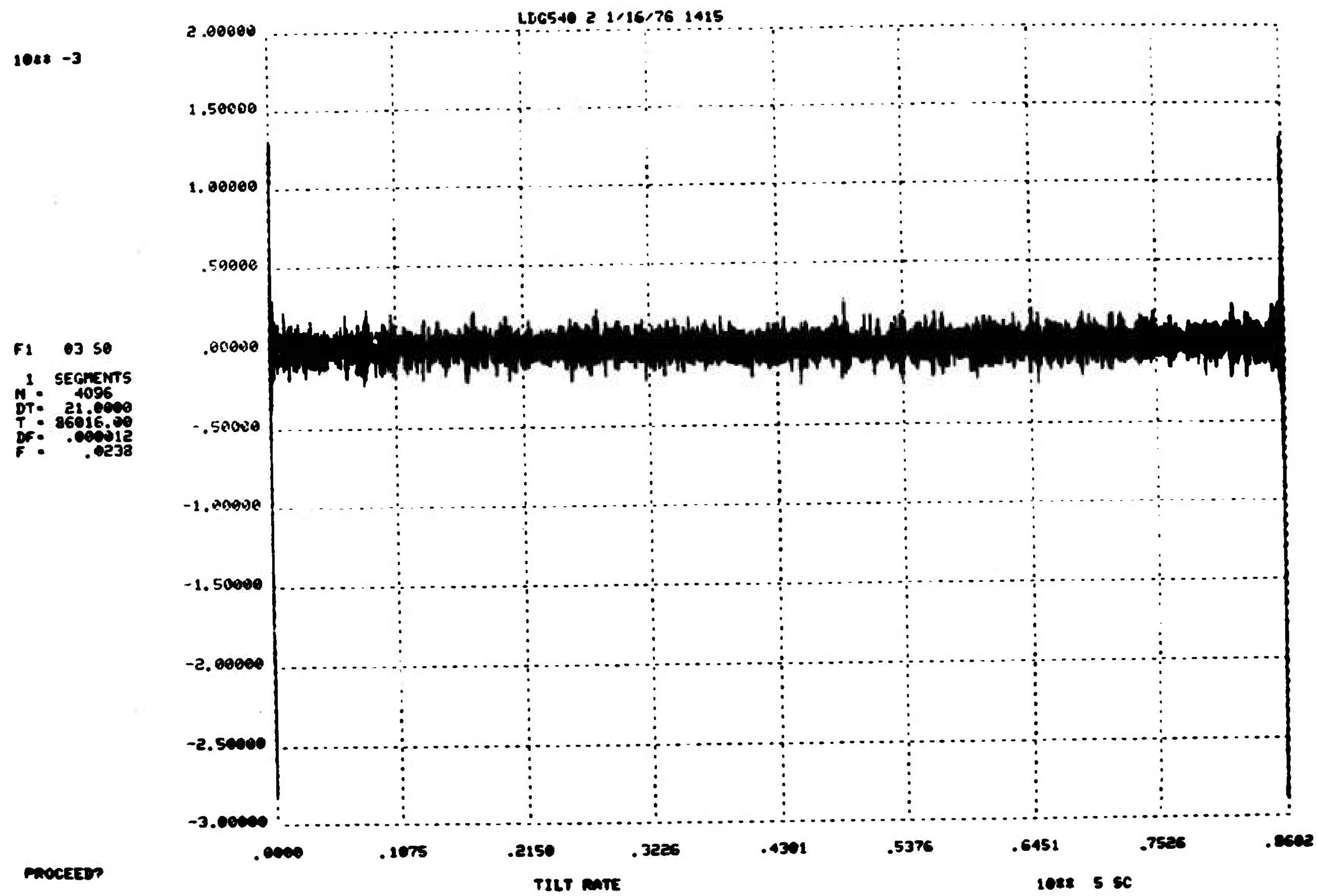

FIGURE D-67. TILT RATE, DEGREE/HOUR (S/N 2 24 HOUR TEST #1)

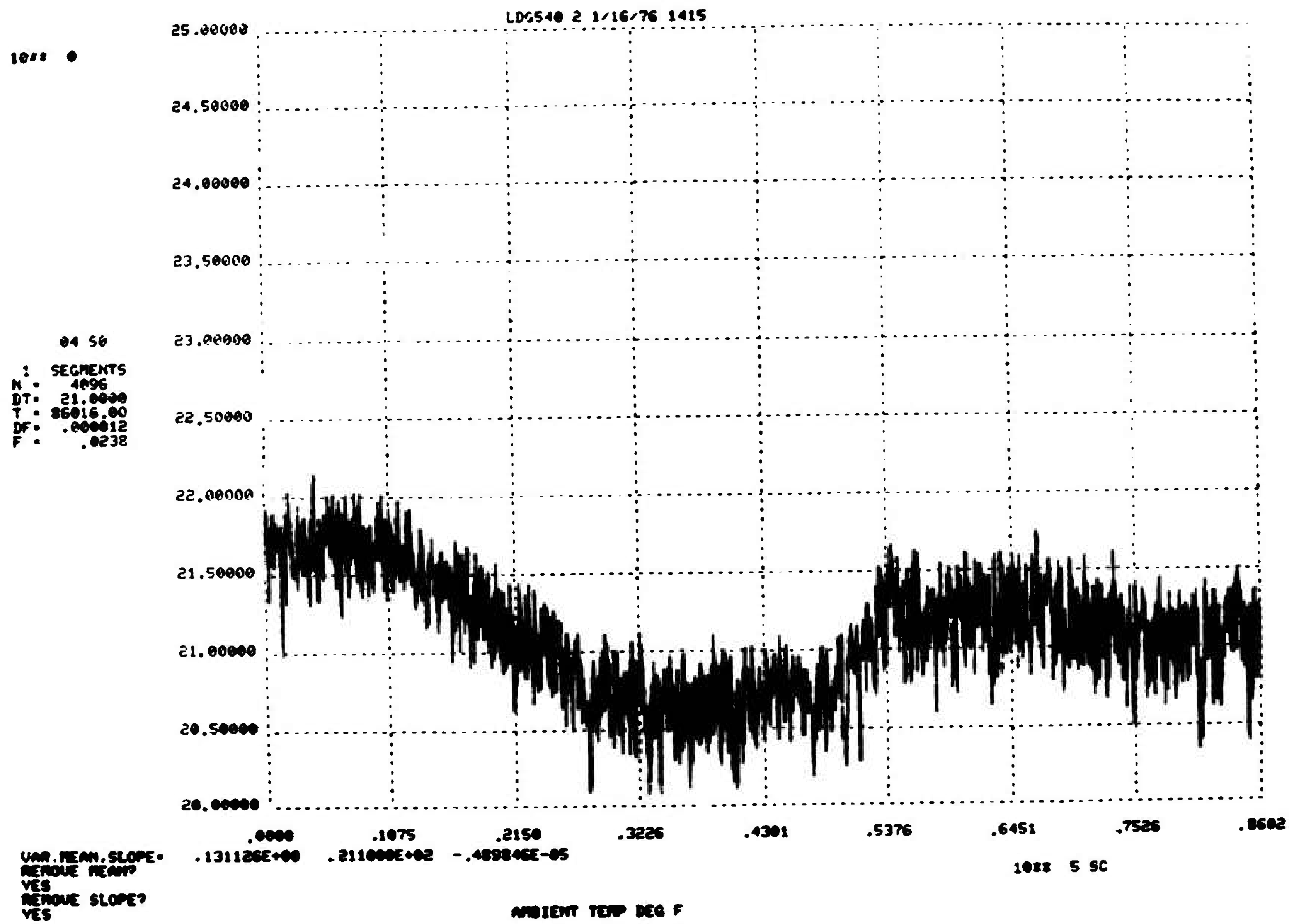

FIGURE D-68. AMBIENT TEMPERATURE, DEGREE F (S/N 2 24 HOUR TEST #1)

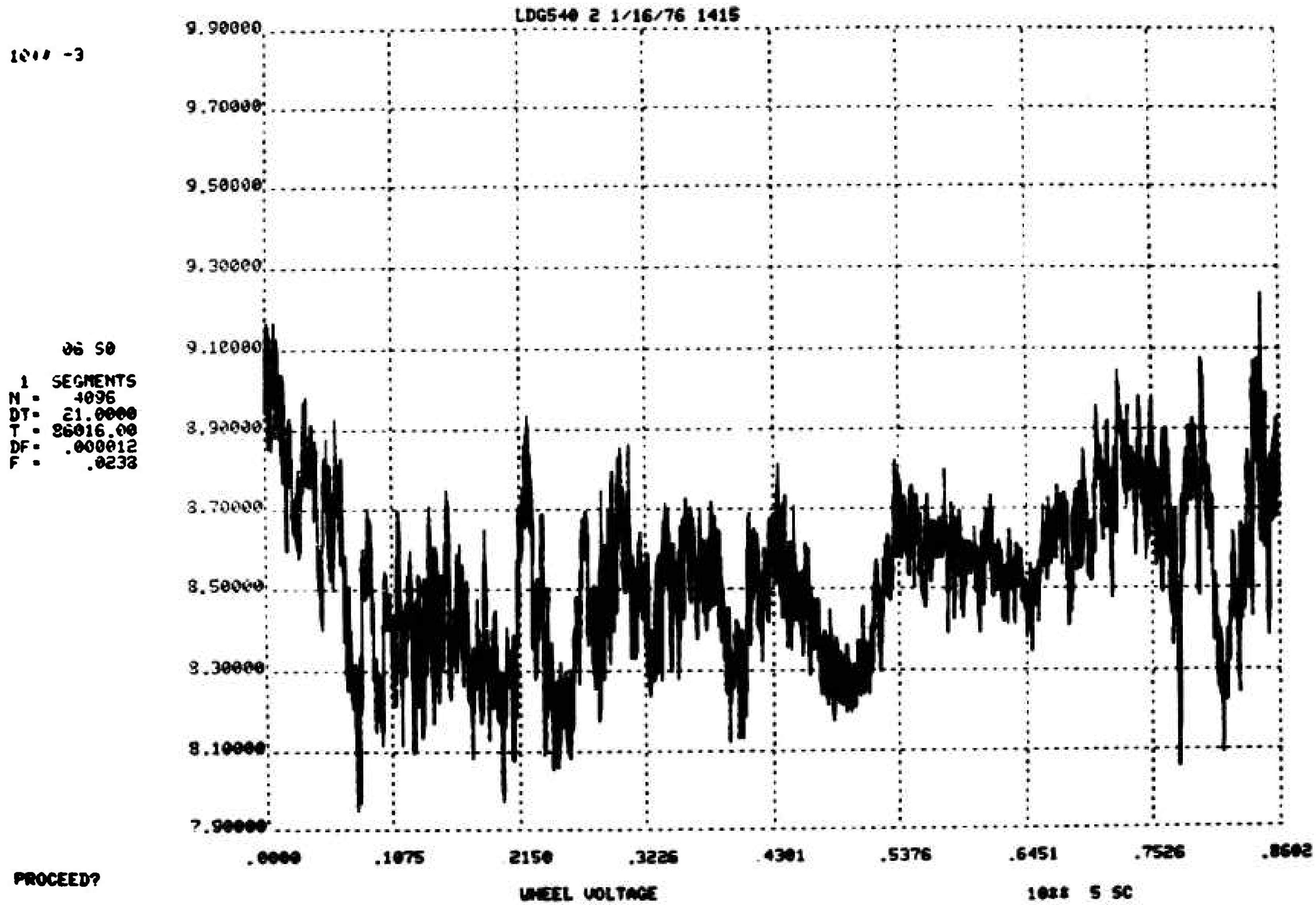

FIGURE D-69. S/N 2 GYRO WHEEL VOLTAGE, VOLTS (24 HOUR TEST #1)

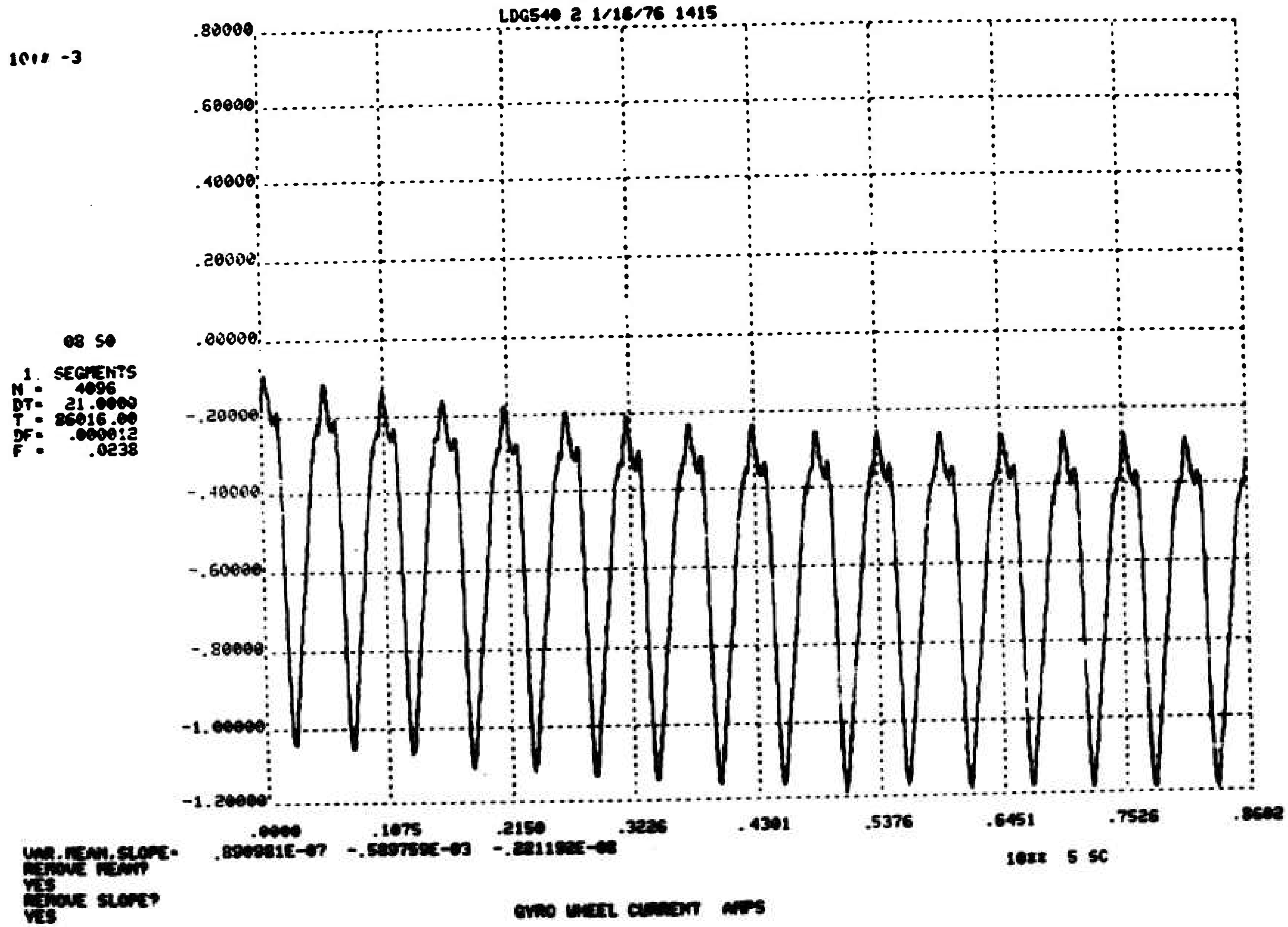

FIGURE D-70. S/N 2 GYRO WHEEL CURRENT, AMPS (24 HOUR TEST #1)

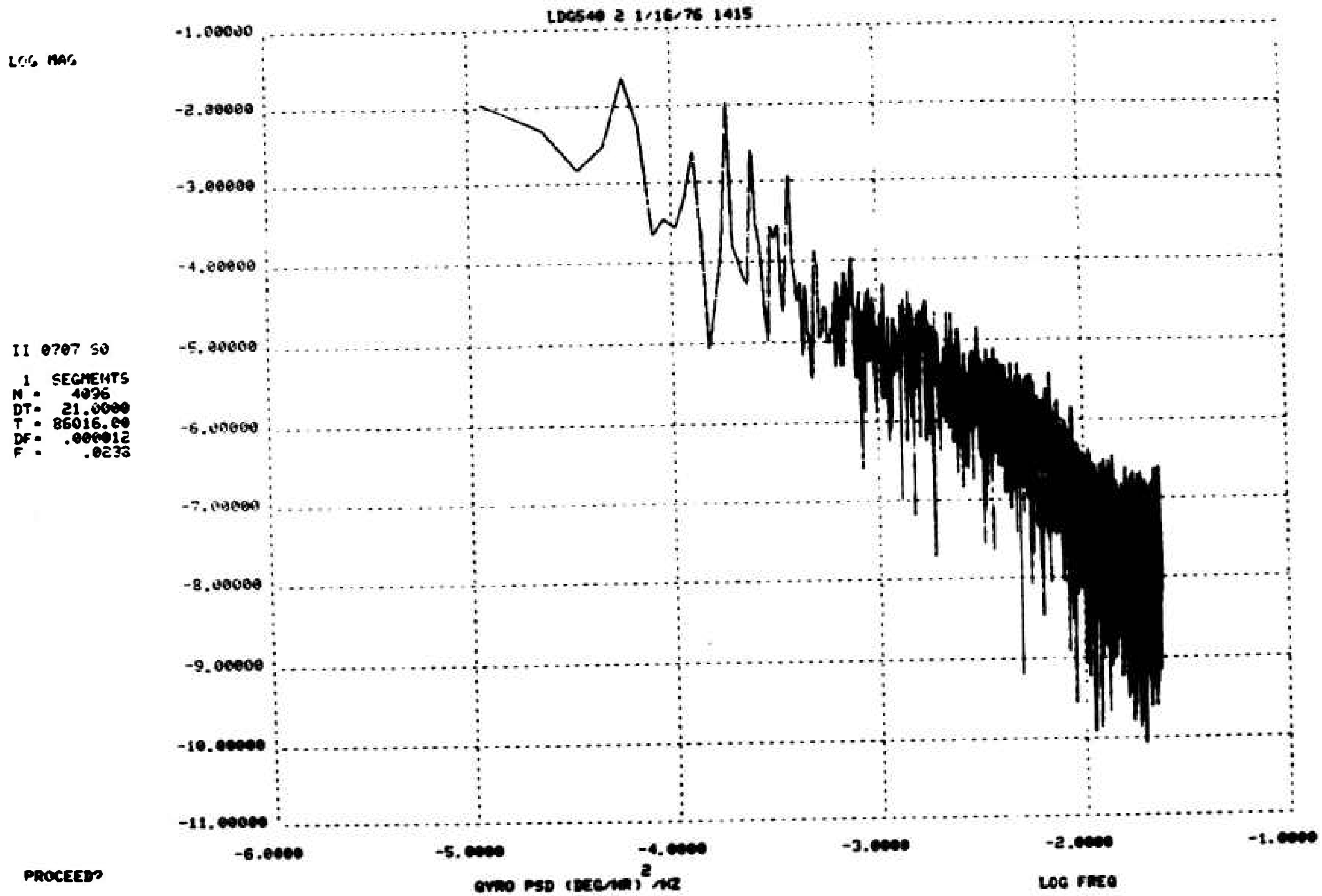

FIGURE D-71. UNSMOOTHED PSD S/N 2 GYRO DATA, (DEGREE/HOUR)^2/HZ (24 HOUR TEST #1)

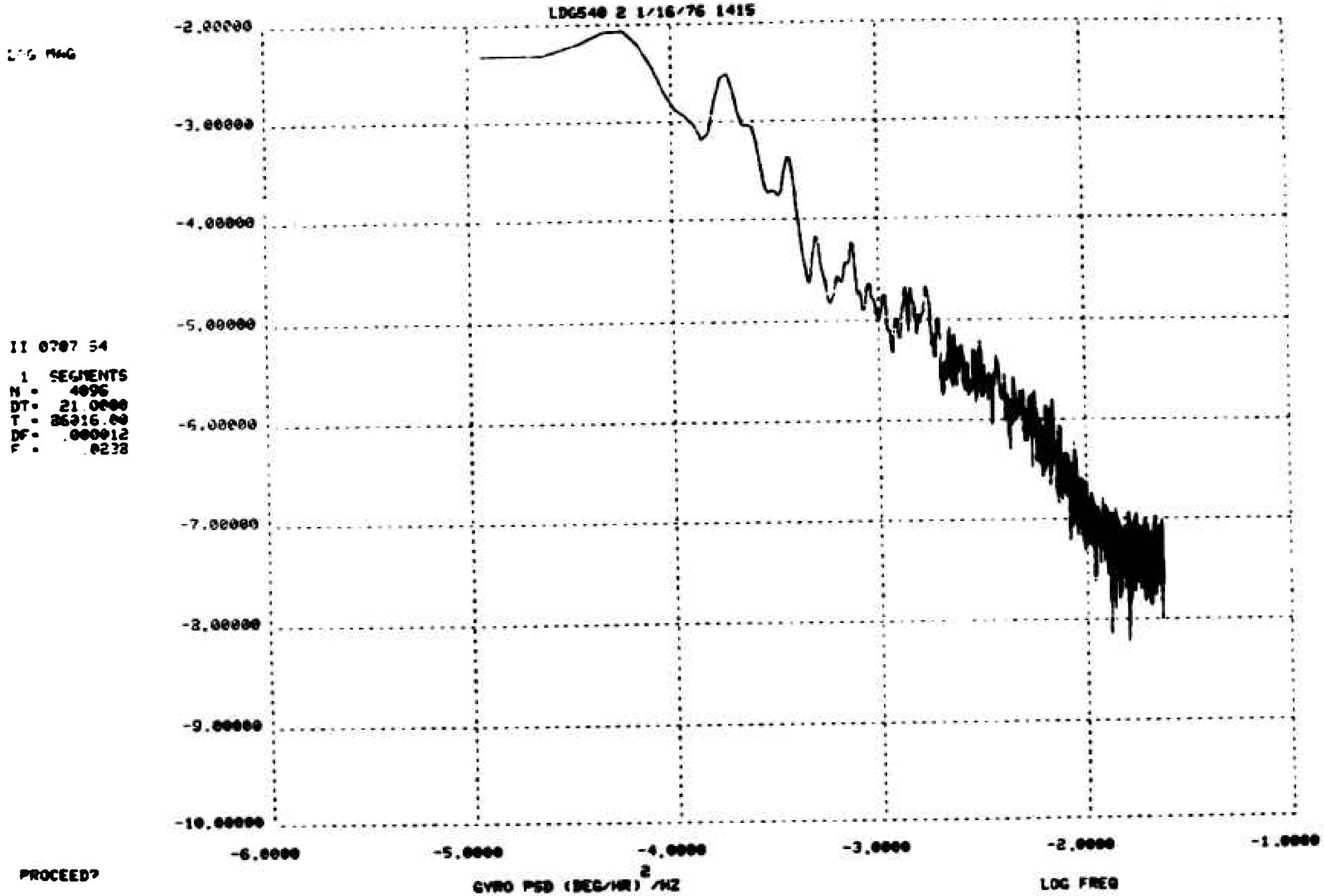

FIGURE D-72. SMOOTHED PSD S/N 2 GYRO DATA, (DEGREE/HOUR)^2/HZ (24 HOUR TEST #1)

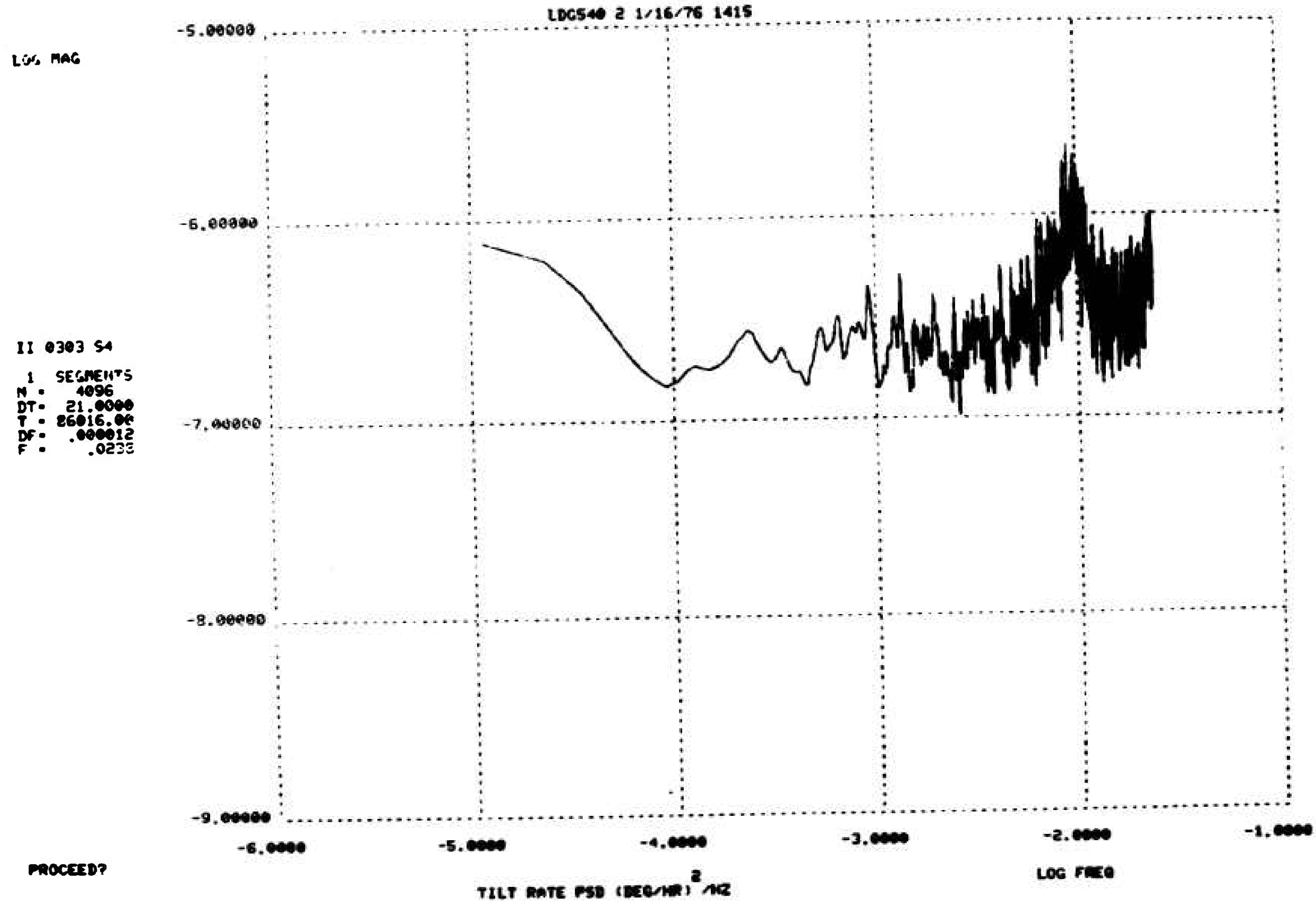

FIGURE D-73. PSD TILT RATE, $(\text{DEGREE/HOUR})^2/\text{HZ}$ (S/N 2 24 HOUR TEST #1)

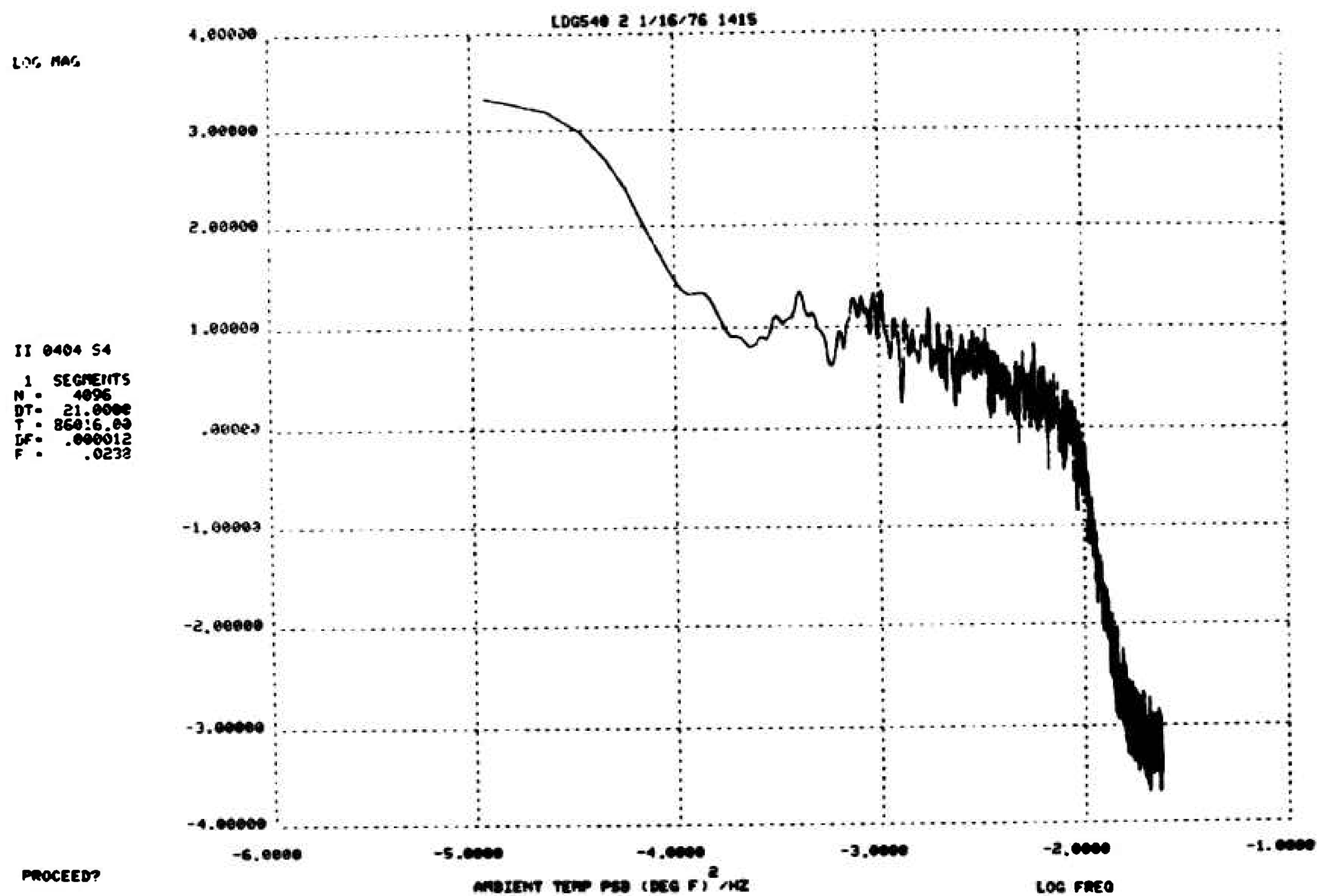

FIGURE D-74. PSD AMBIENT TEMPERATURE (DEGREE F)^2/HZ (S/N 2 24 HOUR TEST #1)

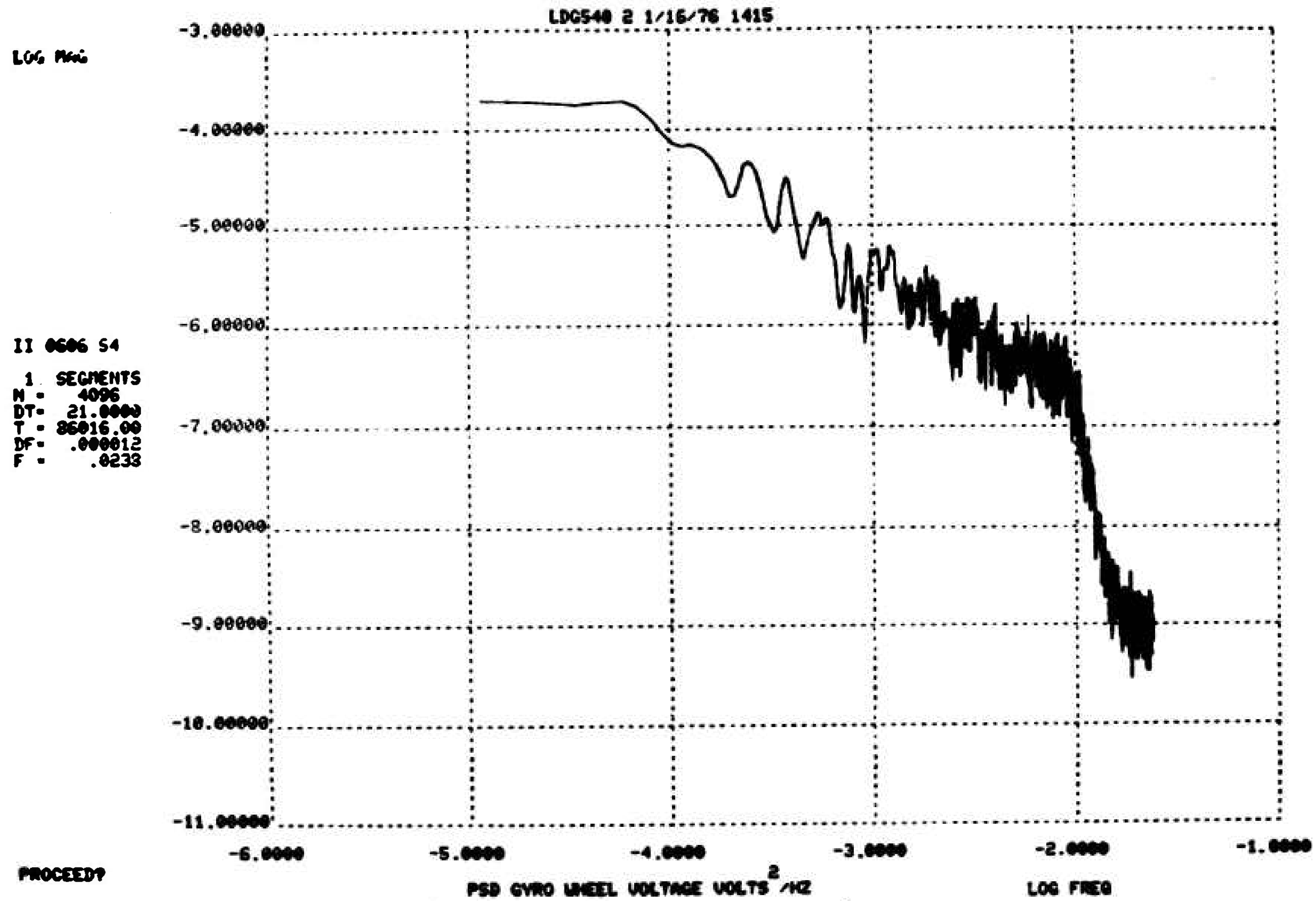

FIGURE D-75. PSD S/N 2 GYRO WHEEL VOLTAGE, $(\mathrm{VOLTS})^2/\mathrm{HZ}$ (24 HOUR TEST #1)

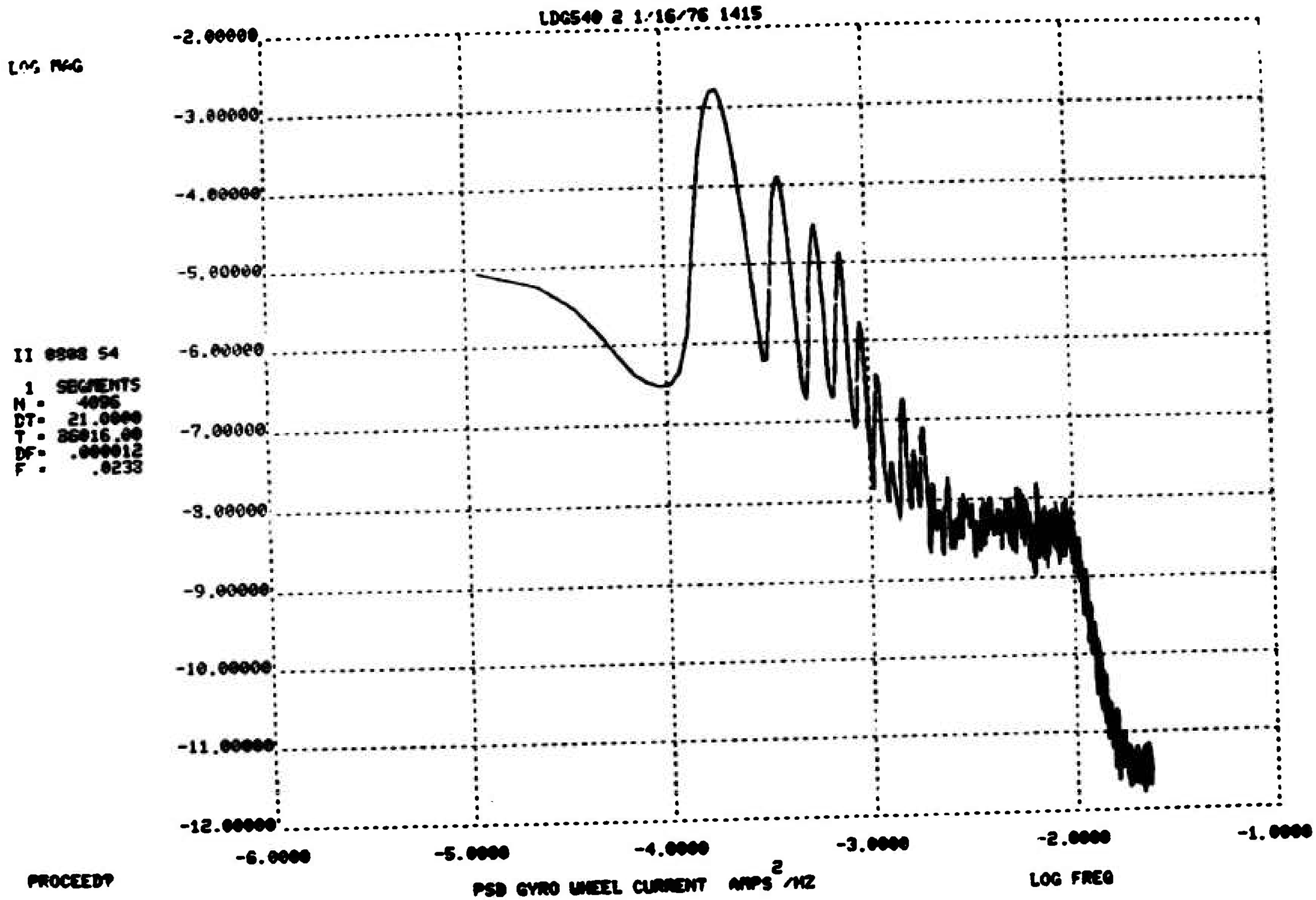

FIGURE D-76. PSD S/N 2 GYRO WHEEL CURRENT, $(AMPS)^2/HZ$ (24 HOUR TEST #1)

24 HOUR TEST #2 S/N 2

Figure D-77 through Figure D-88 show the results of the final twenty-four hour drift test for Gyro S/N 2. The temperature dependence observed in the S/N 1 Gyro 24 hour test appears to also be in the S/N 2 gyro. However, the temperature dependence in Gyro S/N 2, shown by comparing Figures D-77 and D-80, appears to be an inverse relationship.

10** -2

07 50

1 SEGMENTS
N = 4096
DT= 21.0000
T = 86016.00
DF= .000012
F = .0232

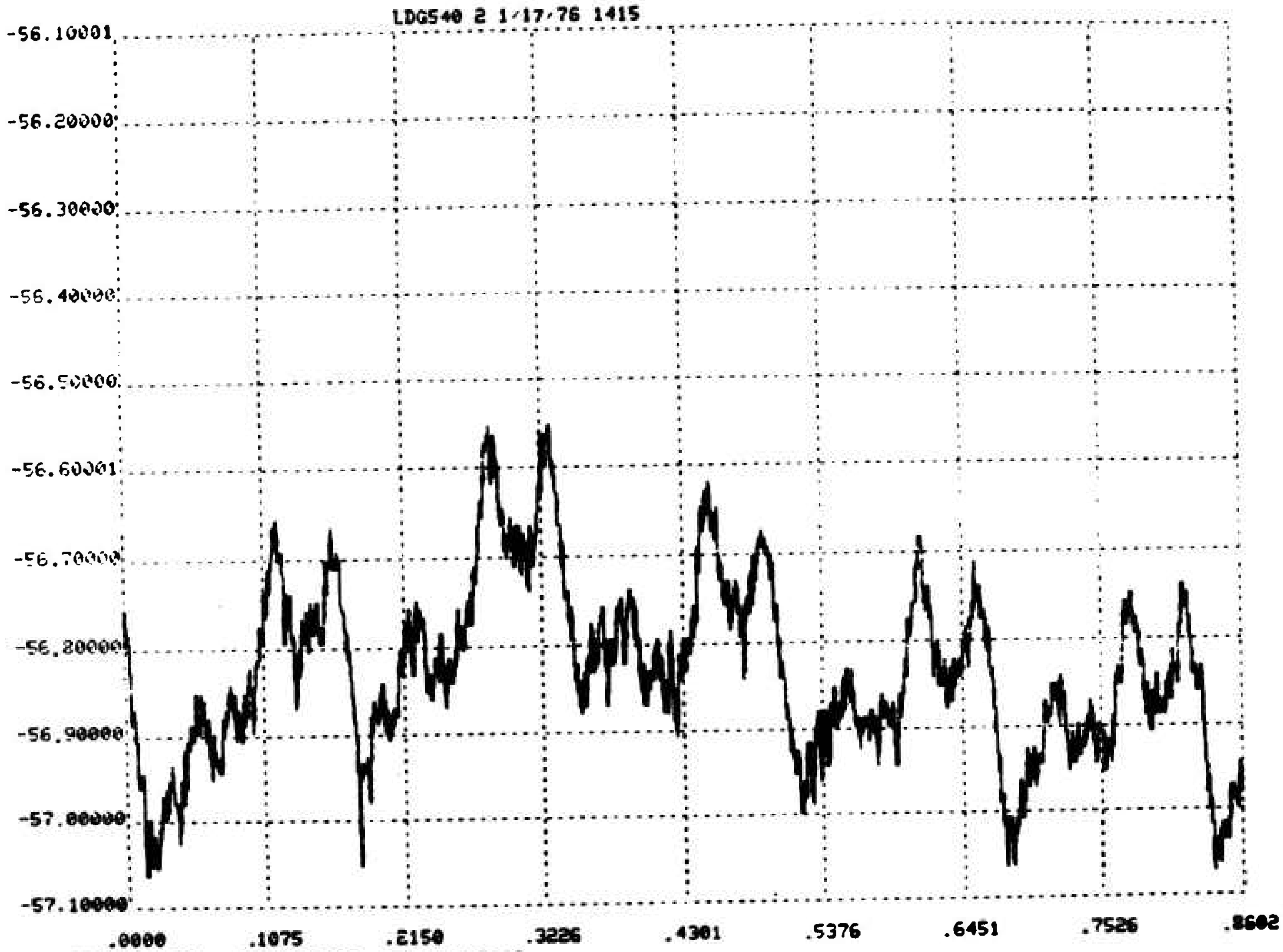

VAR.MEAN.SLOPE= .975940E-06 -.568308E+00 -.781411E-08
REMOVE MEAN?
YES
REMOVE SLOPE?
YES

10** 5 SC

GYRO OUTPUT DEG / HR

FIGURE D-77. S/N 2 GYRO DATA, DEGREE/HOUR (24 HOUR TEST #2)

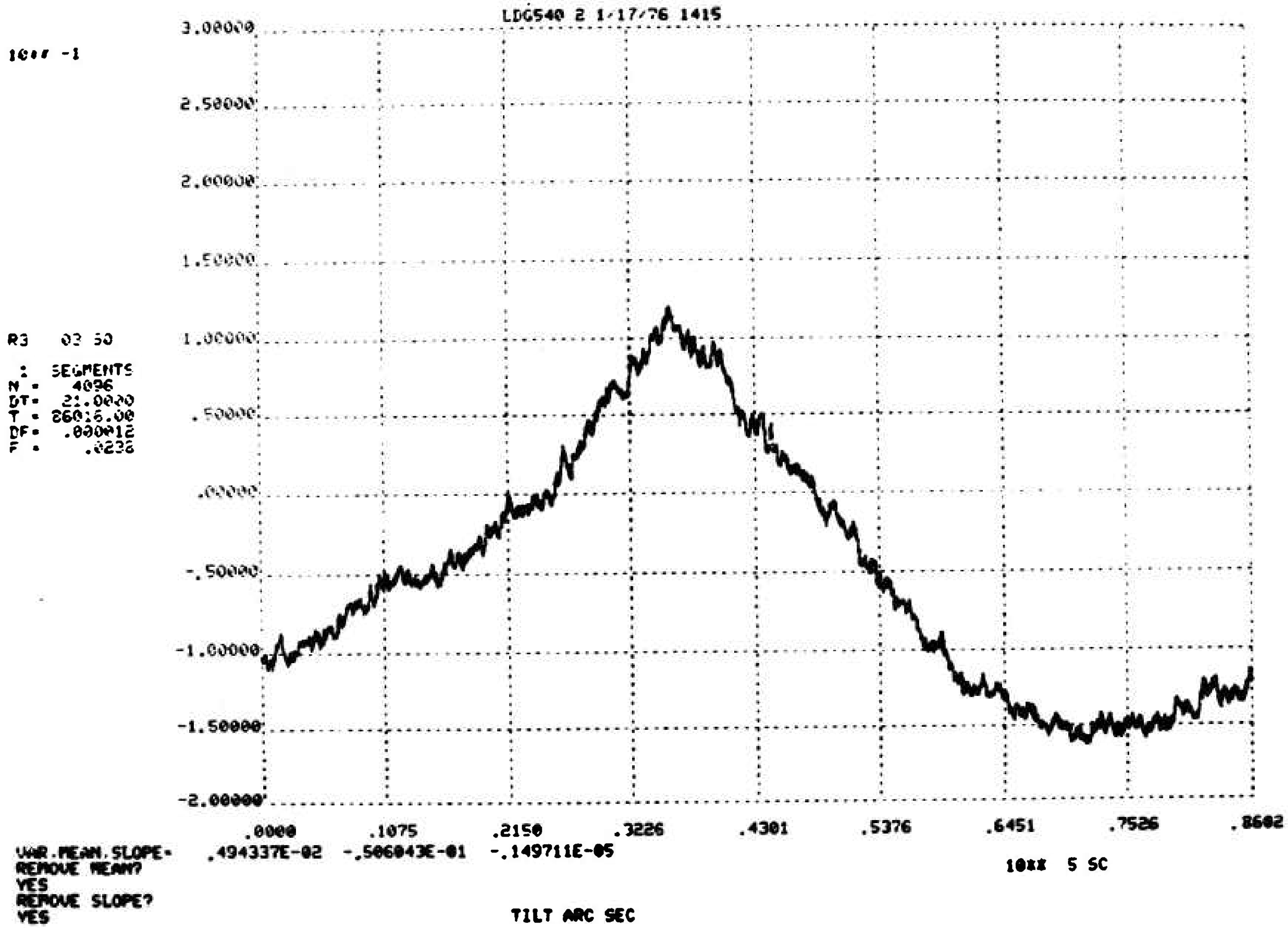

FIGURE D-78. AVERAGE TILT, ARC SECONDS (S/N 2 24 HOUR TEST #2)

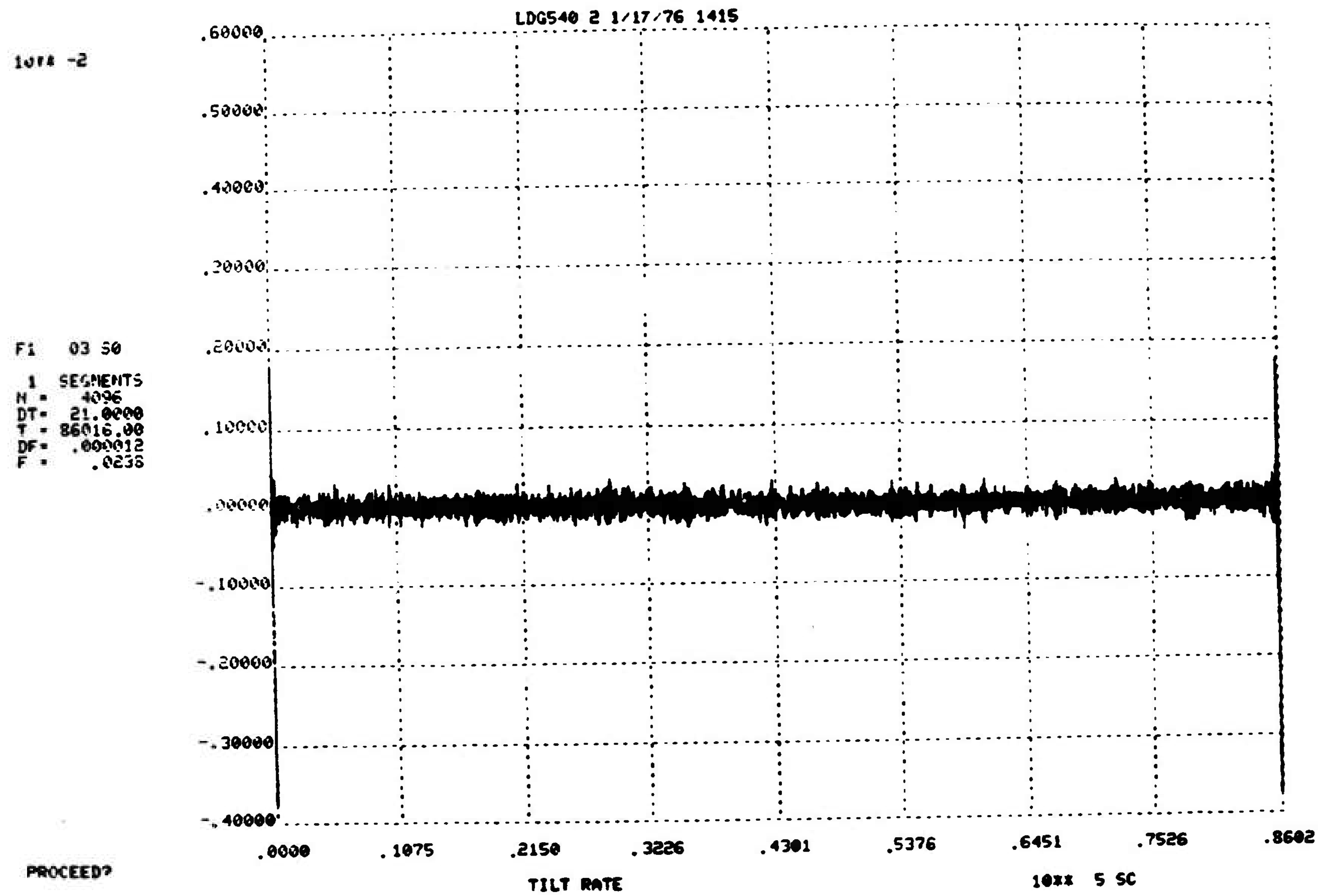

FIGURE D-79. TILT RATE, DEGREE/HOUR (S/N 2 24 HOUR TEST #2)

10** 0

04 50

1 SEGMENTS
N = 4096
DT= 21.0000
T = 86016.00
DF= .000012
F = .0232

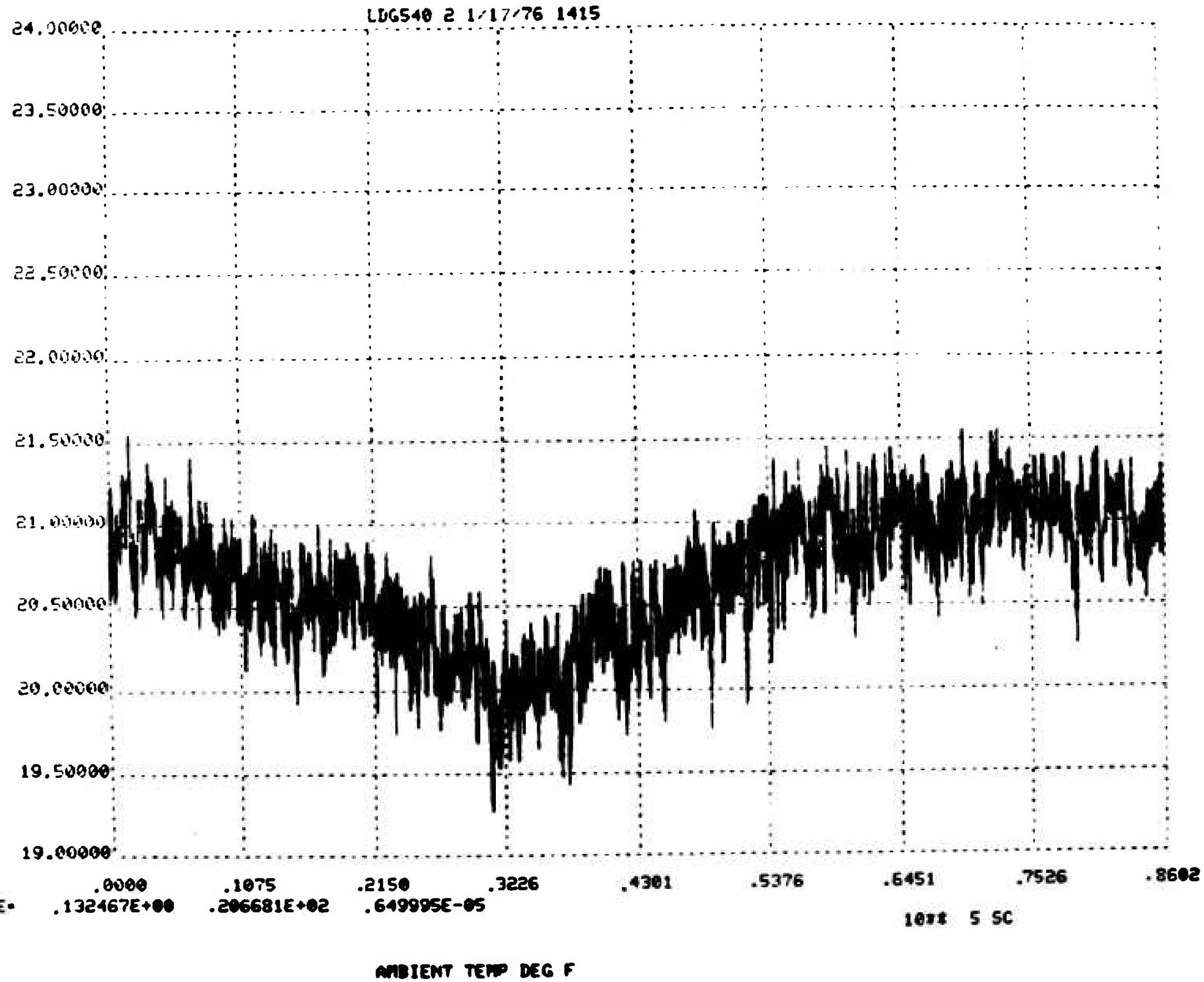

VAR.MEAN.SLOPE= .132467E+00 .206681E+02 .649995E-05
REMOVE MEAN?
YES
REMOVE SLOPE?
YES

FIGURE D-80. AMBIENT TEMPERATURE, DEGREE F (S/N 2 24 HOUR TEST #2)

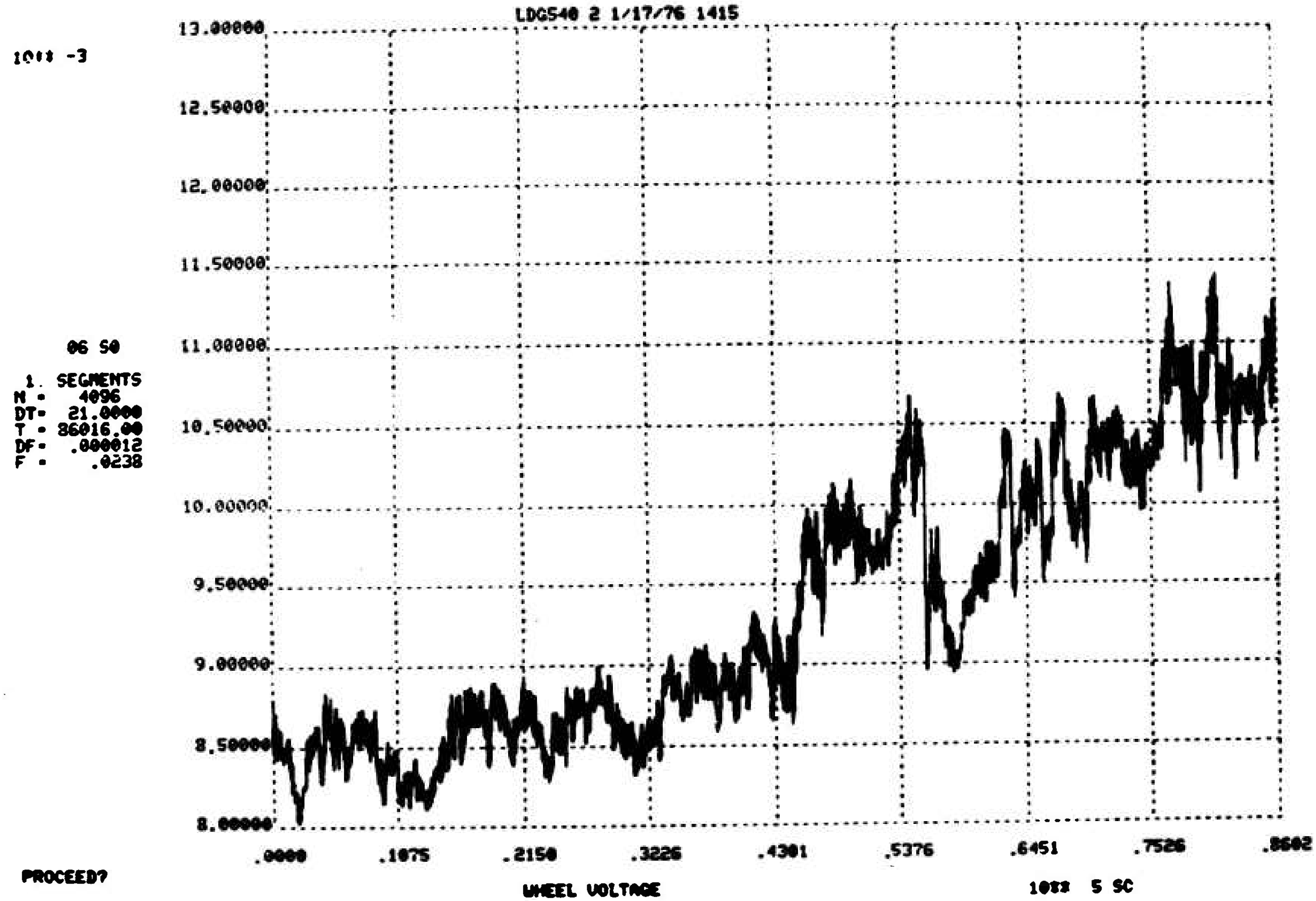

FIGURE D-81. S/N 2 GYRO WHEEL VOLTAGE, VOLTS (24 HOUR TEST #2)

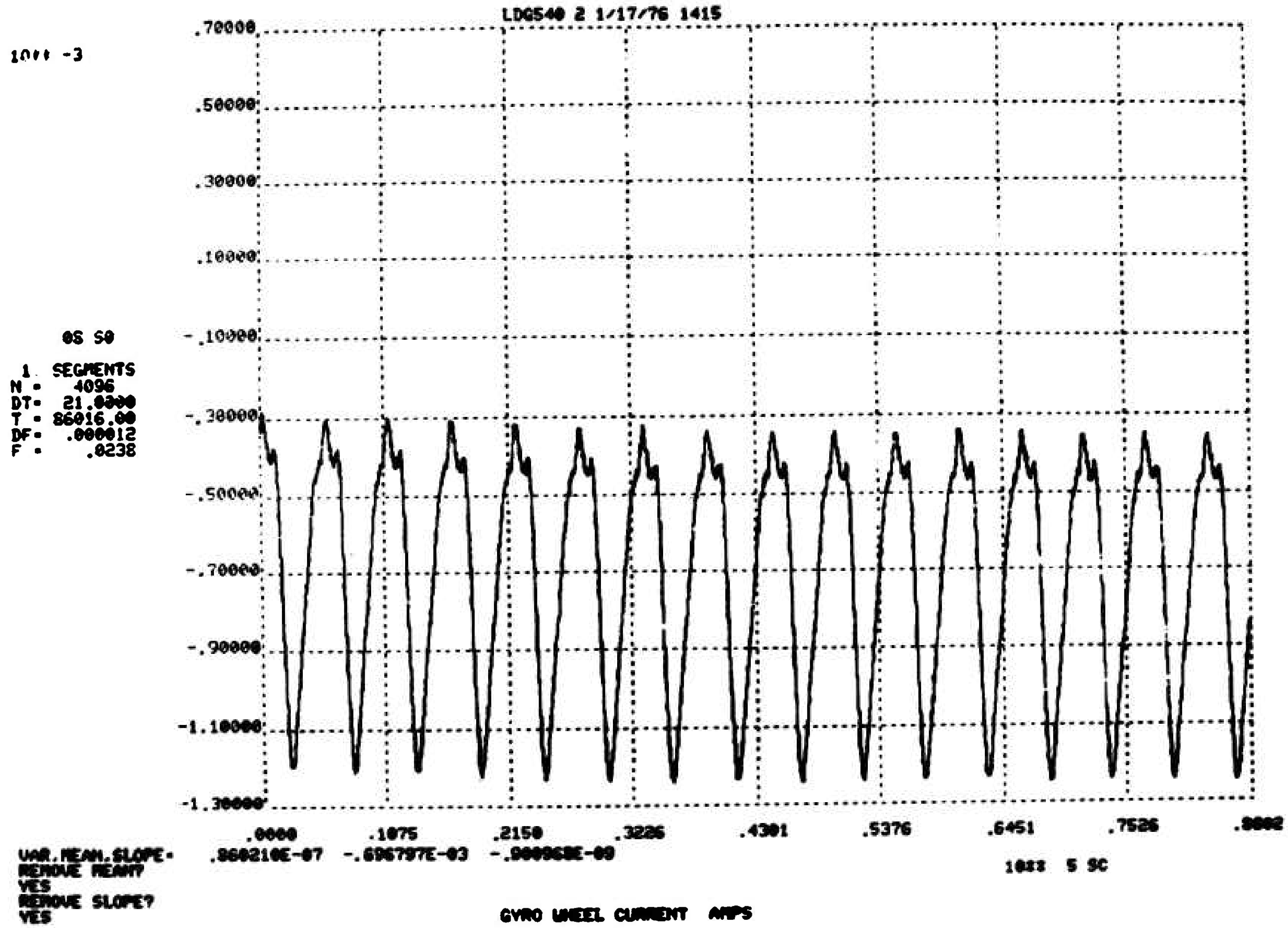

FIGURE D-82. S/N 2 GYRO WHEEL CURRENT, AMPS (24 HOUR TEST #2)

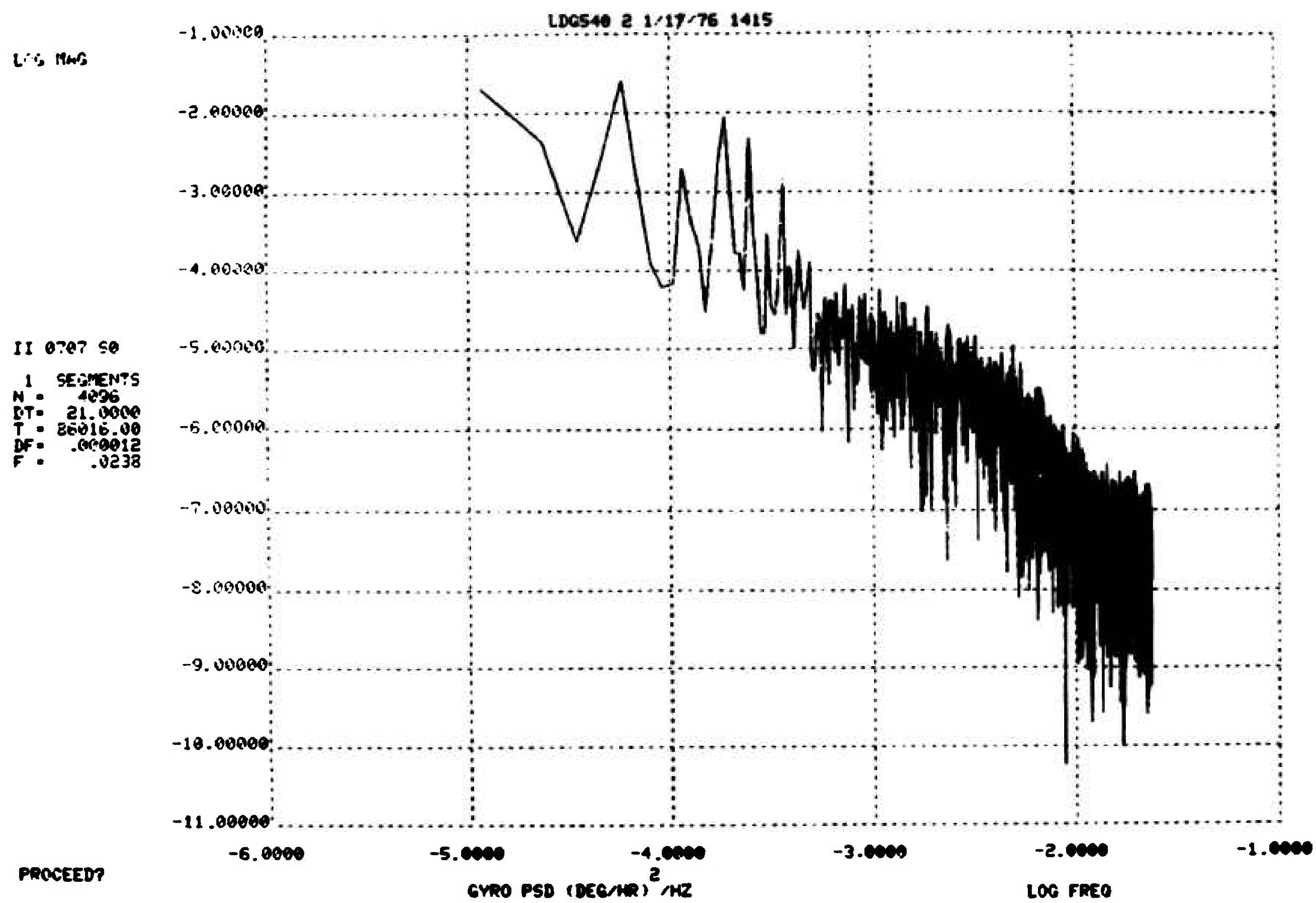

FIGURE D-83. UNSMOOTHED PSD S/N 2 GYRO DATA, $(\text{DEGREE/HOUR})^2/\text{HZ}$ (24 HOUR TEST #2)

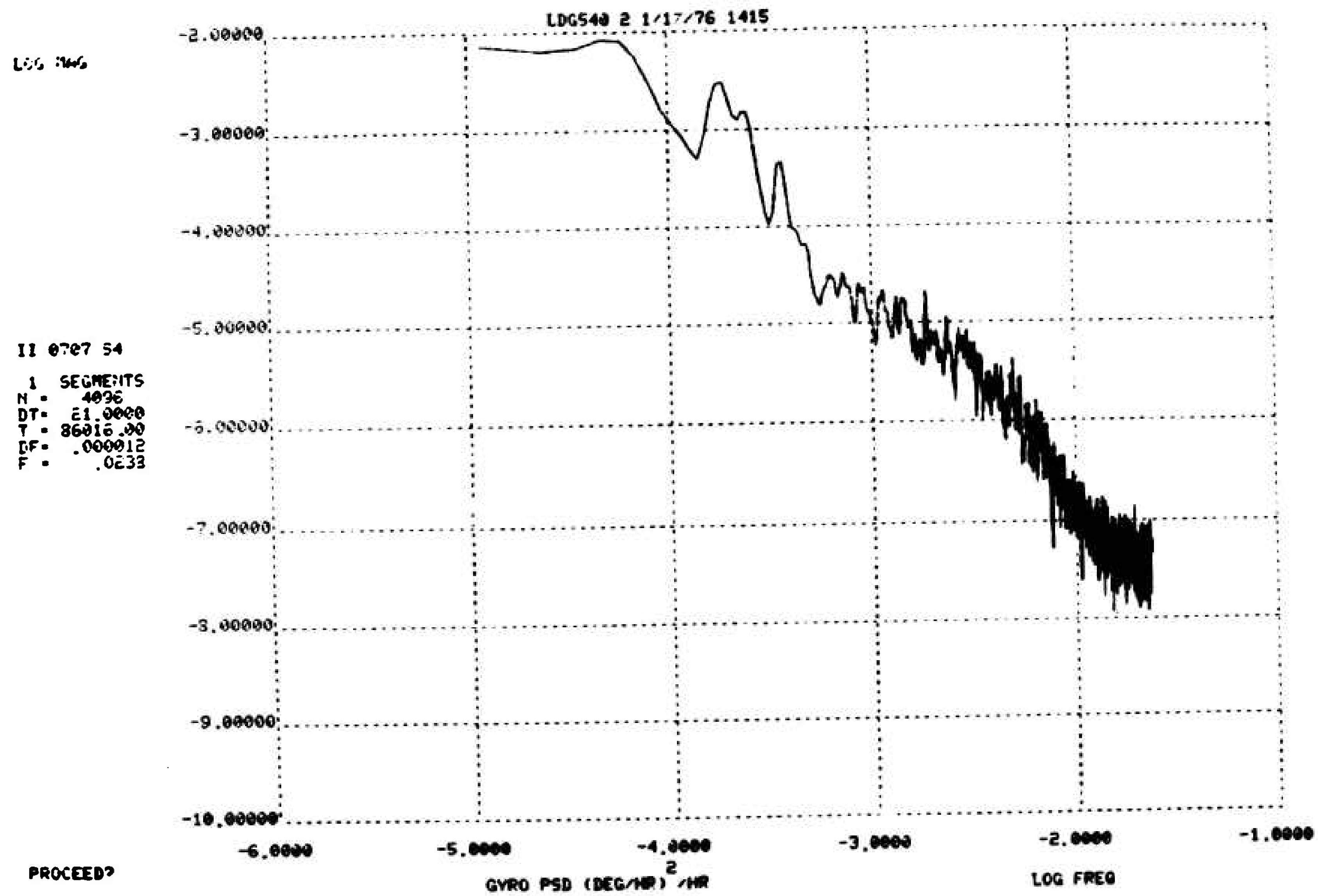

FIGURE D-84. SMOOTHED PSD S/N 2 GYRO DATA, $(\text{DEGREE/HOUR})^2/\text{HZ}$ (24 HOUR TEST #2)

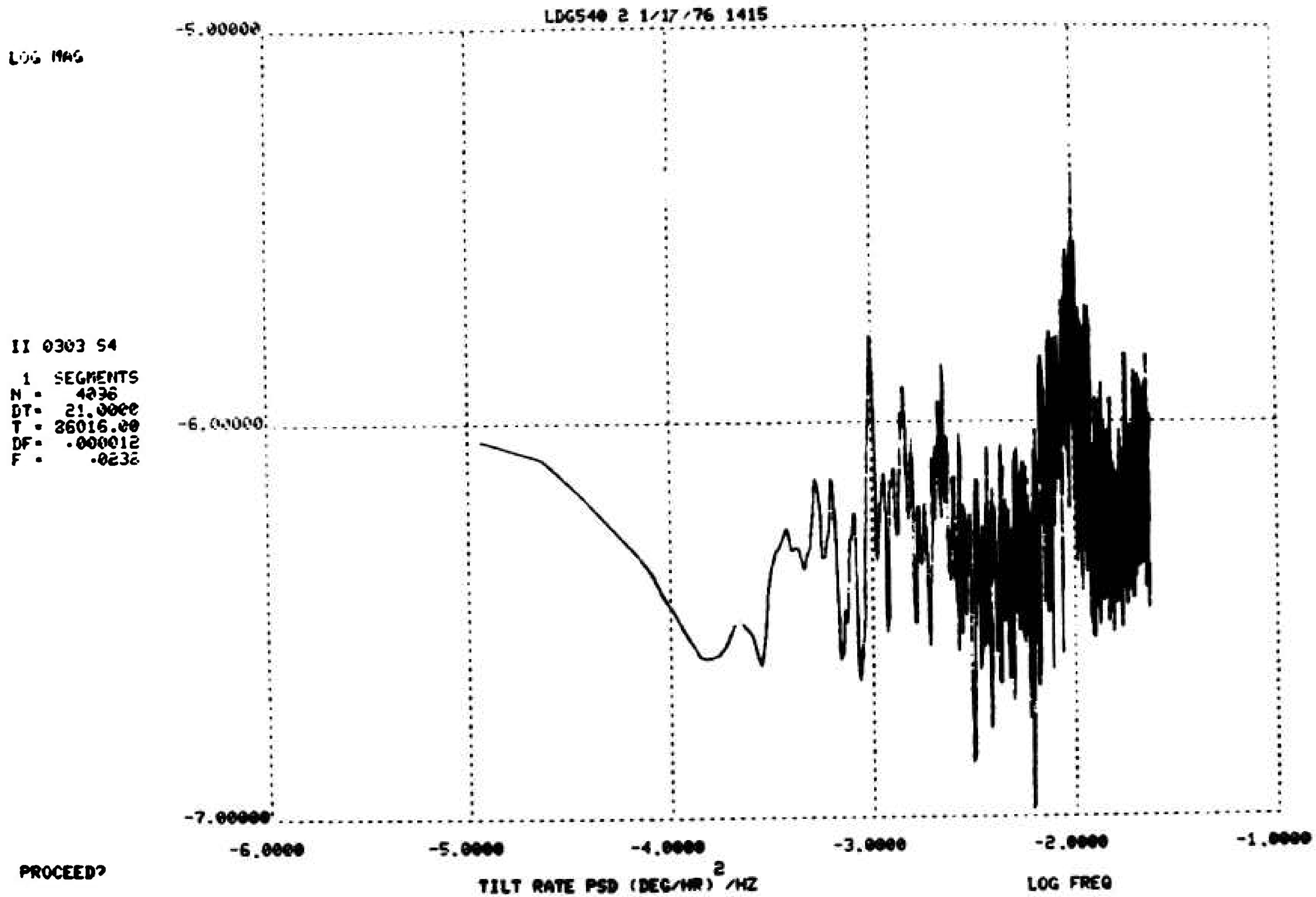

FIGURE D-85. PSD TILT RATE, (DEGREE/HOUR)^2/HZ (S/N 2 24 HOUR TEST #2)

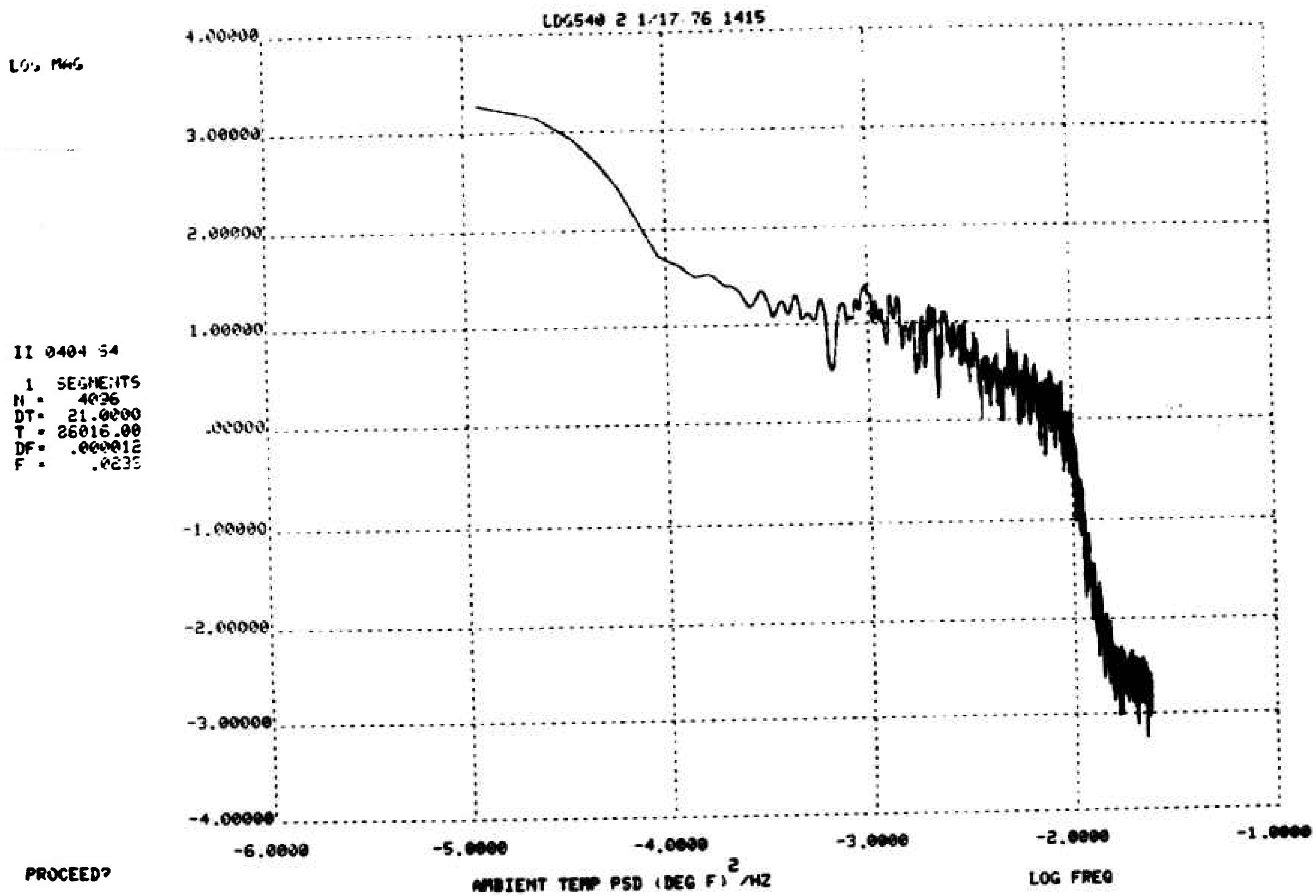

FIGURE D-C6. PSD AMBIENT TEMPERATURE, (DEGREE F)^2/HZ (S/N 2 24 HOUR TEST #2)

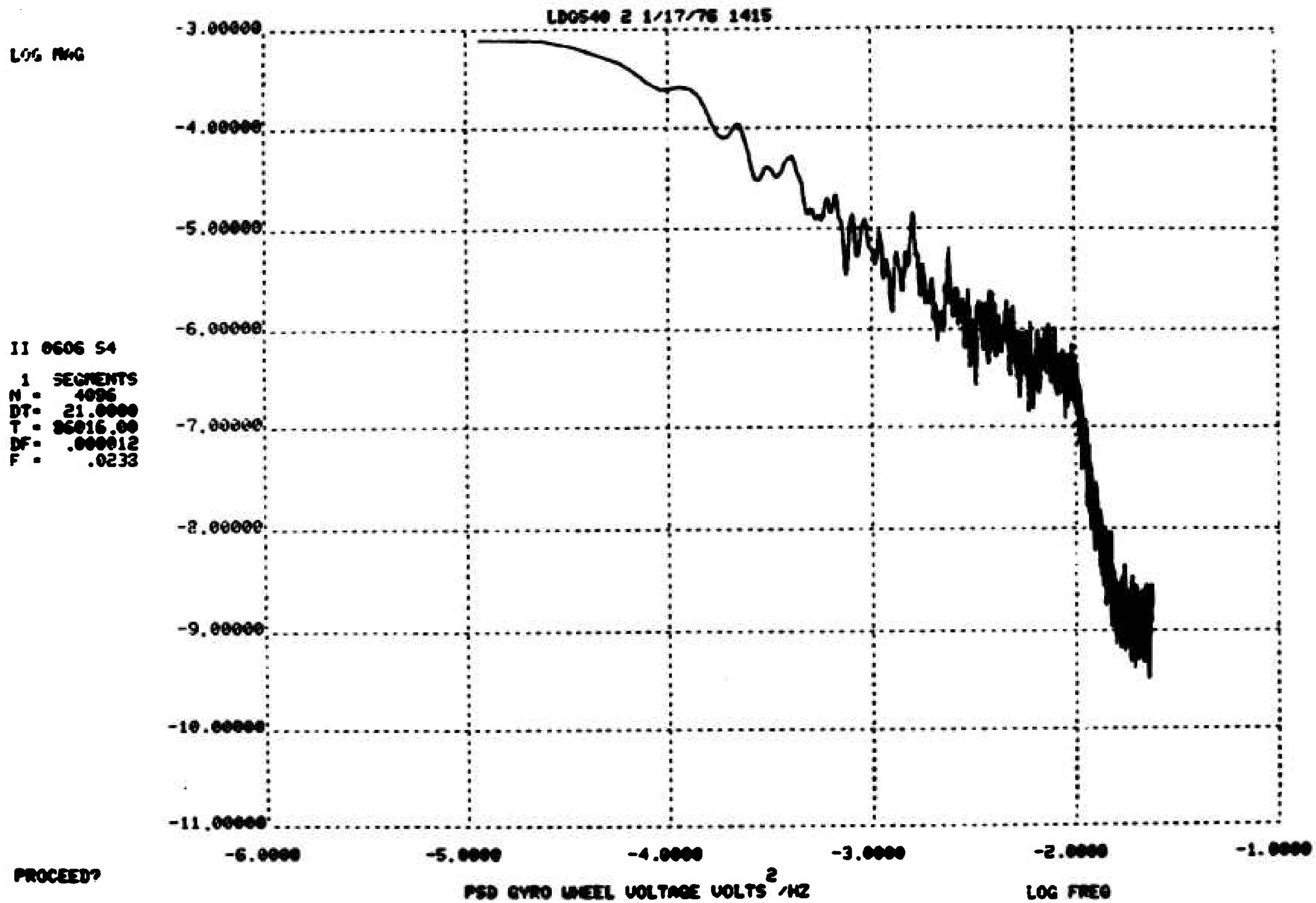

FIGURE D-87. S/N 2 PSD GYRO WHEEL VOLTAGE, $(VOLTS)^2/HZ$ (24 HOUR TEST #2)

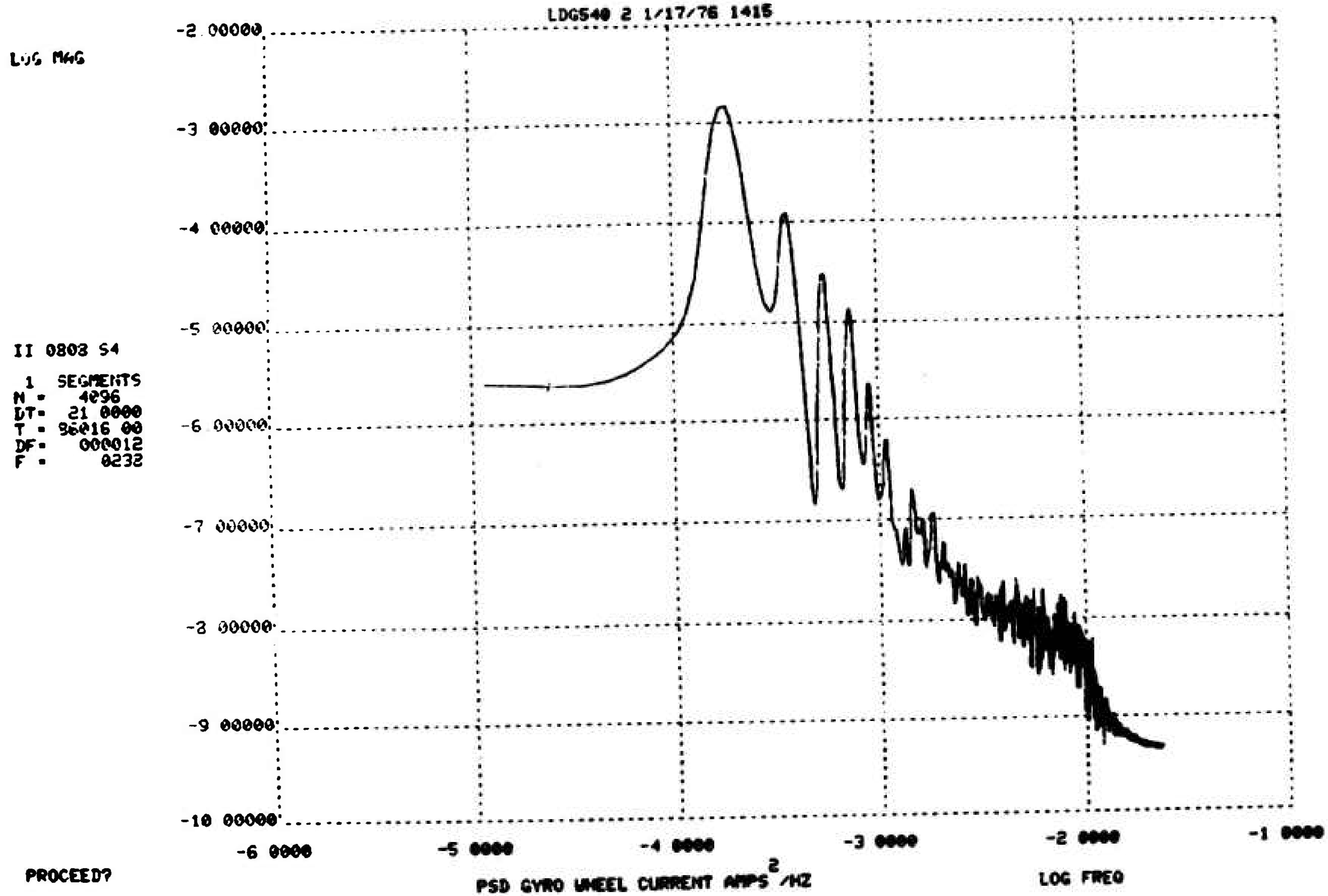

FIGURE D-88. S/N 2 PSD GYRO WHEEL CURRENT, $(AMPS)^2/HZ$ (24 HOUR TEST #2)

1 HOUR TEST S/N 2

Test results for the 1 hour test for Gyro S/N 2 are shown in Figure D-89 through Figure D-99. Comments concerning the influence of noise on the data made for the 1 hour test for Gyro S/N 1 are generally true for this test except for gyro voltage and current. Significant wheel voltage information, above the noise level is found at frequencies below .2 Hz, and the wheel current PSD is significantly above the noise level throughout the test. The spikes at approximately .05 and .1 Hz, can clearly be seen in the gyro PSD, Figure D-95. The cause of the observed spikes is not apparent. A lower amplitude single spike appeared in the 1 hour test for S/N 1 which was apparently related to the gyro case temperature. A similar phenomenon could have been responsible for the spikes observed in S/N 2, however, since the gyro case temperature was not monitored during the S/N 2 tests, justification supporting the hypothesis is lacking.

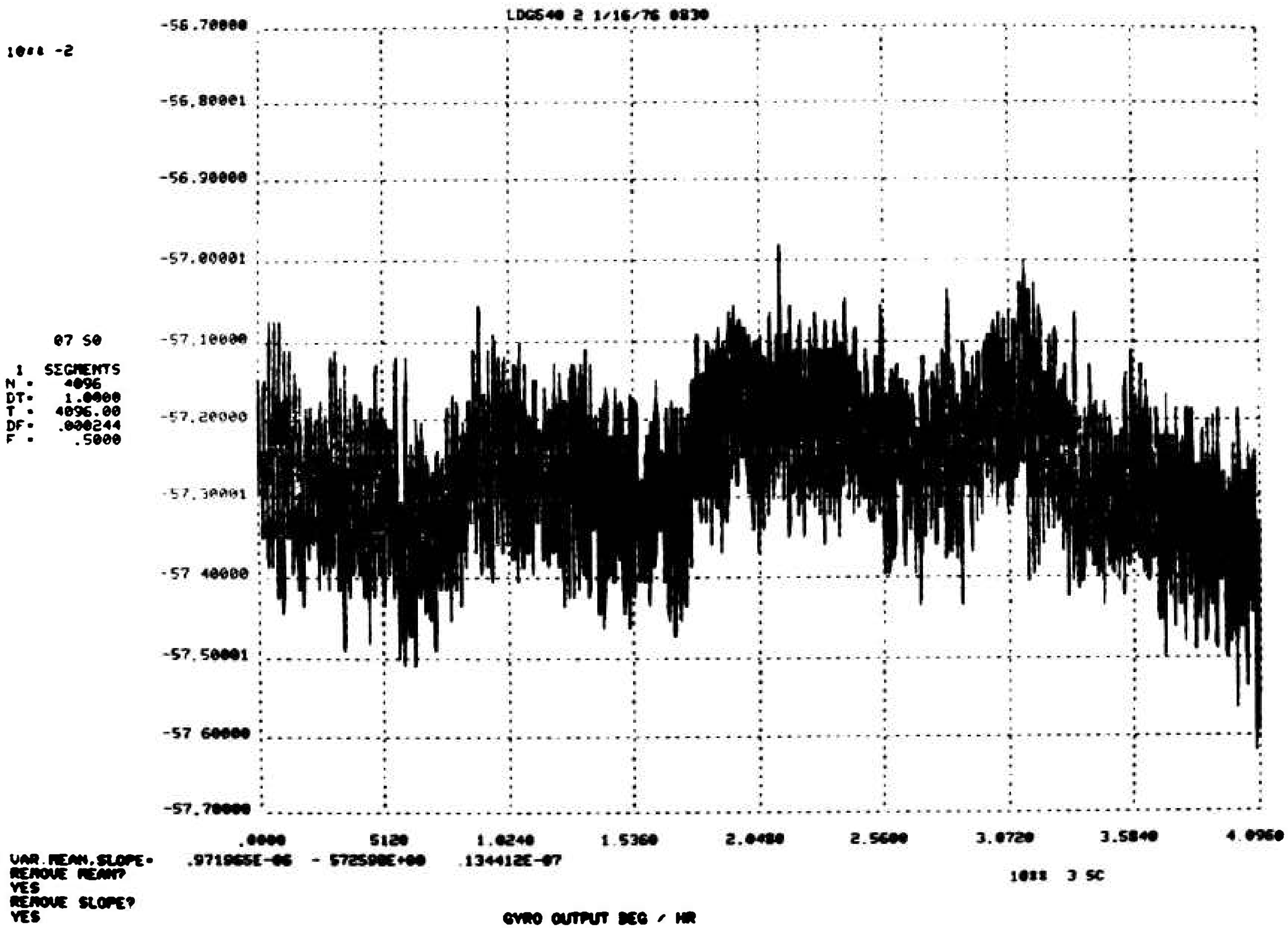

FIGURE D-89. S/N 2 GYRO DATA, DEGREE/HOUR (1 HOUR TEST)

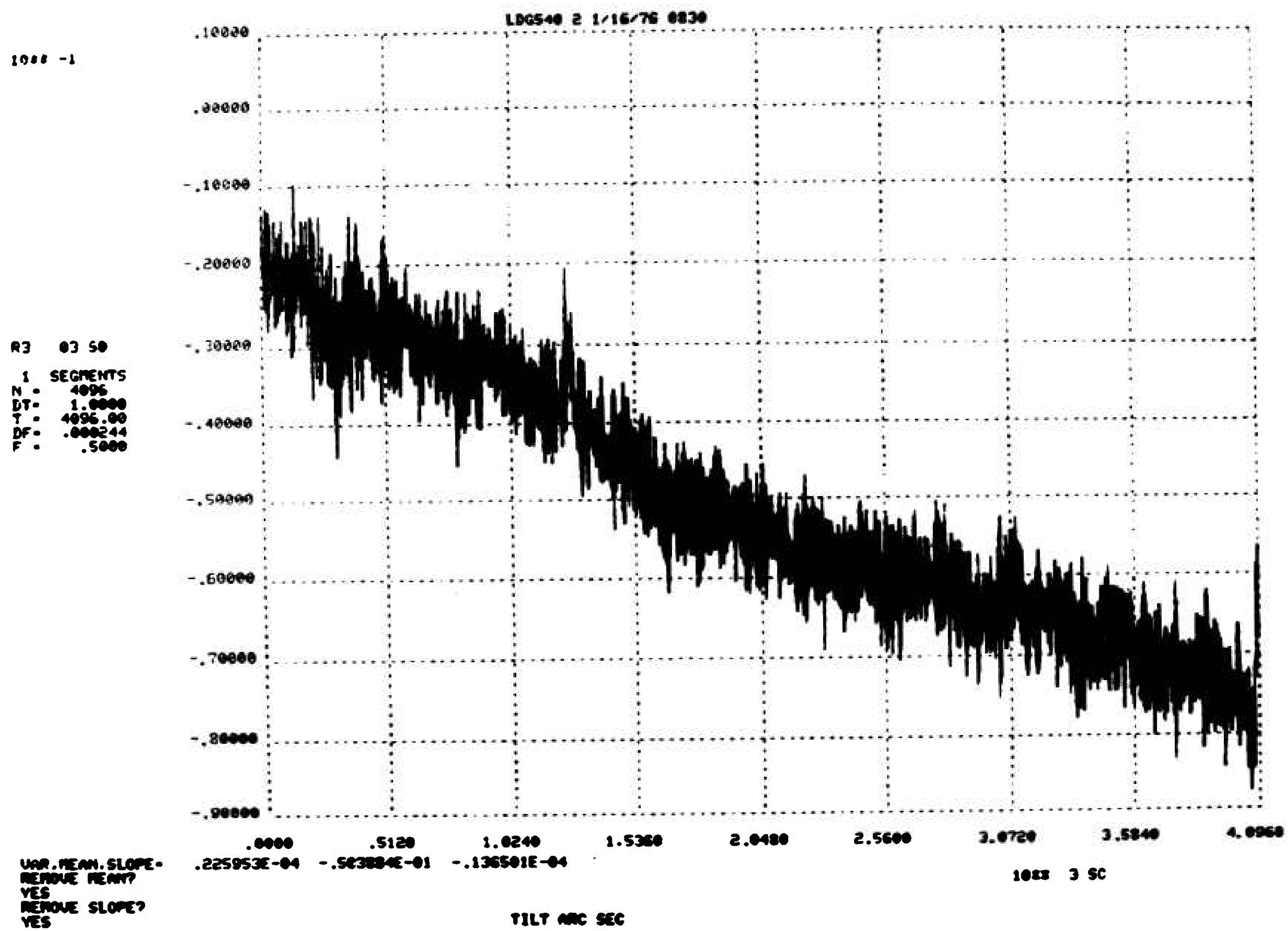

FIGURE D-90. AVERAGE TILT, ARC SECONDS (1 HOUR TEST S/N 2)

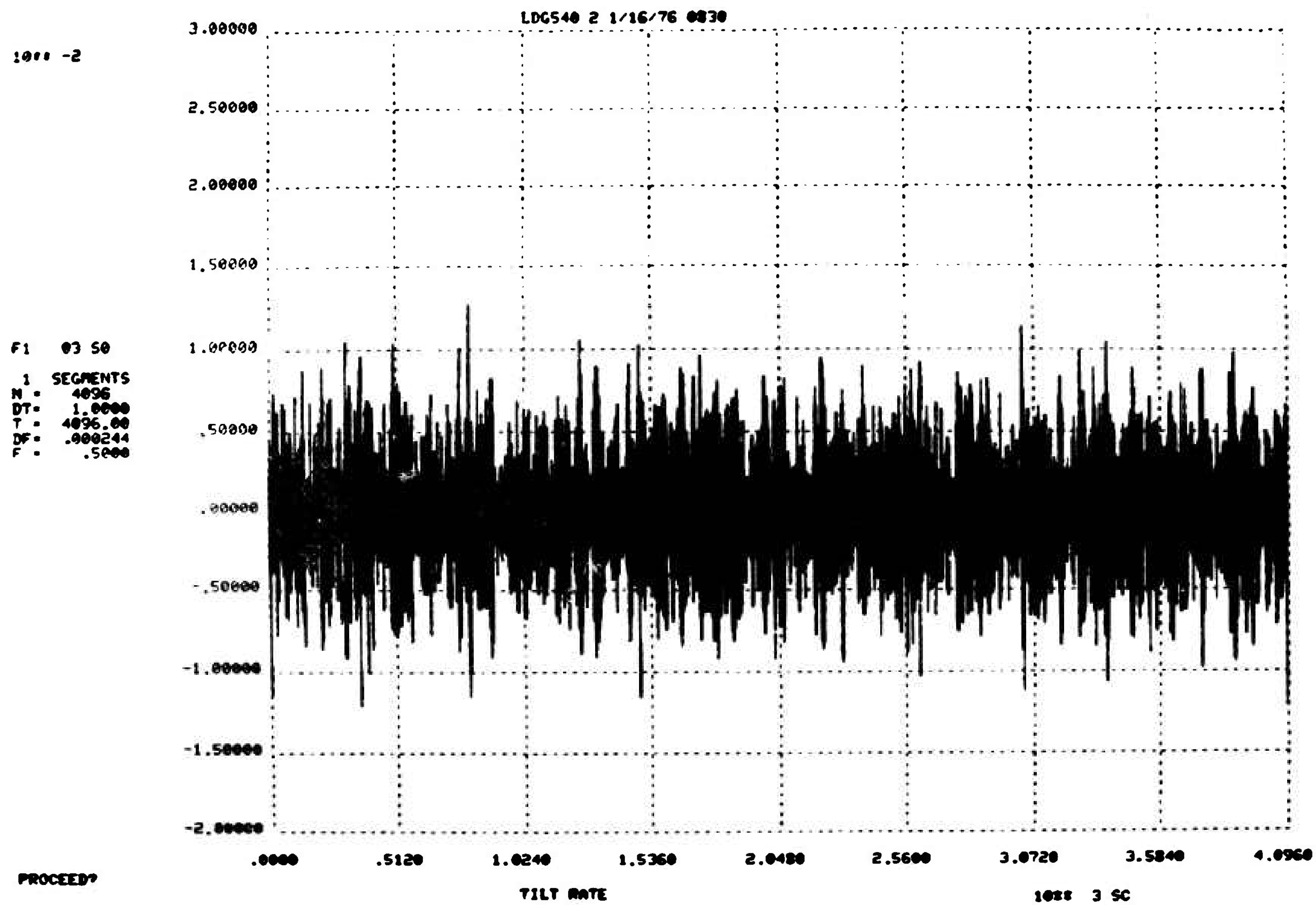

FIGURE D-91. TILT RATE, DEGREE/HOUR (1 HOUR TEST S/N 2)

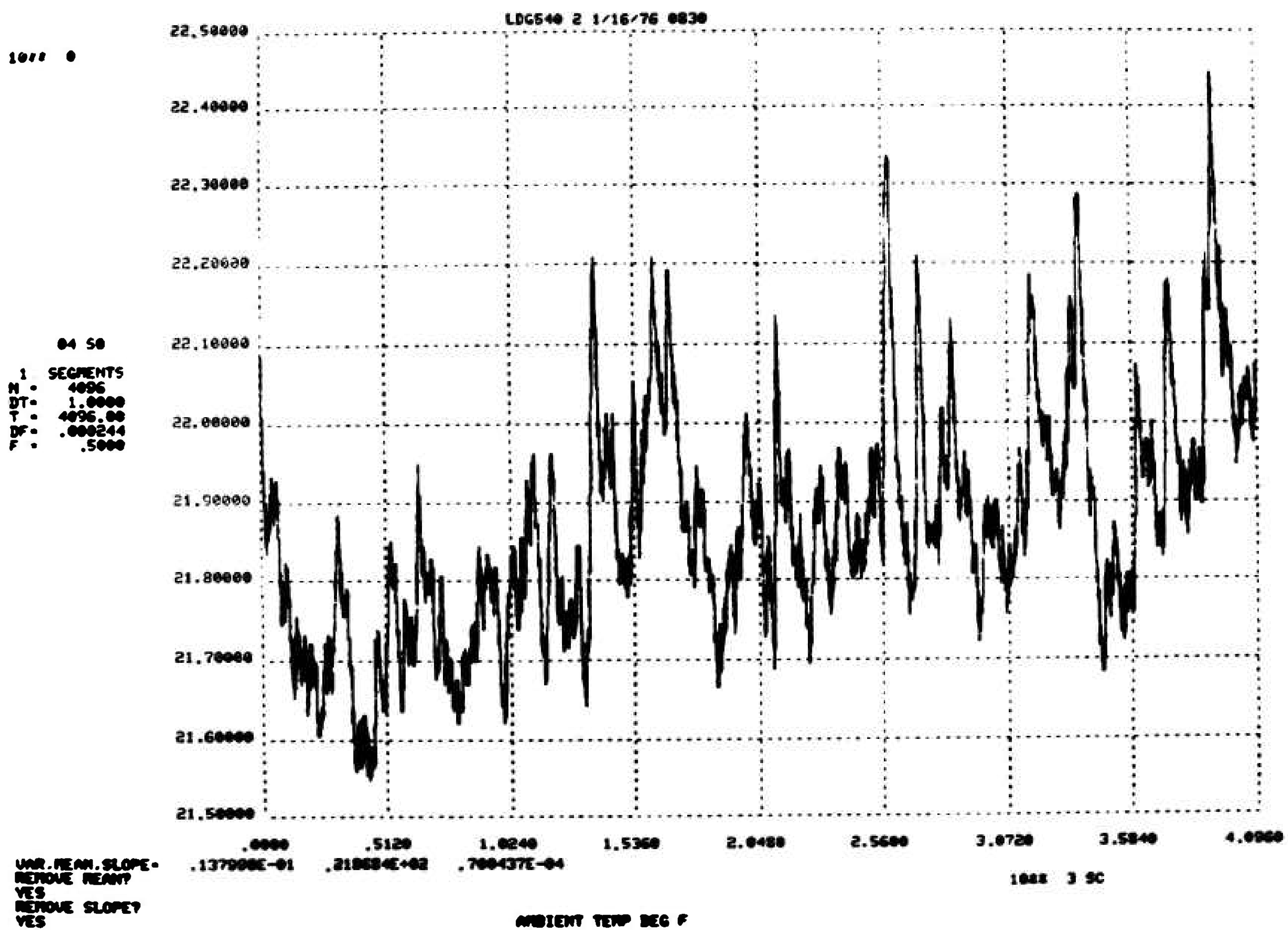

FIGURE D-92. AMBIENT TEMPERATURE, DEGREE F (1 HOUR TEST S/N 2)

1O** -3

06 50

1 SEGMENTS
N = 4096
DT= 1.0000
T = 4096.00
DF= .000244
F = .5000

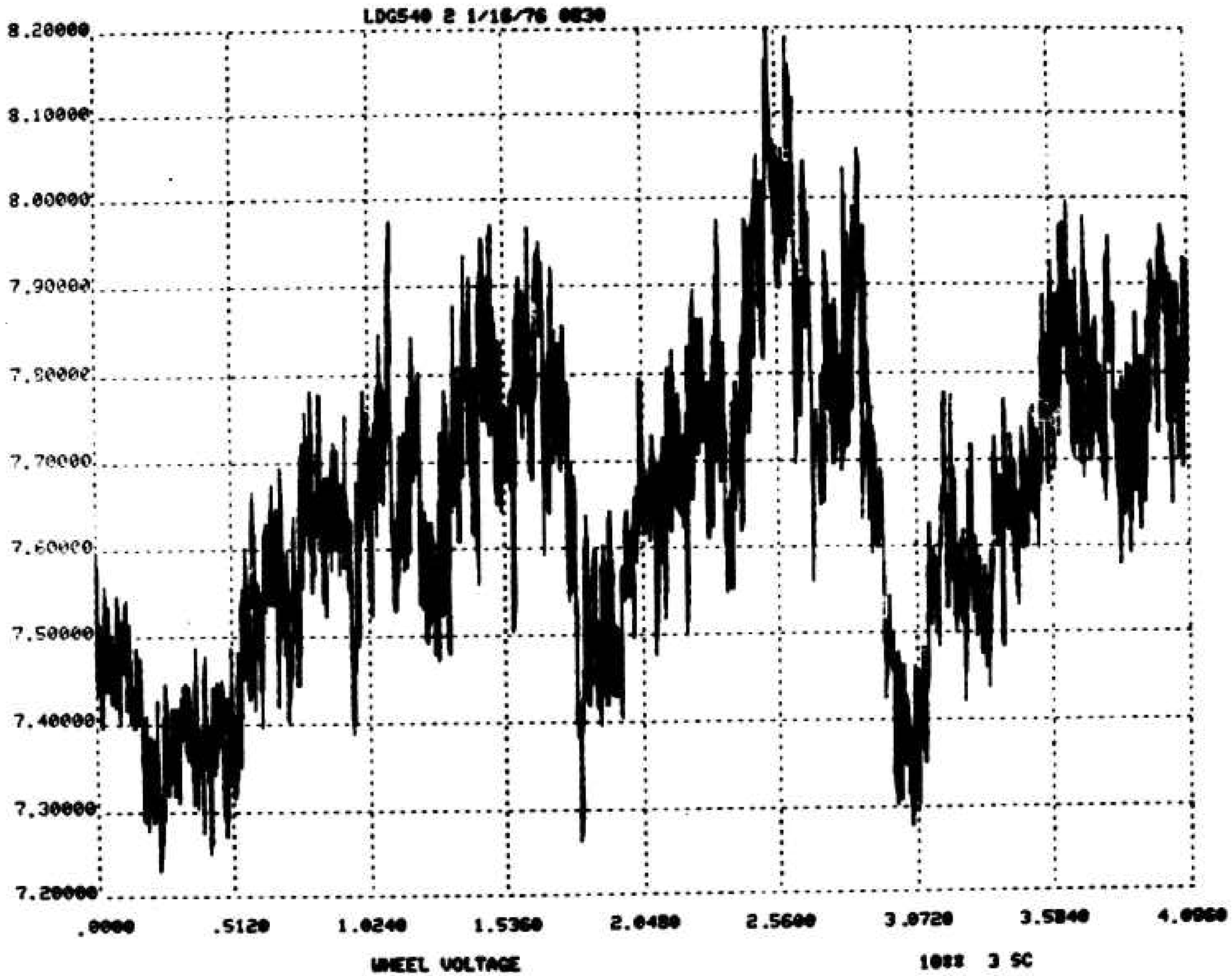

PROCEED?

FIGURE D-93. S/N 2 GYRO WHEEL VOLTAGE, VOLTS (1 HOUR TEST)

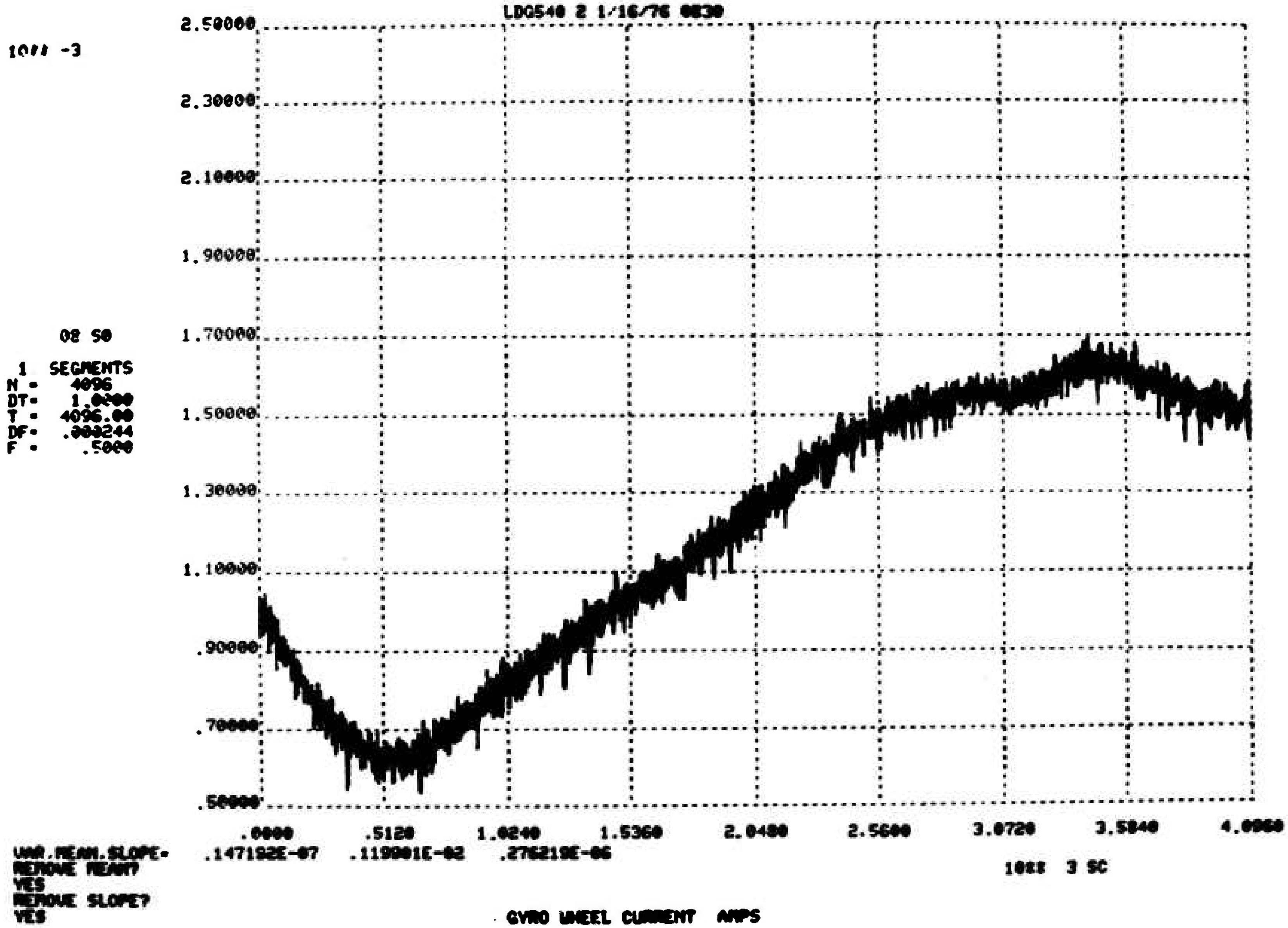

FIGURE D-94. S/N 2 GYRO WHEEL CURRENT, AMPS (1 HOUR TEST)

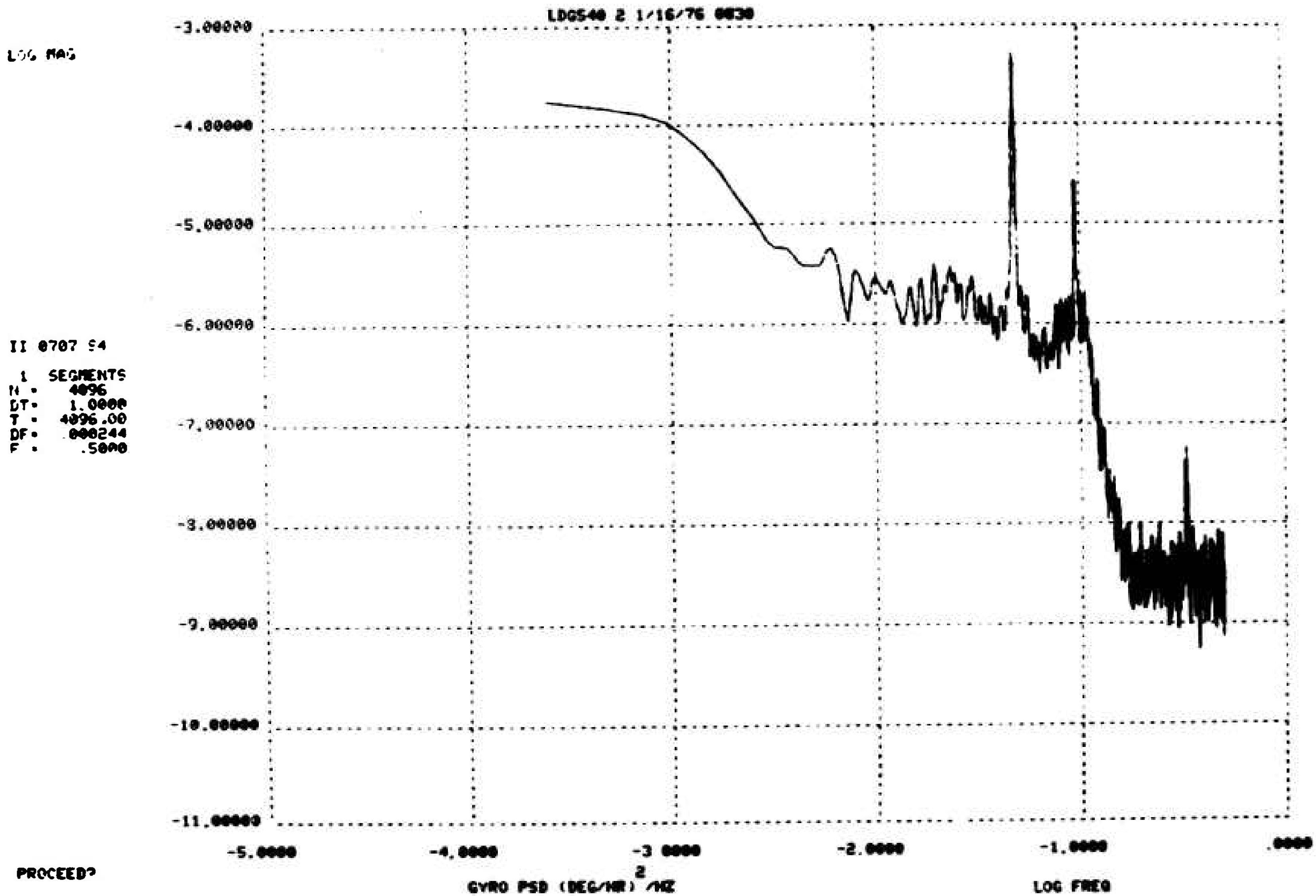

FIGURE D-95. PSD S/N 2 GYRO DATA, (DEGREE/HOUR)^2/HZ (1 HOUR TEST)

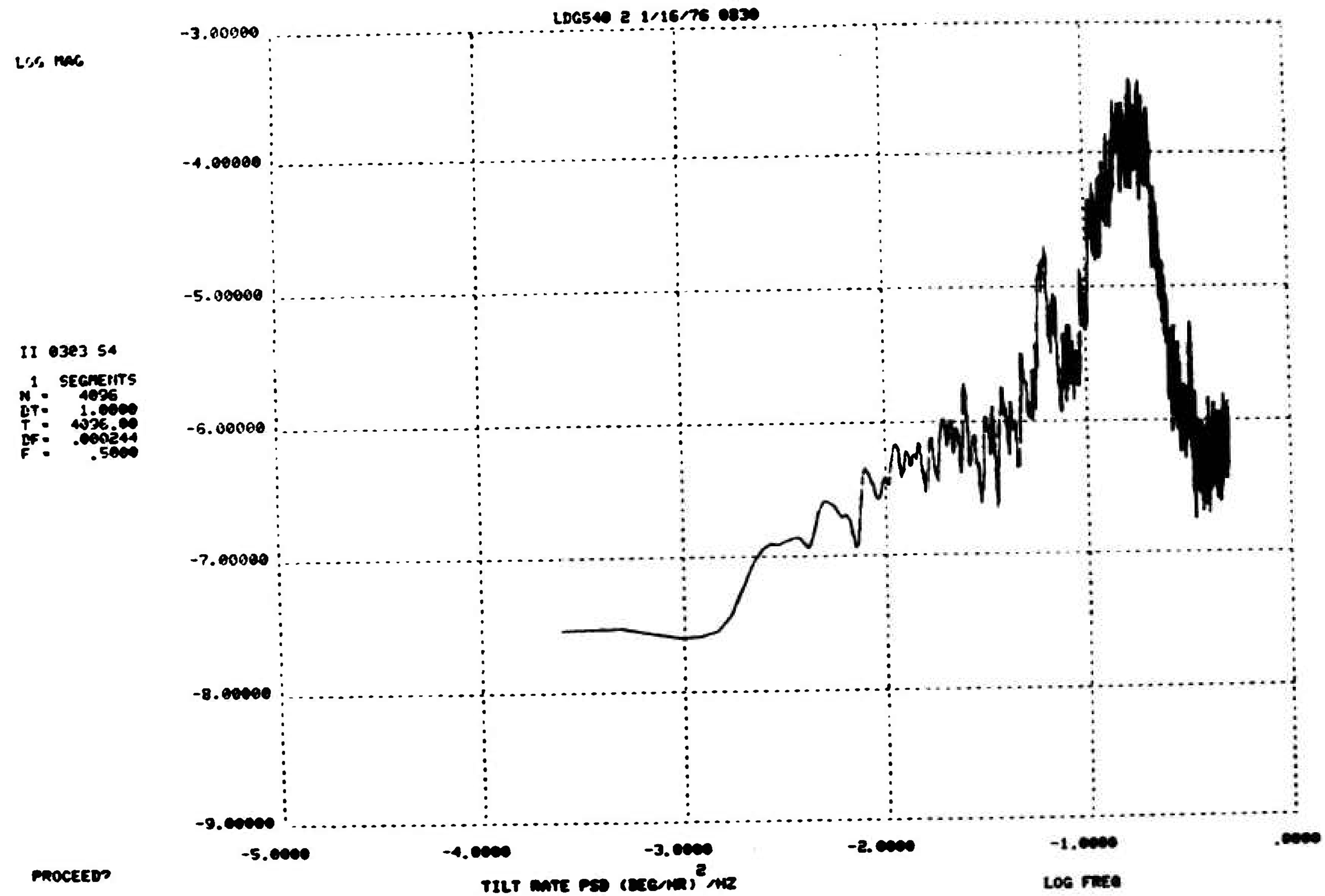

FIGURE D-96. PSD TILT RATE, $(DEGREE/HOUR)^2/HZ$ (1 HOUR TEST S/N 2)

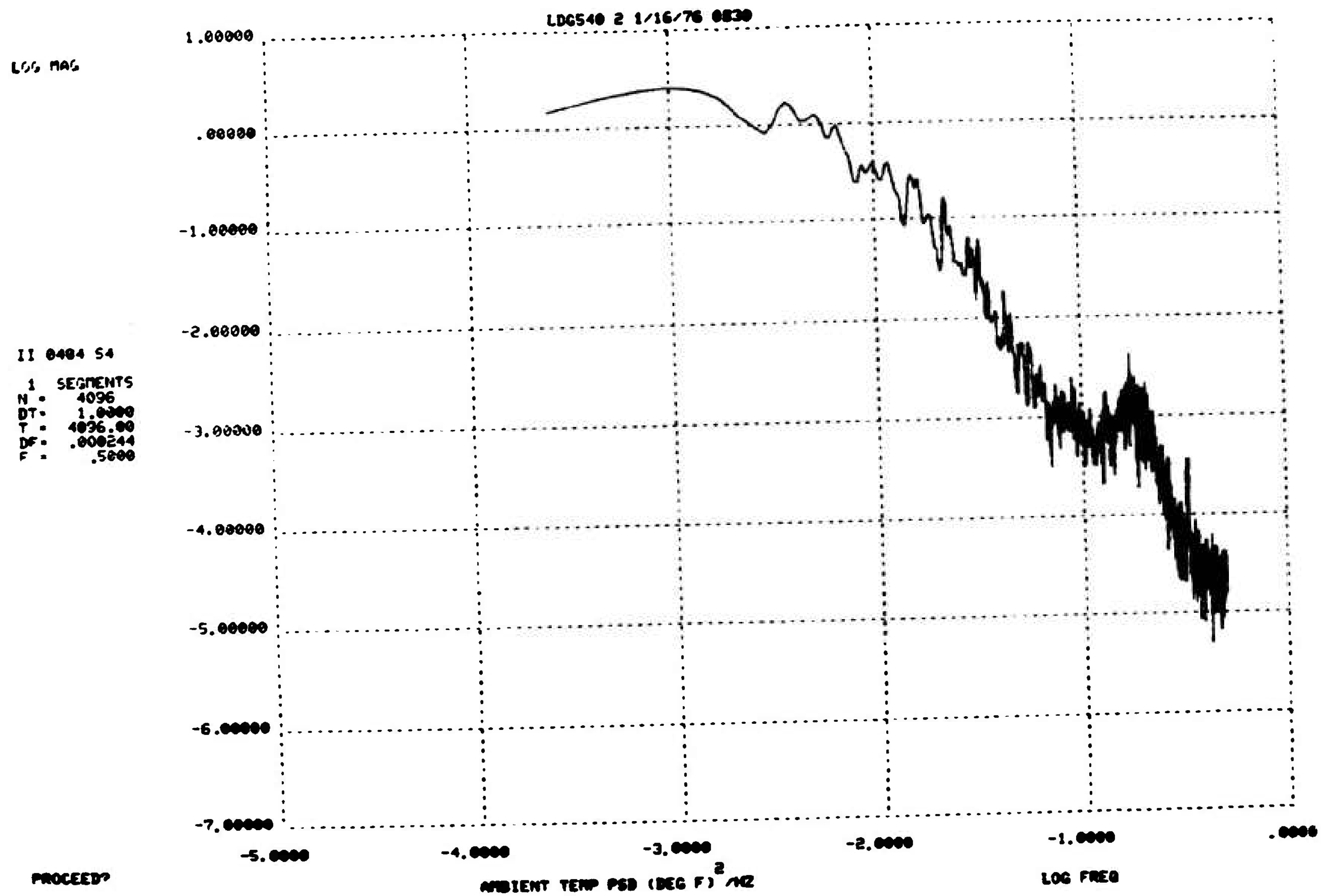

FIGURE D-97. PSD AMBIENT TEMPERATURE, (DEGREE F)/HZ (1 HOUR TEST S/N 2)

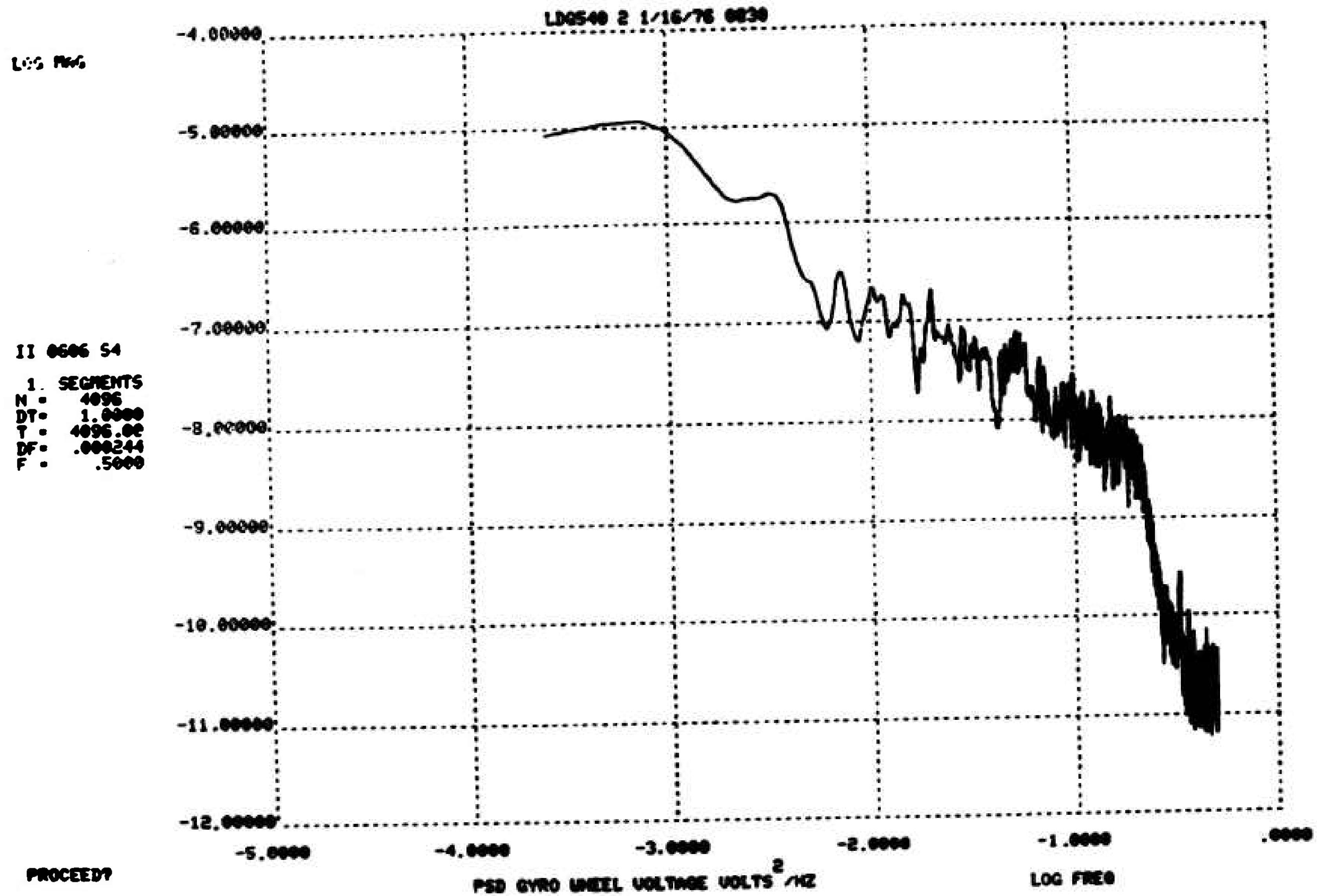

FIGURE D-98. PSD S/N 2 WHEEL VOLTAGE, (VOLTS)^2/HZ (1 HOUR TEST)

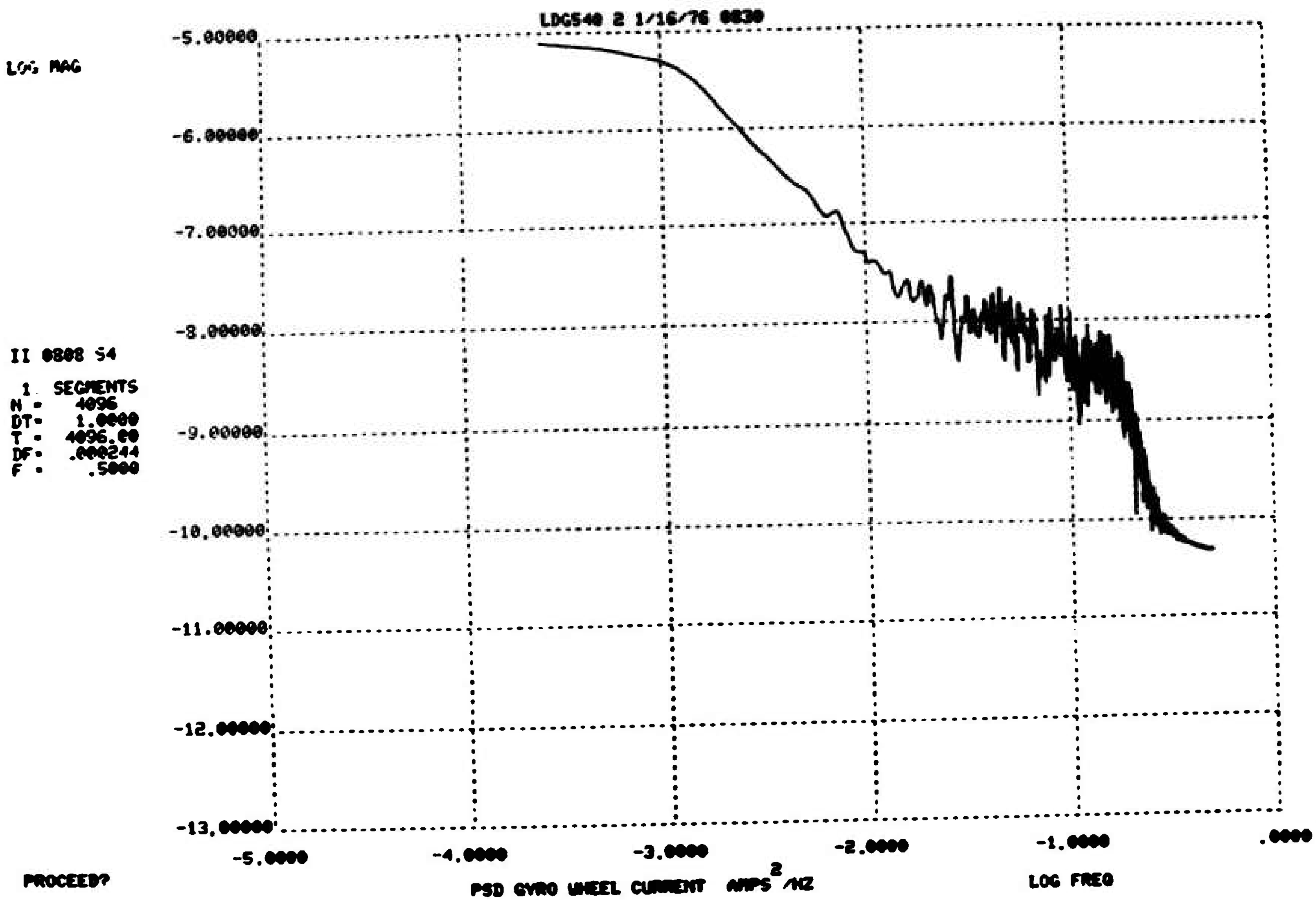

FIGURE D-99. PSD S/N 2 WHEEL CURRENT, $(AMPS)^2/HZ$ (1 HOUR TEST)

3 MINUTE TEST S/N 2

Figures D-100 through D-107 contain the results of the 3 minute test on Gyro S/N 2. An interesting phenomenon occurred toward the beginning of the test. The tilt rate plot, Figure D-102, indicates the test pad was given a jolt of some kind less than 40 seconds after the test started. However, from the gyro data, Figure D-100, it appears there was little or no gyro response to the shock. The low frequency end of the gyro PSD, Figure D-106, is characterized by two peaks, one at approximately .05 Hz and the other at .1 Hz. These two peaks, shown more vividly on the 1 hour test, cause the power levels of S/N 2 to be significantly higher than the corresponding regions shown for S/N 1. Comments on the influence of noise made earlier, concerning the 3 minute test on Gyro S/N 1, also apply to Gyro S/N 2.

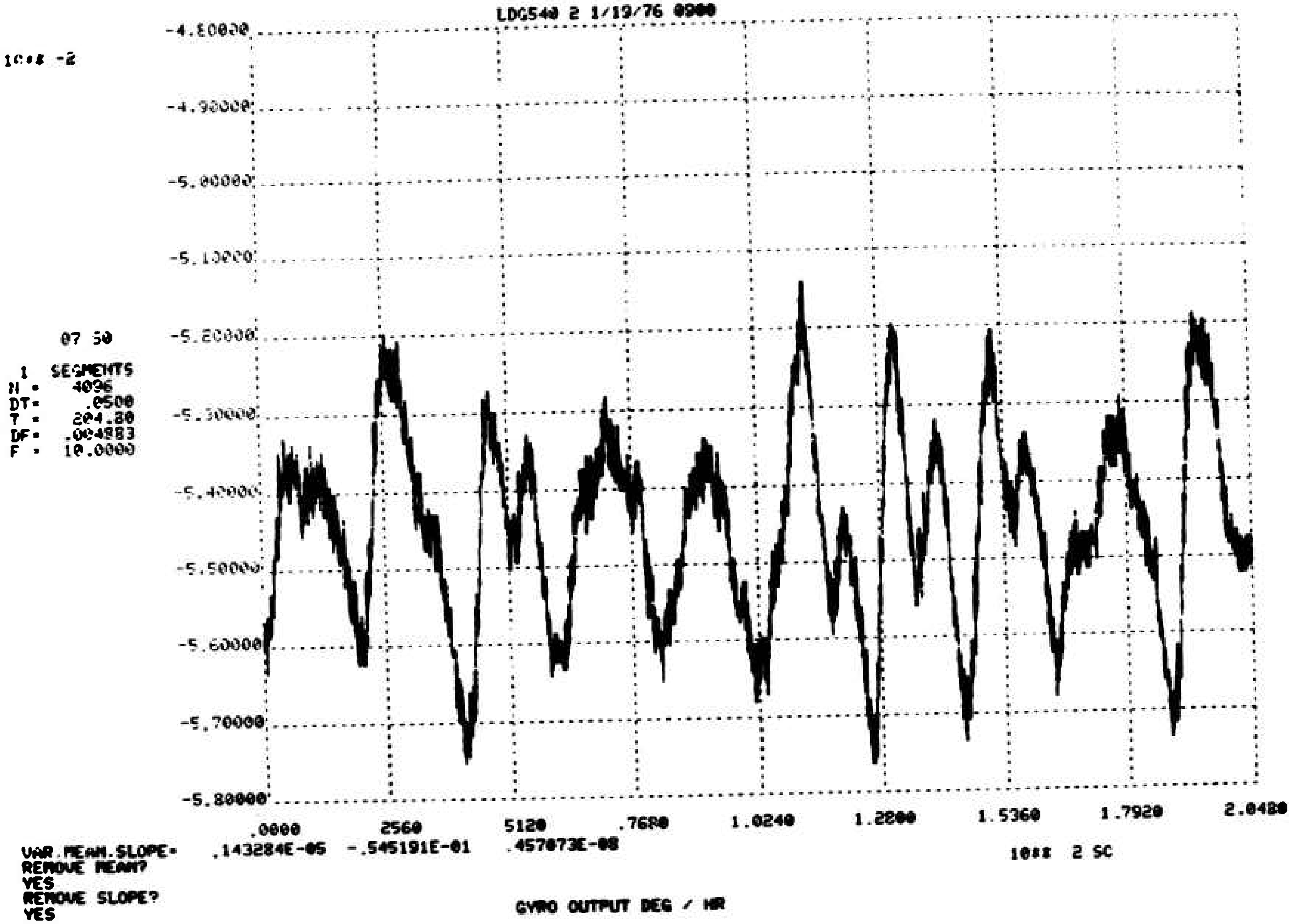

FIGURE D-100. S/N 2 GYRO DATA, DEGREE/HOUR (3 MINUTE TEST)

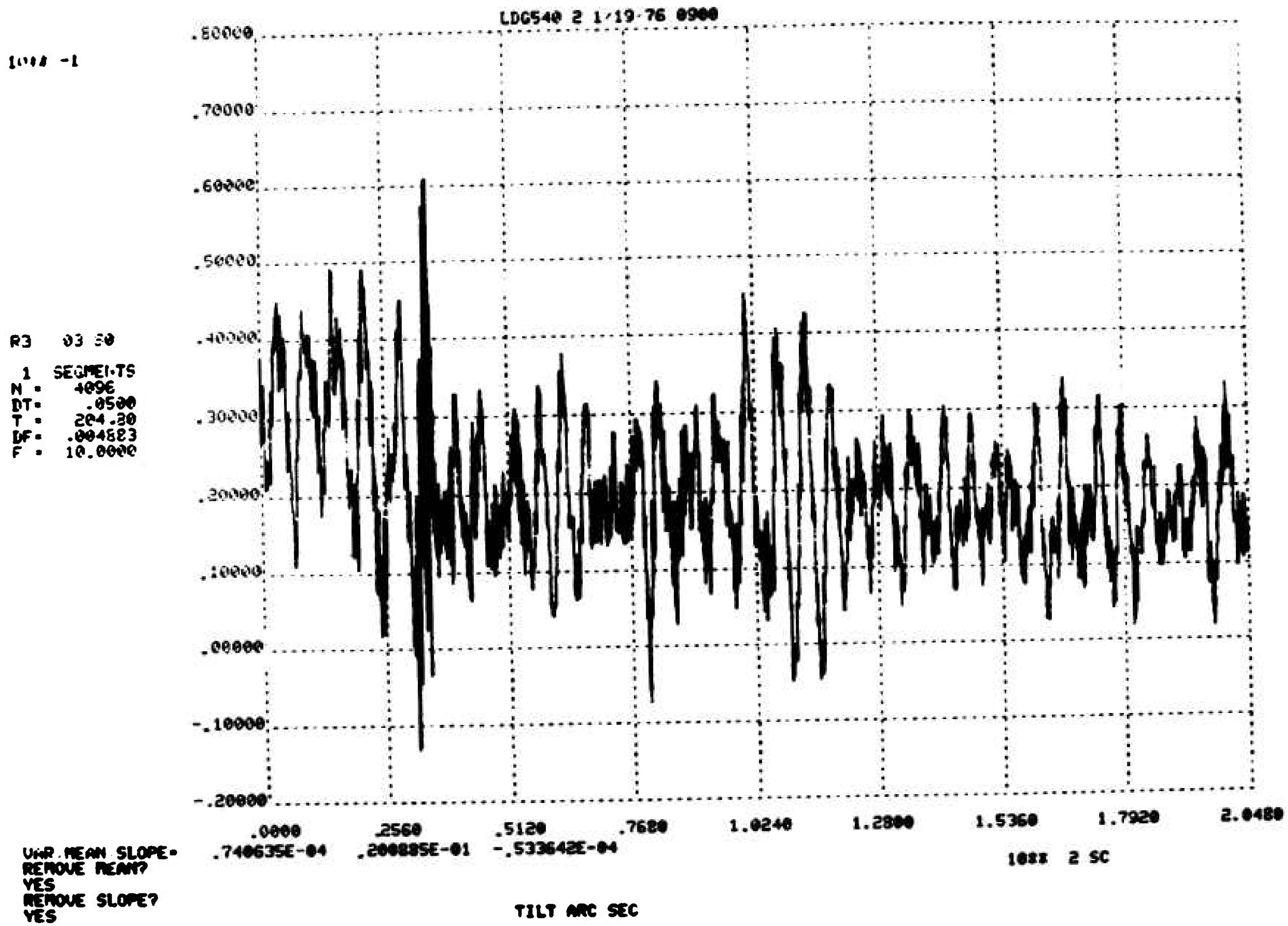

FIGURE D-101. AVERAGE TILT, ARC SECONDS (3 MINUTE TEST S/N 2)

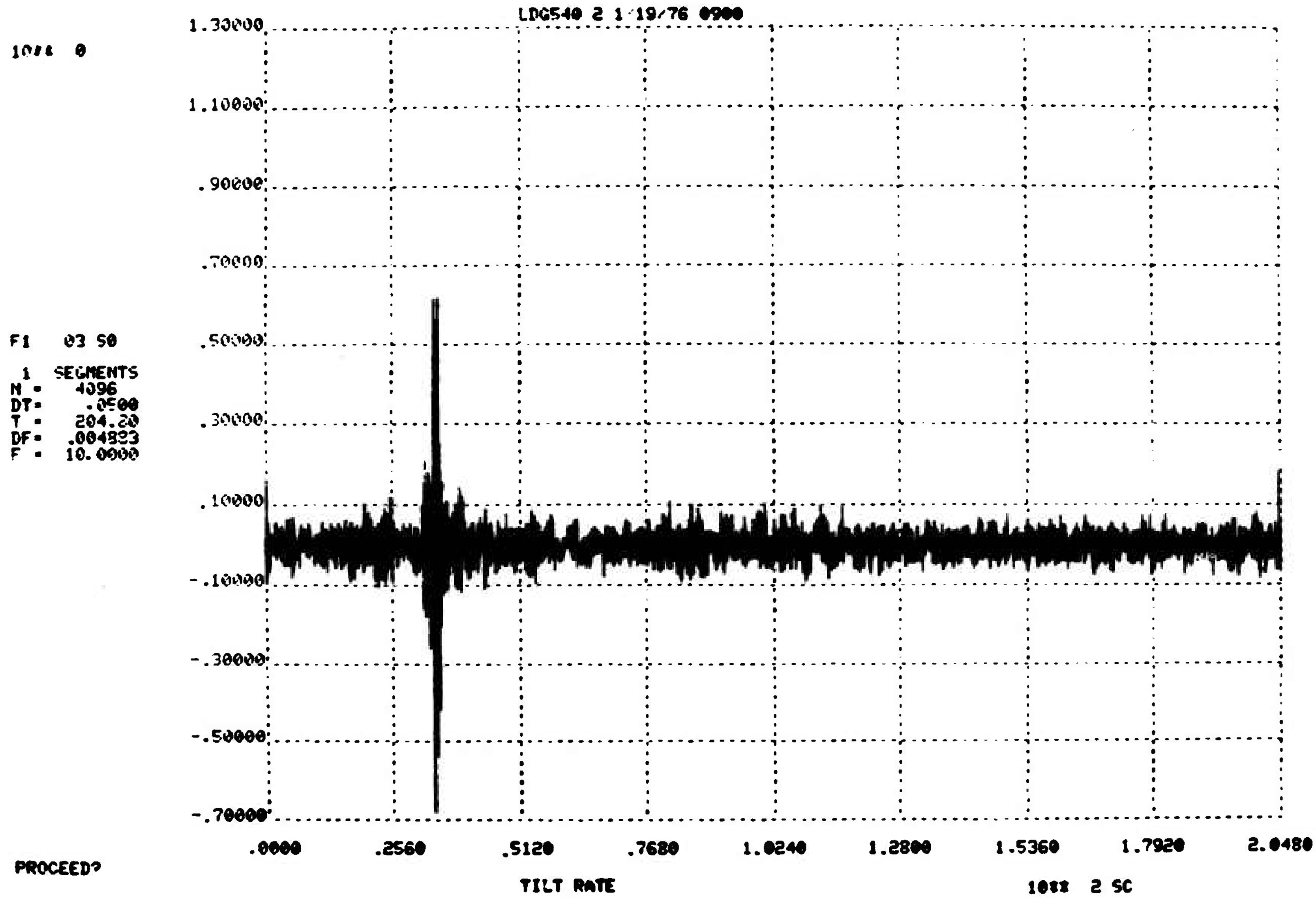

FIGURE D-102. TILT RATE, DEGREE/HOUR (3 MINUTE TEST S/N 2)

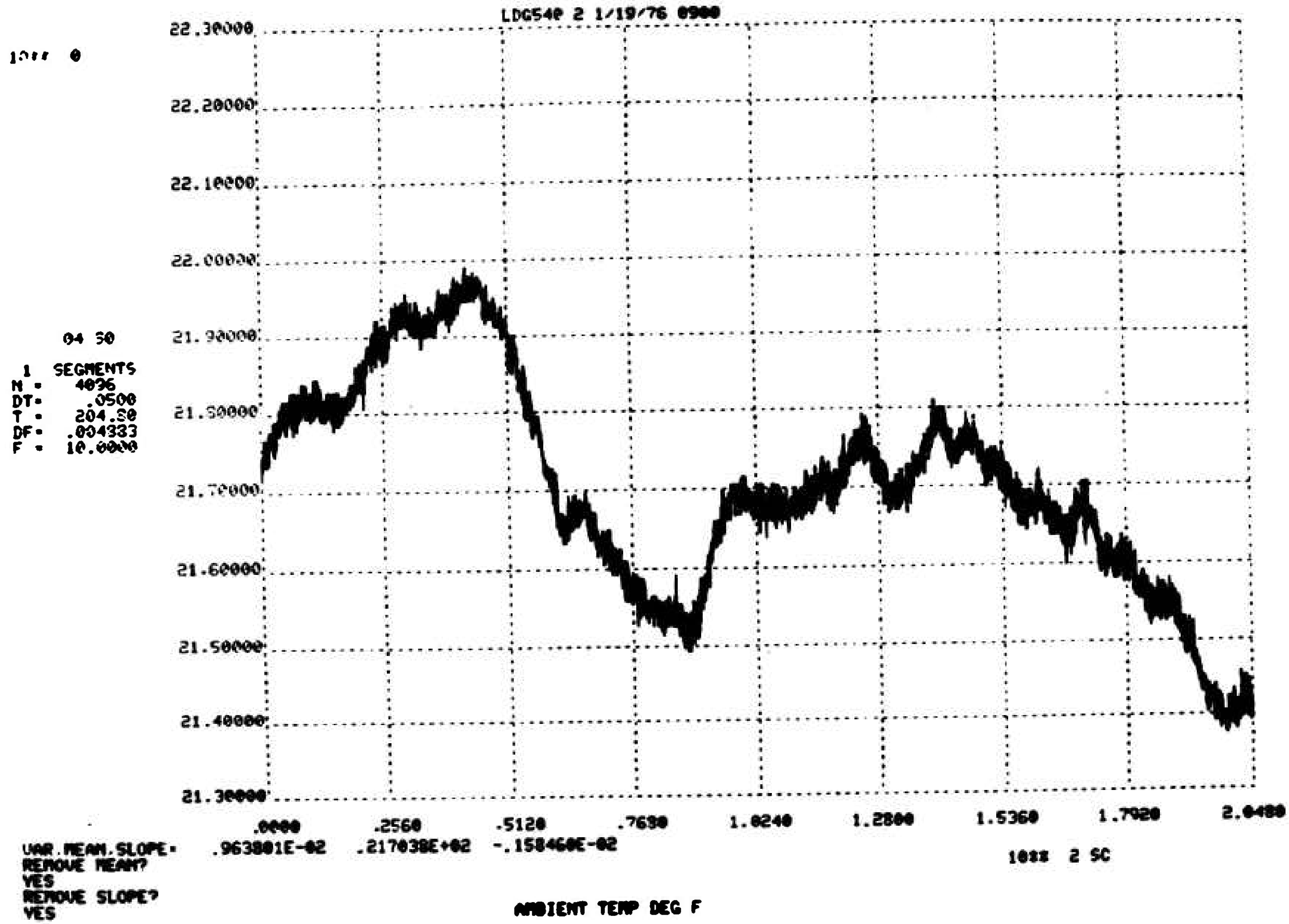

FIGURE D-103. AMBIENT TEMPERATURE, DEGREE F (3 MINUTE TEST S/N 2)

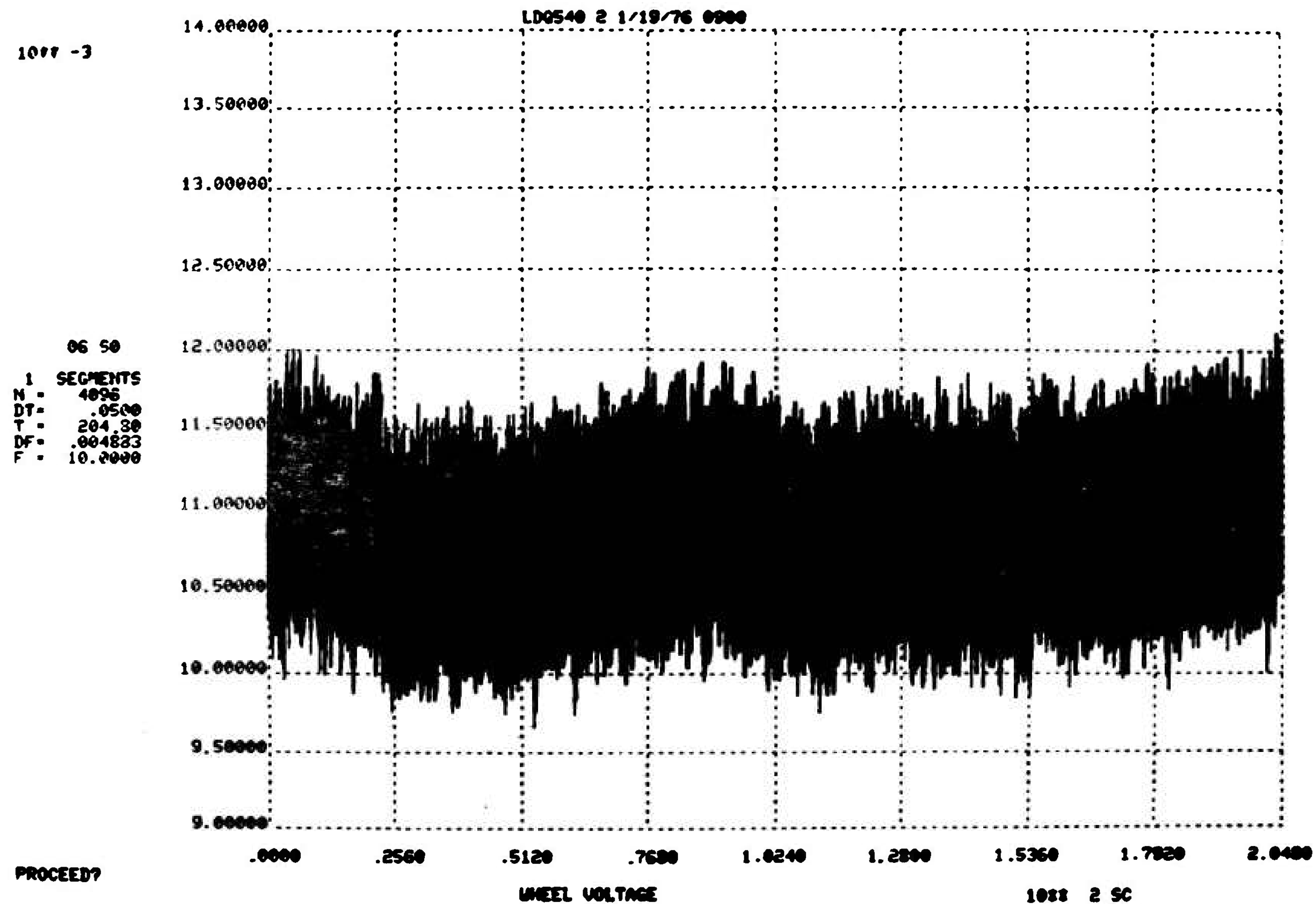

FIGURE D-104. S/N 2 GYRO WHEEL VOLTAGE, VOLTS (3 MINUTE TEST)

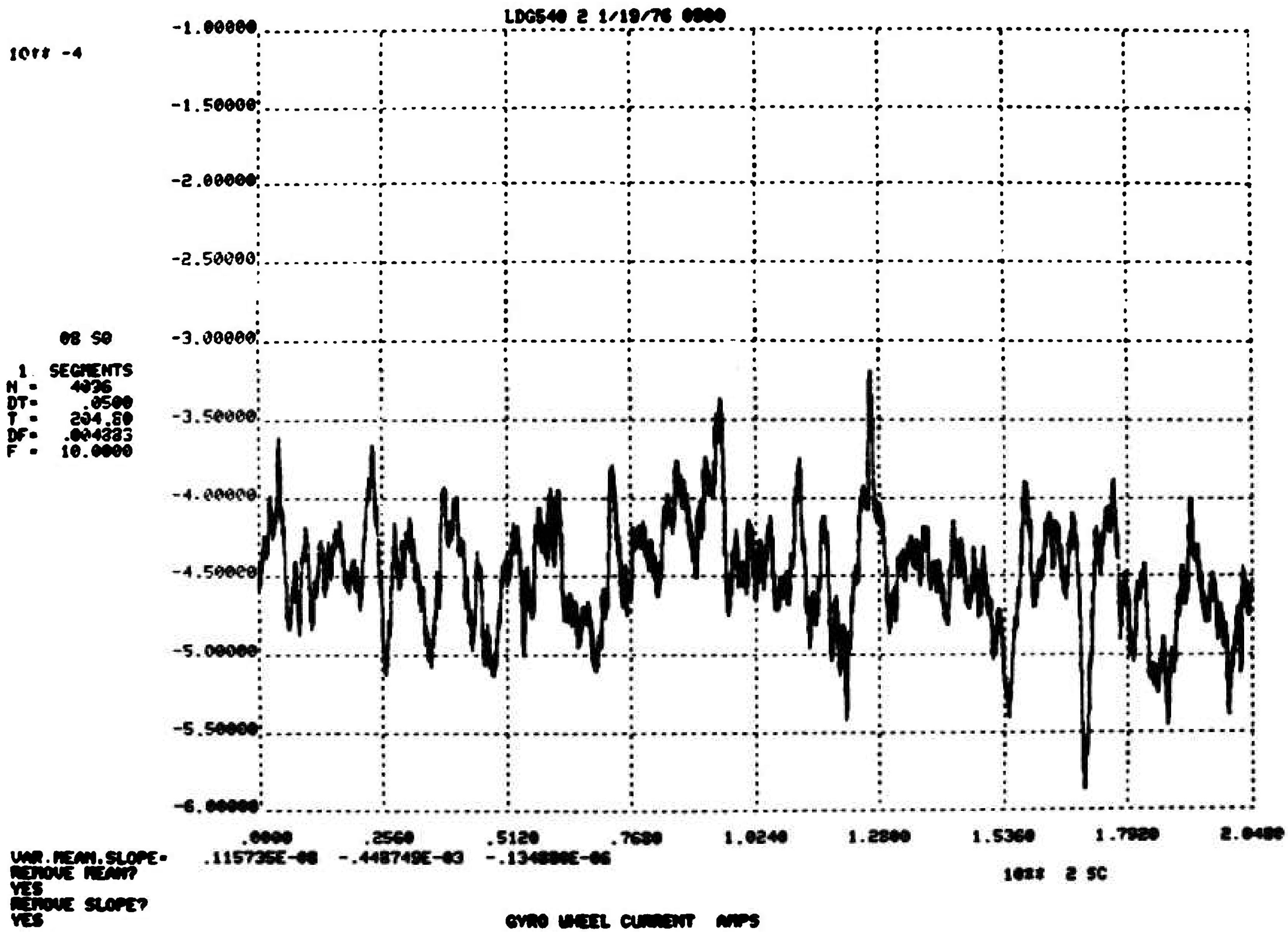

FIGURE D-105. S/N 2 GYRO WHEEL CURRENT, AMPS (3 MINUTE TEST)

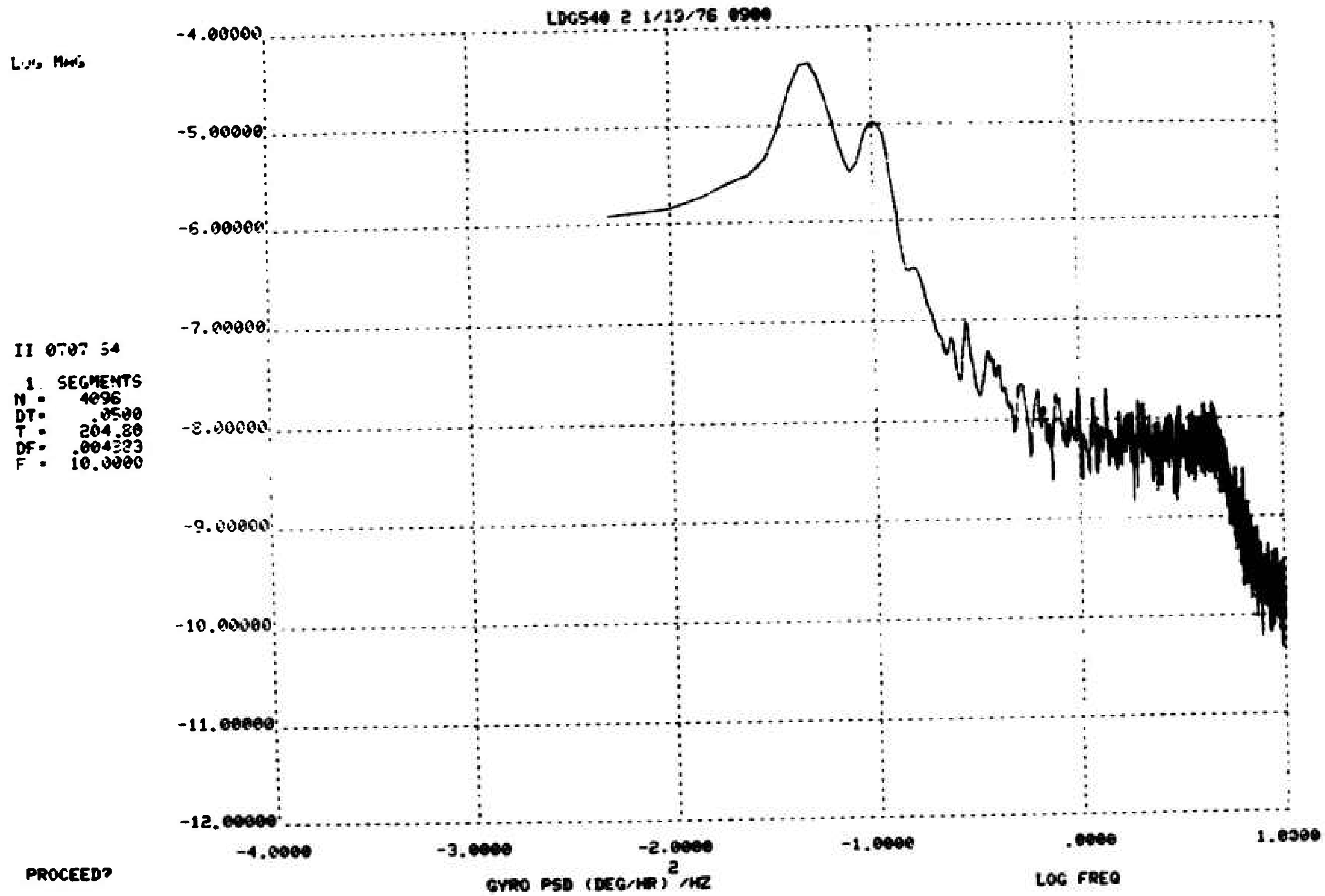

FIGURE D-106. PSD S/N 2 GYRO DATA, (DEGREE/HOUR)^2/HZ (3 MINUTE TEST)

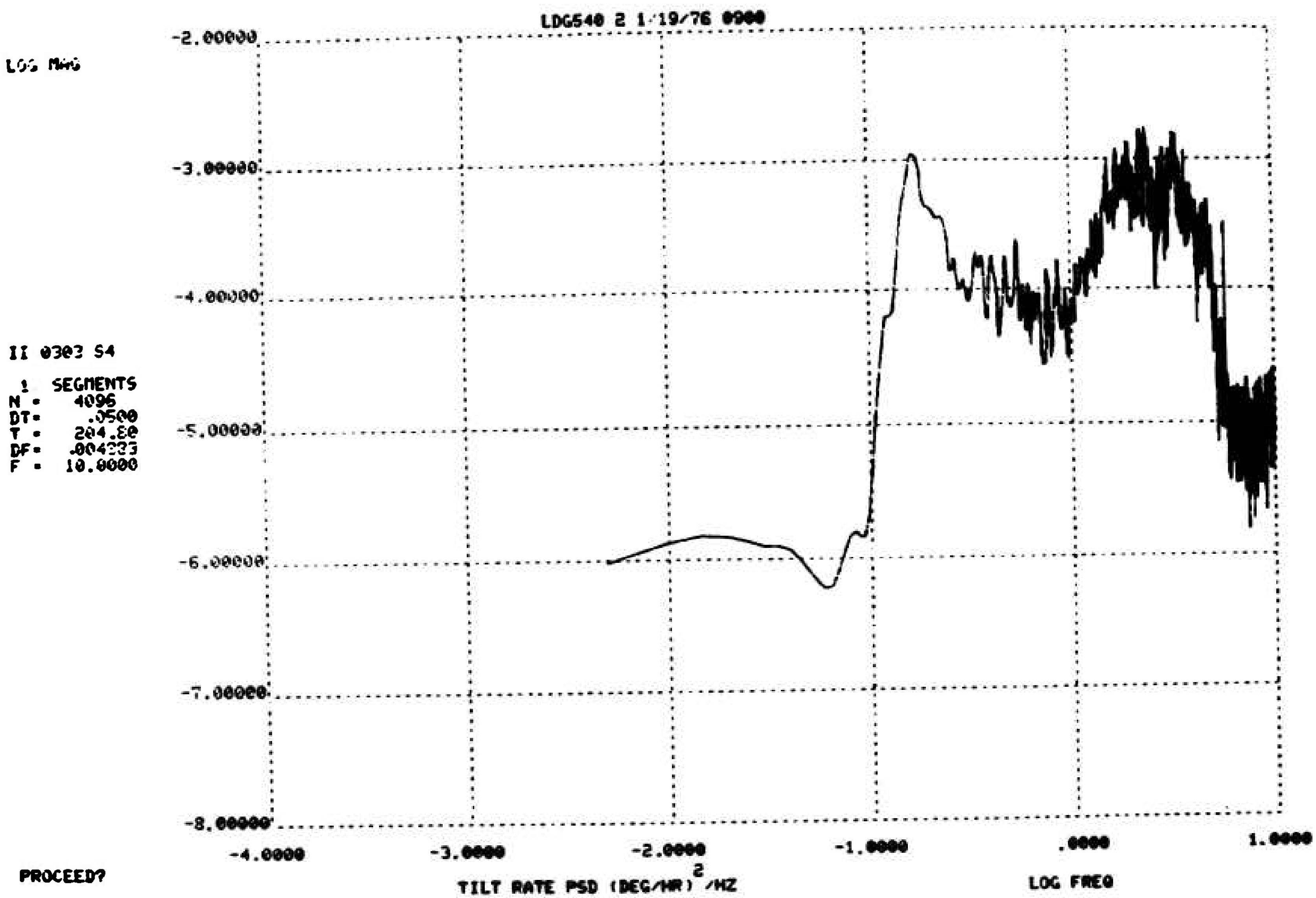

FIGURE D-107. PSD TILT RATE, $(\mathrm{DEGREE/HOUR})^2/\mathrm{HZ}$ (3 MINUTE TEST S/N 2)

APPENDIX E

SHORTED FILTER TEST RESULTS

For the three minute tests, the 816 filter was used on the gyro data and all other signals monitored. Figures E-1 through E-3 show the raw shorted 816 filter data, followed by PSD plots using gyro and tilt rate scaling.

The one hour test used the 3-pole filter on the gyro data, and the 816 filter on all other monitored functions. The 3-pole filter raw data and gyro scaling PSD is presented first, Figures E-4 and E-5, followed by the raw 816 data and appropriately scaled PSD plots in Figures E-6 through E-13.

The twenty-four hour test also used the 3-pole filter on the gyro, and the 816 filter for the rest of the data. Figures E-14 through E-32 presents the twenty-four hour shorted filter test results in the same format as described above for the one hour test.

Note that in both the one hour test, and the twenty-four hour test, two different voltage scalings and two different current scalings are presented. This is because the voltage and current monitoring instruments were set differently for the test on Gyro S/N 2 than they were for Gyro S/N 1. Current scaling of .05 and voltage scaling of .4 apply to the tests on Gyro S/N 1. For all tests on Gyro S/N 2, current scaling of .00158, and voltage scaling of .04 applies.

Note that the sharper cutoff of the 816 Butterworth filter results in a more pronounced knee in the PSD plots than the cascaded 3-pole filters.

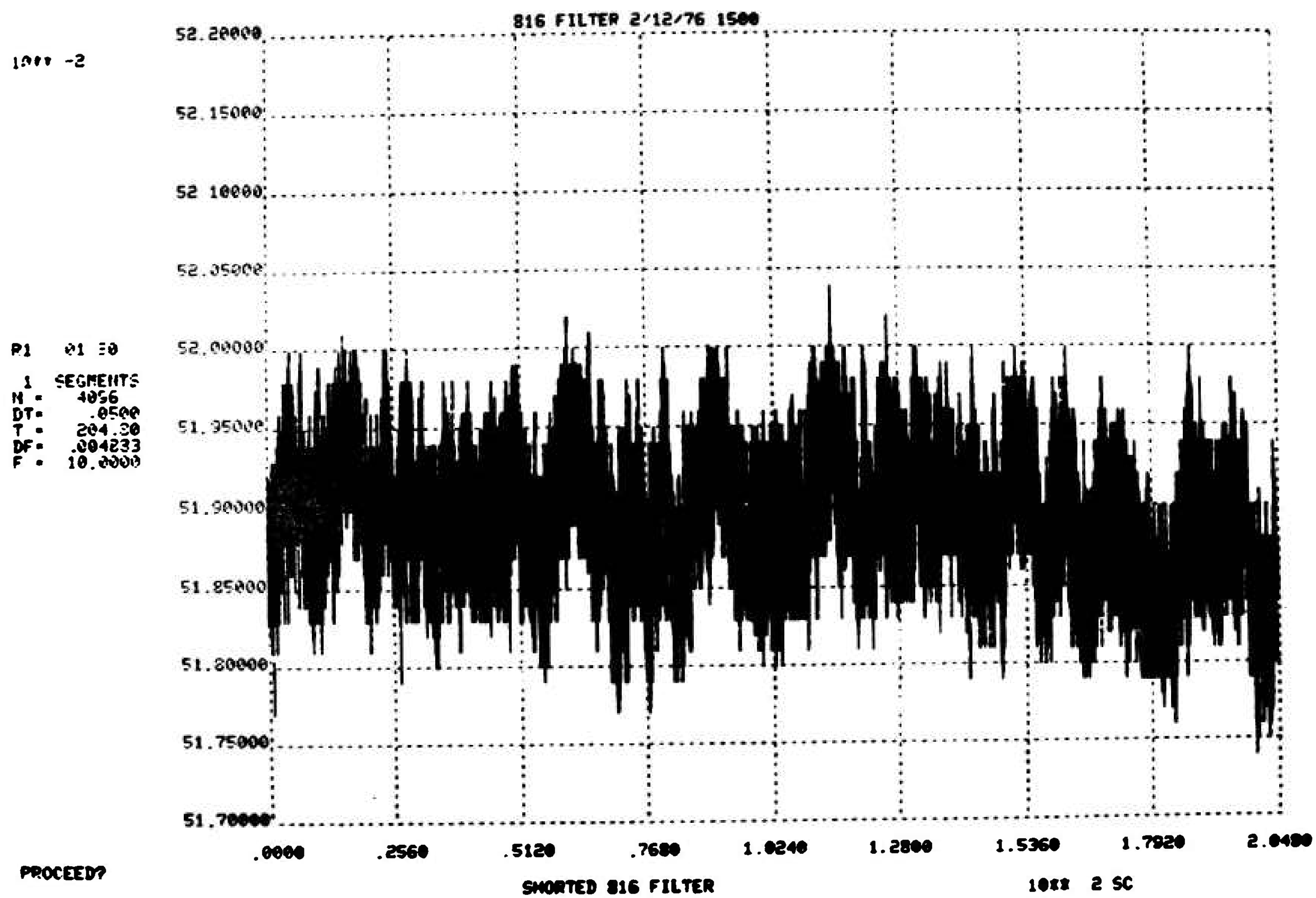

FIGURE E-1. SHORTED 816 FILTER (3 MINUTE TEST) (Volts)

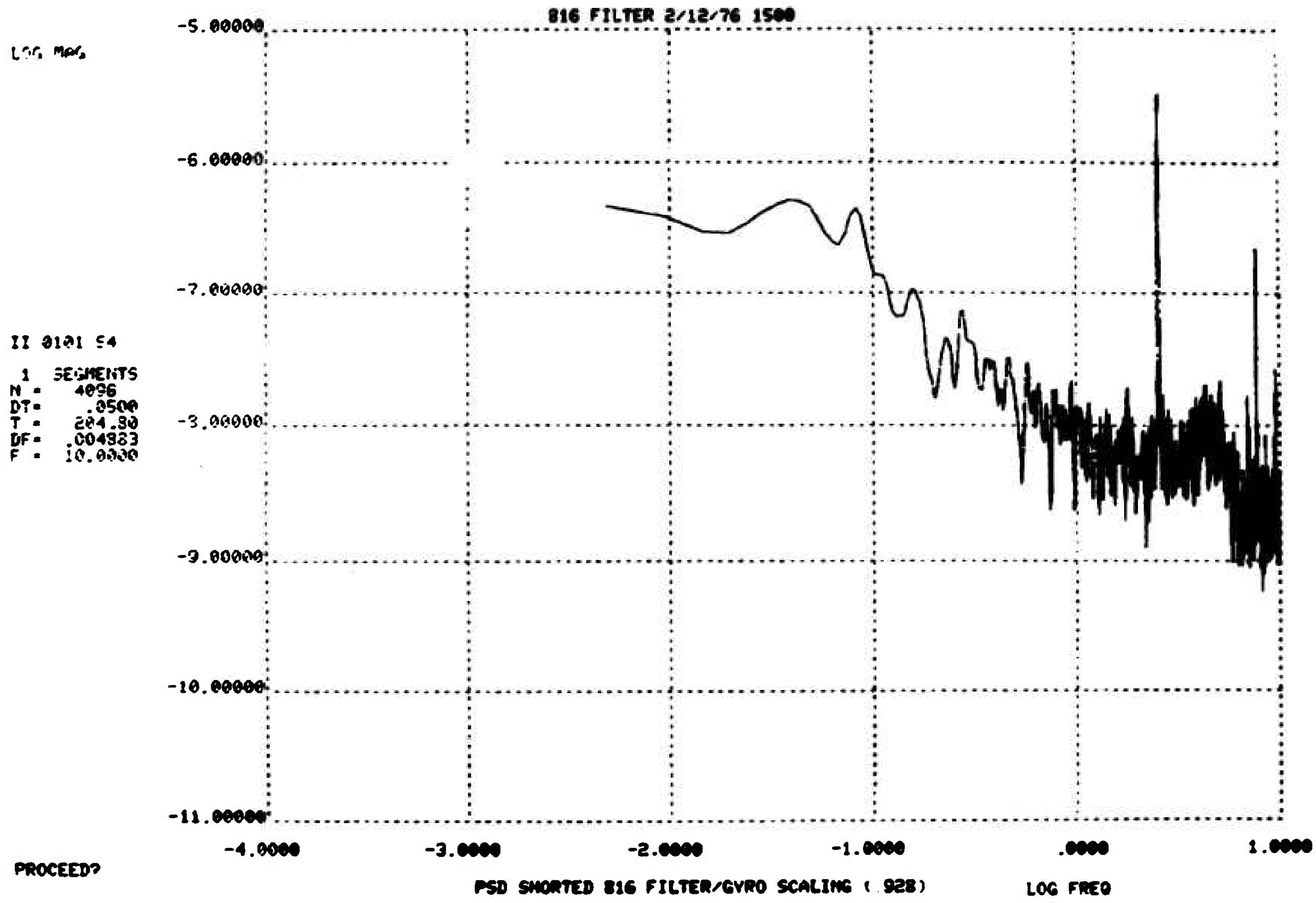

FIGURE E-2. FILTER NOISE PSD/GYRO SCALING (3 MINUTE TEST)

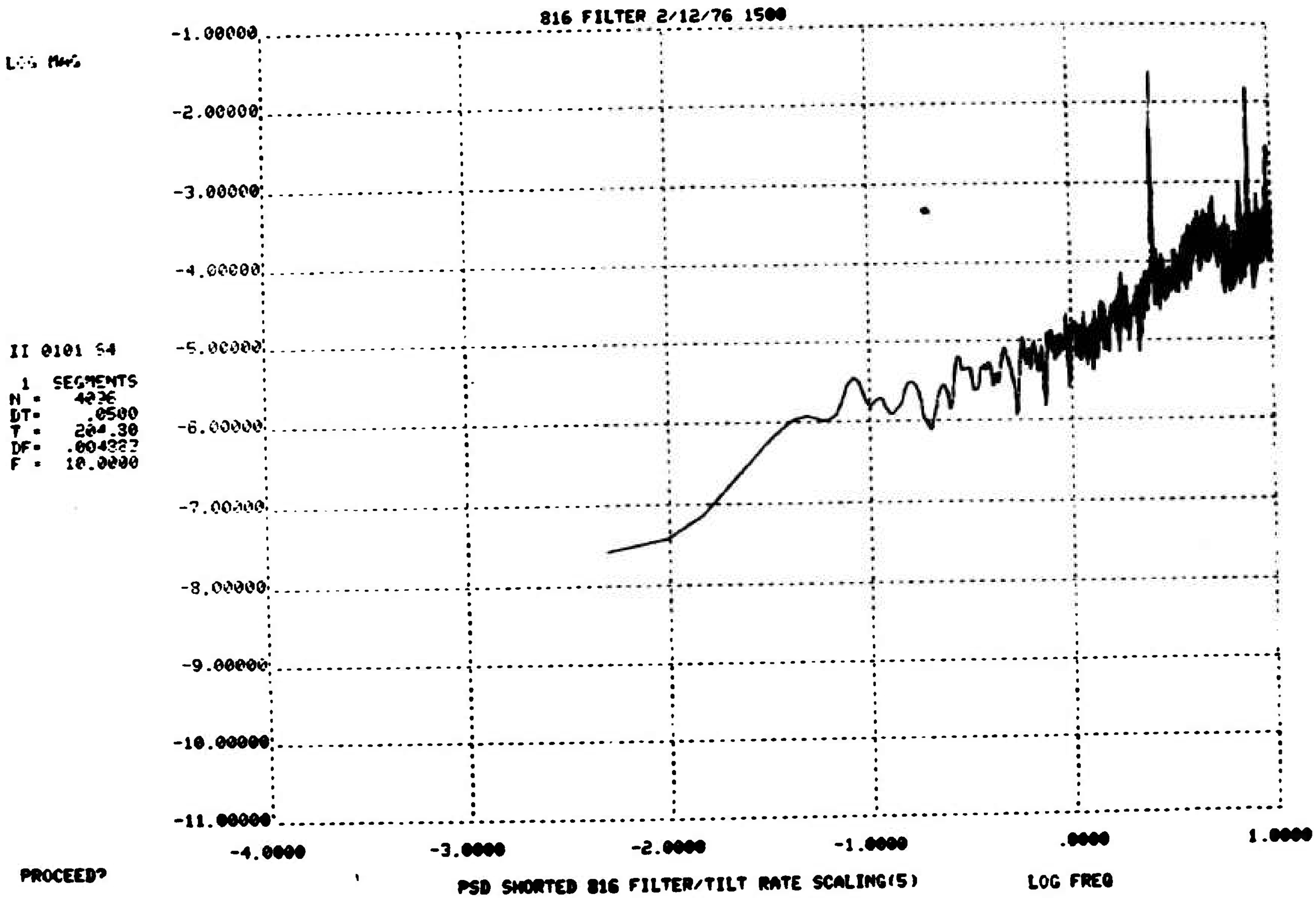

FIGURE E-3. FILTER NOISE PSD/TILT RATE SCALING (3 MINUTE TEST)

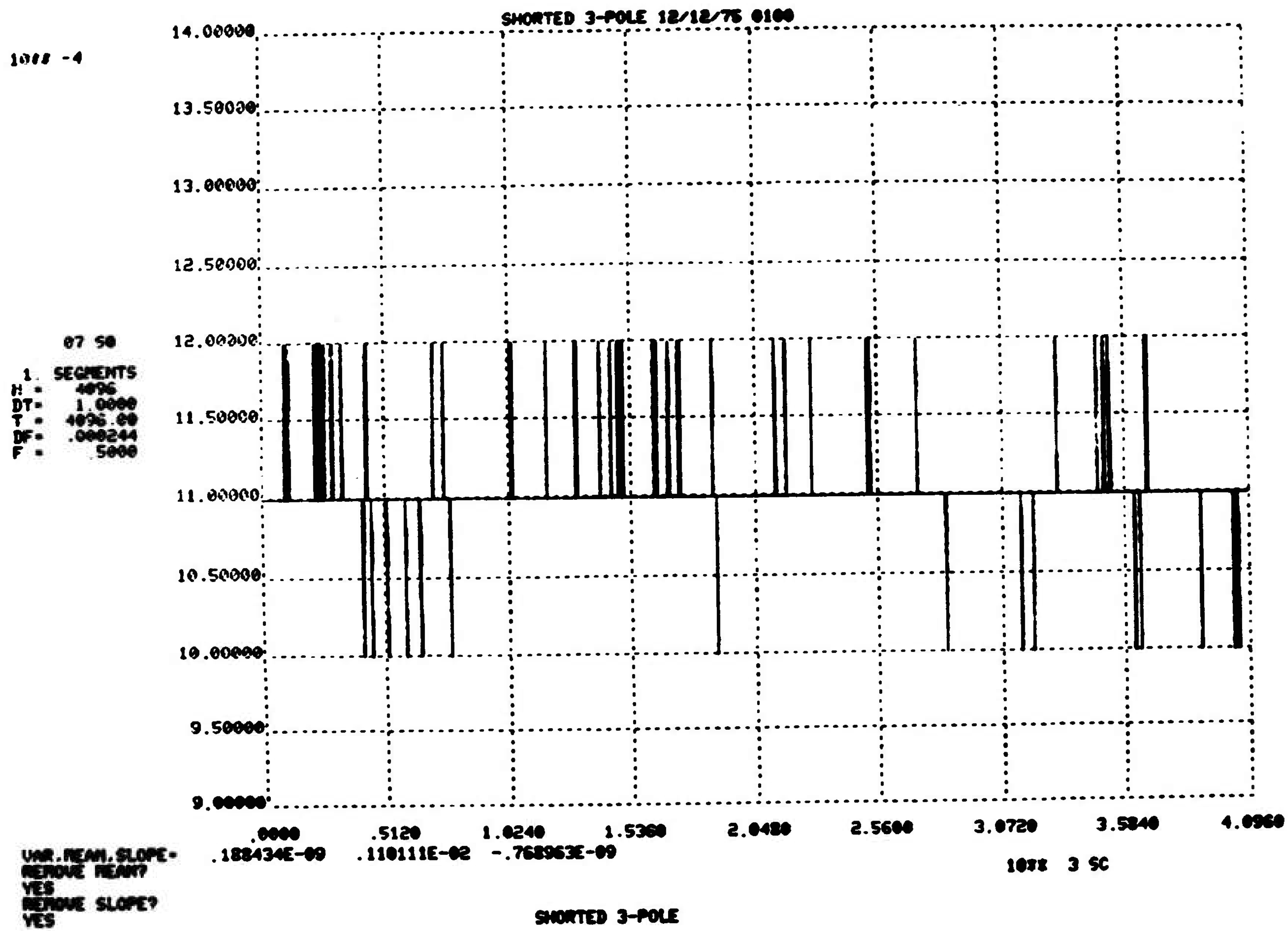

FIGURE E-4. SHORTED 3-POLE FILTER (1 HOUR TEST) (Volts)

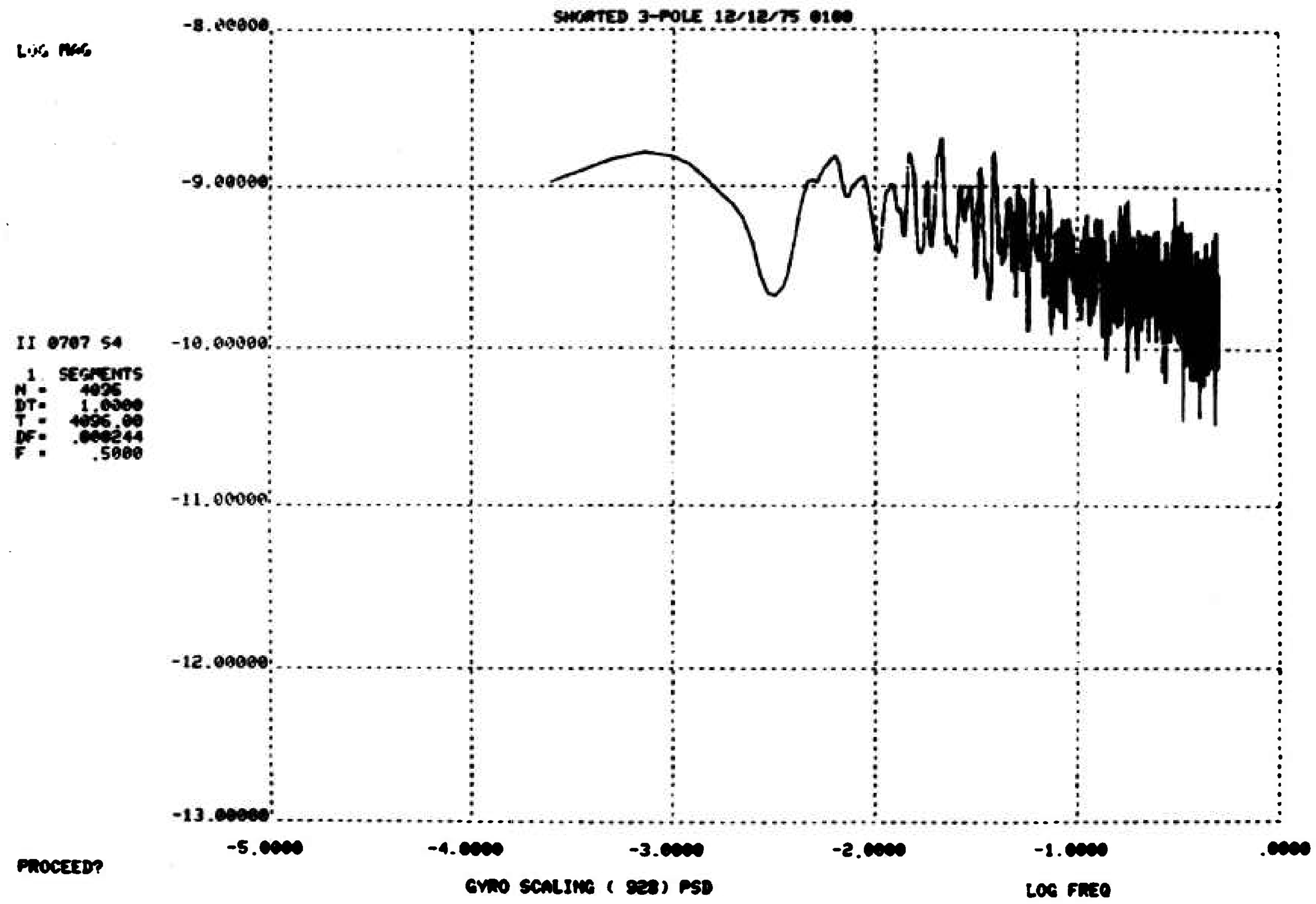

FIGURE E-5. FILTER NOISE PSD/GYRO SCALING (1 HOUR TEST)

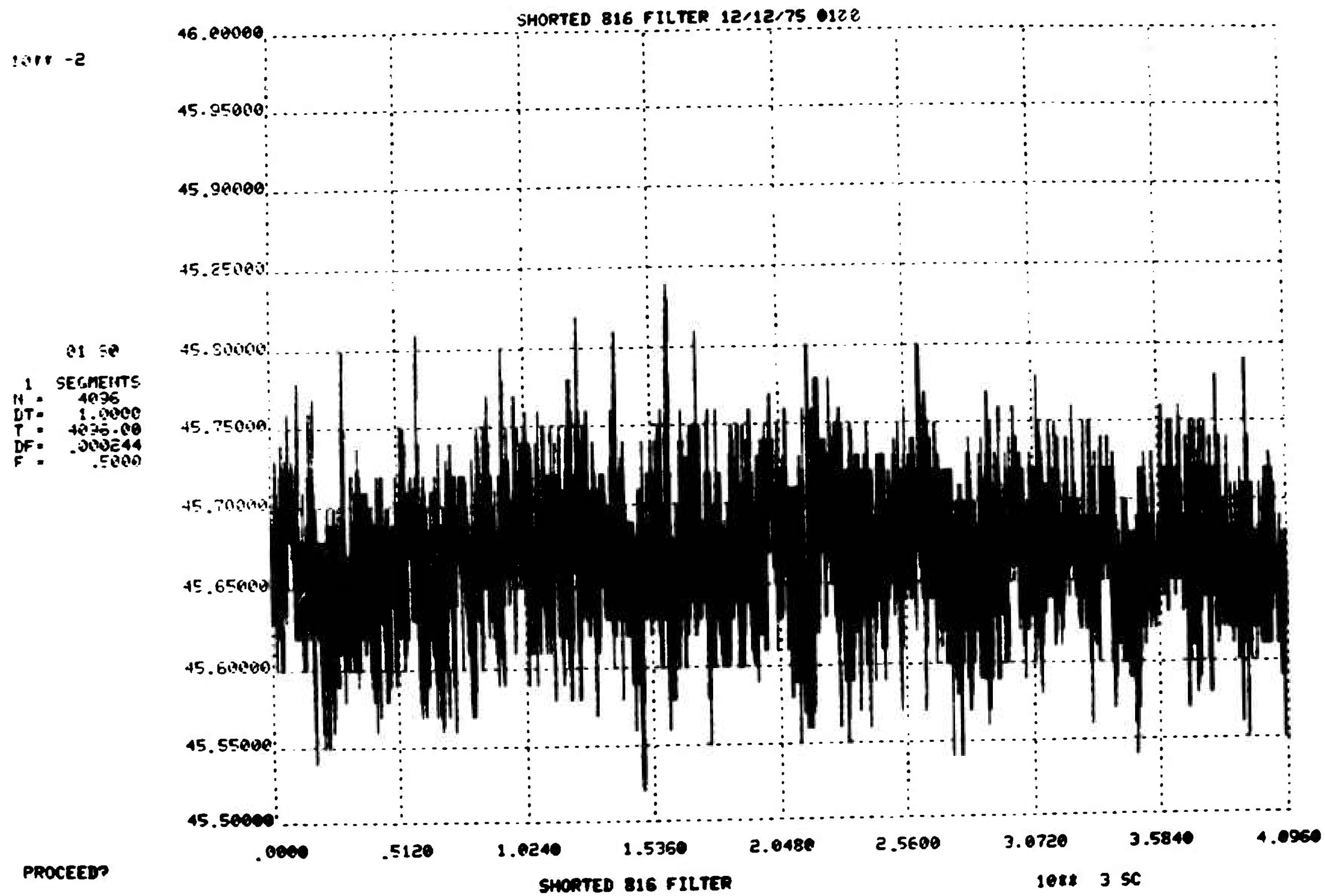

FIGURE E-6. SHORTED 816 FILTER (1 HOUR TEST) (Volts)

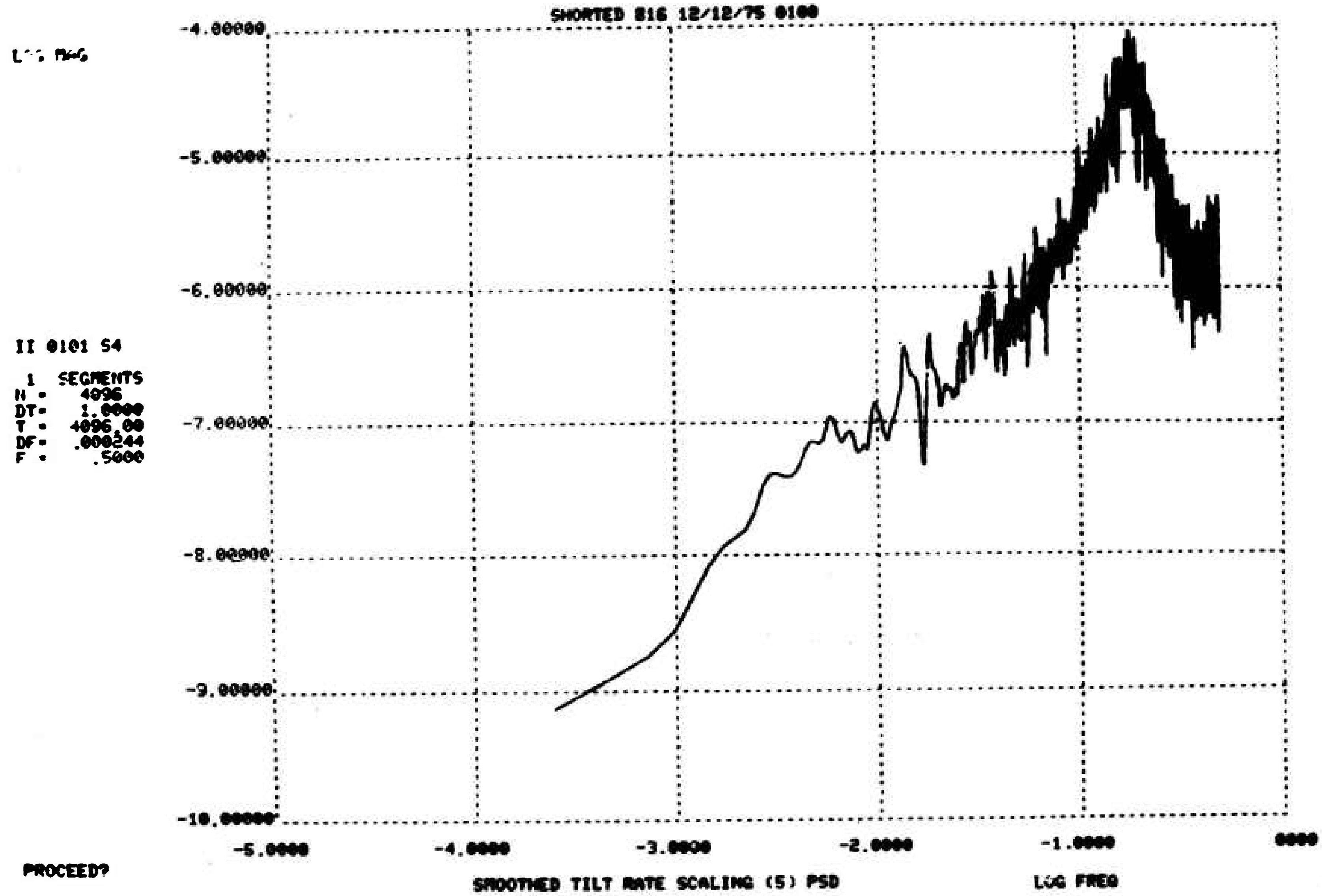

FIGURE E-7. FILTER NOISE PSD/TILT RATE SCALING (1 HOUR TEST)

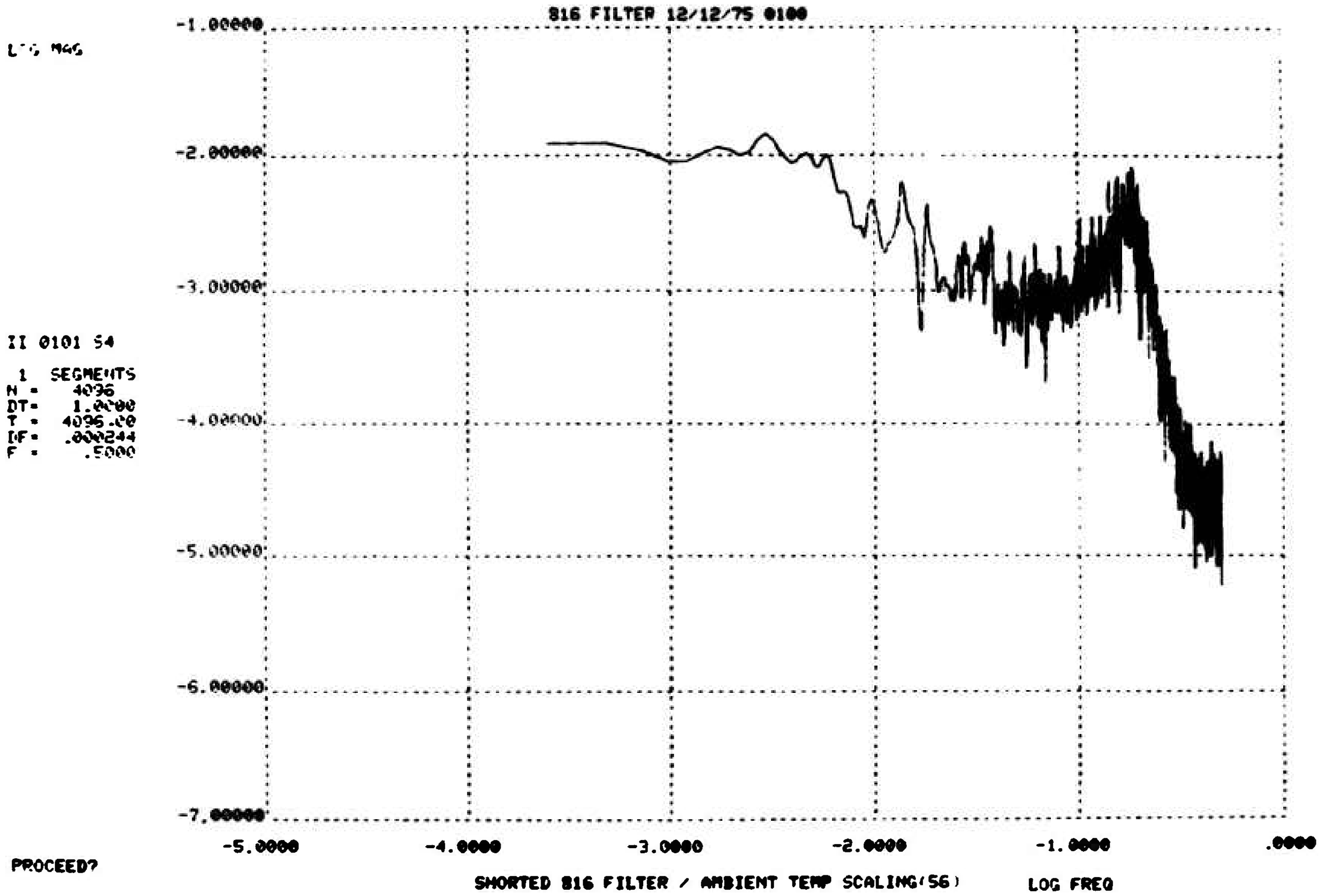

FIGURE E-8. FILTER NOISE PSD/AMBIENT TEMPERATURE SCALING (1 HOUR TEST)

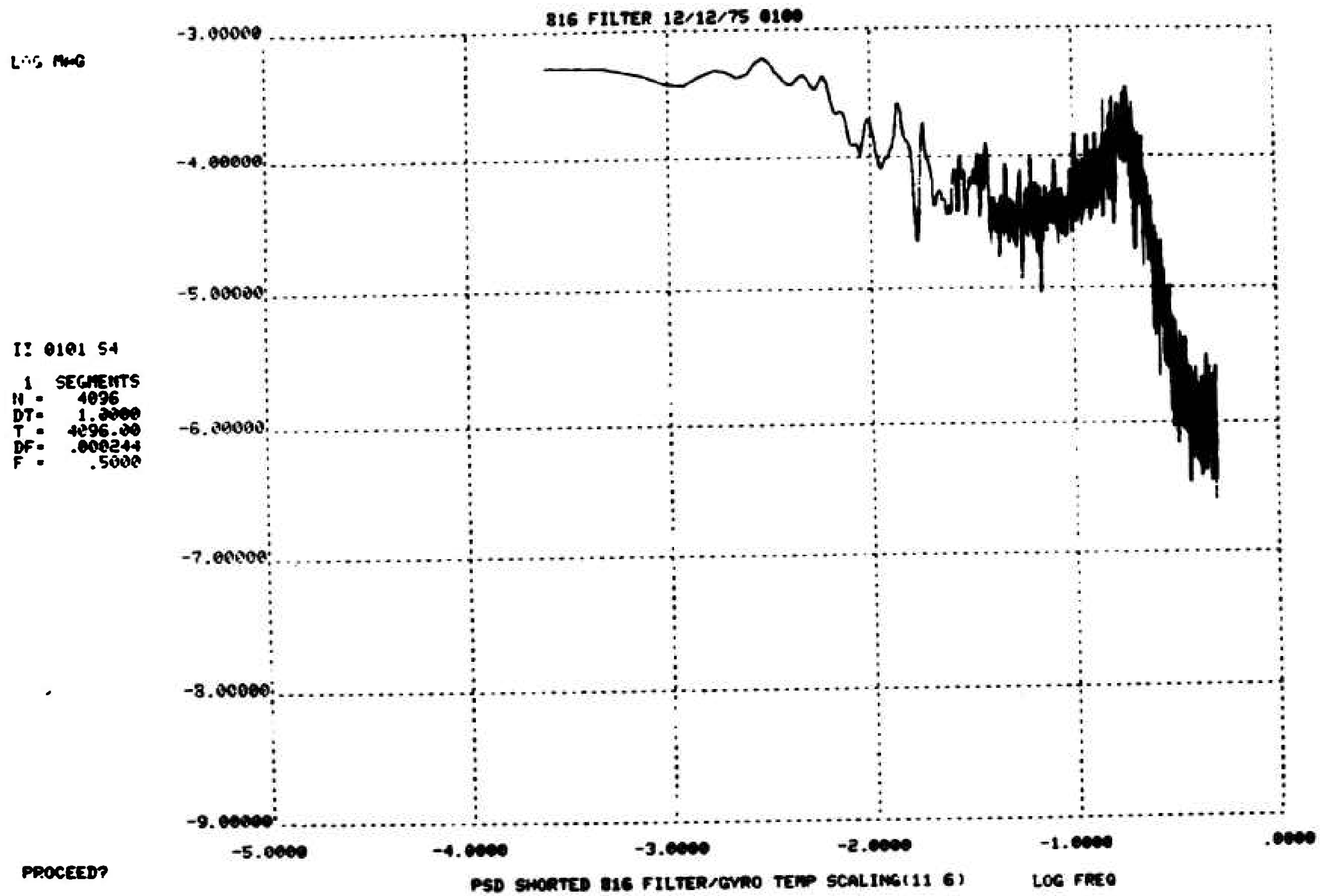

FIGURE E-9. FILTER NOISE PSD/GYRO TEMPERATURE SCALING (1 HOUR TEST)

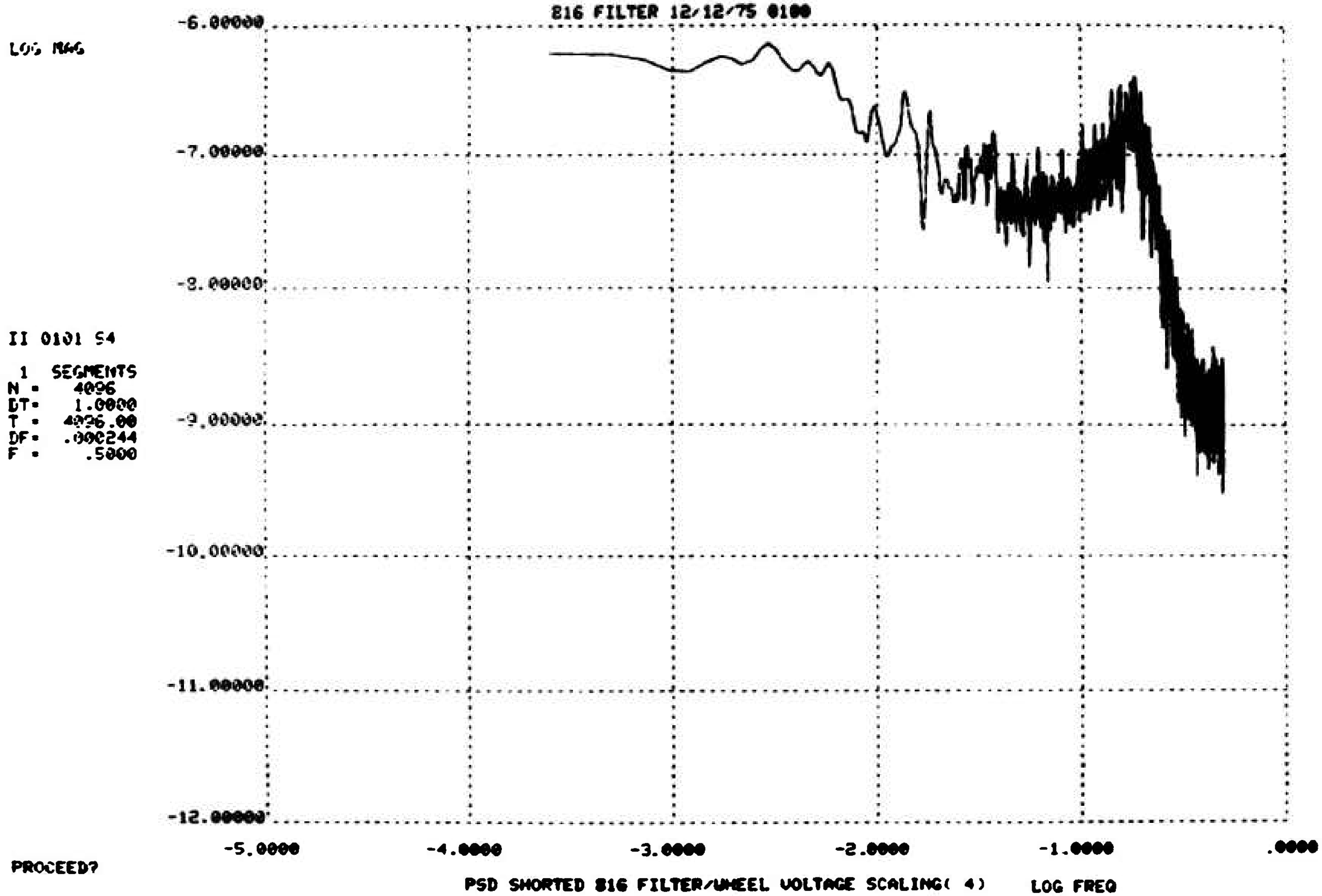

FIGURE E-10. FILTER NOISE PSD/GYRO VOLTAGE .4 SCALING (1 HOUR TEST)

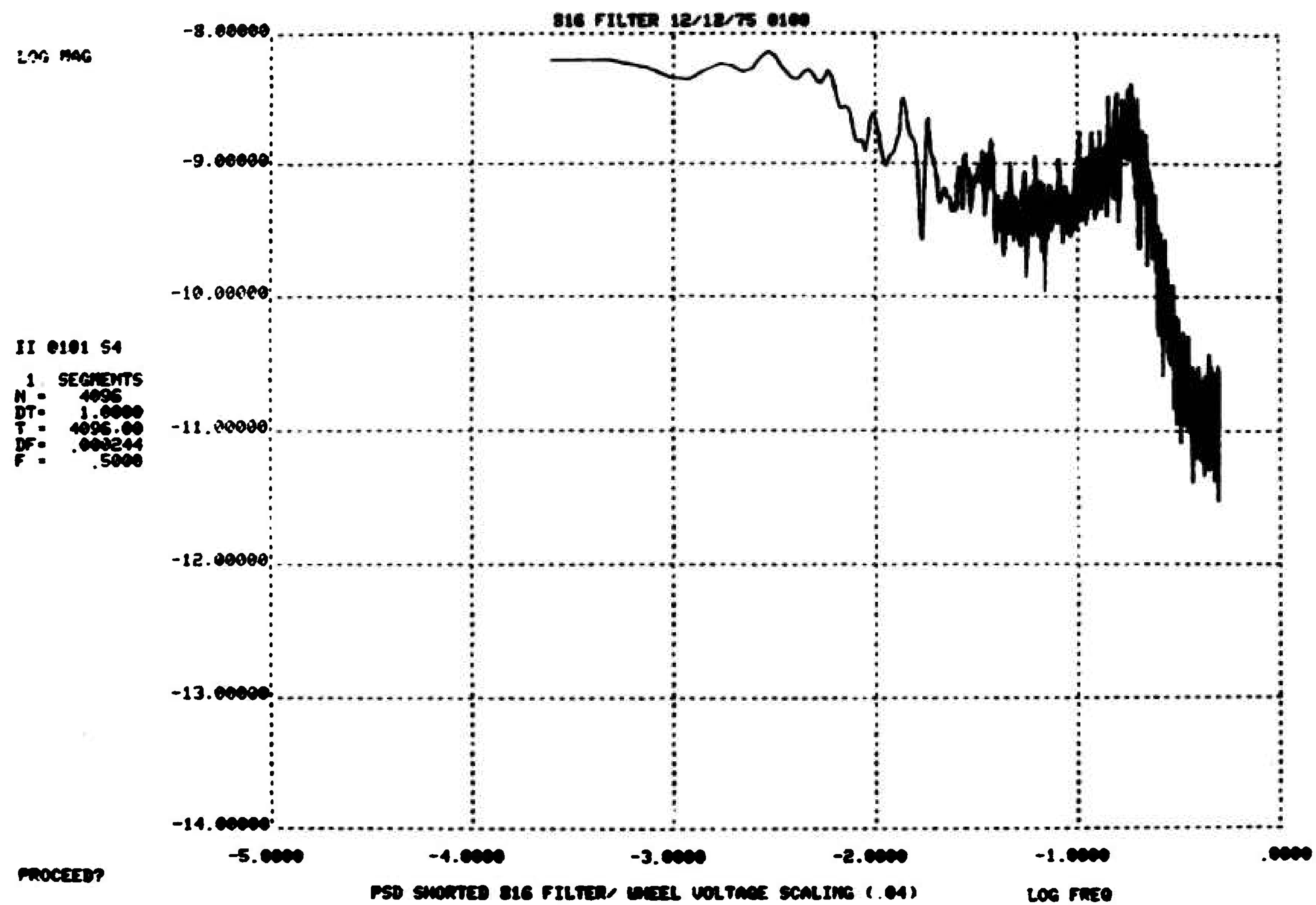

FIGURE E-11. FILTER NOISE PSD/GYRO VOLTAGE .04 SCALING (1 HOUR TEST)

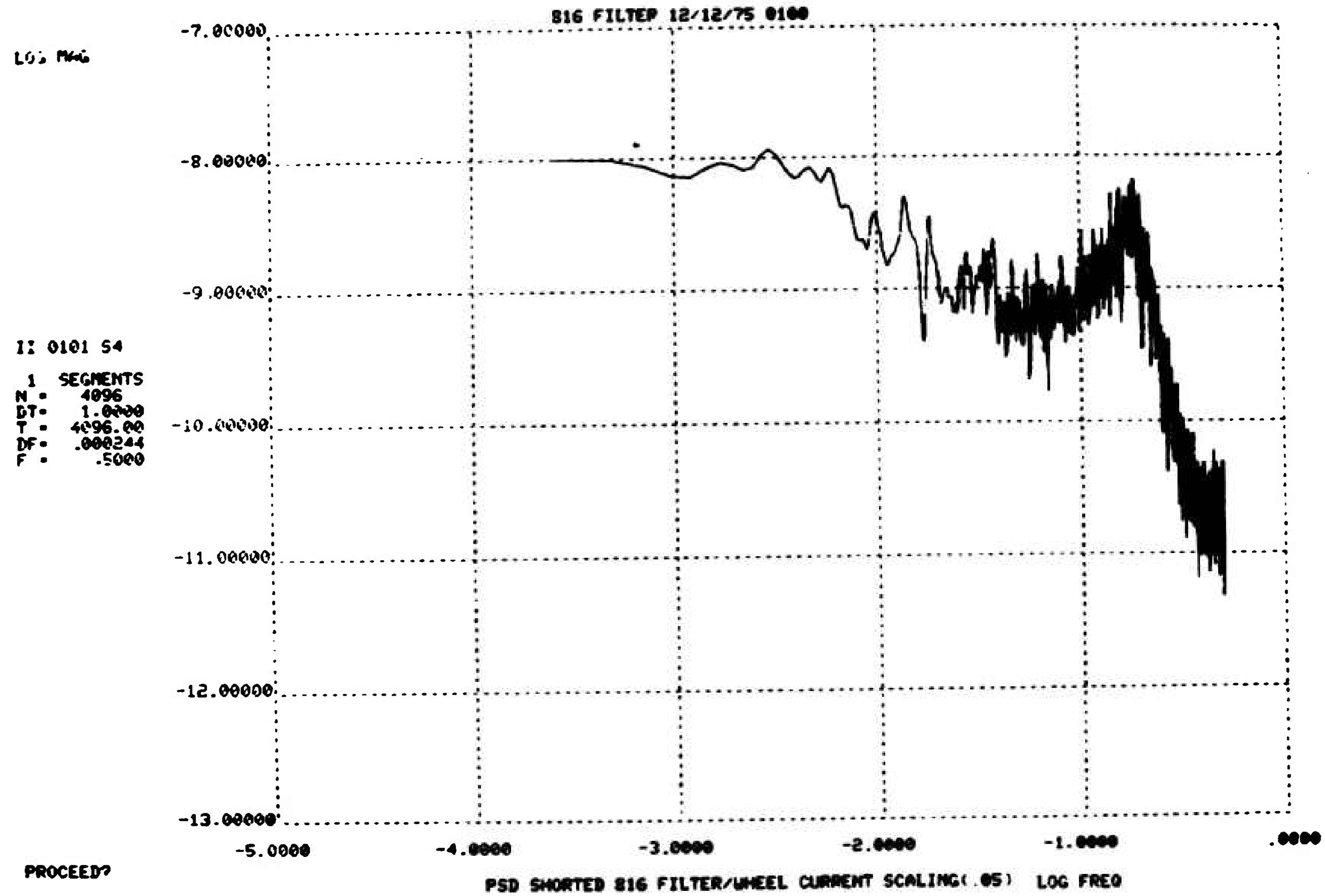

FIGURE E-12. FILTER NOISE PSD/GYRO CURRENT .05 SCALING (1 HOUR TEST)

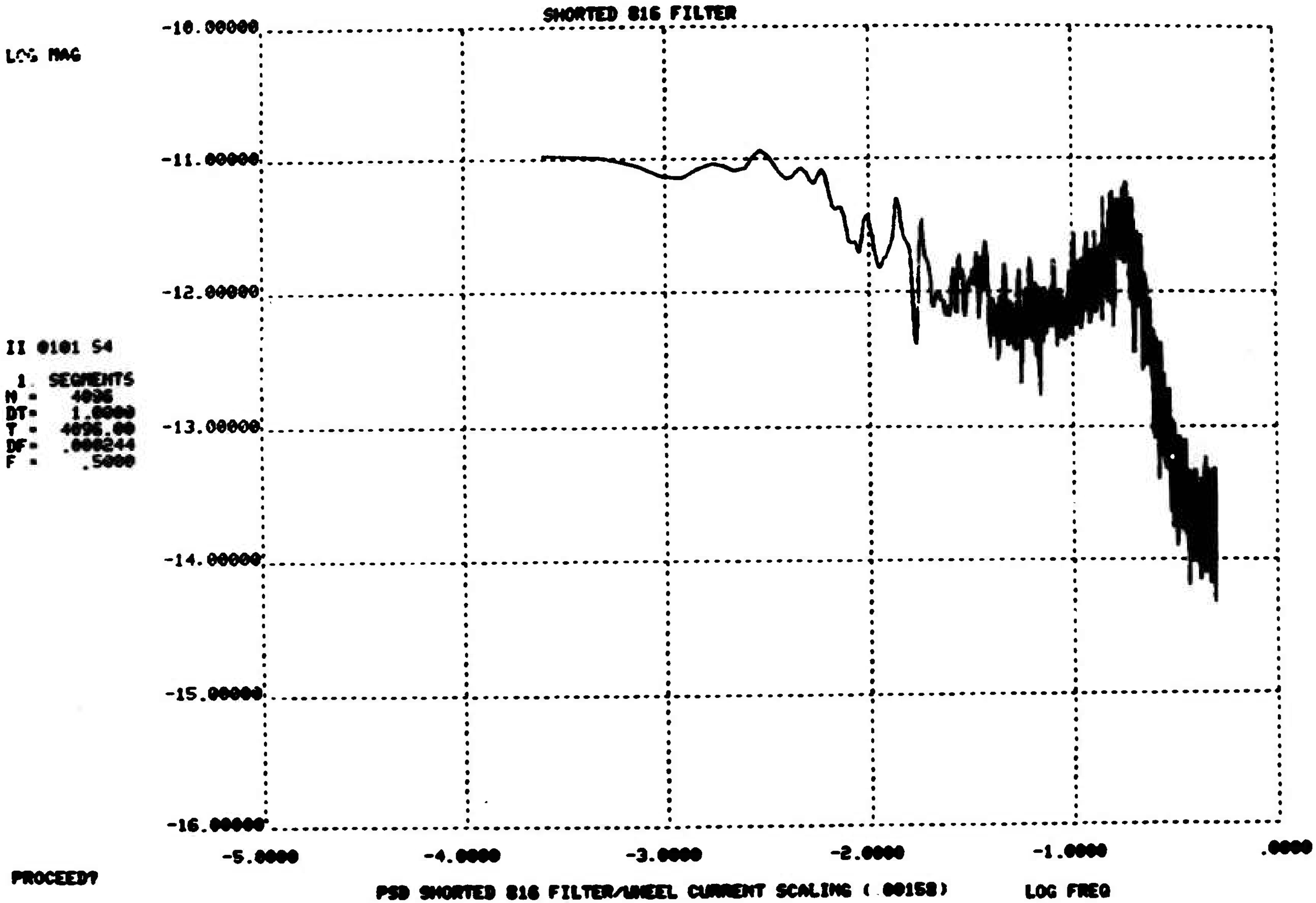

FIGURE E-13. FILTER NOISE PSD/GYRO CURRENT .00158 SCALING (1 HOUR TEST)

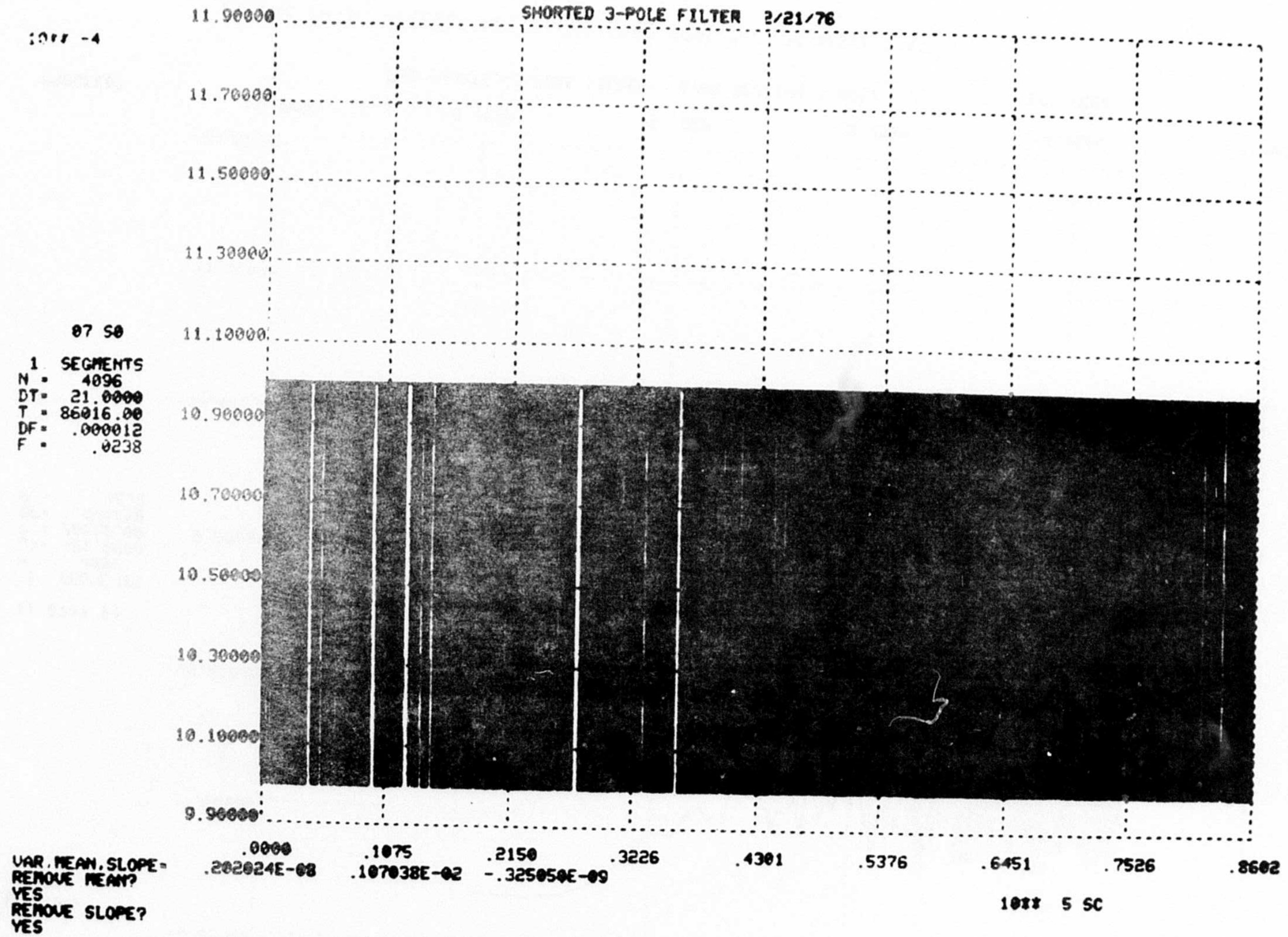

FIGURE E-14. SHORTED 3- POLE FILTER (24 HOUR TEST) (VOLTS)

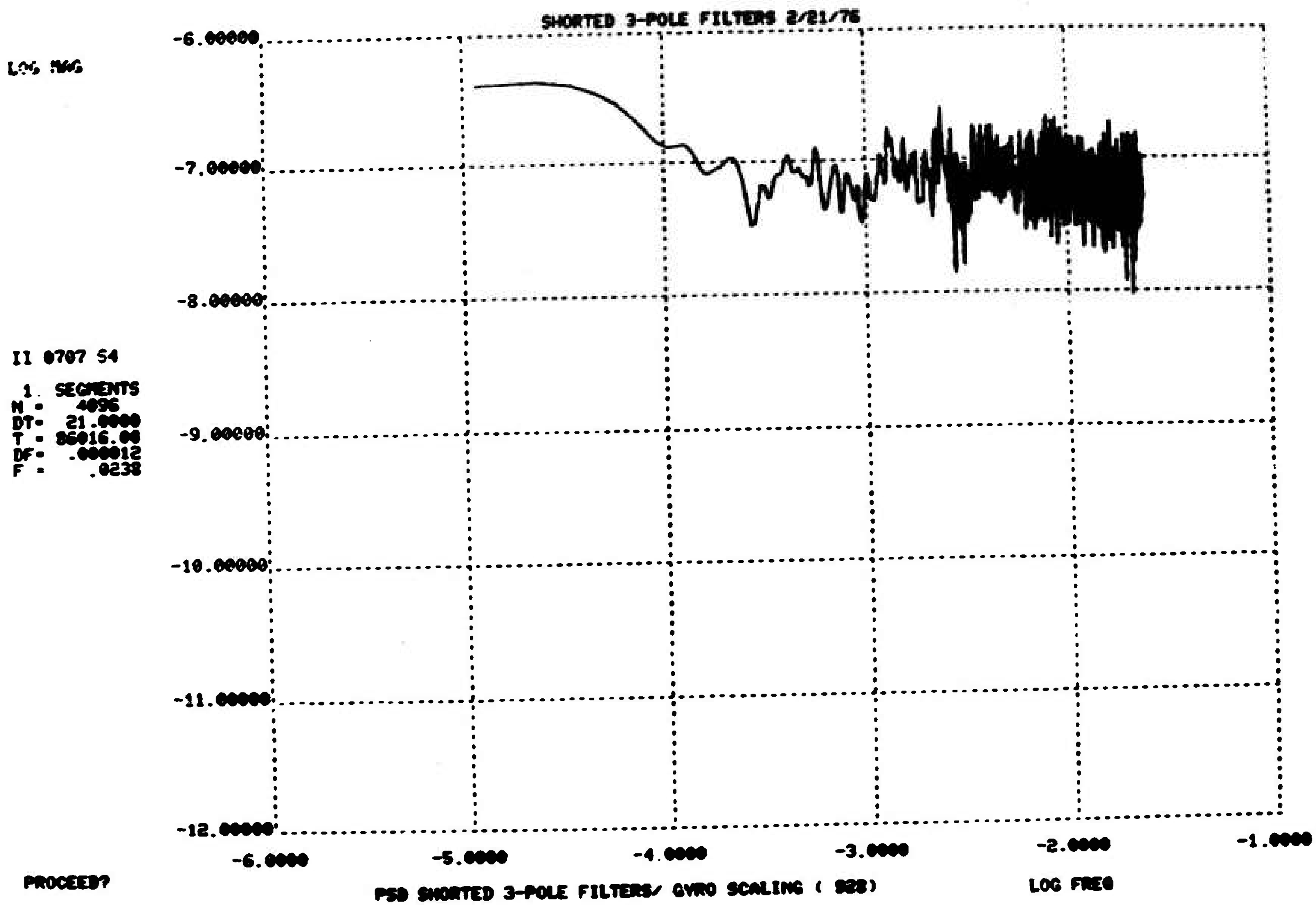

FIGURE E-15. FILTER NOISE PSD/GYRO SCALING (24 HOUR TEST)

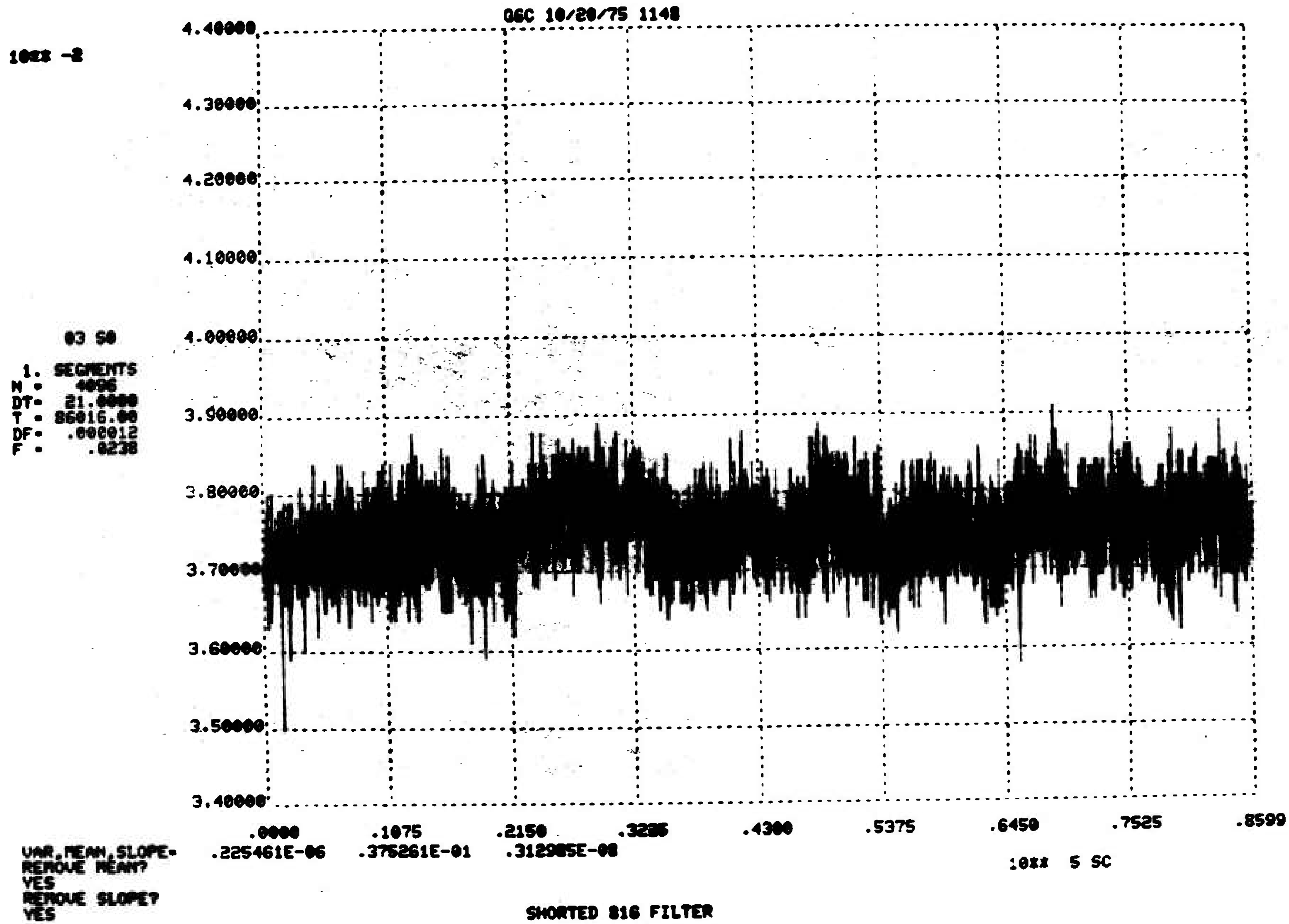

FIGURE E-16. SHORTED 816 FILTER (24 HOUR TEST) (VOLTS)

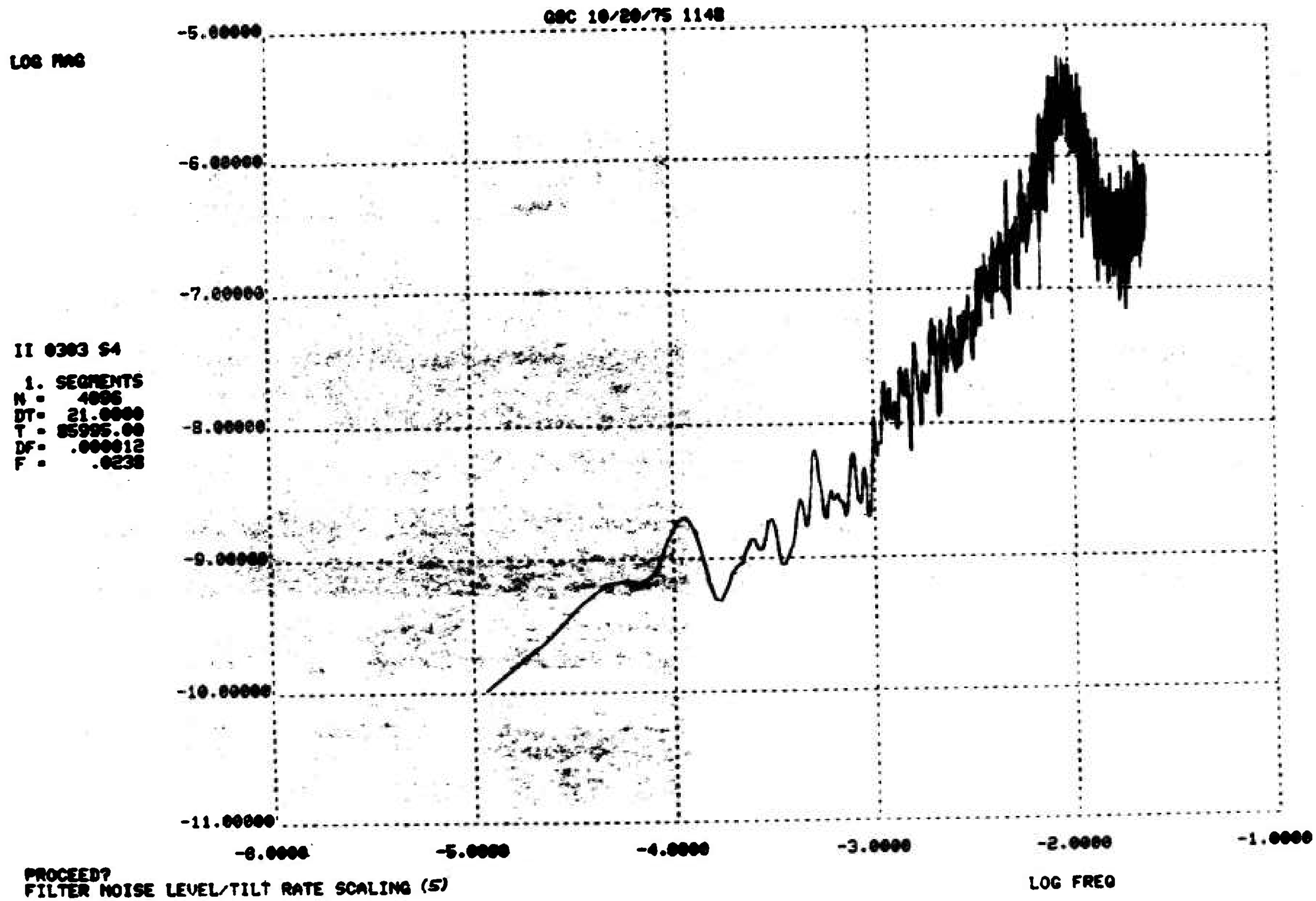

FIGURE E-17. FILTER NOISE PSD/TILT RATE SCALING (24 HOUR TEST)

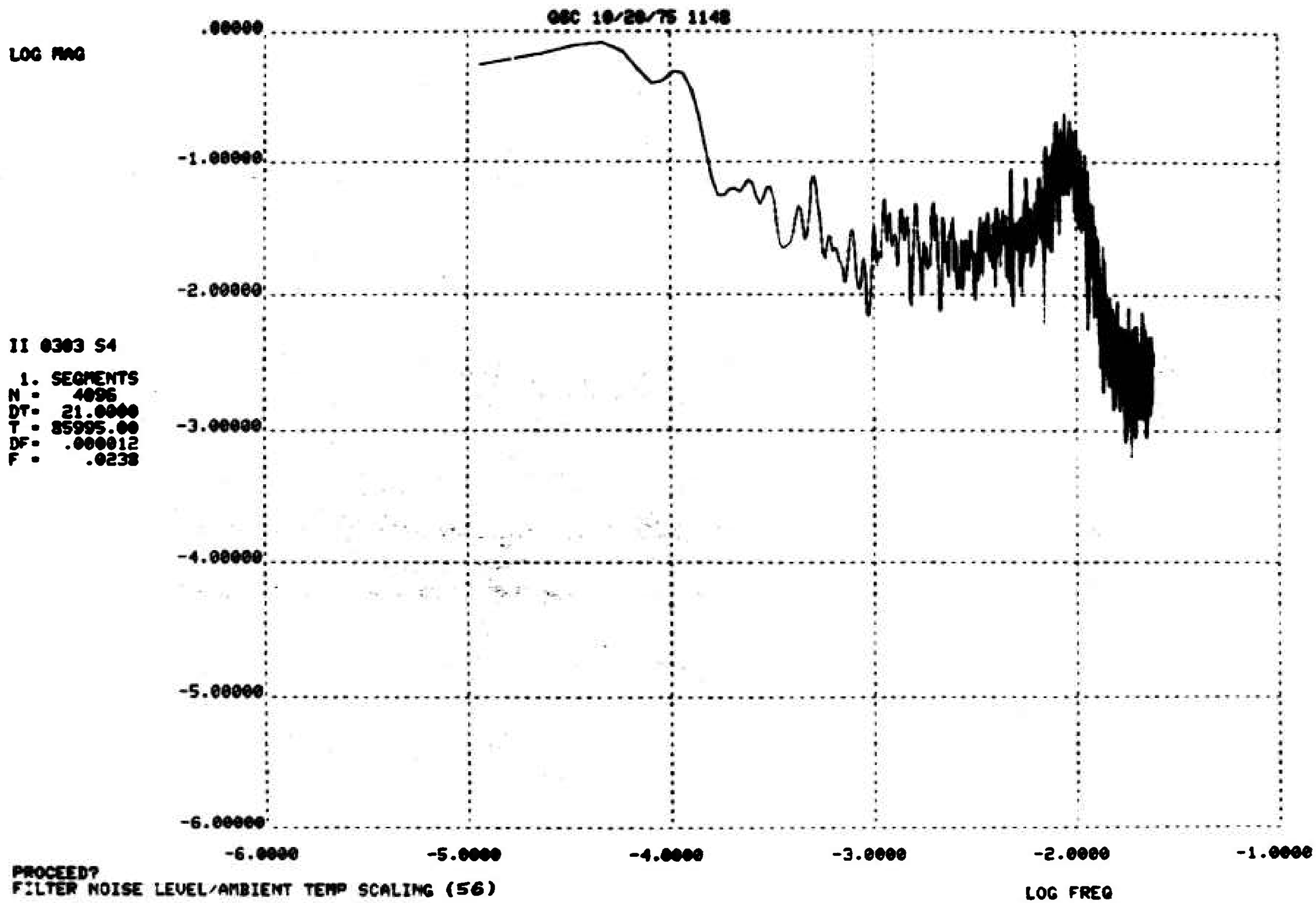

FIGURE E-18. FILTER NOISE PSD/AMBIENT TEMPERATURE SCALING (24 HOUR TEST)

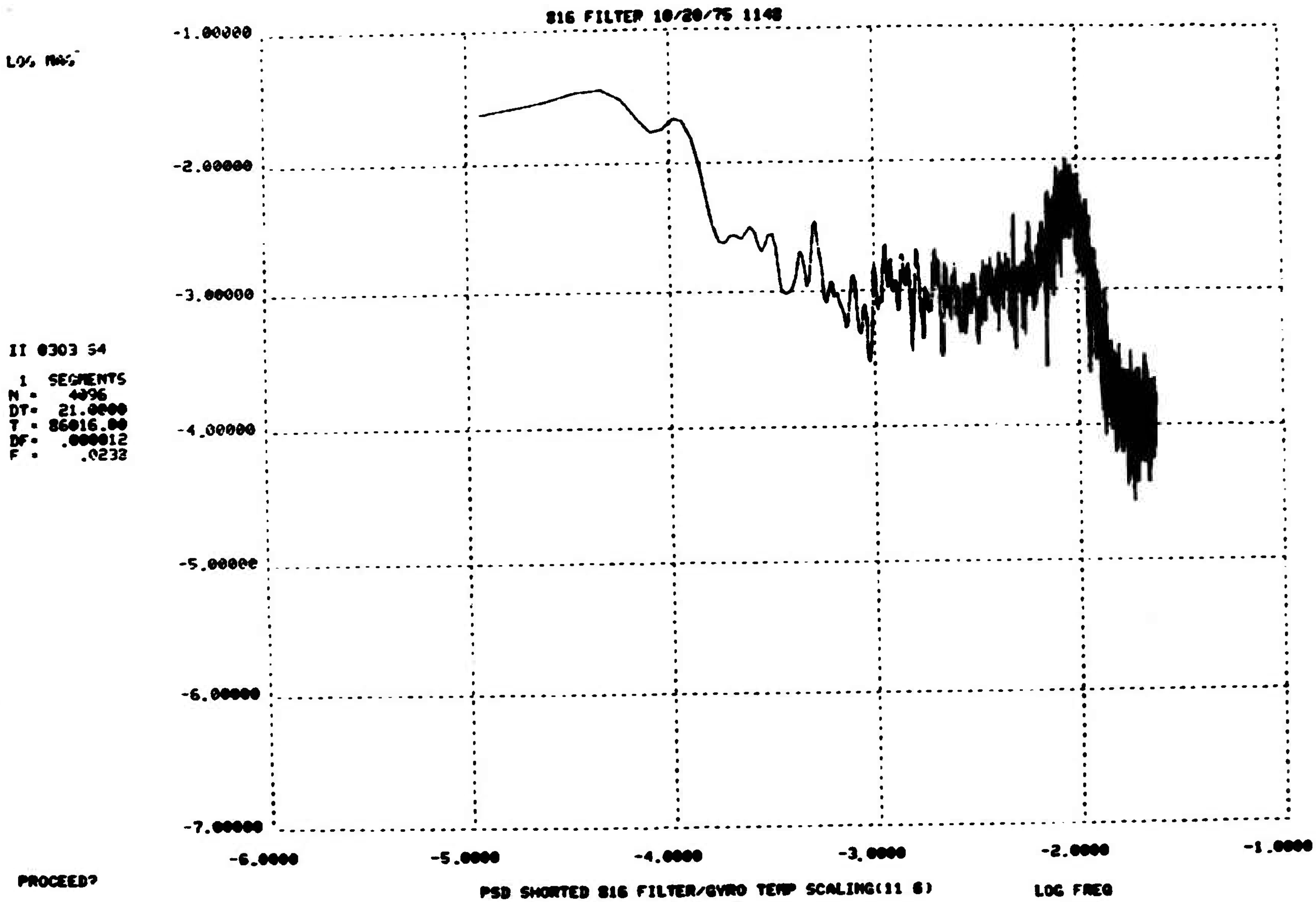

FIGURE E-19. FILTER NOISE PSD/GYRO TEMPERATURE SCALING (24 HOUR TEST)

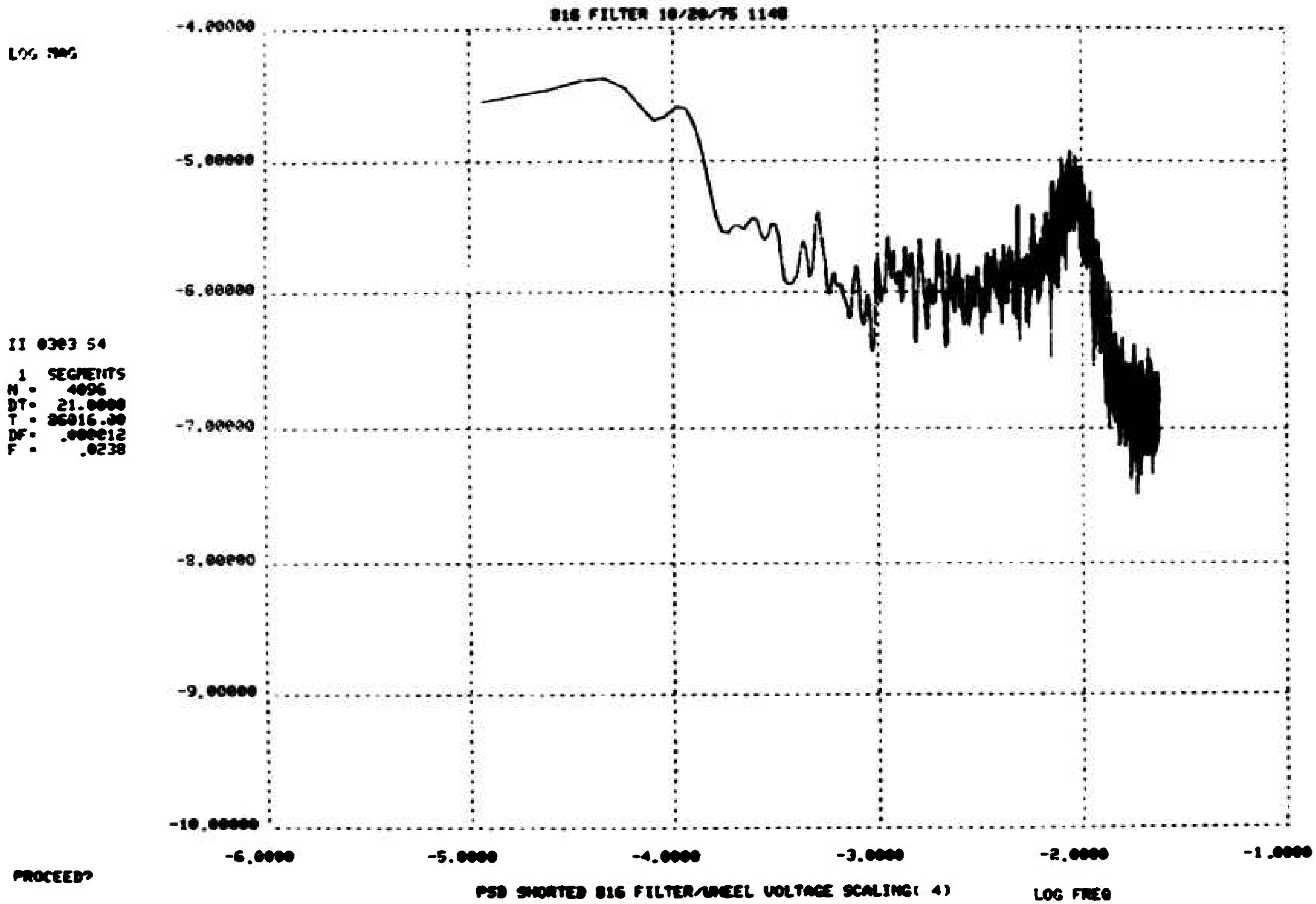

FIGURE E-20. FILTER NOISE PSD/GYRO VOLTAGE .4 SCALING (24 HOUR TEST)

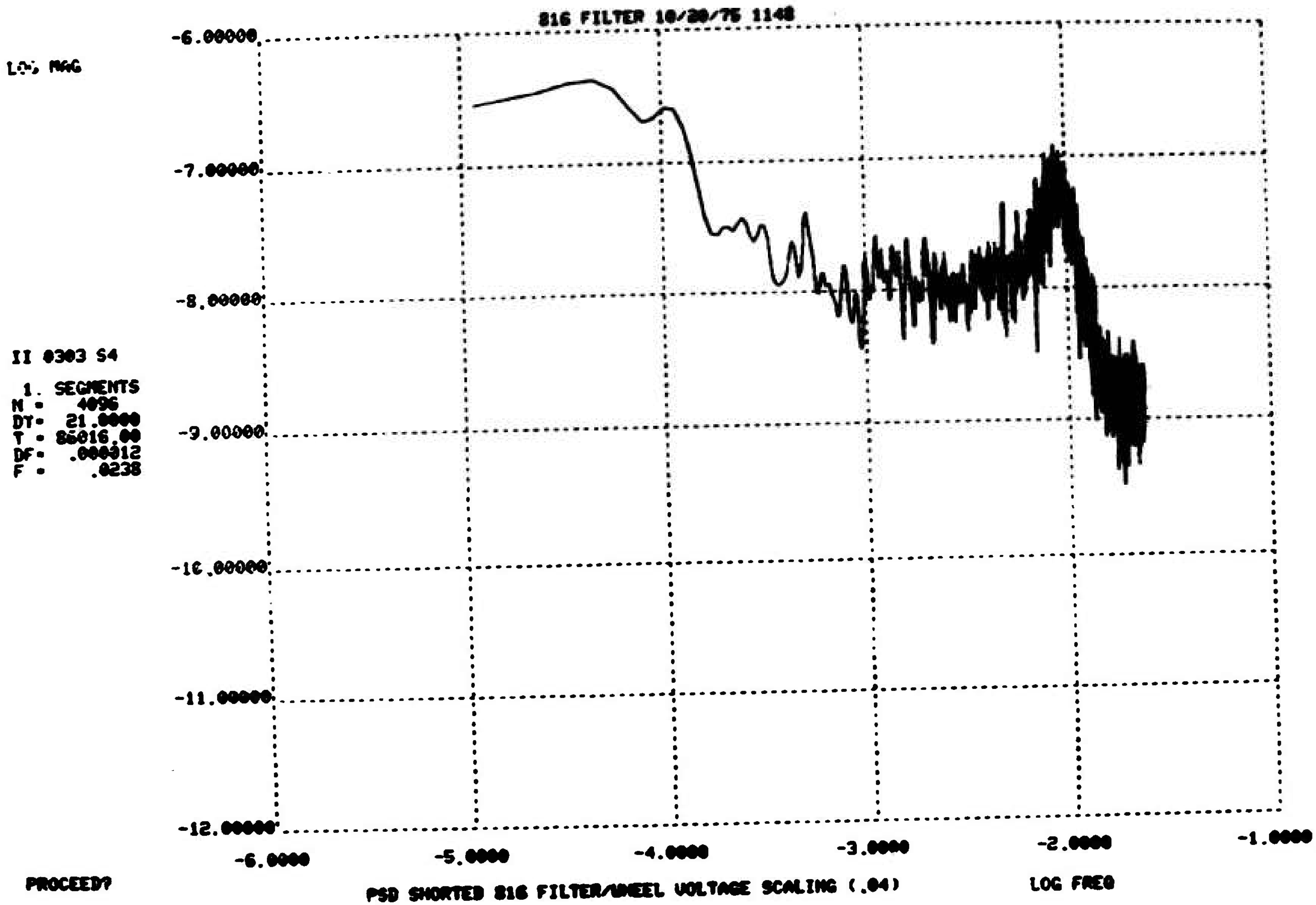

FIGURE E-21. FILTER NOISE PSD/GYRO VOLTAGE .04 SCALING (24 HOUR TEST)

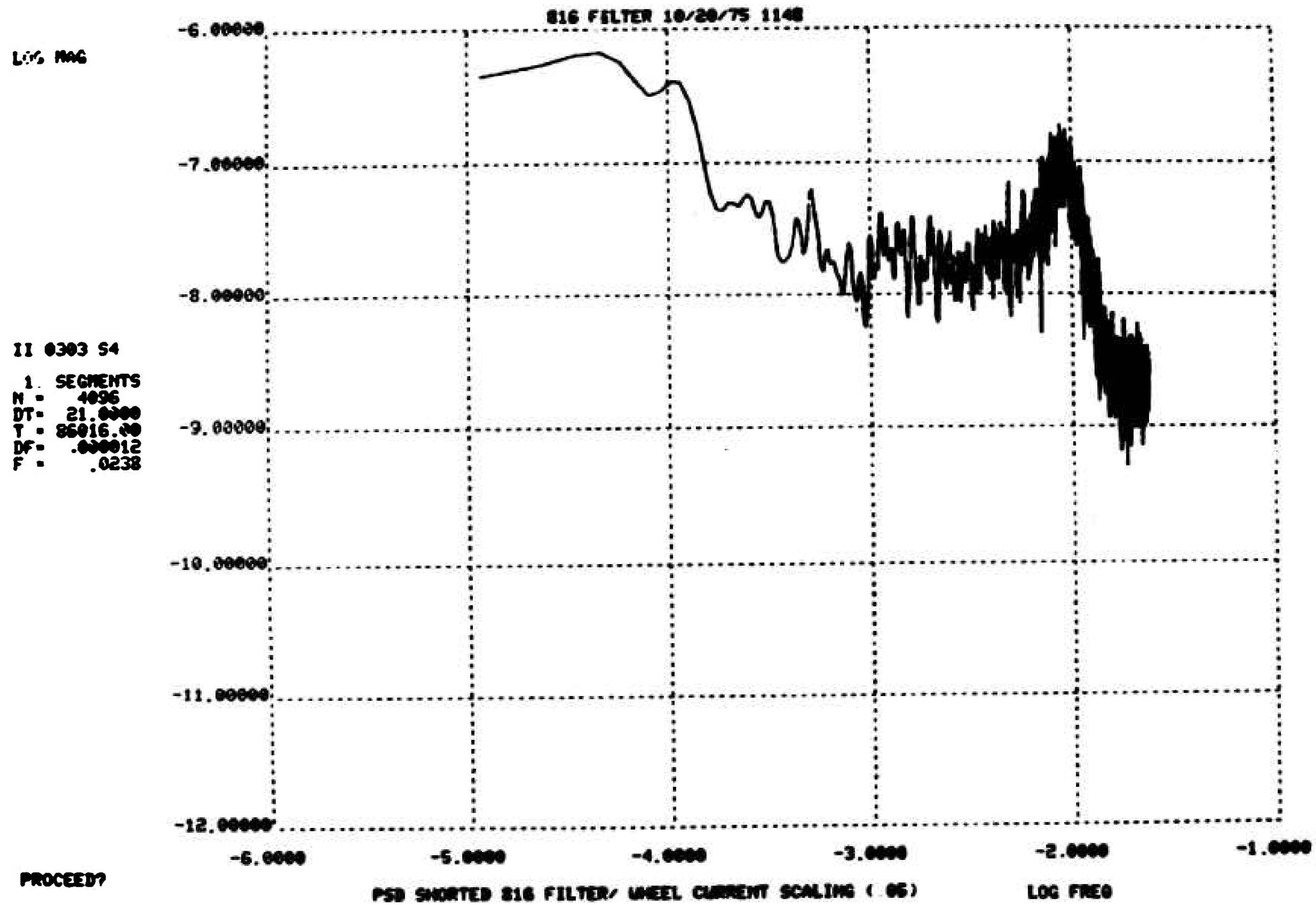

FIGURE E-22. FILTER NOISE PSD/GYRO CURRENT .05 SCALING (24 HOUR TEST)

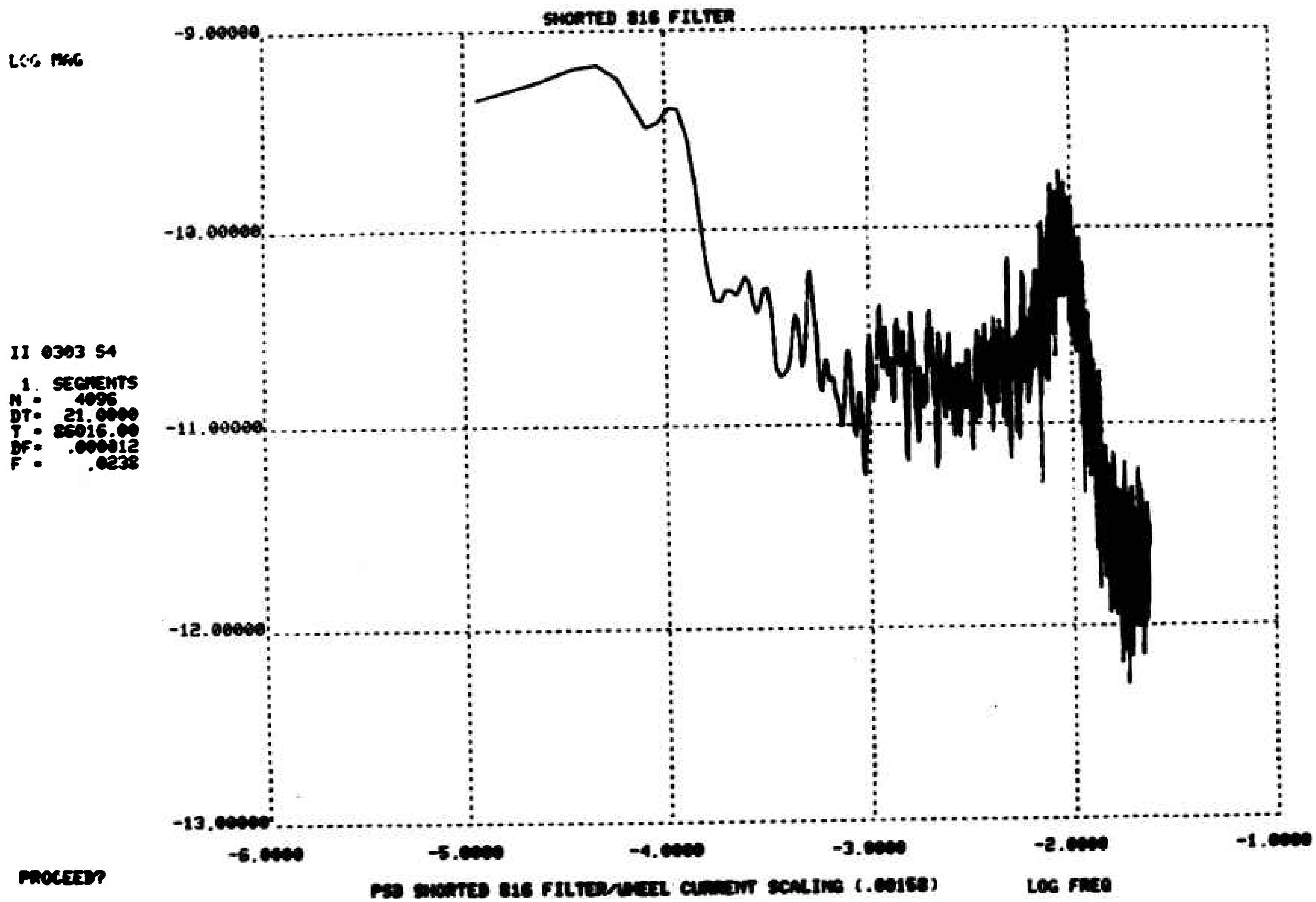

FIGURE E-23. FILTER NOISE PSD/GYRO CURRENT .00158 SCALING (24 HOUR TEST)

APPENDIX F

WHEEL OFF 3 MINUTE AND 1 HOUR TESTS

The gyro output followed by the gyro PSD for the three minute test is shown in Figures F-1 and F-2. Figures F-3 through F-5 show the gyro data, ambient temperature, and gyro case temperature, for the one hour test, followed respectively by their PSD plots in Figures F-6 through F-8. Note that the gyro data plots, Figure F-1 and particularly the one hour test data, Figure F-3, are highly quantized. The gyro PSD plots, Figures F-2 and F-6 look very similar to the corresponding PSD plots of the shorted filter tests presented in Appendix E. Therefore, the gyro torquer loop noise for these tests appears to be as quiet or quieter than the resolution of the data acquisition system. Significant temperature information above data acquisition noise appears to start at frequencies below .04 Hz. This is shown by comparing the ambient temperature and gyro case temperature PSD plots with the appropriately scaled temperature PSD plots in Appendix E.

1011 -2

07 50

1 SEGMENTS
N = 4096
DT= .0500
T = 204.80
DF= .004883
F = 10.0000

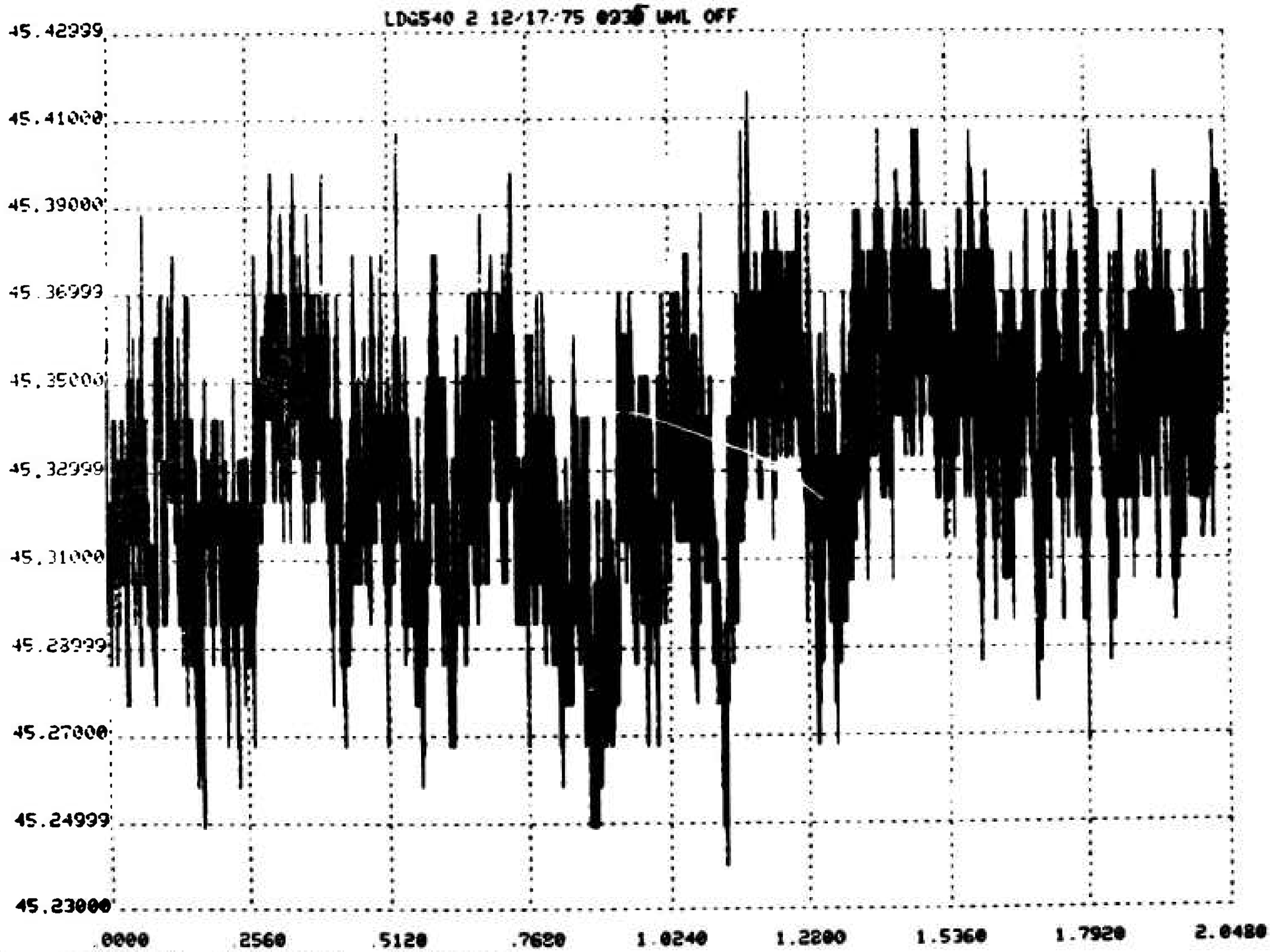

VAR.MEAN.SLOPE= .666118E-07 .453332E+00 .158483E-05
REMOVE MEAN?
YES
REMOVE SLOPE?
YES

GYRO OUTPUT DEG/HR

FIGURE F-1. S/N 2 GYRO DATA, DEGREE/HOUR (WHEEL OFF 3 MINUTE TEST)

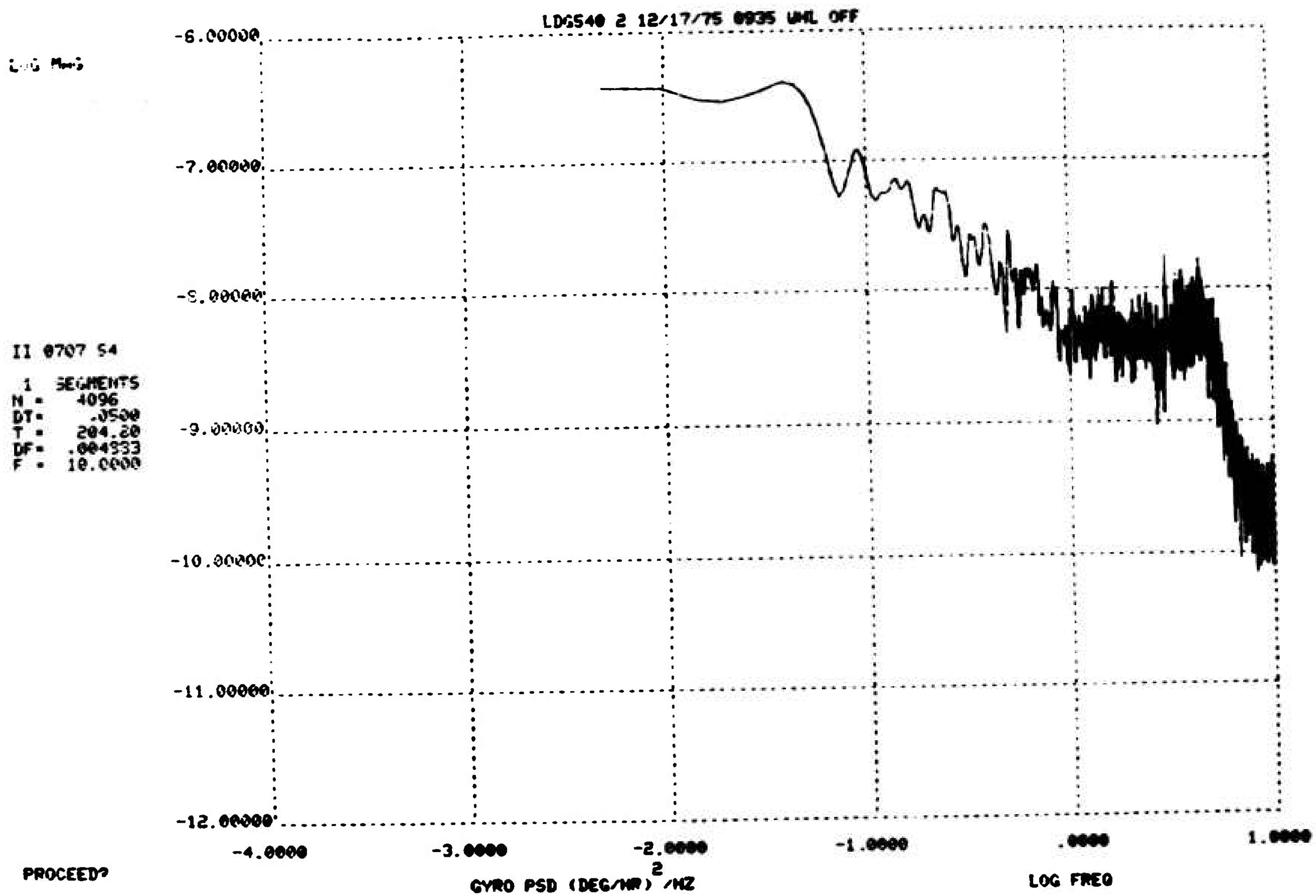

FIGURE F-2. PSD S/N 2 GYRO DATA, (DEGREE/HOUR)^2/HZ (WHEEL OFF 3 MINUTE TEST)

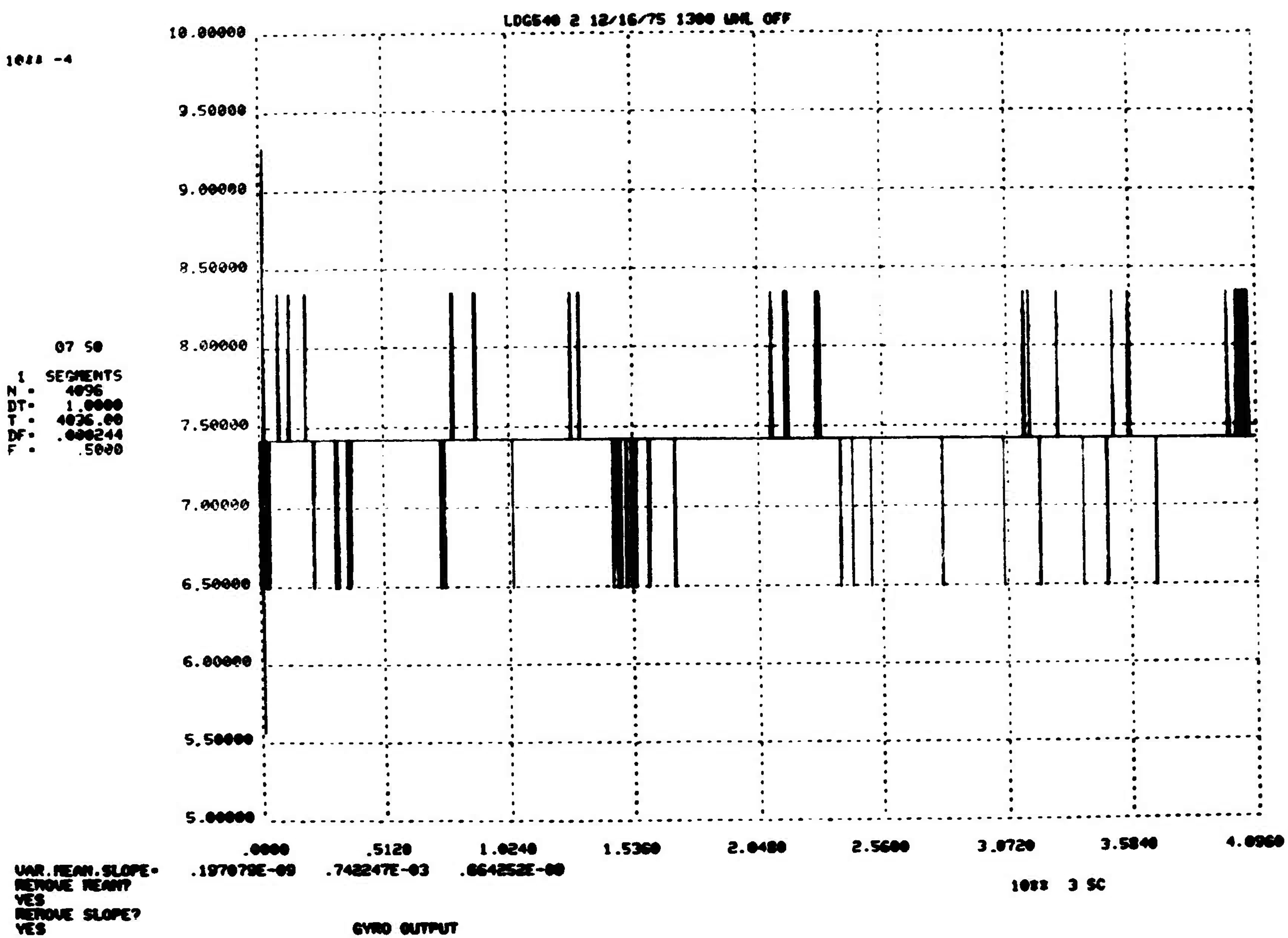

FIGURE F-3. S/N GYRO DATA, DEGREE/HOUR (WHEEL OFF 1 HOUR TEST)

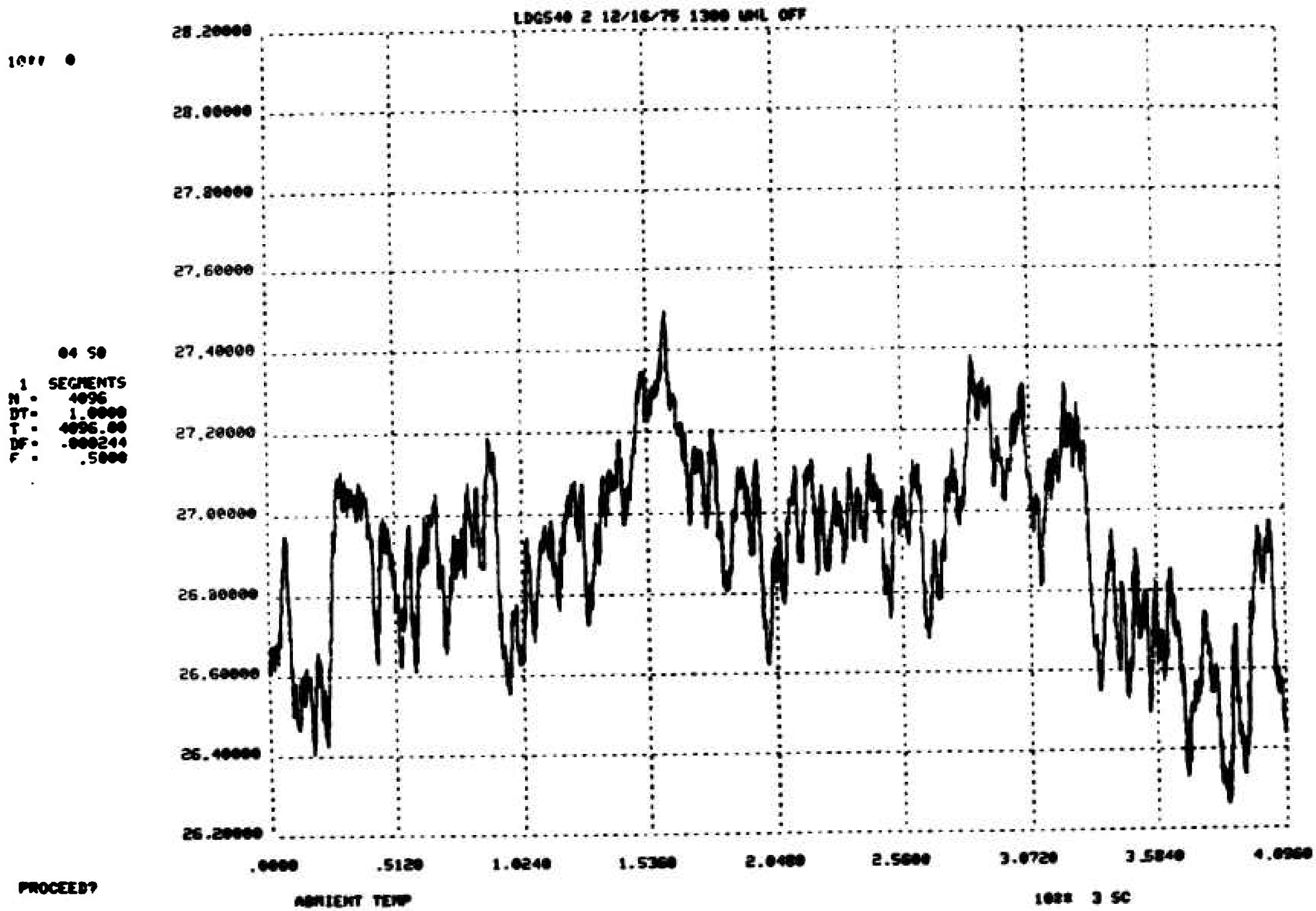

FIGURE F-4. AMBIENT TEMPERATURE, DEGREE F (WHEEL OFF 1 HOUR TEST S/N 2)

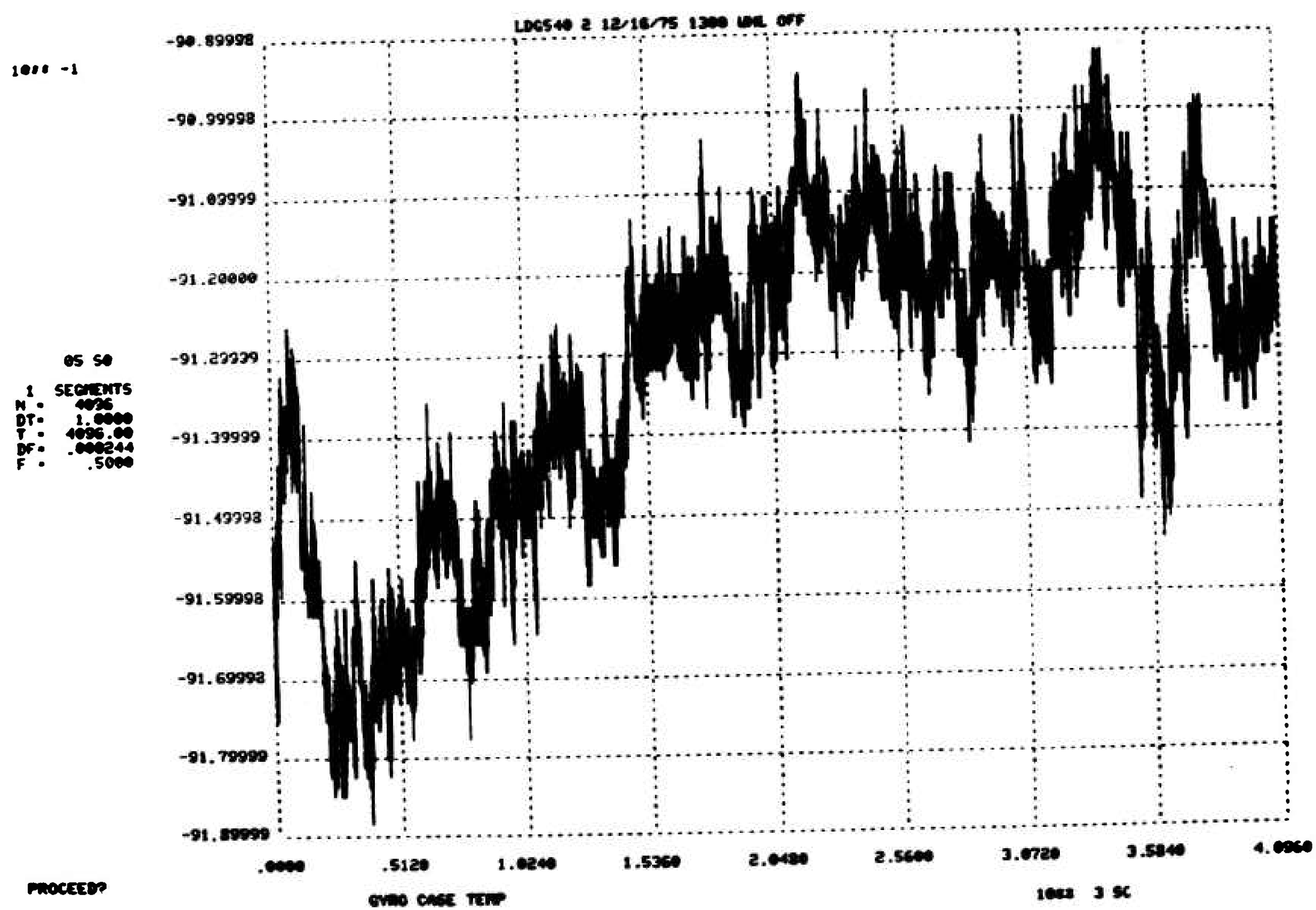

FIGURE F-5. S/N 2 GYRO CASE TEMPERATURE, DEGREE F (WHEEL OFF 1 HOUR TEST)

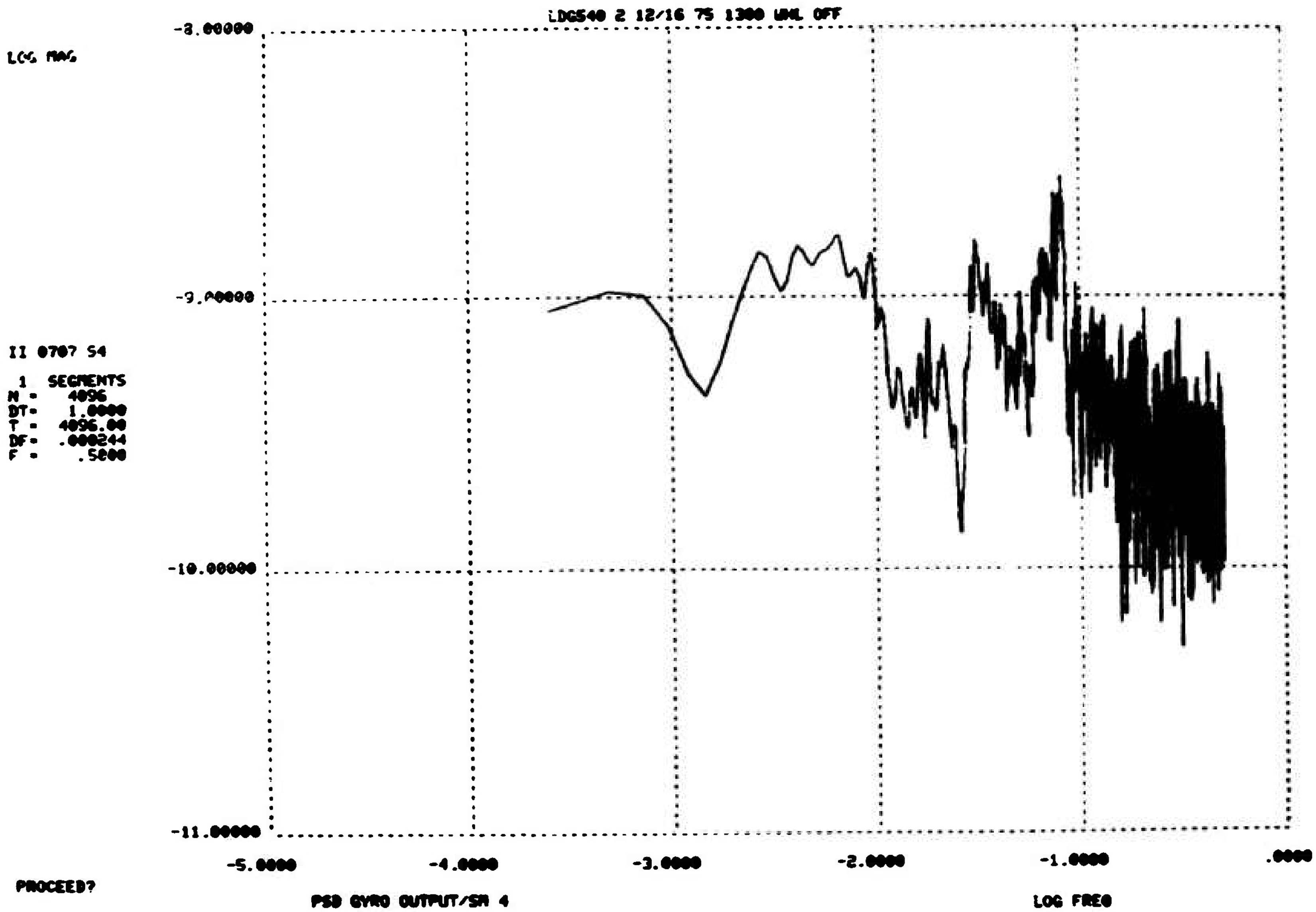

FIGURE F-6. PSD S/N 2 GYRO DATA, $(DEGREE/HOUR)^2/HZ$ (WHEEL OFF 1 HOUR TEST)

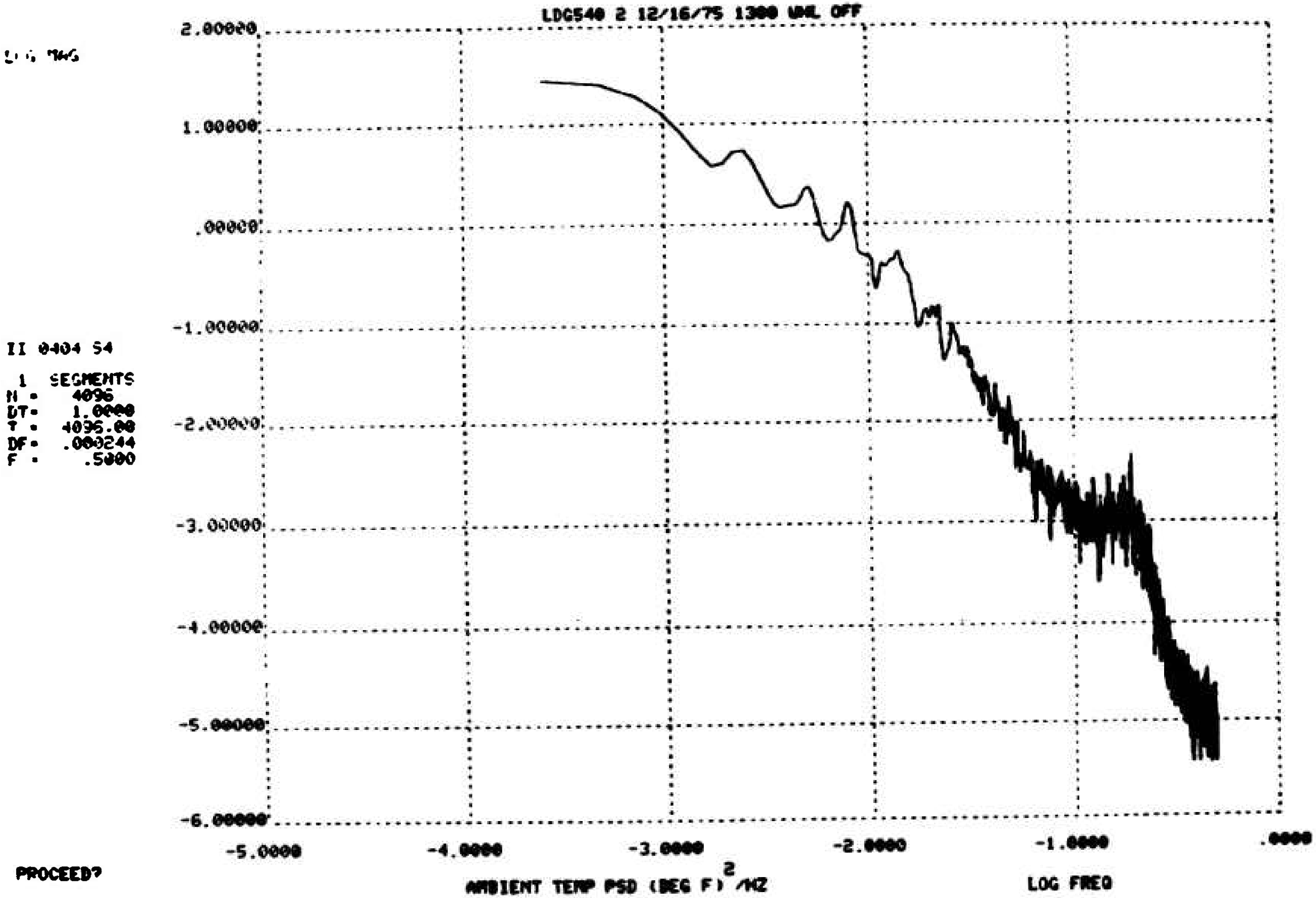

FIGURE F-7. PSD AMBIENT TEMPERATURE, (DEGREE F)^2/HZ (WHEEL OFF 1 HOUR TEST S/N 2)

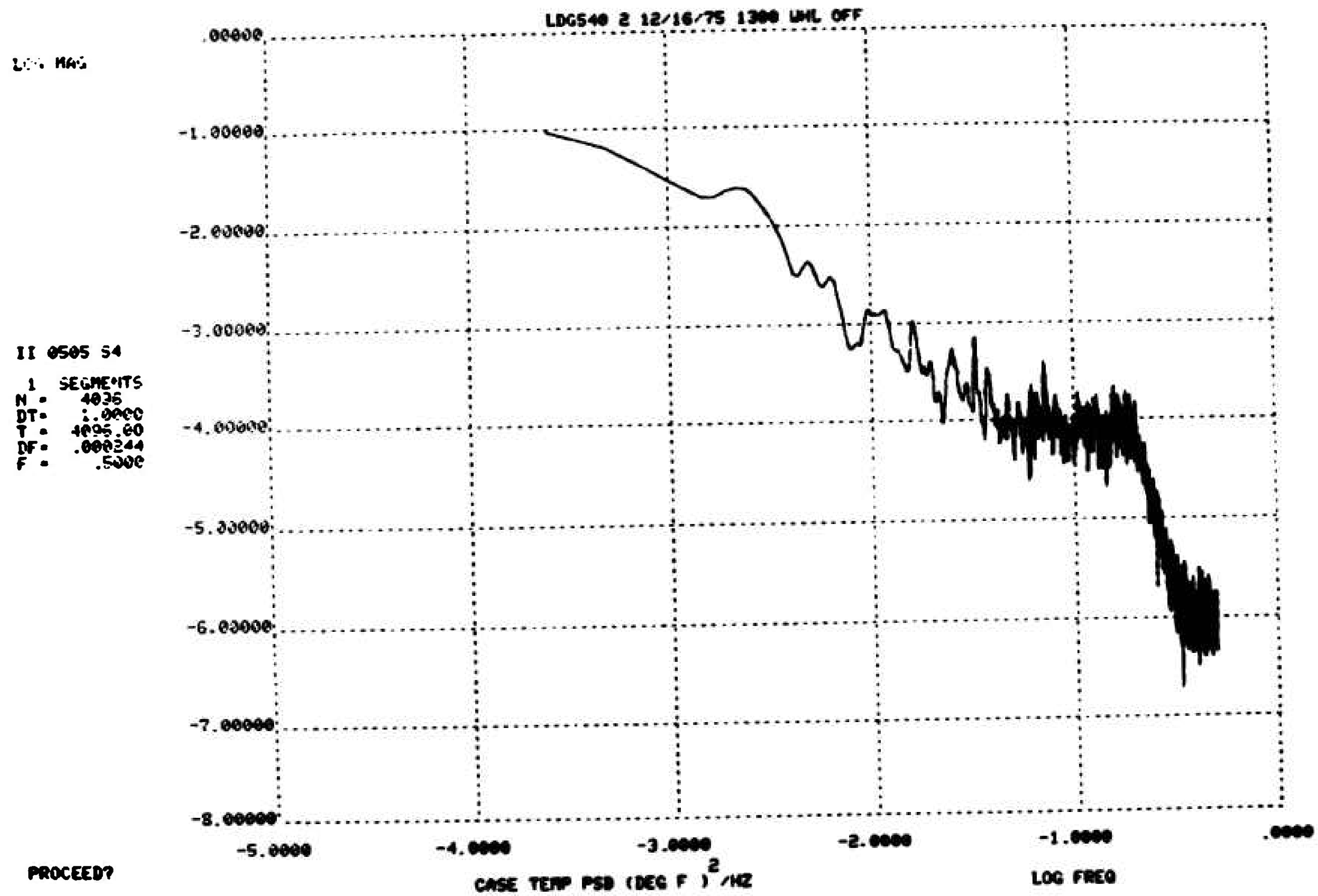

FIGURE F-8. PSD S/N 2 GYRO CASE TEMPERATURE, (DEGREE F)^2/HZ (WHEEL OFF 1 HOUR TEST)

WHEEL OFF 24 HOUR TEST

Figures F-9 through F-14 show the results of the 24 hour wheel off test. The data acquisition system was set up for the twenty-four hour test, however, only about six hours of data was actually taken. The shorter time window reduced the low frequency resolution, but sufficient data was taken to show the trends. As in the earlier tests, the gyro data, Figure F-9, is highly quantized. Also, the gyro PSD, Figure F-12, agrees very closely with the corresponding shorted filter test in Appendix E. The gyro case heater apparently malfunctioned during the test causing the expotential temperature decay seen in the gyro case temperature data, Figure F-11. This causes the PSD of gyro case temperature, Figure F-14, to be greatly distorted in the low frequency region.

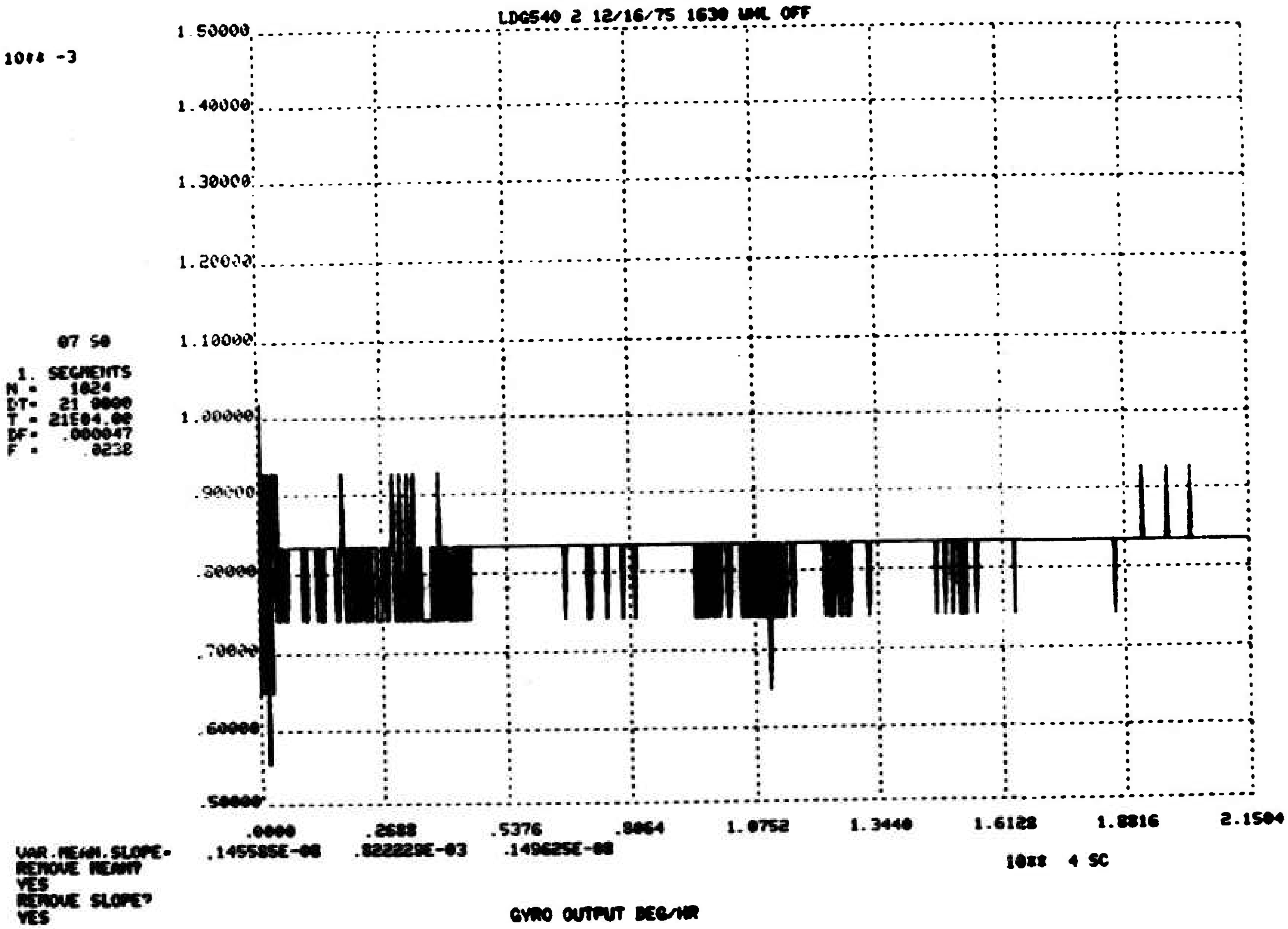

FIGURE F-9. S/N 2 GYRO DATA, DEGREE/HOUR (WHEEL OFF 24 HOUR TEST)

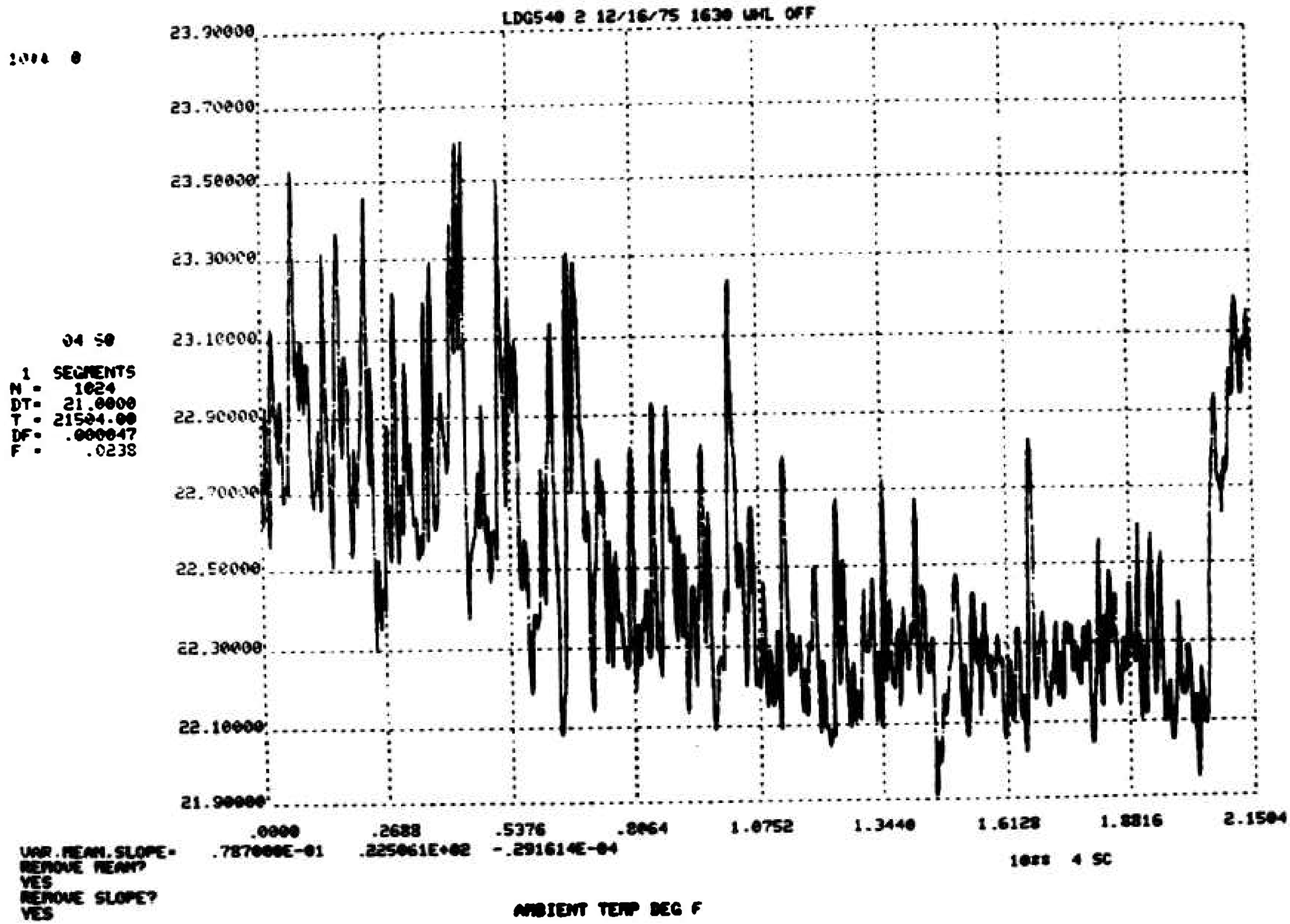

FIGURE F-10. AMBIENT TEMPERATURE, DEGREE F (S/N 2 WHEEL OFF 24 HOUR TEST)

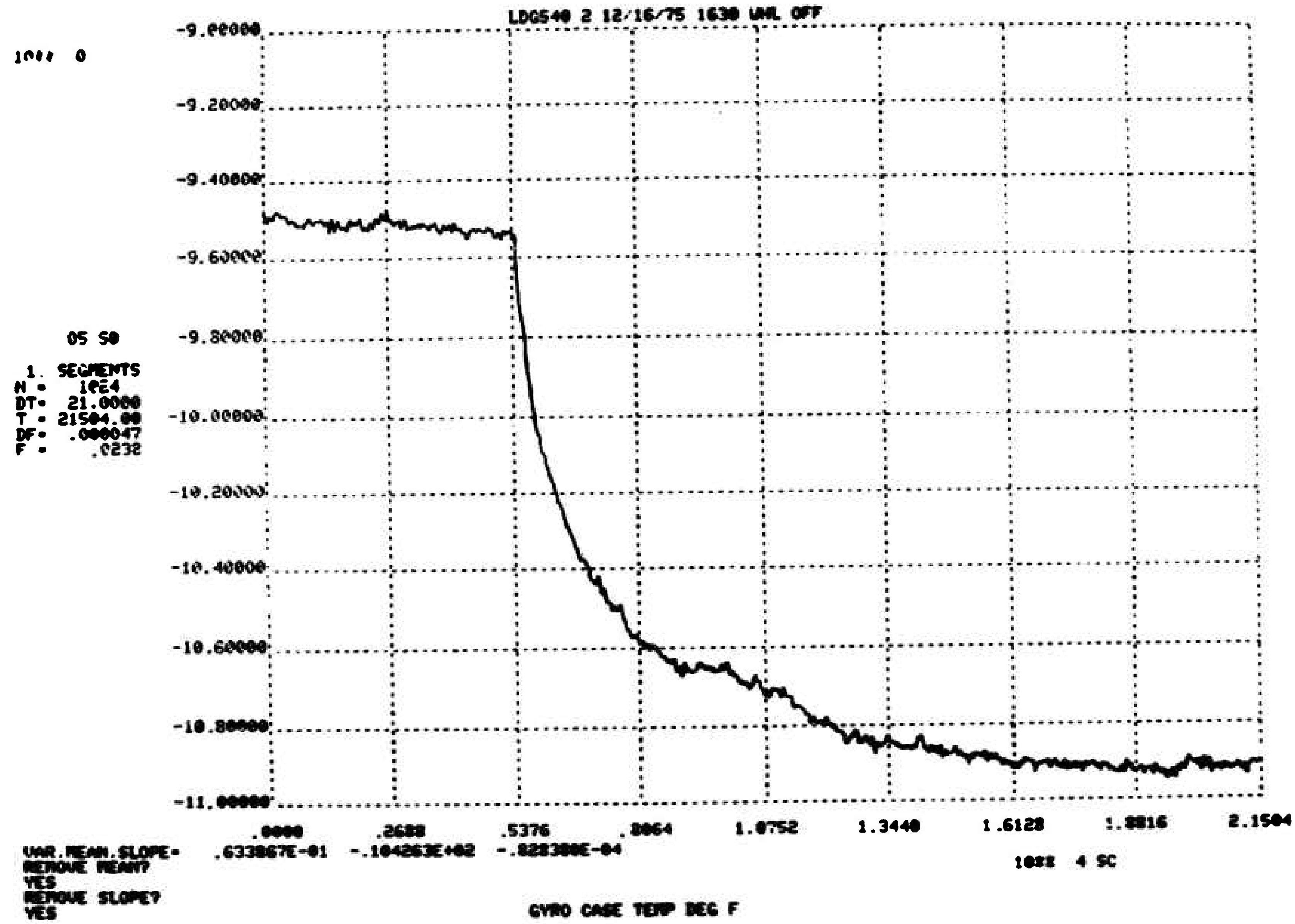

FIGURE F-11. S/N 2 GYRO CASE TEMPERATURE, DEGREE F (WHEEL OFF 24 HOUR TEST)

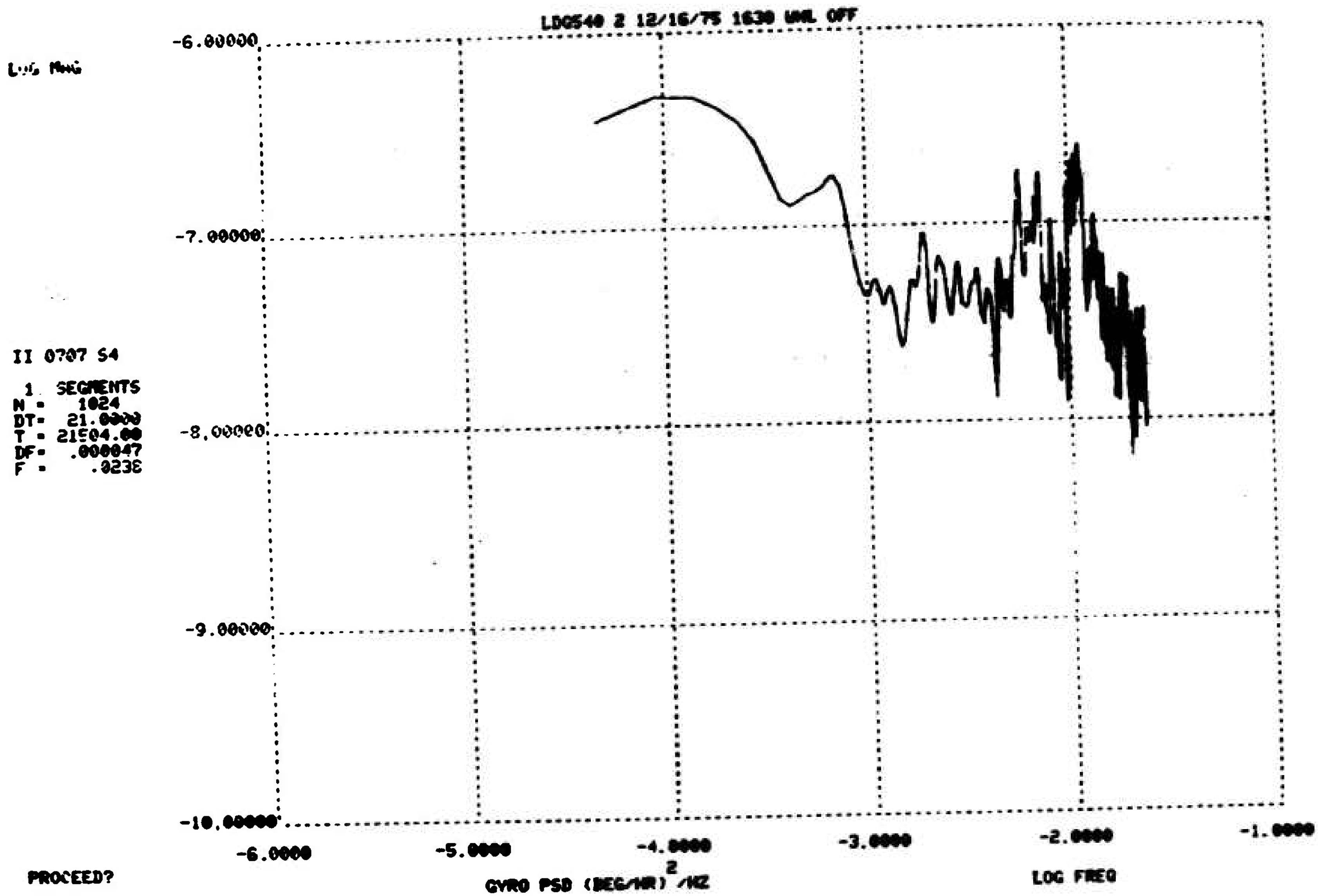

FIGURE F-12. PSD S/N 2 GYRO DATA, $(\text{DEGREE/HOUR})^2/\text{HZ}$ (WHEEL OFF 24 HOUR TEST)

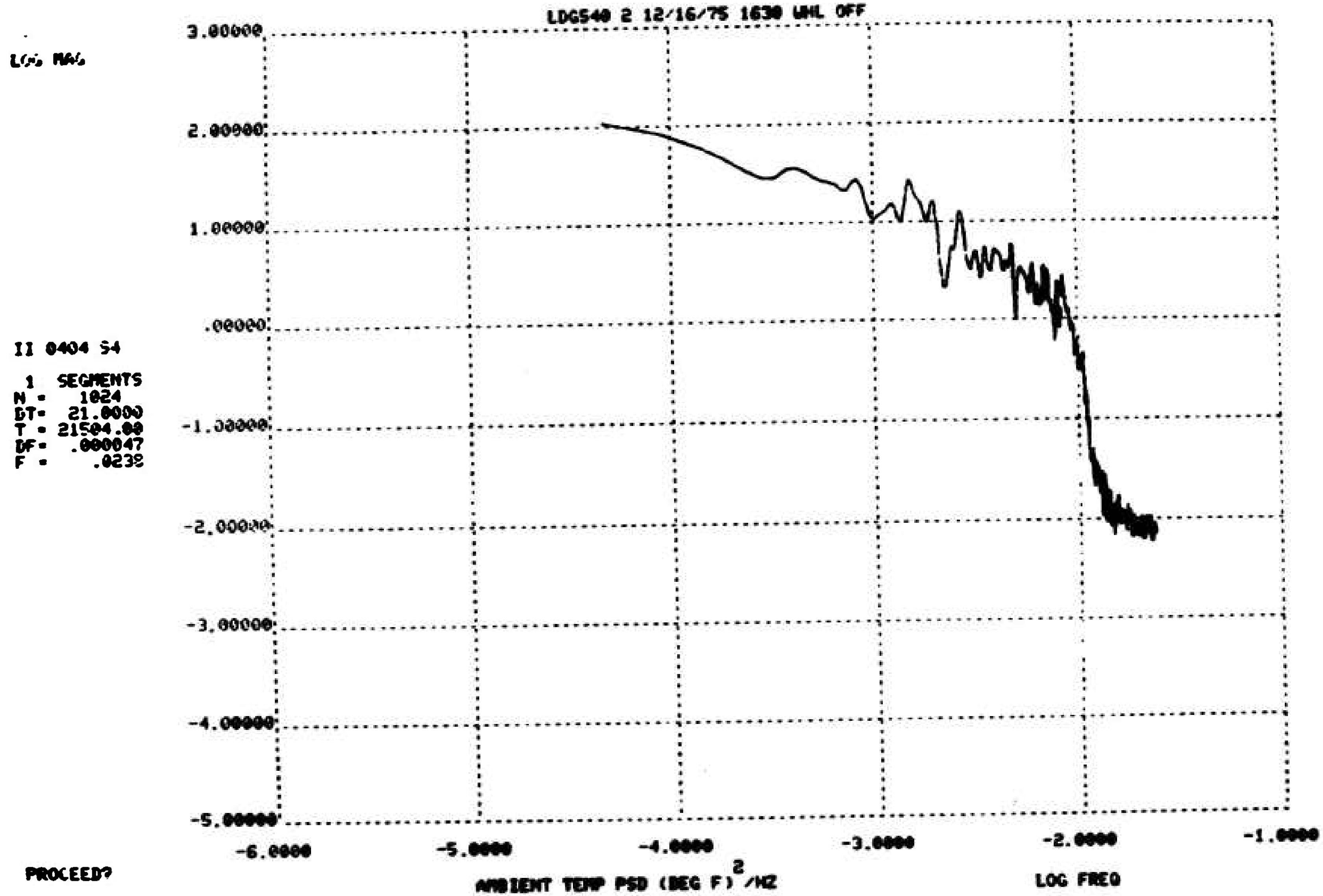

FIGURE F-13. PSD AMBIENT TEMPERATURE, (DEGREE F)^2/HZ (S/N 2 WHEEL OFF 24 HOUR TEST)

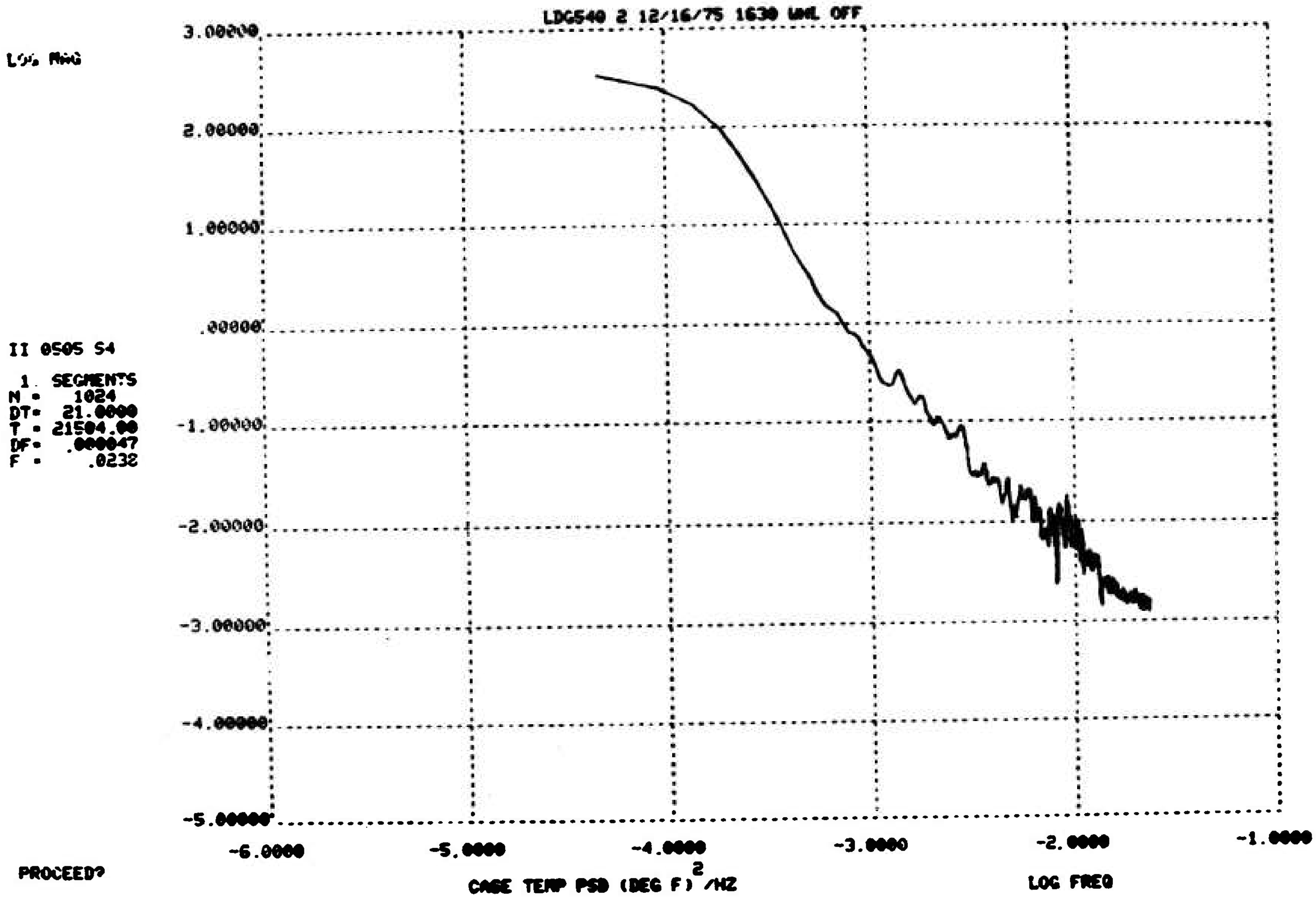

FIGURE F-14. PSD S/N 2 GYRO CASE TEMPERATURE, (DEGREE F)^2/HZ (WHEEL OFF 24 HOUR TEST)

APPENDIX G

OUTPUT AXIS SENSITIVITY TEST RESULTS

Figures G-1 through G-8 show the results of the baseline and output axis sensitivity tests conducted on Gyro S/N #2. The results of the one hour test with the table locked and torquer off are shown in Figures G-1 and G-2. The gyro output does not appear to be significantly noisier than it was when mounted on the pad except in the mid frequency regions. The results of the one hour test with the table unlocked and torquer on but without applied rates are shown in Figures G-3 and G-4.

Finally, Figures G-5 through G-8 show the results of the output axis sensitivity test. Figures G-5 shows the rate voltage applied to the table top which is proportional to the table rate. Figure G-6 shows the PSD of this voltage. The corresponding gyro output and gyro output PSD plots are shown in Figures G-7 and G-8.

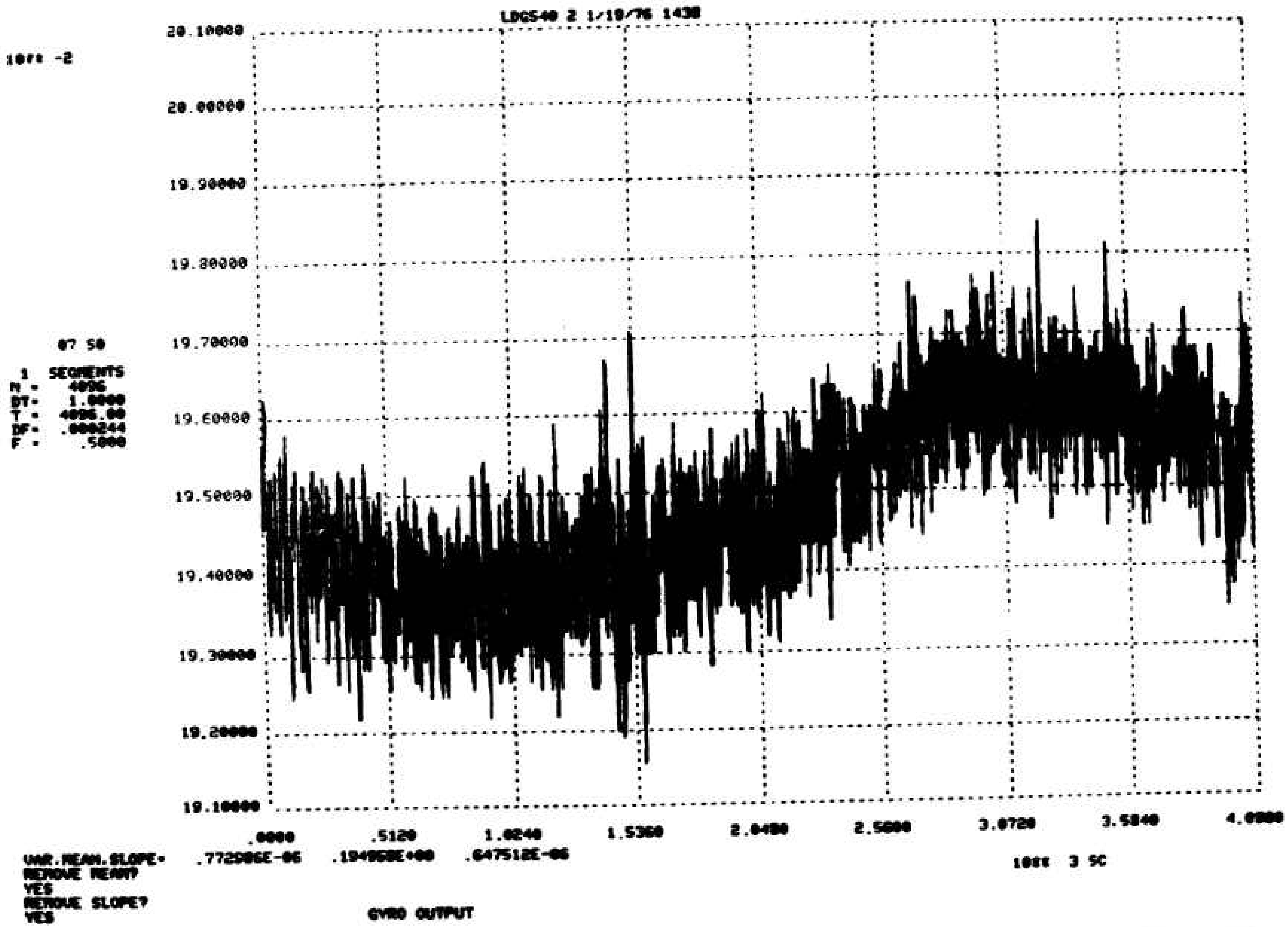

FIGURE G-1 S/N 2 GYRO OUTPUT, DEGREE/HOUR (OA SENSITIVITY WITH TABLE LOCKED)

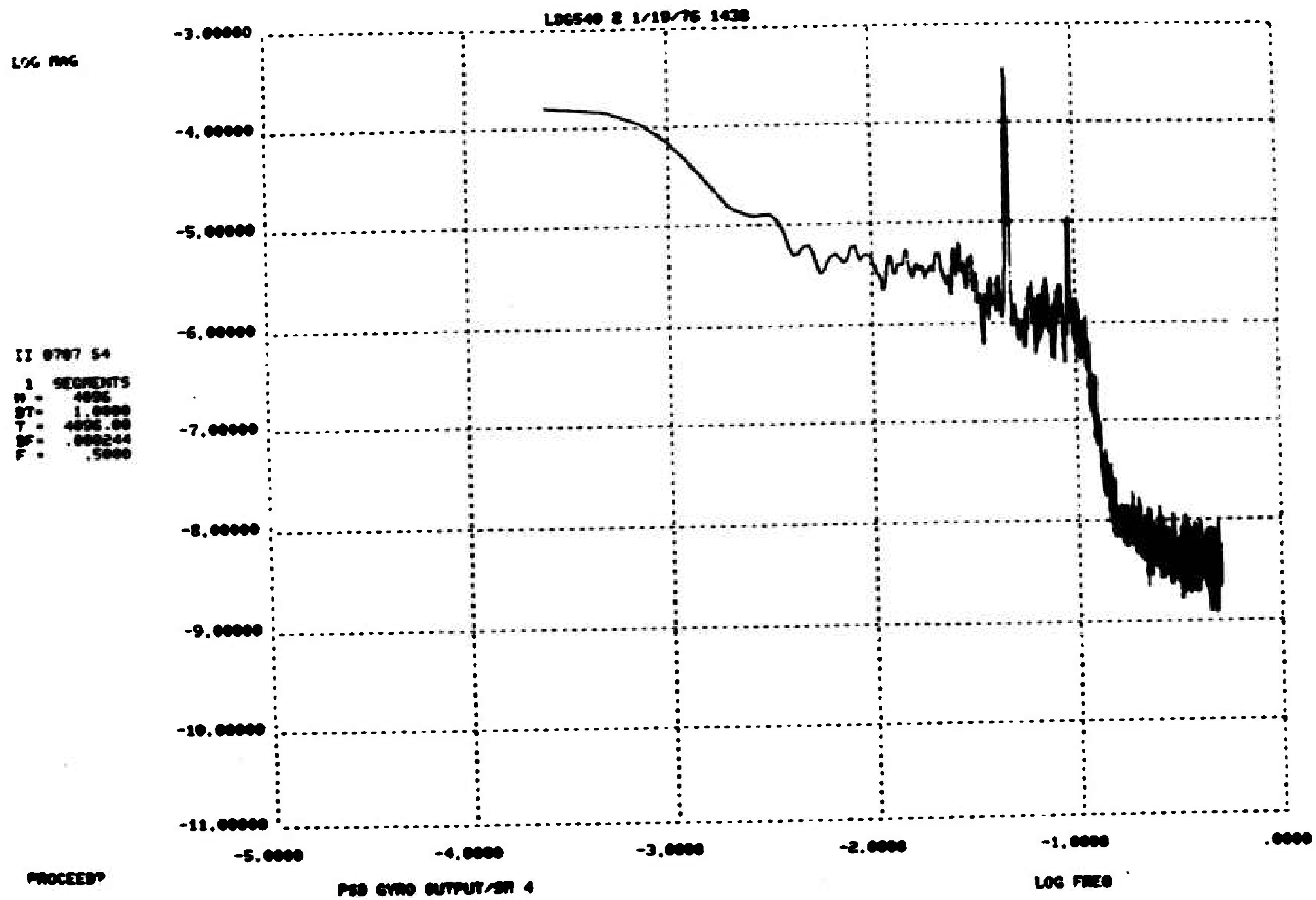

FIGURE G-2. PSD S/N 2 GYRO OUTPUT, $(DEGREE/HOUR)^2/HZ$ (OOA SENSITIVITY WITH TABLE LOCKED)

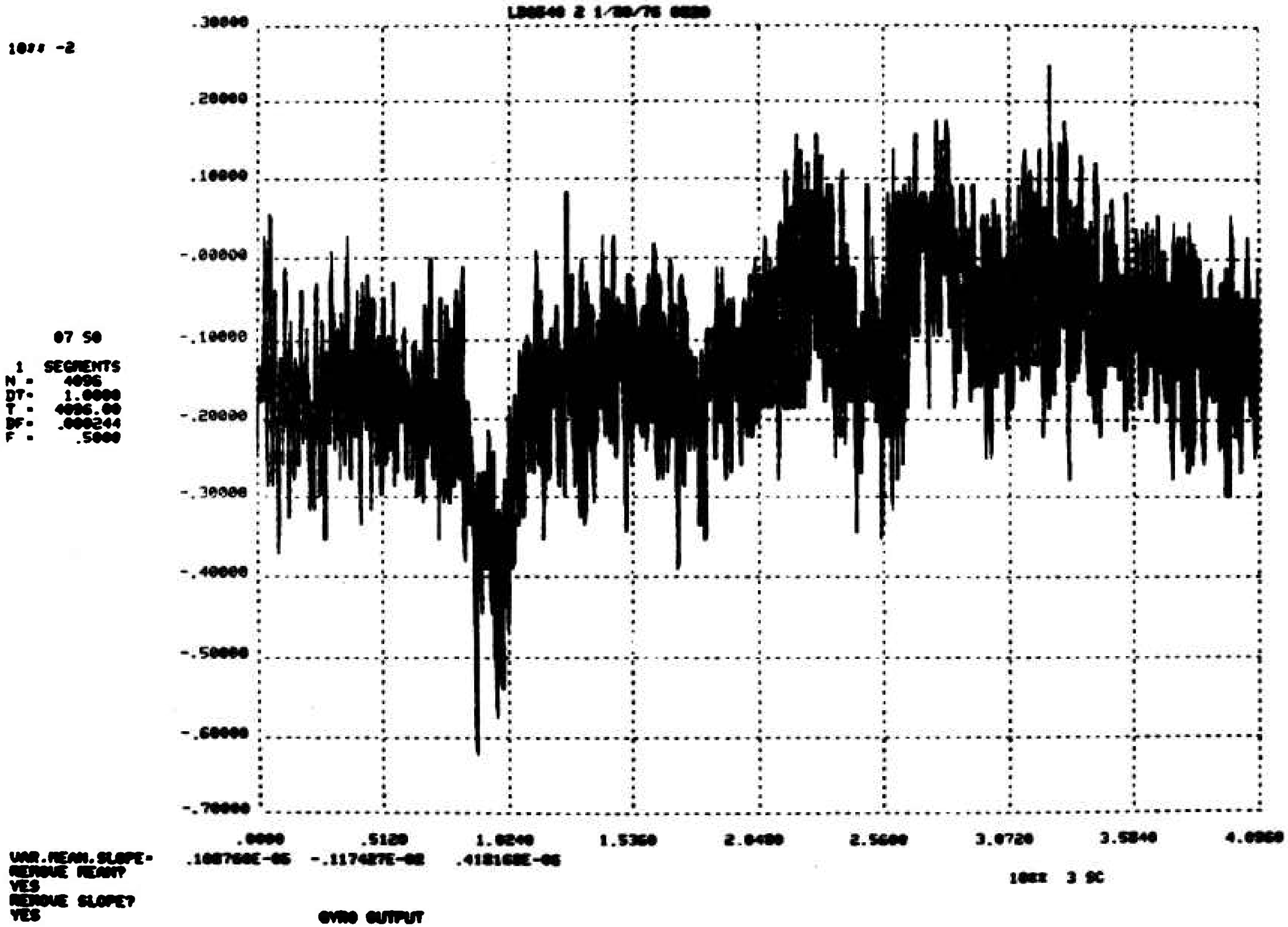

FIGURE G-3. S/N 2 GYRO OUTPUT, DEGREE/HOUR (OA SENSITIVITY WITH TABLE UNLOCKED)

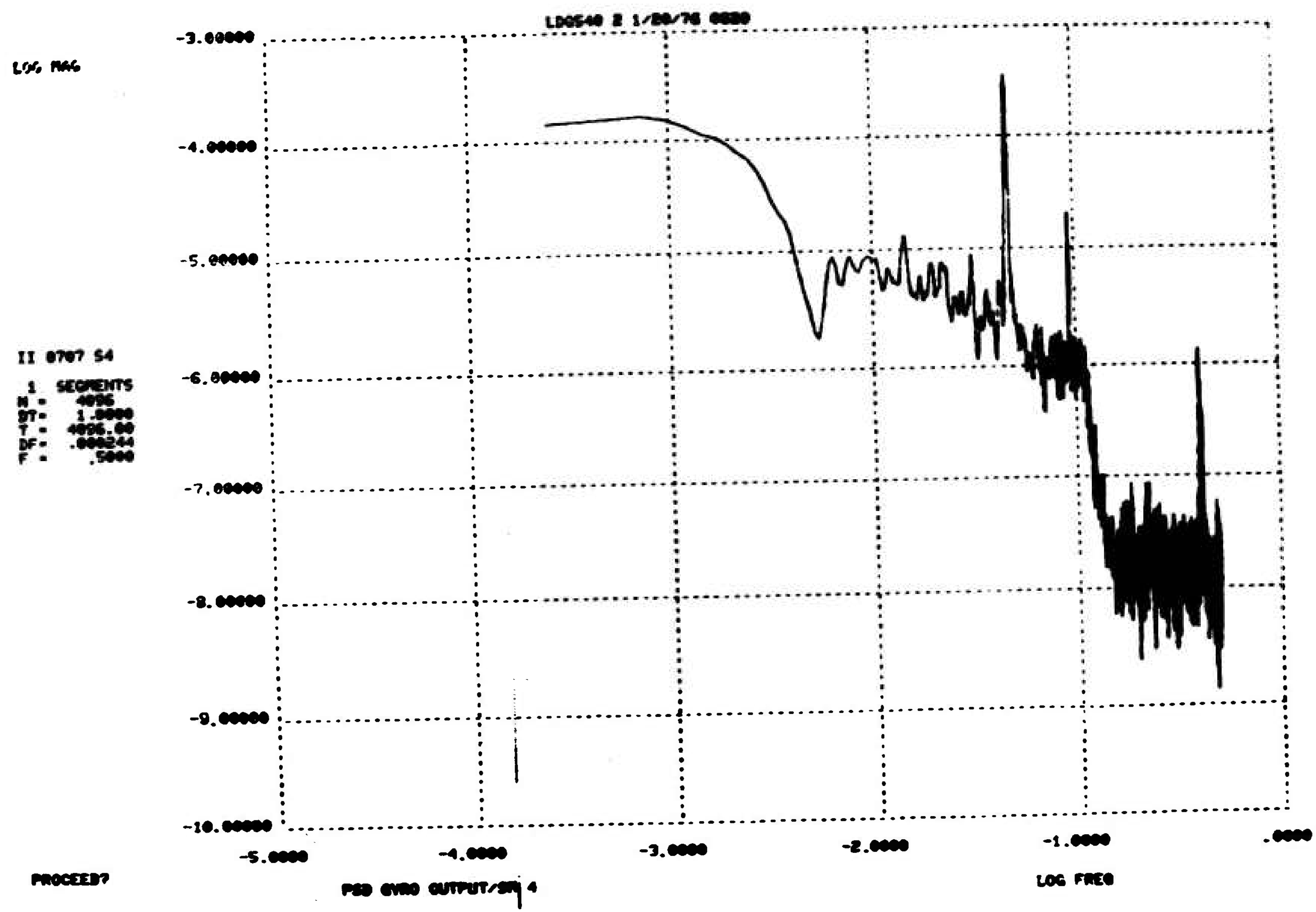

FIGURE G-4. PSD S/N 2 GYRO OUTPUT, $(\text{DEGREE/HOUR})^2/\text{HZ}$ (OA SENSITIVITY WITH TABLE UNLOCKED)

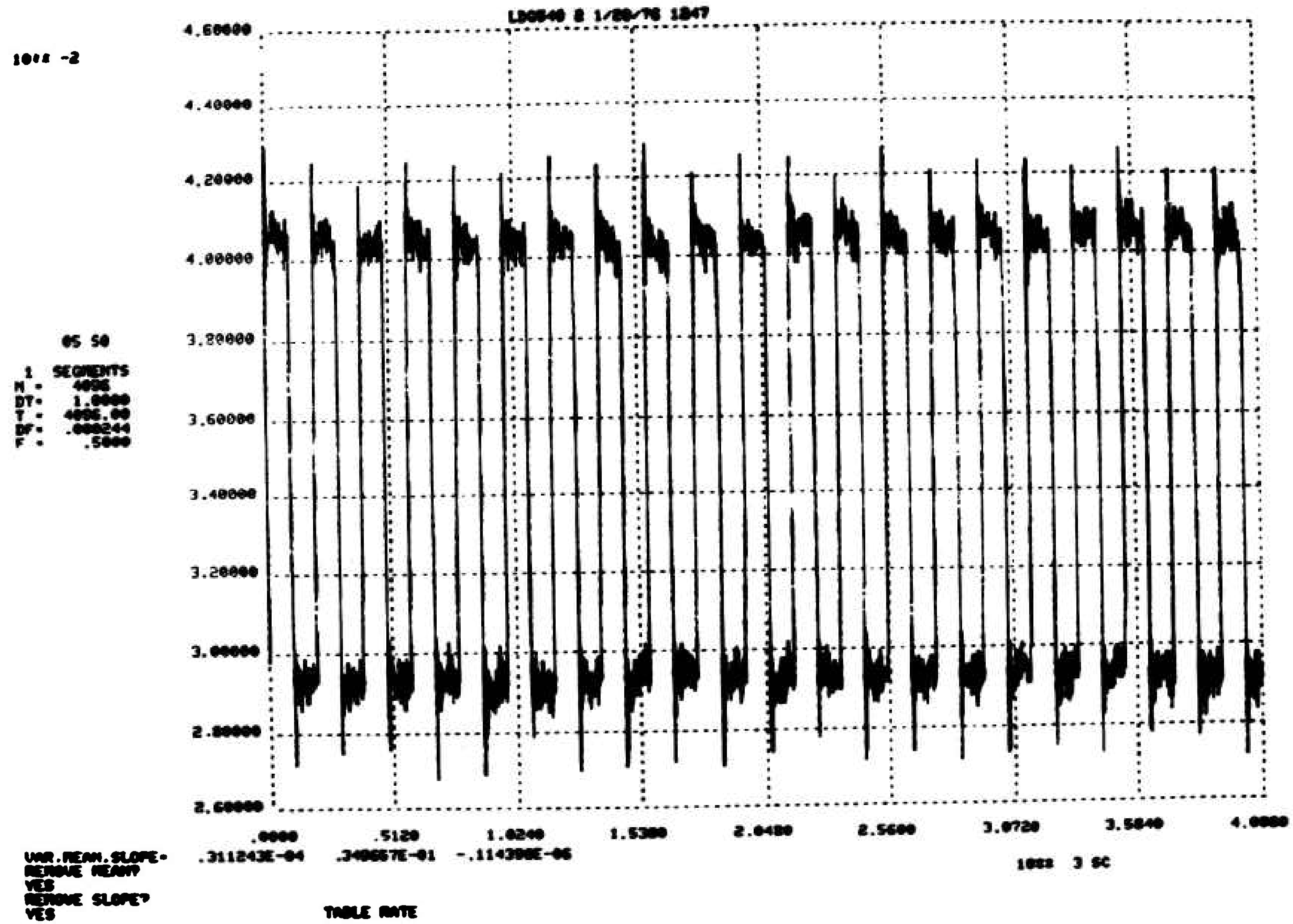

FIGURE G-5. TABLE RATE, DEGREE/HOUR (OA SENSITIVITY WITH TABLE TORQUED)

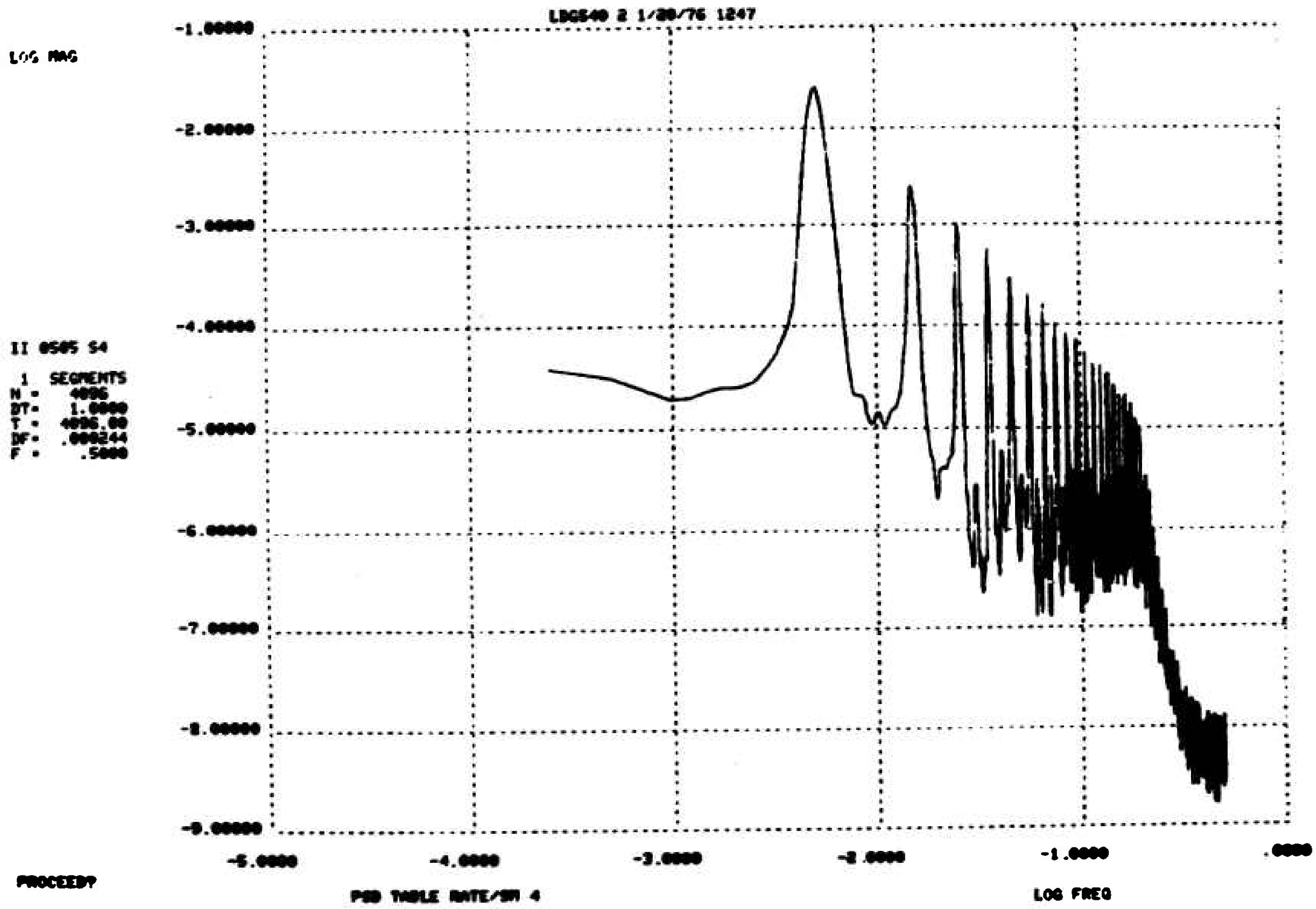

FIGURE G-6. PSD TABLE RATE, $(DEGREE/HOUR)^2/HZ$ (OA SENSITIVITY WITH TABLE TORQUED)

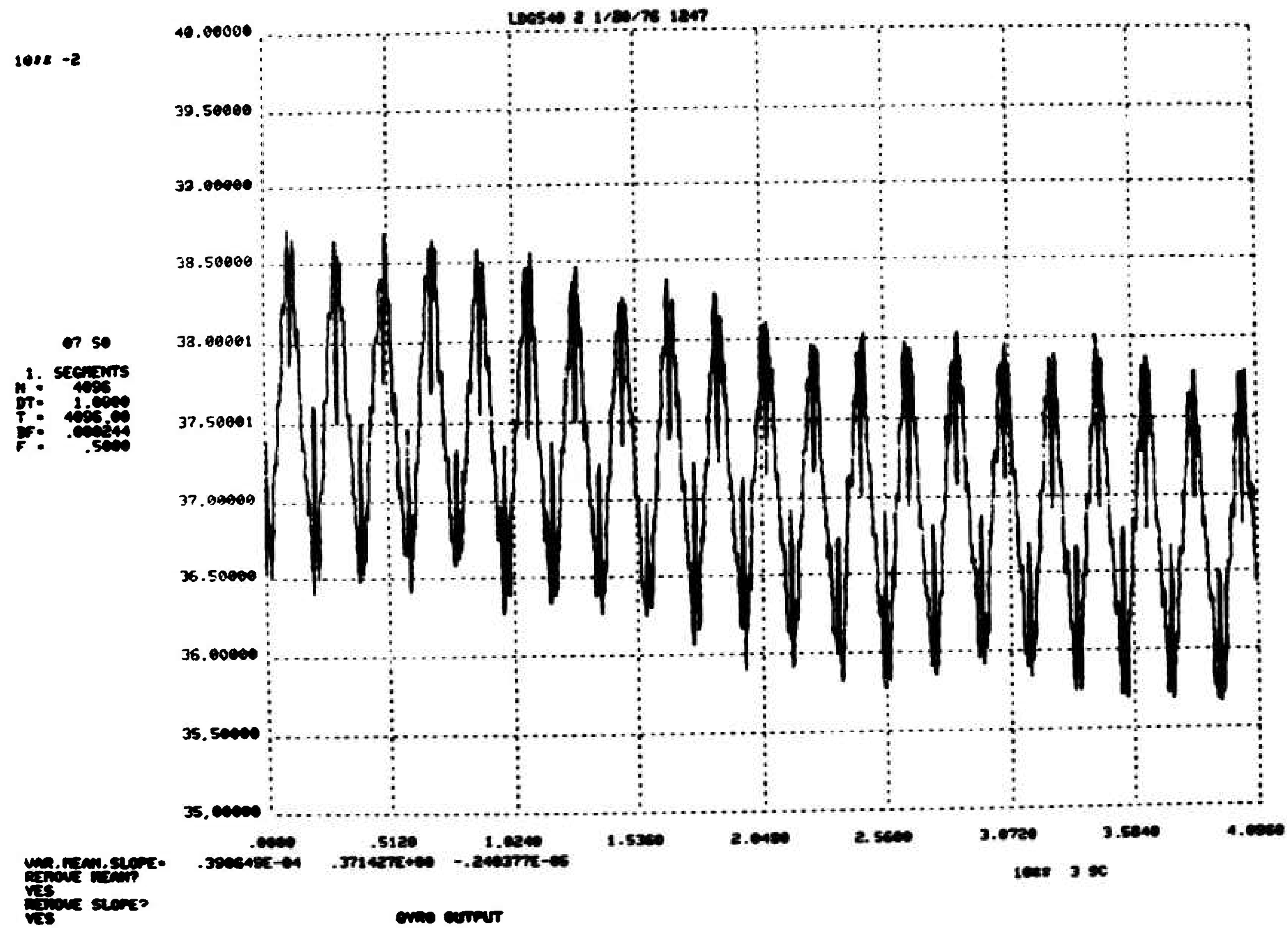

TABLE G-7. S/N 2 GYRO OUTPUT, DEGREE/HOUR (OA SENSITIVITY WITH TABLE TORQUED)

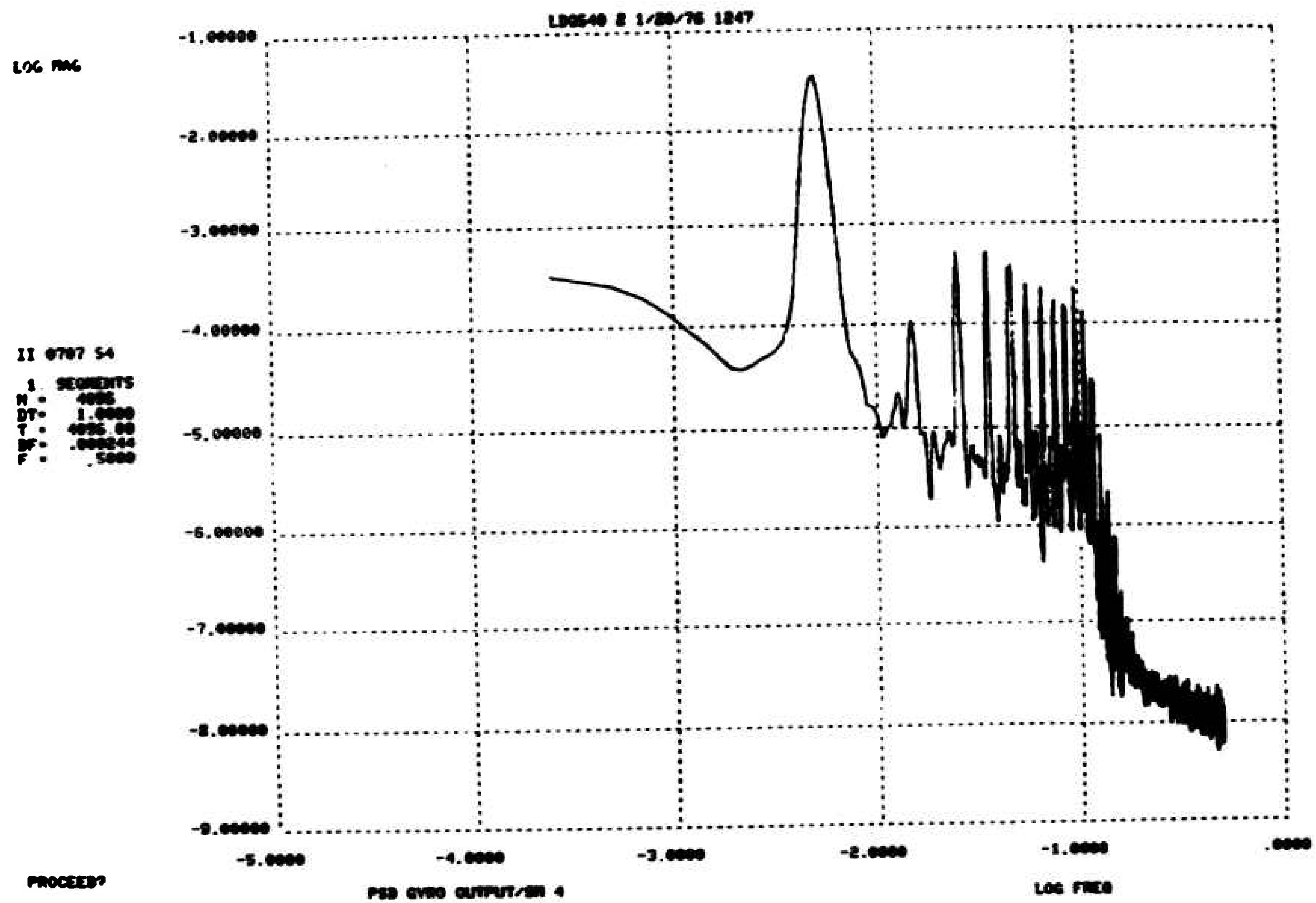

FIGURE G-8. PSD S/N 2 GYRO OUTPUT, $(\text{DEGREE/HOUR})^2/\text{HZ}$ (OA SENSITIVITY WITH TABLE TORQUED)

PRECEDING PAGE BLANK-NOT FILMED

DISTRIBUTION LIST

Defense Documentation Center Cameron Station Alexandria, VA 22314	12 Copies
AFSWC (HO) Kirtland AFB, NM 87117	1 Copy
ADTC (DLOSL) Eglin AFB, FL 32542	7 Copies
ADTC (CS) Eglin AFB, FL 32542	1 Copy
3201 Air Base Group (HO) Eglin AFB, FL 32542	1 Copy
AU Maxwell AFB, AL 31142	1 Copy
6585th Test Group Holloman AFB, NM 88330	
TSL	2 Copies
GDL	1 Copy
GDLC	2 Copies
GDP	3 Copies
GDA	2 Copies
ADTC/TG Eglin AFB, FL 32542	1 Copy
SAMSO/YAD P. O. Box 92960 Worldway Postal Center Los Angeles, CA 90009	5 Copies

REFERENCES

1. William D. Koenigsberg and Ronald A. Harris, Evaluation of Gyro Drift Noise Using Power Spectral Density; E-2770, Charles Stark Draper Laboratory, Cambridge, Mass, June 1973, CONFIDENTIAL.

2. Russell, J. F., Gyroscope Standard Torque-to-Balance Test; MDC-TR-67-79, Central Inertial Guidance Test Facility, Holloman AFB, New Mexico; June 1967.

3. William D. Koenigsberg, Spectral Density Measurements of Passive Tilt Environments, AIAA Paper No. 74-856, Charles Stark Draper Laboratory, Cambridge, Mass, AIAA Mechanics and Control of Flights Conference, Anaheim, California, August 5 - 9, 1974.